Intracoronary ultrasound

Intracoronair ultrageluid

PROEFSCHRIFT

Ter verkrijging van de graad van doctor
aan de Erasmus Universiteit Rotterdam
op gezag van de rector magnificus
Prof. Dr. P.W.C. Akkermans M. Lit.
en volgens het besluit van het college van dekanen

De openbare verdediging zal plaats vinden op
woensdag 20 oktober om 15.45 uur

door

Carlo Di Mario
geboren te Modena, Italie

PROMOTIECOMMISSIE

PROMOTOR : Prof. Dr. P.W. Serruys

CO-PROMOTOR : Dr. P.J. de Feyter

OVERIGE LEDEN: Prof. Dr. J.R.T.C. Roelandt
Prof. Dr. N. Bom
Prof. Dr. R. Erbel

ISBN 90-9006543-1

Cover illustrations
Top: Eccentric plaque in a proximal right coronary artery 6 months after directional coronary atherectomy (calibration = 0.5 mm).
Bottom: Doppler spectrum of the baseline flow velocity in a normal left circumflex artery.

Financial support by the Netherlands Heart Foundation for the publication of this thesis is gratefully acknowledged. Part of the research work reported in this thesis has been performed during a yearly Research Fellowship (1991) of the European Society of Cardiology.

Aan Chiara, Francesco en Andrea

CONTENTS

OVERVIEW OF THIS THESIS

Knowledge of the characteristics of the atherosclerotic plaque (eccentricity, composition, effect of initial dilatation or ablation) and of the flow modifications induced by a coronary stenosis would establish more precisely the severity of the lesion under evaluation, improve the planning and guidance of therapeutic interventions, and facilitate the detection of subsequent complications. The miniaturization of the ultrasound catheters and the development of Doppler probes with guidewire technology have permitted the application of these techniques during diagnostic or therapeutic procedures in the Cardiac Catheterization Laboratory. In this thesis, the application of catheter-based ultrasound probes for the assessment of function and morphology of the coronary arterial tree is addressed. In particular, after a general introduction to the physical principles and probe technology in catheter-based diagnostic intracoronary techniques (Chapter I), Chapter II and III discuss the application of intracoronary ultrasound for the quantitative assessment of arterial dimensions and the reconstruction of three-dimensional images of arterial segments. Chapter IV, V and VI report the results of experimental studies carried out to validate the accuracy of intravascular ultrasound for the assessment of wall morphology and pathology and of acute changes of arterial compliance and to study the effects of changes of the angle of incidence of the ultrasound beam.

Using Doppler guidewires, changes in flow velocity distal to a stenosis can be studied, providing information on the functional characteristics of the stenosis under assessment complementary to the morphological evaluation obtained with two-dimensional ultrasound imaging. In Chapter VII and VIII the physical and technical background of intracoronary Doppler is discussed and the advantages of a spectral analysis of the Doppler signal are established based on the comparison with the results obtained with a conventional zero-crossing detector. Based on the limitations of the conventional indexes of stenosis severity in the assessment of the results of coronary interventions (Chapter X), alternative indexes based on flow velocity measurements are proposed. Chapter IX explores the possibility of using the maximal velocity of the stenotic jet in the evaluation of the severity of a stenosis based on the continuity equation. Chapters X, XI and XII report the results obtained using a simultaneous assessment of pressure gradient and flow velocity, allowing the examination of stenosis hemodynamics as in an isolated hydraulic conduit. In Chapter XIII the possibility to study the relation between coronary pressure and flow velocity is tested in arteries with and without coronary stenoses. The potential usefulness of this approach, validated in animal models, for the assessment of an impaired coronary conductance due to the presence of a flow limiting stenosis or to the presence of a reduced maximal vasodilatation of the distal resistance vessels is discussed. In the final chapter of this thesis, the response of large conduit arteries and resistance vessels to endothelium-dependent vasodilators such as acetylcholine is assessed using quantitative angiography and intracoronary Doppler.

Part 1

Introduction to catheter-based intracoronary diagnostic techniques

CHAPTER 1

INTRACORONARY IMAGING AND NON-IMAGING TECHNIQUES FOR GUIDANCE OF CORONARY INTERVENTIONS

Carlo Di Mario, M.D., Jose Baptista, M.D., Peter de Jaegere, M.D., Ph.D., Pim J. de Feyter, M.D., Ph.D., Jos R.T.C. Roelandt, M.D., Ph.D., Patrick W. Serruys, M.D., Ph.D.

From the Intracoronary Imaging Laboratory and Cardiac Catheterization Laboratory, Thoraxcenter, Rotterdam, The Netherlands

INTRODUCTION

Coronary angiography is used during interventional procedures to assess the morphologic characteristics and to measure the absolute and relative dimensions of the stenotic segment. Computer-assisted quantitative coronary angiography has greatly increased the accuracy of these measurements, yielding precise and reproducible results [1,2]. However, multiple characteristics of the stenotic segment (minimal luminal cross-sectional area and percent cross-sectional area stenosis, length, entrance and exit angles) must be determined to assess the functional severity of a coronary stenosis [3,4]. Angiographic measurements of the reference segment can be misleading because of the presence of a diffuse atherosclerotic narrowing, of post-stenotic ectasia or of intraluminal defects, as frequently observed after coronary interventions. Further, angiography provides no information on plaque composition and no direct measurement of plaque thickness and eccentricity. Angiography has also a low sensitivity in the detection of thrombosis and wall dissection. To overcome these limitations, new techniques have been developed to obtain a more complete and precise assessment of the morphological and functional characteristics of coronary stenoses using intracoronary probes. This manuscript reviews the role and limitations of four new catheter-based imaging and non-imaging techniques during coronary intervention.

TWO-DIMENSIONAL INTRACORONARY ULTRASOUND IMAGING

Intravascular ultrasound has the unique advantage of studying vessel wall morphology and pathology beneath the endothelial surface [5,6]. Although earlier prototypes have been described and tested in the seventies [7], the major impetus for the development of intracoronary ultrasound into a practical tool was a consequence of the introduction of catheter-based interventions for treatment of atherosclerotic disease both in coronary and peripheral arteries. The safety of the use of new generation intracoronary ultrasound probes has been confirmed in a recent multicentric survey, reviewing 1,904 examinations in 1,837 patients (Yock et al., personal communication). Minor complications (spasm, reversible occlusion, dissection) occurred in 64/1904 arteries studied (3.5%). Seven major complications (myocardial infarction, bypass surgery) occurred and in 3 cases were considered "certainly" related to the ultrasound study (0.16%). No deaths were considered as possibly or certainly related to the ultrasound study. The major complications predominantly occurred (6/7) during interventional procedures.

Technique

Two approaches are currently applied to obtain cross-sectional images of the vessel wall. One approach is based on mechanical rotation of a single crystal (single element mechanical system) while in the other several crystals are mounted around

the tip of the catheter and used in sequence to scan around the circumference (multielement electronic system). Advantages and disadvantages of the two systems can be summarized as follows:

Single element mechanical systems: Mechanical rotation of the ultrasound element permits to circumferentially scan the vessel wall perpendicular to the long axis of the catheter. Rotating an acoustic reflector in front of a fixed transducer is an alternative approach. The principle is simple but realizing a driving mechanism while keeping the catheter fully flexible and steerable as well as its miniaturization are challenging problems. Distortion of the image because of an unequal rotation of the element/mirror at the catheter tip is a limitation of these systems. The advantages of the mechanical probes are imaging with high resolution and absence of near-field artifact.

Multi-element electronic systems: Sixty-four transducer elements are mounted around the circumference of the tip of a catheter which is as thin as an angioplasty intracoronary catheter. The signal is processed and multiplexed via ultra-miniaturized integrated circuits contained in the tip of the catheter. Each transducer element transmits and receives independently. Thus, this dynamic aperture array differs from phased array technology in which elements are activated in concert. Advantages of the system are: the catheter shaft, containing conductive wires only, is very flexible; a central lumen is available for guide-wire insertion; no distortion of the image due to inhomogeneous mechanical rotation is present. Disadvantages are a near-field artifact around the tip of the catheter, so that structures close to the catheter tip are not imaged, and the limited resolution and dynamic range of the system.

ADVANTAGES OF INTRACORONARY ULTRASOUND

Intracoronary ultrasound has three major advantages in comparison with angiography for the assessment of wall pathology.

1. *Detection of wall pathology in apparently normal angiographic segments*: Glagov et al [9] have shown that coronary arteries undergo a progressive enlargement in relation to increases in plaque area, so that a reduction of lumen area is delayed until the atherosclerotic lesion occupies more than 40% of the area circumscribed by the internal elastic lamina. These findings explain why angiographically normal arterial segments may show an extensive atherosclerotic involvement at autopsy [9], by direct surgical inspection and on intraoperative epicardial high-frequency echograms. Intravascular ultrasound has confirmed that significant and diffuse atherosclerotic changes may be present in angiographically normal arterial segments (Figure 1) [9,10,11]. Furthermore, intravascular ultrasound can facilitate the assessment of the severity of intermediate lesions or of lesions not clearly visualized with angiography (ostial lesions, proximal lesions not clearly visualized in multiple projections with angiography).

Detection of plaque eccentricity: An accurate assessment of lumen eccentricity with angiography requires an angiogram perpendicular to the maximal plaque thickness. Angiography determines the eccentricity of a stenosis comparing the proximal and

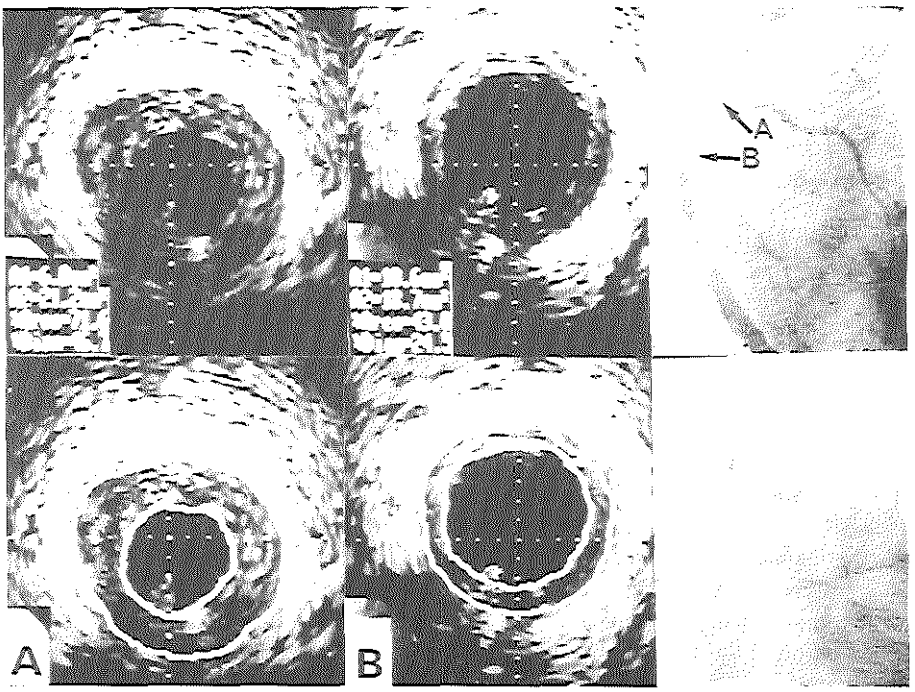

Fig. 1. Ultrasonic image (left panel, A) showing a large concentric plaque at the site of a moderate stenosis in a proximal right coronary artery (position A, indicated with an arrow in the corresponding angiogram, right panel). Also in the position indicated with B, apparently normal in the angiographic image, a diffuse intimal thickening induces a 43% cross-sectional area stenosis.
Calibration: 0.5 mm.

distal segments of the vessel, assumed as "normal" reference segments so that a misinterpretation is possible if the eccentric plaque also involves the reference segments. Intravascular ultrasound detects the eccentricity of the lesion from a direct measurement of the maximal and minimal thickness of the plaque so that the eccentricity index calculated with intravascular ultrasound is independent from the characteristics of the contiguous segments [12]. The advantage of the direct visualization of eccentric plaques is obvious in the guidance of percutaneous recanalization techniques which allow selective removal of atheromatous plaque, avoiding potentially dangerous procedures in areas of thin, normal wall [13].

Study of plaque composition: Two types of atherosclerotic plaques can be distinguished (Figure 2). "Hard" plaques are seen as highly echogenic lesions and are likely to be composed of dense fibrous tissue. The additional presence of shadowing and duplicate echoes indicates the presence of calcific deposits. "Soft" plaques are lesions with low echogenicity and may consist of thrombus, fibromuscular tissue or loose collagen. Occasionally, markedly hypoechoic areas can be identified within the plaque and are suggestive of lipid deposition or intraplaque necrotic degeneration. Most atherosclerotic lesions are complex plaques with multiple components, thus

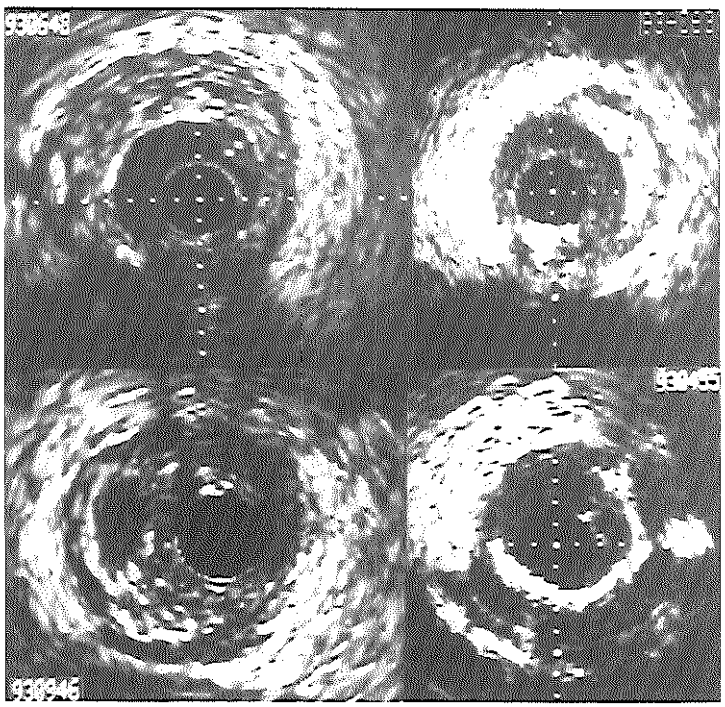

Fig. 2. Examples of different echographic characteristics of atherosclerotic plaques in 4 different patients. Upper left panel: predominantly "soft" plaque with a small calcification with shadowing at 9:00 o'clock. Upper right panel: eccentric non-calcific "hard" plaque. Note that the plaque echogenicity is similar to the echogenicity of the vascular adventitia. Lower left panel: mixed plaque with an inner area of low echogenicity surrounded by a more echogenic structure. The image is suggestive of an area of lipid deposition enclosed in a fibrous cap. Lower right panel: diffuse subendothelial calcification with shadowing and duplicate echoes (napkin's ring).

explaining why most of the stenotic segments undergoing balloon dilatation show areas of different echographic characteristics within the plaque ("mixed" plaques). Different echogenic characteristics of the culprit lesion have been reported in patients with stable and unstable syndromes. A prevalence of soft plaques with fewer intralesional calcium deposits has been reported by Hodgson et al [14]. In our experience, although echogenically "soft" material was present in almost all the 57 unstable lesions studied, the overall echographic characteristics of the plaque were similar in stable and unstable syndromes [15].

Knowledge of plaque composition may be helpful for deciding which lesions are more suitable for which specific treatment modality. "Soft" plaques are more likely to be dilated by compression, stretching and superficial intimal tears. Alternatively, "hard" or clearly calcific plaques have a higher risk of extensive dissection [16]. The presence of diffuse subendothelial calcification is associated with a lower success rate and higher risk of complications after directional coronary atherectomy, suggesting that alternative techniques such as rotational atherectomy should be used [17]. Using

this last technique, intracoronary ultrasound has shown that the neo-lumen is more circular and regular after treatment of "hard"/calcific lesions than after treatment of "soft" plaques [18]. On the contrary, after directional atherectomy a smaller amount of tissue is retrieved in the presence of "hard" or calcific lesions and more complications occur [19]. However, when "hard" lesions have been treated with directional atherectomy, they seem to be less prone to restenosis [19].

Mechanism of coronary interventions and restenosis

The possibility to measure lumen area and area inside the external elastic lamina before and after coronary interventions allows one to study the mechanism of balloon dilatation. Wall stretching with or without wall dissection has been reported as the main operative mechanism of balloon angioplasty in both coronary [20] and peripheral arteries [21]. A significant plaque compression (absolute reduction of plaque area) has been more recently reported [22,23]. The evaluation of a single cross-section, at the site of the minimal luminal cross-sectional area before and after angioplasty, may be insufficient for a complete assessment of the mechanism of balloon dilatation, thus explaining the differences in the results reported in the literature. In 18 coronary stenoses treated with balloon angioplasty and examined with three-dimensional intracoronary ultrasound, Mintz et al [24] noted the presence of an axial redistribution of the plaque away from the narrowest cross-sectional area, without significant changes in the total plaque volume. Intracoronary ultrasound has shown that gain in luminal area is primarily achieved by plaque removal with directional coronary atherectomy [13,20] (Figure 3). However, the measurement of plaque area before and after directional coronary atherectomy allows the detection of individual cases with an unchanged or almost unchanged plaque area after treatment. These different mechanisms may have a prognostic value to predict the long-term result after atherectomy.

Immediate complications and long-term results can be predicted based on the morphological findings after the interventional procedure [16]. Pathology studies have shown that intimal splits or cracks with localized medial dissection are normal operative mechanisms of balloon angioplasty. Extensive medial tears (> 50% of the

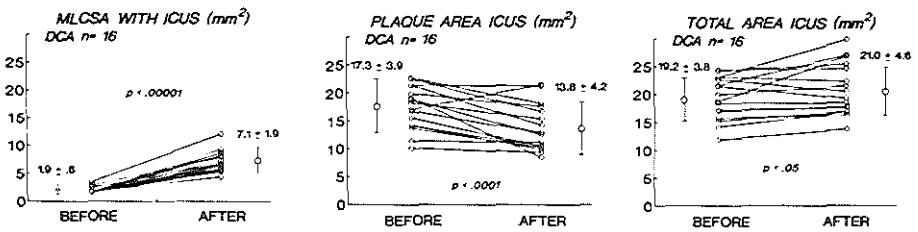

Fig. 3. From left to right minimal luminal cross-sectional area (MLCSA), plaque area and total area changes in 16 patients treated with directional coronary atherectomy. Although a significant plaque reduction occurred in most cases, accounting for most of the lumen gain, note the presence of individual cases with a minimal plaque decrease and in whom wall stretching (total area increase) was the mechanism of lumen enlargement.

vessel circumference), however, are at risk of abrupt closure [25,26]. A "smooth-walled" appearance is the most common angiographic pattern after balloon dilatation (41%), followed by intimal flaps (22%) and intraluminal haziness (17%) [27]. The presence of a dissection flap on angiography is a predictor of abrupt occlusion after angioplasty, resulting in a 6.5 fold increase of a major complication in the following 24 hours [28]. The identification of patients at high risk, requiring a prophylactic treatment such as stent implantation, however, is not possible based on the angiographic findings. Furthermore, the presence of an angiographically visible dissection immediately after balloon angioplasty is not a predictor of late restenosis [29]. Intravascular ultrasound is more sensitive than angiography in detecting development of dissections following interventional procedures [30-34] and can identify circumferential and longitudinal extension of a dissection post-angioplasty [35,36] (Figure 4). An increased risk of abrupt occlusion requiring stent implantation or emergency coronary bypass graft implantation was observed in the presence of circular dissections [20], major tears being observed 4 times more commonly in the adverse outcome group. These lesions also showed an increased risk of long-term restenosis (> 50%) [37]. At the other extreme, a higher restenosis rate has been reported in the absence of intimal dissection, when only plaque stretching is the mechanism of lumen enlargement [33].

Intravascular ultrasound has confirmed previous observations from in vitro models showing that tears tend to occur at the junction between normal wall and plaque or

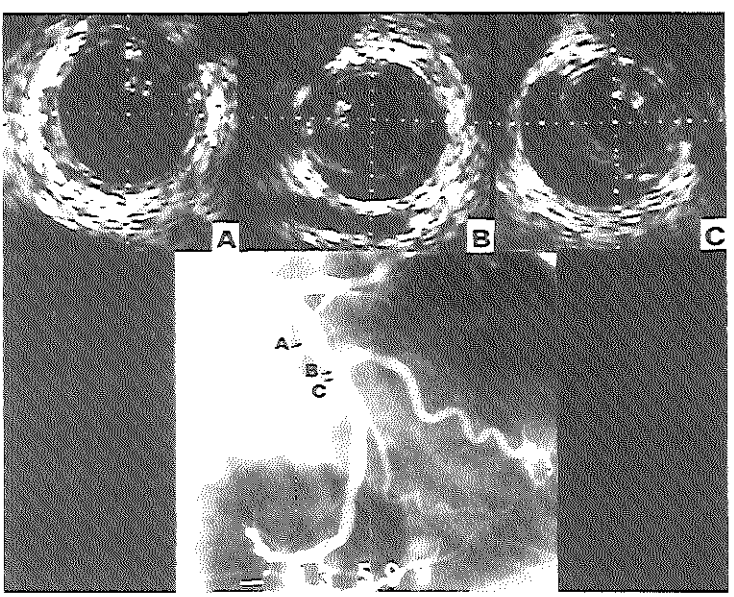

Fig. 4. Large dissection after PTCA in a large circumflex artery. The dissection starts at the origin of the obtuse marginal branch (B) and forms a large false lumen (C) for around 1.5 cm distally. Note that only an intraluminal filling defect is observed in the corresponding angiographic image. Calibration: 0.5 mm.

between "soft" tissue and calcific plates [38]. The qualitative and quantitative information provided by intravascular ultrasound may be used to reconstruct computerized models of the vessel and measure the wall stress in order to predict risk and location of wall dissections [39].

Intravascular ultrasound gives a new insight into the causative mechanism of restenosis. Based on the results of serial intravascular ultrasound studies [40], the importance of neo-intimal hyperplasia in the process of restenosis has to be questioned. The increase in plaque area observed at the stenosis site from the measurements obtained immediately after angioplasty to the measurements obtained at 6 months' follow-up, accounted for only 32% of the loss in luminal gain [40]. Further, no significant changes of the echographic characteristics of the plaque were observed from the initial study to the follow-up study [41]. Based on these findings, mechanisms which must be considered as an alternative to or in combination with neo-intimal hyperplasia are an overestimation of the initial luminal area gain by angiography because of undetected intraluminal flaps (pseudorestenosis), late thrombotic obliteration of dissection planes and a process of chronic recoil.

The metallic struts of current generation stents are poorly visible with fluoroscopy but are highly echogenic and show a clear and characteristic pattern with intravascular ultrasound [42]. An incomplete apposition of the struts to the vessel wall results in an increased risk of thrombosis and can be identified more easily with ultrasound than with angiography. A more frequent situation is the incomplete expansion of the stent due to the rigidity of the stenotic plaque. This suboptimal deployment, especially if the expansion of the stent is asymmetric, is not easily detected by angiography and prevents the normalization of luminal dimensions and restoration of a regular circular cross-sectional area. Ultrasound-guided inflations of short balloons within the stent can be used for the optimization of stent deployment. Intravascular ultrasound can also elucidate the mechanisms of restenosis within the stented segment and distinguish stent compression from neo-intimal proliferation [43].

Limitations

The miniaturization of the currently available ultrasound catheter is still insufficient to allow the study of a clinically significant stenosis and of distal coronary arteries. Prototype catheter systems smaller than 3 Fr are now under clinical evaluation.

All the elements of the catheter, including the distal end where the echo-transducer is mounted, must be fully flexible in order to allow safe and successful negotiation of tortuous vessels, especially in intracoronary application. Furthermore, with currently available intravascular ultrasound systems, the image quality is not consistently adequate to allow a complete evaluation of vascular dimensions and morphological changes.

Limited steerability of the intravascular ultrasound catheters precludes correction for a non-coaxial or eccentric intravascular position. The perpendicularity of the ultrasound beam to the vascular wall influences the intensity with which the structure

is visualized and partial drop-outs occur above a critical angle of incidence [44]. In addition, the "blooming " effect induced by off-axis position of the catheter results in an overestimation of the vascular lumen and wall [45].

Intravascular ultrasound is an expensive technology. The additional diagnostic and prognostic information during recanalization procedures must be confirmed in large studies to determine if the expected benefit outweighs the cost.

Future developments

Efforts are being made to combine intravascular imaging with ablation techniques, so that the echographic cross-sectional image can be used for accurate application of the selected atherectomy technique aiming at maximal plaque removal without damage to the underlying vessel wall [46,47].

Forward imaging would make assessment of vascular disease more comprehensive and guidance of interventions more practical.

The implementation of software systems for on-line automatic quantification and three-dimensional reconstruction [48], providing spatial orientation and safe application of ablation devices, is a research goal (Figure 5).

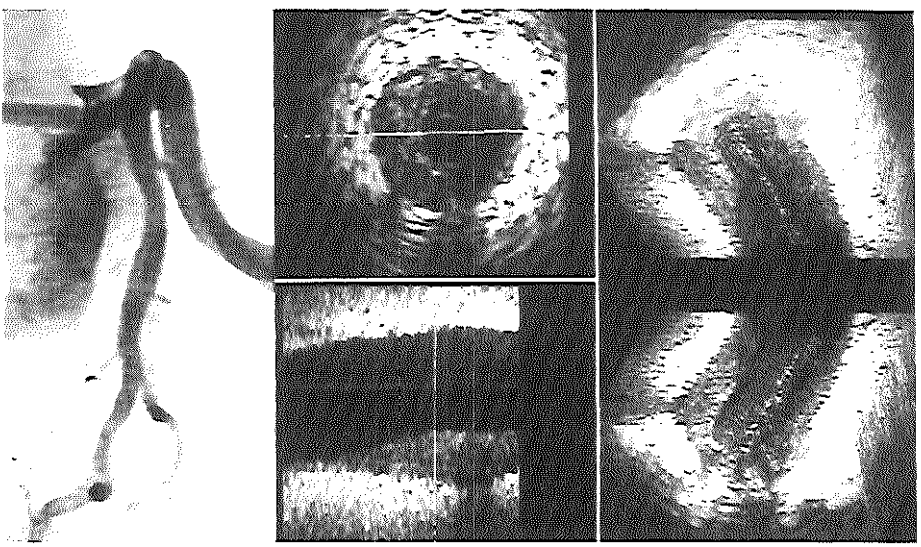

Fig. 5. Three-dimensional reconstruction of a proximal left anterior descending coronary artery after directional coronary atherectomy. An almost complete normalization of the lumen has been achieved as shown by the angiogram (left panel) and confirmed by the longitudinal view of the reconstructed segment (lower image of the mid-panel). The longitudinal view and the three-dimensional image (right panel), however, show length, thickness and circumferential extension of a large residual plaque, facilitating a further selective plaque removal. In the three-dimensional images on the right panel, note the presence of artifacts due to the catheter strut on the internal surface of the two half cylinders ("open-shell" format).

Analysis of the backscatter signals would allow a more accurate and quantitative characterization of plaque components.

An improvement in image quality and a further miniaturization and increased flexibility of the ultrasound probes seem to be conflicting objectives with difficult technical solutions. The use of a miniaturized motor unit which can rotate the ultrasonic crystal at high speed avoiding a connection with an external unit is an example of the many possible revolutionary technical solutions tested in this rapidly evolving field.

FIBEROPTIC INTRACORONARY ANGIOSCOPY

The use of optical fibers in medicine has found a new application for the assessment of the surface of the vessel wall. Although the initial experiences have been reported in the early eighties, only in the last few years has a larger clinical application been possible due to the miniaturization of the angioscopes, the improvement in resolution afforded by the use of multiple microscopic fibers and the incorporation of effective systems to occlude and flush the vessel proximal to the angioscope.

Technique

The angioscope used at the Thoraxcenter (ImageCath, Baxter Laboratories, Irvine, California) is mounted at the tip of a Monorail type catheter with a diameter of 4.5 F (1.43 mm). This catheter features a compliant cuff which can be inflated at low pressure proximal to the stenosis to a diameter of up to 5 mm, a flush port distal to this cuff and a movable optical bundle with an extension range of 5 cm. The imaging bundle is composed of 3,000 individual optical fibers of 2 μm diameter and terminates at a grin lens constructed with a gradient index of refraction so that all the images tend to appear in focus regardless of the distance from the lens. The central imaging bundle is surrounded by 12 light fibers of 120 μm of diameter, coupled to a light source located at the base of the catheter and with an illuminating power of 100,000 lux, although only an effective illumination power of 45 lux is delivered at the tip of the catheter. After positioning of the angioscope over the wire in the segment to be examined, the balloon is inflated and a continuous flushing with Ringer's lactate is performed at infusion rates variable from 30 to 50 ml/min. Once the crystalloid solution has cleared the image field from blood, the tip of the catheter is advanced to explore the lesion under study.

Angioscopic characteristics of the lesion

In vitro studies have confirmed the ability of intracoronary angioscopy to detect ulcerated plaques and thrombi [49]. In a histopathological comparison with ultrasound [50], angioscopy showed a sensitivity of 100% for the detection of thrombi, significantly higher than the sensitivity observed with ultrasound (57%).

Fig. 6. Digital angiogram of the left coronary angiogram in a patient with post-infarction angina. An eccentric lesion with smooth contours and without contrast staining is present in the mid-segment of the left anterior descending coronary artery. The corresponding angioscopic image shows an area of mural thrombosis proximal to the lesion and a red protruding thrombus at the site of the narrowing.

Angioscopy has been used intraoperatively to define the mechanism of unstable angina, showing the presence of arterial thrombosis, undetected by angiography, in the vast majority of the cases [51] (Figure 6). Our experience [52-53] includes 27 patients admitted to hospital within 2 weeks from the study because of unstable angina, 11 patient with chronic stable angina, 17 patients with recurrence of pain within 2 weeks after acute myocardial infarction. A complex lumen shape and an ulcerated vessel surface were present in 18 and 9% respectively of the patients with stable angina but were predominant in the group with unstable and post-infarction angina pectoris (48 and 50%, respectively, both $p < 0.05$). Thrombosis was present in 74% of the patients with an unstable syndrome vs 18% of the cases with stable angina pectoris. It is noteworthy that the thrombus had the characteristics of a mass protruding into the vessel lumen in 14/23 patients (61%) with unstable syndromes. Only mural thrombi were observed in the patients with stable angina. Different characteristics of the thrombi were observed in patients with unstable angina and after acute myocardial infarction, with a prevalence of occlusive thrombi and of red

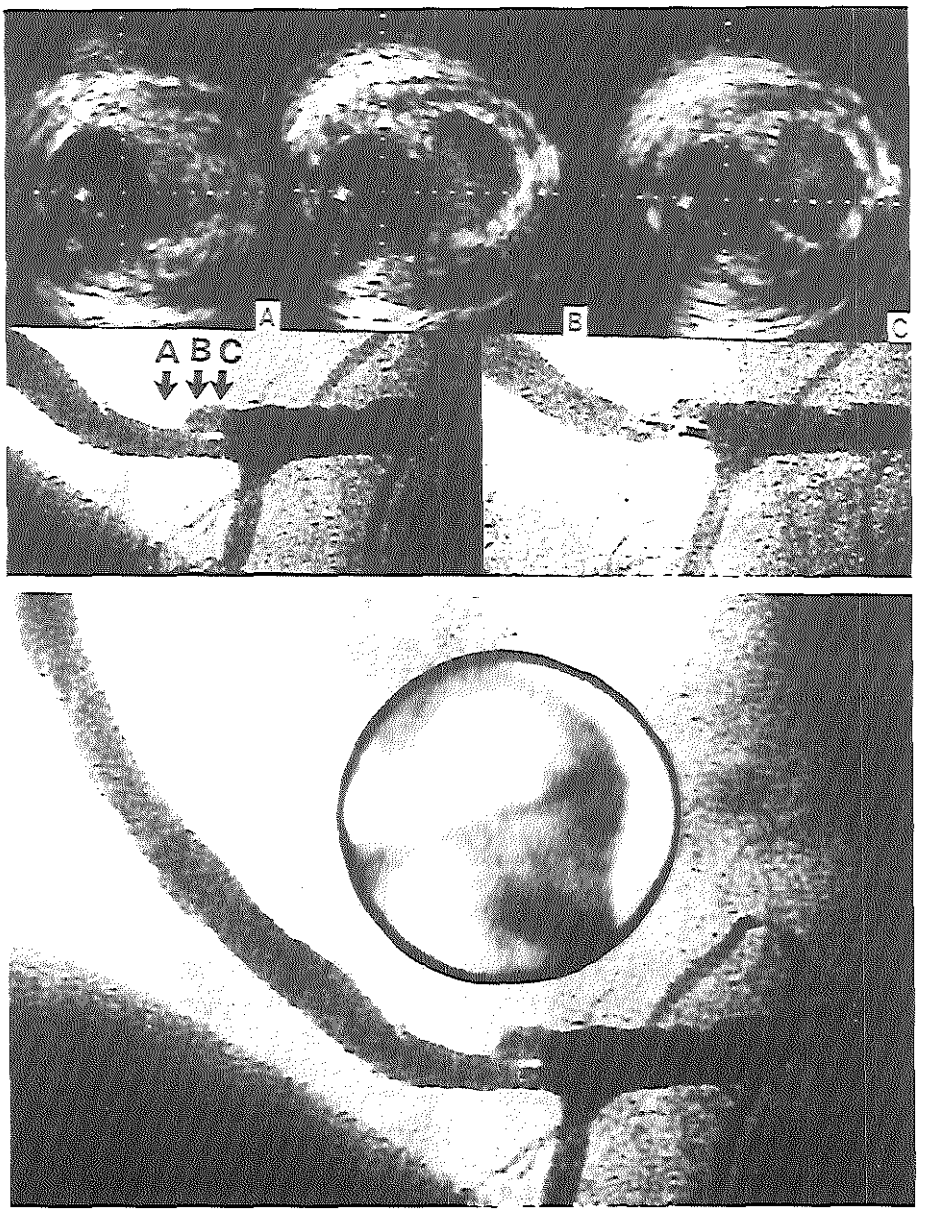

Fig. 7. Digital angiograms showing a complex plaque in the mid-segment of a saphenous vein graft 7 years after implantation. Three ultrasonic cross-sections obtained from proximal to distal at the site of the lesion (top panel, A, B and C) show the presence of a soft eccentric plaque containing a cavity communicating retrogradely with the vessel lumen. The corresponding angioscopic image (lower panel) shows a friable lesion composed of red-greyish material and suggestive of organizing thrombi.

thrombi in this last group [54]. The greyish appearance of the thrombus in unstable angina was correlated to the presence of a platelet rich matrix, as opposed to the red appearance of the thrombus during acute myocardial infarction, composed of a red blood cells trapped in a fibrin matrix. The same authors [55] have reported that xanthomatous plaques are more frequent in unstable syndromes than in patients with chronic stable angina. A high frequency of intravascular thrombi was observed also in degenerated venous bypass grafts prior to balloon angioplasty [56]. Friable lesions, composed of fragmented or loosely adherent plaque lining the vessel wall, and spontaneous dissections were also frequent in degenerated grafts (Figure 7).

Application during coronary interventions

Angioscopy has a higher sensitivity than angiography in the detection of wall dissections after coronary interventions [57,58,59]. Superficial dissections, appearing as mobile whitish intraluminal fronds, may also be present before interventions, due to the trauma induced by the angioplasty guidewire and are an almost constant finding after coronary interventions. Plaque fractures, appearing as deep crevices extending into the wall of the vessel, are more rare (Figure 8). In comparison with intravascular ultrasound, angioscopy has a higher sensitivity in the detection of small

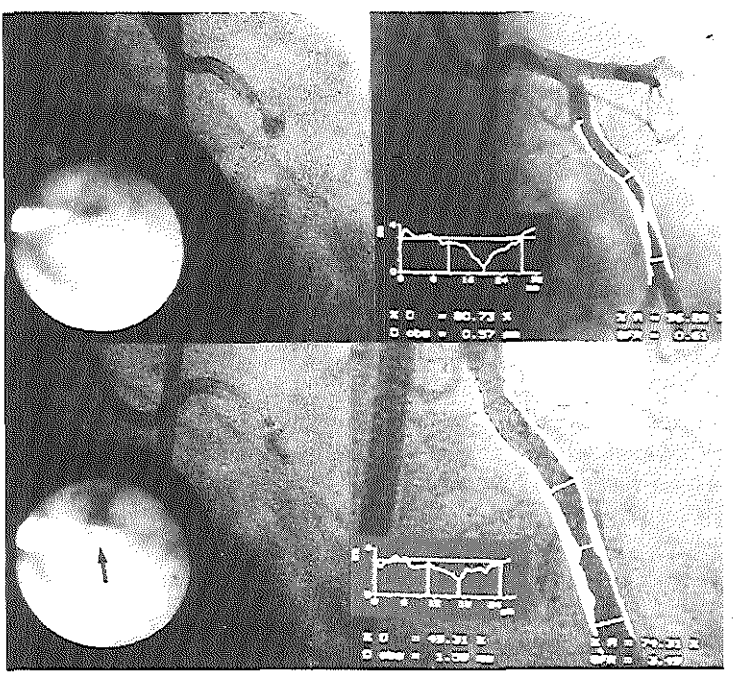

Fig. 8. Right panel: quantitative angiographic measurements before and after angioplasty of a large circumflex artery. Lumen enlargement after angioplasty is evident also in the corresponding angioscopic images before and after intervention. A deep tear induced by balloon inflation and not detected with angiography is indicated by an arrow.

superficial tears but, for deeper dissections, is unable to study depth and longitudinal extension of the plaque fracture. In an in vitro setting angioscopy has also been used successfully to remove experimentally induced intimal flaps using a microbiopsy forceps under visual guidance [57]. In our experience including 17 patients studied with angioscopy before and after balloon angioplasty and 12 patients studied before and after directional coronary atherectomy, newly developed multiple superficial flaps or deep dissections were observed with angioscopy in 65 and 24% of the lesions, respectively [60]. A newly developed thrombus or the increase of a preexisting thrombus was also frequent after these interventions (38%) but remained undetected by angiography and intravascular ultrasound. An increase of the amount of thrombotic material in the first hours after balloon angioplasty has been documented with implications for acute complications and long-term restenosis [61].

The development of acute occlusion after angioplasty can be the result of a massive thrombosis or of an extensive dissection. Angioscopy has the potential to determine the mechanism of occlusion and provide information guiding appropriate therapy. In 10 patients studied by angioscopy immediately following an abrupt occlusion after PTCA, Jain et al. [62] reported that a dissection was by far the most frequent cause of occlusion (80%).

During stent deployment, angioscopy can provide additional information with the identification of presence and extension of wall thrombosis, visualization of plaque bulging at the stent articulation and of incomplete stent apposition to the wall [63].

In 5 restenotic lesions late after balloon angioplasty, a pearl-white appearance was observed, consistent with a fibrous proliferation [64].

Limitations and future developments

Fiberoptic angioscopy requires transient vessel occlusion and continuous flushing with a transparent crystalloid solution. Although significant arrhythmias are not normally observed during the short interval required for an angioscopic study (60-90 s per insertion), discomfort to the patient remains a limitation of the technique. The use of oxygen-carrying solutions has been proposed, with the aim to prolong the study and reduce patient's symptoms. Their high viscosity, however, prevents an effective high-flow infusion.

The most frequent cause of inadequate visualization by angioscopy is the eccentric position of the angioscope within the vessel lumen, with images limited to a small quadrant of the vessel wall. Improved steerability of the catheter or of the optical bundle may obviate this limitation in the future. An increase in the number of imaging optical fibers is desirable to further improve resolution.

The subjective perception of colours is prone to a large interobserver variability, increased by the effect of variations of light intensity. An automatic measurement of colour intensity may facilitate a reproducible and objective classification of wall changes and may show a better correlation with the morphologic characteristics of the examined structures [65]. Angioscopy is unable to provide quantitative measurements of lumen dimensions. With the use of a light-wire projecting a circumferential light bundle at a known distance from the angioscope, quantitative

measurements have been obtained in our laboratory. A malalignment of the angioscope with the long axis of the vessel, however, remains a potential limitation [66].

The dream of the interventional cardiologist is the incorporation of the angioscope in an interventional device, allowing a continuous visual assessment of the plaque removal comparable to the use of laparoscopy or endoscopy during percutaneous cholecystectomy or sphynterotomy. The optical fibers used to deliver the laser energy in the laser atherectomy catheters can also be used for imaging purposes. Further, there is increasing evidence that the replacement of blood with saline required during angioscopic runs, increases the efficacy of laser ablation. These two elements suggest that efforts should be concentrated in the development of a combined laser catheter/angioscope system.

TRANS-STENOTIC PRESSURE GRADIENT MEASURED WITH PRESSURE MICROSENSORS

Andreas Grüntzig, the inventor of coronary angioplasty, made use of the transstenotic pressure gradient to guide the progression of the balloon catheter in the coronary tree up to the targeted stenotic lesion, to demonstrate the severity of the stenotic lesion and to assess the results of the intervention [67,68]. The physiological value of measurements performed through the lumen of the balloon catheter has always been questioned since the catheter impedes flow by its presence. Experimental data obtained in dog femoral arteries suggest that the "true" stenosis gradient is overestimated in a predictable manner dependent on the ratio of the catheter diameter over the stenosis diameter [69]. The further miniaturization of the balloon catheter, the introduction of the movable guidewire and of the Monorail technique soon rendered measurement of pressure gradient less applicable.

The interest for the use of post-stenotic pressure measurements in the Catheterization Laboratory has been revived by the development of ultraminiaturized transducers, allowing a high-fidelity measurement of post-stenotic pressure with a negligible additional reduction of cross-sectional area [70].

Technique

The pressure microsensor is located 3 cm proximal to the flexible tip of a 0.018" guidewire (diameter 0.45 mm, cross-sectional area 0.17 mm^2, Radi Medical Systems, Uppsala, Sweden). Light is emitted from a control unit through a beam splitter and is transmitted to the sensor element along an optical fiber integrated in the guidewire. The sensor element consists of a silicon cantilever with a mirror integrated into its free end. Deflection of the mirror induced by the elastic movement of the sensor in response to changes in the external pressure modulates the reflected light. The signal is then transmitted back through the same optical fiber and is detected by a photo diode in the control unit. The system has been validated in vitro with regard to signal transfer characteristics, linearity and frequency response [70].

Fluid-filled guidewire systems have also been designed and successfully tested in vitro and in vivo [71]. These transducers have the advantage of lower cost and ease of use but cannot provide a phasic pressure recording.

Application for the assessment of stenosis severity

Baseline and hyperemic pressure gradients correlate well with angiographic measurements and with stenosis flow reserve [72]. More recently, Pijls et al. [73] have proposed a set of hydrodynamic equations based only on coronary pressure measurements to quantify separately the transstenotic flow from the contribution of the coronary collateral circulation. Measurements of absolute coronary flow using positron emission tomography have been used to validate in humans the myocardial flow reserve calculated from pressure measurements. A practical drawback of the technique is that a post-stenotic pressure during balloon occlusion (wedge pressure) is required for the relative estimation of anterograde transstenotic flow and collateral flow, limiting the application of this technique for diagnostic purposes.

POST-STENOTIC FLOW VELOCITY MEASURED WITH A DOPPLER-TIPPED ANGIOPLASTY GUIDEWIRE

Technique

The Doppler angioplasty guidewire is a 0.018″ or 0.014″ 175 cm long flexible and steerable guidewire with a floppy shapable distal end mounting a 12-15 MHz piezoelectric transducer at the tip (Cardiometrics Inc., Mountain View, CA) [74]. The sample volume is positioned at a distance of 5.2 mm from the transducer and has an approximate width of 2.25 mm due to the divergent ultrasound beam so that a large part of the flow velocity profile is included in the sample volume also in case of eccentric positions of the Doppler guidewire. After real-time processing of the quadrature audio signal a fast-Fourier transform algorithm is used to increase the reliability of the analysis [75], the Doppler system calculates and displays on-line several spectral variables including the instantaneous peak velocity and the time-averaged (mean of 2 beats) peak velocity. The flow velocity measurements obtained with this system have been validated in vitro and in an animal model using simultaneous electromagnetic flow measurements for comparison [74]. Mean flow velocity is calculated as time-averaged peak velocity/2, assuming a fully developed parabolic flow velocity profile 76].

Application during coronary interventions

Monitoring and assessment of the results of coronary interventions
The Doppler guidewire can be used to assess the severity of the lesion to be treated before angioplasty. During the dilatation, the Doppler guidewire is left in place distal to the lesion in order to continuously record the Doppler signal and monitor the

development of collateral flow, the restoration of flow after balloon deflation, the phase of post-occlusive reactive hyperemia and, incidently, the development of flow limiting complications. Immediately after the inflation, the balloon is withdrawn into the guiding catheter in order to avoid the residual obstruction of flow due to the presence of the deflated balloon across the lesion. The restoration of anterograde flow can be immediately detected during the deflation of the balloon, before the disappearance of electrocardiographic changes or of symptoms. The rapid flow velocity increase in the phase of post-occlusion reactive hyperemia can be used to assess the adequacy of lumen enlargement post-angioplasty immediately after the deflation of the balloon (Figure 9).

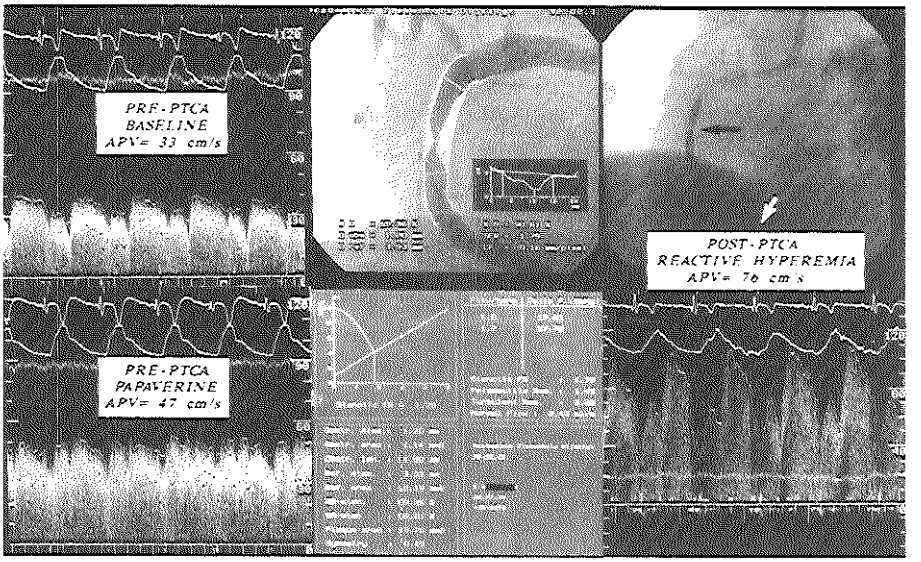

Fig. 9. Left panels: Flow velocity measurements distal to a severe stenosis of the right coronary artery in baseline conditions and at peak hyperemia induced by the injection of papaverine intracoronary. APV- time-averaged peak velocity.
Mid-panels: On-line quantitative angiographic measurement (Philips DCI ACA analysis package, Eindhoven, The Netherlands). Absolute and relative measurements of stenosis severity are showed in the lower panel, reporting also a plot of the stenosis flow reserve.
Right panels: The black arrow shows a clear indentation of the balloon during inflation. Note the Doppler guidewire, positioned distal to the stenosis (white arrow). Immediately after balloon deflation a rapid increase of flow velocity occurs in the post-ischemic period. Note the increase in time-averaged peak velocity and maximal diastolic velocity (from 47 cm/s and 52 cm/s before PTCA to 76 and 110 cm/s after PTCA, respectively). Note also the relative decrease of the systolic component after PTCA.

In a study by Serruys et al. [77] on 34 patients, coronary flow reserve, expressed as the ratio of hyperemic/baseline flow velocity, showed a moderate but significant increase post-PTCA (from 1.75 ± 0.55 to 2.39 ± 0.75 ,$p < 0.005$). A comparable flow velocity increase was observed post-PTCA in the phase of the maximal reactive hyperemia recorded following balloon dilatation and at the peak effect of a

papaverine injection (45 ± 22 cm/s peak reactive hyperemia vs 47 ± 20 cm/s after papaverine, NS). The ratio between mean diastolic and mean systolic flow velocity measured during baseline conditions distal to the stenosis was 1.51 ± 0.58 pre-PTCA, significantly lower than the ratio measured in 39 normal/near-normal arteries (2.09 ± 0.90, $p < 0.001$). After angioplasty, the diastolic/systolic flow velocity ratio increased from 1.51 ± 0.58 to 2.16 ± 0.98 ($p < 0.001$) and did not differ from the control group.

Segal et al. [78] have also recently reported their results after balloon angioplasty in 38 patients. Twelve patients without significant coronary artery disease served as a control group. Following angioplasty, the time-averaged peak velocity in the distal vessel increased from 19 ± 12 to 35 ± 16 cm/s ($p < 0.01$), whereas in the proximal vessel velocity increased to a lesser extent (pre-angioplasty 34 ± 18 cm/s vs post-angioplasty 41 ± 14 cm/s, $p=0.04$). Coronary flow reserve did not increase significantly after angioplasty whether measured in either the distal or proximal coronary artery ($p < 0.10$). When measured distal to significant stenoses (> 70 %) before angioplasty, the diastolic/systolic flow patterns were noted to be abnormal with low diastolic to systolic flow ratios (1.3 ± 0.5) when compared to coronary arteries in patients without significant stenoses (diastolic to systolic flow ratio = 1.8 ± 0.5, $p < 0.01$). Phasic velocity patterns normalized with significant increases in diastolic to systolic flow ratios (1.9 ± 0.6, $p < 0.01$) within 10-15 minutes following successful balloon angioplasty. In the proximal vessel, phasic diastolic/systolic flow patterns were not significantly different than in normal vessels (diastolic to systolic flow ratios = 1.8 ± 0.8 vs 1.8 ± 0.5, $p < 0.10$) and diastolic to systolic flow ratios did not increase significantly following angioplasty ($p < 0.10$).

Similar findings have been reported by Ofili et al. [79] before and after angioplasty in 32 patients, 15 with angiographic normal arteries and 27 with significantly stenosed arteries. After angioplasty, improvement in the phasic pattern, increase in the total velocity integral and the peak diastolic velocity during hyperemia in the distal region were noted. The mean and peak diastolic velocity during hyperemia were also significantly higher in the proximal and distal stenotic regions compared to the pre-angioplasty values. An additional indicator of a satisfactory result was the improvement in the ratio of proximal to distal mean velocity which correlated with the angiographic success of the procedure. The distal mean velocity increased 200% compared to 90% for proximal mean velocity ($p < 0.05$), which resulted in near equalization and normalization of proximal and distal velocities and significant reduction in the proximal to distal mean velocity. Systolic velocity integrals were also significantly lower following angioplasty (2.1 ± 1.2 vs 1.2 ± 0.3, $p < 0.02$).

Rationale for application of velocity indices during interventions

Coronary flow reserve: The ratio of maximal flow to baseline flow (coronary flow reserve, CFR) is a well-established methodology to provide a normalized index which is comparable in arteries of different diameter and in different subjects and has been shown to be well correlated with the severity of coronary stenoses [80] (Figure 10). The possibility of measuring coronary flow velocity with a Doppler guidewire

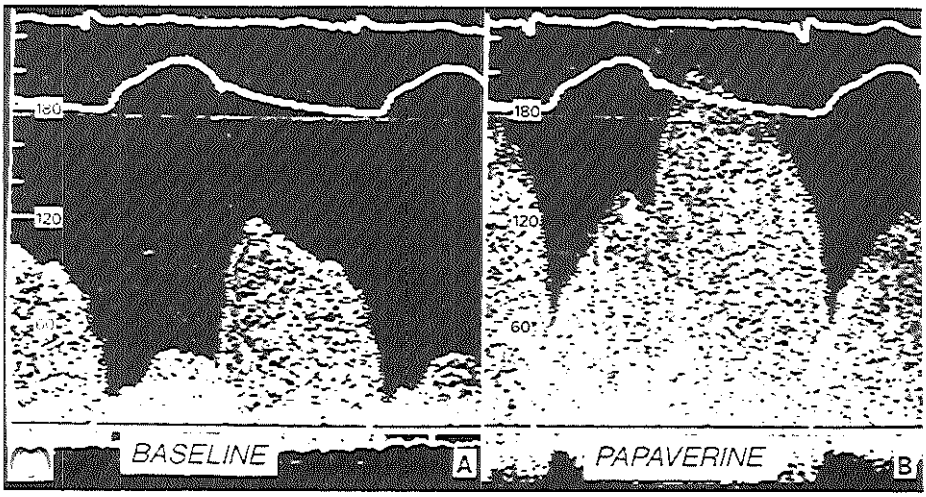

Fig. 10. Flow velocity measurements distal to an angiographically intermediate lesion of the left anterior descending coronary artery before and after intracoronary injection of 12.5 mg of papaverine i.c.

positioned distal to a stenosis avoids one of the major problems present with the use of Doppler catheters, the necessity to maintain the probe proximal to the stenosis. Confusing effects due to the interposition of side-branches between the site of the measurement and the stenosis can preclude a correct assessment of the velocity changes induced by the stenosis. As a ratio. however, CFR is influenced by changes in resting myocardial flow and by factors modifying the slope of the flow-pressure relationship during maximal hyperemia such as the presence of myocardial hypertrophy and changes in pre-load, heart rate and myocardial contractility [81-83]. Furthermore, the ratio between maximal hyperemic flow, which is linearly related to changes of driving pressure, and baseline flow, which is relatively independent from pressure changes in the autoregulatory range, is inherently variable with the level of aortic pressure at the time of measurement [11]. Coronary flow reserve, measured in clinical studies using Doppler or videodensitometry, correlated well with the angiographically measured stenosis severity only in very selected subsets of patients [84-86], but this index could not be successfully applied to a large population of patients with coronary artery disease [87]. Furthermore, after coronary interventions the increase in baseline flow and/or the persistence of an impaired vasodilatory response of the distal vasculature explains the unsuccessful results obtained using CFR for the immediate assessment of the effects of interventional procedures [88,89,90,91,77,78,79].

Diastolic to systolic flow velocity ratio: In contrast with the flow characteristics of most arterial beds, coronary arterial blood flow has a distinctive and unique phasic pattern. Blood flow is higher in diastole and lower in systole (Figure 10). The classical experiments of Sabistorn and Gregg have confirmed that the systolic reduction of arterial coronary flow is due to the contraction of the heart [92]. Squeezing of the capillary network was considered the cause of the flow changes

during the cardiac cycle and was attributed to the increase in tissue pressure consequent to the myocardial compression in the presence of a high systolic intraventricular pressure. More recently, an increased systolic stiffness of the cardiac myocytes has been proposed as a possible alternative [93,94].

Experimental and intraoperative human studies have shown that the contribution of the systolic components is increased distal to a stenosis [95-98]. A significant difference between distal diastolic to systolic velocity ratio was observed between normal arteries and arteries with significant stenosis [77,99,100] as well as in arteries examined before and after coronary angioplasty [77,78,79]. A limitation to the possible application of this index for the assessment of the hemodynamic severity of individual stenoses is the different pattern normally observed in the right and left coronary arteries and the variability of the diastolic to systolic velocity ratio and the changes of this ratio due to changes in cardiac contractility.

Proximal to distal velocity ratio: Only a moderate decrease of mean velocity, inversely proportional to the moderate increase in total cross-sectional area, occurs from proximal to distal segments in the epicardial coronary arteries. The uniform pattern of velocity decrease in epicardial normal arteries is drastically modified in the presence of a significant coronary stenosis, which induces a reduction of the post-stenotic velocity due to redistribution of flow in the lower resistance branches proximal to the stenosis. The ratio of proximal to distal mean velocity was significantly lower in normal arteries than in arteries with significant stenoses (1.1 ± 0.2 vs 2.4 ± 0.7, $p < 0.001$) [101]. A trend towards a normalization of the proximal to distal velocity ratio has also been observed after coronary angioplasty [78,79]. Despite these significant differences in the total population studied, a significant overlap was observed in patients with and without flow-limiting coronary stenoses. Furthermore, in the absence of important side-branches between the site of the proximal measurement and stenosis (very proximal stenosis, middle segment of the right coronary artery, bypass grafts) no redistribution of flow may occur and, for the principle of continuity of flow, constant proximal and distal velocities are measured.

Instantaneous hyperemic velocity-pressure or pressure gradient relation: To overcome the limitations of the above mentioned indices, Mancini et al proposed the assessment of the instantaneous relation between aortic pressure and coronary flow during maximal hyperemia in the phase of progressive flow decrease (mid- and end-diastole) [102]. In their experimental preparation, electromagnetic flowmeters were used to measure coronary flow and left ventricular pressure was used to define the start- and end-points for the measurement, avoiding the diastolic phase influenced by the rapid cardiac relaxation and the phase of isovolumetric myocardial contraction. In separate series of experiments [102-103], the slope of the instantaneous hyperemic diastolic flow-pressure relation (IHDFPS) was shown to be independent from changes in heart rate, preload, aortic pressure and cardiac contractility. The IHDFPS showed a better correlation with the severity of coronary stenoses induced by epicardial constrictors than the conventional CFR. The measurement of coronary conductance obtained with this index was highly correlated with the measurement obtained using microspheres. In humans, selective measurements of instantaneous coronary flow cannot be easily performed in the cardiac catheterization laboratory. Intracoronary

Doppler, however, can accurately measure instantaneous flow velocities during the cardiac cycle [74,76]. Using Doppler-tipped guidewires the velocity measurements can be obtained distal to the stenosis, so that the flow changes will certainly reflect the severity of the lesion under study.

We have studied feasibility, reproducibility and independency from the hemodynamic parameters at the time of the assessment of the IHDVPS in 52 arteries with < 30% diameter stenosis [104]. Sensitivity and specificity of the IHDVPS for the assessment of a flow-limiting stenosis was established by comparing the measurements of IHDVPS in the control group with the measurements obtained in 24 arteries with ≥30% diameter stenosis.

Using a cut-off value of ≥0.8 $cm \cdot s^{-1} \cdot mmHg^{-1}$, the sensitivity and specificity of this index in the detection of the absence of a ≥30% diameter stenosis were 95 and 91%, respectively, with a sensitivity slightly greater than coronary flow reserve. Despite the potential interest of these initial observations, the assessment of a larger group of patients with flow limiting stenoses is required to establish the potential advantage of IHDVPS over CFR in the assessment of an impairment of coronary conductance. Furthermore, additional studies should address the value of this index for the assessment of changes of coronary conductance after coronary interventions. In this respect, the IHDVPS has the great potential advantage over CFR to be independent from hemodynamic changes and from changes in baseline velocity.

The measurement of the relation between proximal coronary pressure and flow velocity distal to the stenosis explores both the changes in coronary conductance due to the presence of a stenosis and the vasodilatory capacity of the distal coronary circulation. An independent assessment of these two components can be obtained if the pressure distal to the stenosis can be simultaneously measured.

In a series of animal experiments performed by Gould et al. [105], the relation between transstenotic pressure and flow velocity showed an excellent correlation with the severity of experimentally induced coronary stenoses. The simultaneous measurement of the transstenotic pressure gradient and flow velocity has several practical advantages. The possible misinterpretation of a low flow increase during maximal vasodilation is avoided because the simultaneous recording of the transstenotic pressure gradient discriminates a low flow increase due to a hemodynamically severe stenosis (high pressure gradient) from a low flow increase due to an impairment of the distal vasodilatory mechanisms or to a competition of flow through a well-developed collateral circulation (low pressure gradient). Conversely, when a low maximal flow is present due to factors not dependent on the stenosis resistance, the measurement of a low transstenotic pressure gradient can be misleading and suggests the presence of a non-significant stenosis.

Although the maximal flow and, consequently, the maximal transstenotic gradient is determined also by factors independent from the stenosis resistance, the pressure gradient/flow relation is intimately correlated with the stenosis hemodynamics. Using a high-fidelity pressure transducer mounted on an angioplasty guidewire in combination with a separate Doppler guidewire, this approach has been recently applied in humans [77,106,107]. The initial results of the analysis of the instantaneous pressure gradient-velocity relation suggest that this technique can repro-

ducibly and accurately assess parameters which more precisely characterize the physiologic significance of coronary stenoses.

CONCLUSIONS

Coronary angiography provides a rapid overview and effective road-map during diagnostic or interventional procedures, has a low cost and enjoys a widespread availability. These advantages, coupled with the continuous improvement in image quality and possibility of on-line quantitative analysis, suggest that angiography will continue to be the principal imaging technique for coronary interventional procedures. However, knowledge on the qualitative and quantitative characteristics of the plaque is not available with angiography. Intracoronary ultrasound can image and quantitatively assess the vessel wall under the endothelial surface and is, at present, the technique with the greatest potential to become an established diagnostic technique for guidance of coronary interventions, especially when a selective plaque removal must be performed. The field of application of angioscopy is more limited, essentially including the qualitative assessment of the characteristics of the vessel wall surface. However, for this specific application and especially for the study of unstable plaques, angioscopy has an accuracy and resolution unmatched by any other imaging modality.

The development of quantitative angiography and the introduction of new imaging techniques can not replace the functional methods for the assessment of stenosis severity. The measurement of the transstenotic pressure gradient and of the post-stenotic flow velocity using miniaturized sensors with guidewire technology offers an alternative to the conventional non-invasive methods which is immediately applicable in the Catheterization Laboratory during interventional procedures. The complexity of the coronary circulation, however, impairs the possibility to establish simple cut-off criteria to identify the presence of a flow-limiting stenosis. For intermediate lesions or in the presence of variable hemodynamic conditions, the accuracy of the assessment can be improved by the application of more complex indices proposed and validated in animal laboratories and based on the instantaneous relationship between pressure or pressure gradient and flow velocity.

All these new techniques require technical improvements to further increase the quality of the image/signal and facilitate the integration in interventional procedures. Also at the present stage of development, however, the additional morphological and functional information provided by these techniques can modify the strategy of the operator in a substantial number of interventions [63,108]. However, still missing is a clear evidence that the modification in treatment modalities driven by these new techniques leads to a consistent improvement of the immediate results of the intervention and to a significant long-term clinical benefit. For intravascular ultrasound and Doppler, pilot studies (GUIDE II, PICTURE, VALID II, DEBATE) have been started to establish the ultrasonic/Doppler measurements and indexes with the best diagnostic and prognostic accuracy and which should be used in larger randomized trials aimed at the comparison of an interventional strategy based only

on angiography and a strategy based also on these new diagnostic methods. Ultimately, only a positive result of this type of trial may transform these promising research tools into diagnostic techniques of daily clinical use during coronary interventions.

ACKNOWLEDGMENTS

The authors wish to thank the entire Staff of the Cardiac Catheterization Laboratory, University Hospital Dijkzigt, Rotterdam for their dedication to facilitate the integration of these new techniques in interventional procedures. The expert secretarial assistance of Ms. Marja Lems is gratefully acknowledged.

REFERENCES

1. Di Mario C, Haase J, den Boer A, Reiber JHC, Serruys PW. Videodensitometry versus edge detection for the assessment of in vivo intracoronary phantoms. Am Heart J 1992; 124: 1181-89.
2. Haase J, Di Mario C, Slager CJ, van der Giessen WJ, den Boer A, de Feyter PJ, Reiber JHC, Verdouw PD, Serruys PW. In-vivo validation of on-line and off-line geometric coronary measurements using insertion of stenosis phantoms in porcine coronary arteries. Cathet Cardiovasc Diagn 1992;27:16-27.
3. Young DF, Vholvin NR, Roth AC. Pressure drop across artificially induced stenoses in the femoral arteries of dogs. Circ Res 1975;36:735-743.
4. Lipscomb K, Hooten S. Effect of stenotic dimensions and blood flow on the hemodynamic significance of model coronary arterial stenoses. Am J Cardiol 1978; 42; 781-92.
5. Roelandt JRTC, Di Mario C, de Feyter PJ, et al. Intravascular Ultrasound: instrumentation, image interpretation, promises and pitfalls. In Hanrath P, Uebis R, Krebs W (eds):"Cardiovascular Imaging by Ultrasound", Kluwer Academic Publishers, Dordrecht-Boston-London, 1992, pp. 325-341.
6. Yock PG, Linker DT. Intravascular ultrasound. Looking below the surface of vascular disease. Circulation 1990; 81: 1715-18.
7. Bom N, Lancee CT, Rijsterborgh H, ten Hoff H, Roelandt JRTC. Intravascular ultrasound. From idea to clinical application. In Roelandt J, Gussenhoven EJ, Bom N (eds): Intravascular ultrasound. Kluwer Academic Publishers, Dordrecht, 1993, p. 3-13.
8. Glagov S, Weisenberg E, Zarins CK, et al. Compensatory enlargement of human atherosclerotic coronary arteries. N Engl J Med 1987; 316: 1371-75.
9. Escaned J, Haase J, Di Mario C, et al. Undetected coronary atheroma during quantitative angiographic analysis demonstrated by intravascular ultrasound and histological morphometry (abstr). Eur Heart J 1993; 14: 426.
10. Hermiller JB, Tenaglia AN, Kisslo KB, Stack RS, Davidson CJ. In vivo validation of compensatory enlargement of atherosclerotic coronary arteries. Am J Cardiol 1993; 71: 665-68.
11. Erbel R, Ge J, Schumann D, et al. Differentiation of coronary syndromes with intracoronary ultrasound. In Roelandt J, Gussenhoven EJ, Bom N (eds): Intravascular ultrasound. Kluwer Academic Publishers, Dordrecht, 1993, p. 33-39.
12. Honye J, Ashit J, Tobis JM, et al. Atherosclerotic plaque eccentricity; a comparison of angiography and intravascular ultrasound imaging (abstr). Circulation 1991; 64: II-701.
13. Kimura BJ, Fitzgerald PJ, Sudhir K, Amidon TM, Strunk BL, Yock PG. Guidance of directional coronary atherectomy by intracoronary ultrasound imaging. Am Heart J 1992; 124: 1385-1369.
14. Hodgson McJB, Reddy KG, Suneja R, Nair RN, Lesnefsky EJ, Sheehan HM. Intracoronary ultrasound imaging: correlation of plaque morphology with angiography, clinical syndrome and procedural results in patients undergoing coronary angioplasty. J Am Coll Cardiol 1993; 21: 35-44.

15. de Feyter PJ, Escaned J, Di Mario C, et al. Combined intracoronary ultrasound and angioscopic imaging in patients with unstable angina. Target lesion characteristics (abstr). Eur Heart J 1993; 14: 25.
16. Tenaglia AN, Buller CE, Kisslo KB, Phillips HR, Stack RS. Intracoronary ultrasound predictors of adverse outcomes after coronary artery interventions. J Am Coll Cardiol 1992; 20: 1385-90.
17. Fitzgerald PJ, Muhlberger VA, Moes NY, et al. Calcium location within plaque as a predictor of atherectomy tissue retrieval: an intravascular ultrasound study (abstr). Circulation 1992; 86: 516.
18. Kovach JA, Mintz GS, Pichard AD, et al. Sequential intravascular ultrasound imaging characterizes mechanism of luminal enlargement after rotational atherectomy (abstr). Circulation 1992; 86: 532.
19. Suarez de Leto J, Romero M, Medina A, et al. Intracoronary assessment of directional coronary atherectomy: Immediate and long-term findings. J Am Coll Cardiol 1993; 21: 298-307.
20. Tenaglia AN, Buller CE, Kisslo KB, Stack RS, Davidson CJ. Mechanisms of balloon angioplasty and directional coronary atherectomy as assessed by intracoronary ultrasound. J Am Coll Cardiol 1992; 20: 685-91.
21. The SHK, Gussenhoven EJ, Zhong Y, Li W, van Egmond F, Pieterman H, van Urk H, Gerritsen P, Borst C, Wilson RA, Bom N. Effect of balloon angioplasty on femoral artery evaluated with intravascular ultrasound imaging. Circulation 1992; 86: 483-93.
22. Losordo DW, Rosenfield K, Pieczek A, Baker K, Harding M, Isner JM. How does angioplasty work? Serial analysis of human iliac arteries using intravascular ultrasound. Circulation 1992; 86: 1845-58.
23. Baptista J, Di Mario C, Ozaki Y, et al. Determinants of lumen and plaque changes after balloon angioplasty. A quantitative ultrasound study (abstr). J Am Coll Cardiol, submitted.
24. Mintz G, Kovach JA, Park KS. Conservation of plaque mass: a volumetric intravascular ultrasound analysis of patients before and after percutaneous transluminal coronary angioplasty (abstr). J Am Coll Cardiol 1993; 21: 484A.
24. Mintz GS, Douek P, Pichard AD, et al. Intravascular ultrasound comparison of de novo and restenotic coronary artery lesions (abstr). J Am Coll Cardiol 1993; 21: 118.
25. Waller BF. Morphologic correlates of coronary angiographic patterns at the site of percutaneous coronary angioplasty. Clin Cardiol 1988; 11: 817-22.
26. Waller BF, Orr CM, Pinkerton CA, van Tassel J, Peters T, Slack JD. Coronary balloon angioplasty dissections: " the Good, the Bad and the Ugly". J Am Coll Cardiol 1992; 20: 701-06.
27. Holmes DR Jr, Vliestra RE, Mock MB. Angiographic changes produced by percutaneous transluminal coronary angioplasty. Am J Cardiol 1983; 51: 676-81.
28. Bredlau C, Roubin GS, Leimgruber PP, Douglas JS, King SB, Gruentzig AR. In-hospital morbidity and mortality in patients undergoing elective coronary angioplasty. Circulation 1985; 72: 1044-52.
29. Hermans WRM, Rensing BJ, Foley DP, Deckers JW, Rutsch W, Emanuelsson H, Serruys PW. Therapeutic dissection after successful coronary balloon angioplasty.: no influence on restenosis or on clinical outcome in 693 patients. J Am Coll Cardiol 1992; 20: 767-80.
30. Yock PG, Fitzgerald PJ, Linker DT, et al. Intravascular ultrasound guidance for catheter based coronary interventions. J Am Coll Cardiol 1991; 6: 39B-45B.
31. Yock PG, Fitzgerald PJ, Sudhir K. Intracoronary ultrasound scanning: clinical experience and new insights. In Roelandt J, Gussenhoven EJ, Bom N (eds): Intravascular ultrasound. Kluwer Academic Publishers, Dordrecht, 1993, p. 17-28.
32. Werner GS, Sold G, Buchwald A, Wiegand V. Intravascular ultrasound imaging of human coronary arteries after percutaneous transluminal angioplasty: morphologic and quantitative assessment. Am Heart J 1991; 122: 212-20.
33. Honye J, Mahon DJ, White CJ, Ramee SR, Tobis JM. Morphological effects of coronary balloon angioplasty in vivo assessed by intravascular ultrasound imaging. Circulation 1992; 85: 1012-25.
34. Violaris AG, Linnemeier TJ, Campbell S, et al. Intravascular ultrasound imaging combined with coronary angioplasty. Lancet 1992; 339: 1571-72.
36. Kearney P, Erbel R, Ge J, et al. Mechanisms of angioplasty analyzed by coronary ultrasound before and after intervention. Eur Heart J 1993; 14: 327.
37. Görge G, Erbel R, Gerber T, et al. Intravascular ultrasound after PTCA and clinical outcome. A six months follow-up study. Abstracts Xth Symp. Echocardiology, Rotterdam, p.65.

38. Fitzgerald PJ, Pots TA, Yock PG. Contribution of localized calcium deposits to dissection after angioplasty. An observational study using intracoronary ultrasound. Circulation 1992; 86: 64-70.
39. Lee RT, Loree HM, Cheng GC, Lieberman EH, Jaramillo N, Schoen FJ. Computational structural analysis based on intravascular ultrasound imaging before in vitro angioplasty: prediction of plaque fracture locations. J Am Coll Cardiol 1993; 21: 777-82.
35. Coy KM, Park JC, Fishbein MC, Laas T, Diamond GA, Adler L, Maurer G, Siegel RJ. In Vitro validation of three dimensional intravascular ultrasound for the evaluation of arterial injury after balloon angioplasty. J Am Colll cardiol 1992; 20: 692-700.
40. Mintz G, Kovach JA, Park KS. Conservation of plaque mass: a volumetric intravascular ultrasound analysis of patients before and after percutaneous transluminal coronary angioplasty (abstr). J Am Coll Cardiol 1993; 21: 484A.
41. Mintz GS, Douek P, Pichard AD, et al. Intravascular ultrasound comparison of de novo and restenotic coronary artery lesions (abstr). J Am Coll Cardiol 1993; 21: 118.
42. Slepian MJ. Application of intraluminal ultrasound imaging to vascular stenting. Int J Card Imaging 1991; 6: 285-311.
43. Laskey WK, Brady ST, Kussmaul WG, Waxler AR, Krol J, Herrmann HC, Hirshfeld JW, Sehgal C. Intravascular ultrasonic assessment of the results of coronary artery stenting. Am Heart J 1993; 125: 1576-83.
44. Di Mario C, Madretsma S, Linker D, The SHK, Bom N, Serruys PW, Gussenhoven EJ, Roelandt JRTC. The angle of incidence of the ultrasonic beam: a critical factor for image quality in intravascular ultrasonography. Am Heart J 1992; 125: 442-48.
45. Nishimura RC, Edwards WD, Warnes CA, et al. Intravascular ultrasound imaging:in vitro validation and pathologic correlation. J Am Coll Cardiol 1990; 16, 145-54.
46. Crowley RJ, Hamm MA, Joshi SH, et al. Ultrasound guided therapeutic catheters: recent developments and clinical results. Int J Cardiac Imag 1991; 6: 145-156.
47. Aretz HT, Gregory KW, Martinelli OMA, et al. Ultrasound guidance of laser atherectomy. Int J Cardiac Imag 1991; 6: 231-238.
48. Di Mario C, Wenguang L, Linker DT, Gussenhoven EJ, Serruys PW, Roelandt JRTC. Three-dimensional reconstruction in intravascular ultrasound. Promises and practical problems. Int J Cardiac Imag 1993; 63-67.
49. Hombach V, Hoher M, Kochs M, et al. Pathophysiology of unstable angina pectoris. Correlations with coronary angioscopic imaging. Eur Heart J 1988; 9: 40-45.
50. Siegel RJ, Ariani M, Fishbein MC, et al. Histopathologic validation of angioscopy and intravascular ultrasound. Circulation 1991; 84: 109-17.
51. Sherman CT, Litvack F, Forrester J et al. Coronary angioscopy in patients with unstable angina pectoris. N Eng J Med 1986; 315: 913-19.
52. Baptista J, de Feyter PJ, Di Mario C, et al. Angioscopy in stable and unstable coronary syndromes. J Am Coll Cardiol, submitted.
53. Escaned J, Di Mario C, Serruys PW, et al. The use of angioscopy in percutaneous coronary interventions. J Interv Cardiol 1993; in press.
54. Mizuno K, Satomura K, Ambrose JA, et al. Angioscopic evaluation of coronary artery thrombi in acute coronary syndromes. N Eng J Med 1992; 326; 287-291.
55. Mizuno K, Miyamoto A, Nakamura H, et al. Angioscopic coronary macromorphology in patients with acute coronary disorders. Lancet 1991; 337: 809-12.
56. White CJ, Ramee SR, Collins TJ, et al. Percutaneous angioscopy of saphenous vein coronary bypass grafts. J Am Coll Cardiol 1993; 21: 1181-85.
57. Neville RF, Yasuhara H, Watanabe BI, et al. Endovascular management of arterial intimal defects. An experimental comparison by arteriography, angioscopy and intravascular ultrasonography. J Vasc Surg 1991; 13: 496-502.
58. Siegel RJ, Chae JS, Forrester JS, Ruiz CE. Angiography, angioscopy and ultrasound imaging before and after percutaneous balloon angioplasty. Am Heart J 1990; 120: 1086-90.
59. Ramee SR, White CJ, Collins TJ, et al. Percutaneous angioscopy during coronary angioplasty using a steerable microangioscope. J Am Coll Cardiol 1991; 17: 100-05.

60. Baptista J, Di Mario C, de Feyter PJ, et al. Wall changes after directional atherectomy and balloon angioplasty. A combined echographic-angioscopic study. J Am Coll Cardiol; submitted.
61. den Heijer P, van Dijk RB, Pentinga ML, Lie KI. Serial angioscopy during the first hour after sucessful PTCA (abstr). Circulation 1992; 86: 458.
62. Jain SP, White CJ, Collins TJ, et al. Etiologies of acute occlusion after PTCA. Angioscopic morphology (abstr). J Am Coll Cardiol 1993; 21: 484.
63. Denardo SJ, Schatz RA, Teirstein PS, et al. Coronary angioscopy before and after stent deployment. J Am Coll Cardiol 1993; in press.
64. White CJ, Ramee SR, Mesa JE, et al. Percutaneous coronary angioscopy in patients with restenosis after coronary angioplasty. J Am Coll Cardiol 1991; 17: 46-49.
65. Baptista J, Slager CJ, Di Mario C, Oomen J, de Feyter PJ, Serruys PW. Automatic computer-assisted colour quantification. Analysis of in vivo coronary angioscopic images. Circulation; submitted.
66. Slager CJ, Oomen J, Serruys PW, et al. Quantitative angioscopic measurements using a light-wire. Circulation; submitted.
67. Grüntzig AR, Senning A, Siegenthaler WE. Nonoperative dilatation of coronary-artery stenosis: percutaneous transluminal coronary angioplasty. N Engl J Med 1979; 301: 61-8.
68. Serruys PW, Wijns W, Reiber JHC, de Feyter PJ, van den Brand M, Piscione F, Hugenholtz PG. Values and limitations of transstenotic pressure gradients measured during percutaneous coronary angioplasty. Herz 1985; 10: 337-342.
69. Leiboff R, Bren G, Katz R, Korhegi R, Katzen B, Ross A. Determinants of transstenotic gradients observed during angioplasty: an experimental model. Am J Cardiol 1983; 52: 1311-1317.
70. Emanuelsson H, Dohnal M, Lamm C, Tenerz L. Initial experiences with a miniaturized pressure transducer during coronary angioplasty. Cath Cardiovasc Diagn 1991; 24: 137-143.
71. de Bruyne B, Pijls NHJ, Paulus WJ, Vantrimpont PJ, Sys SU. Transstenotic coronary pressure gradient measurement in humans: in vitro and in vivo evaluation of a new pressure monitoring angioplasty guidewire. J Am Coll Cardiol 1993; 22: 119-26.
72. Lamm C, Dohnal M, Serruys PW, Emanuelsson H. High-fidelity translesional pressure gradients during percutaneous transluminal coronary angioplasty. Correlation with quantitative coronary angiography. Am Heart J 1993; 126: 66-75.
73. Pijls NHJ, van Son JAM, Kirkeeide RL, de Bruyne B, Gould KL. Experimental basis of determining maximum coronary, myocardial and collateral blood flow by pressure measurements for assessing functional stenosis severity before and after percutaneous transluminal coronary angioplasty. Circulation 1993; 86: 1354-61.
74. Doucette JW, Douglas Corl P, Payne HP, Flynn AE, Goto M, Nassi M, Segal J. Validation of a Doppler guide wire for intravascular measurement of coronary artery flow velocity. Circulation 1992; 85: 1899-1911.
75. Di Mario C, Roelandt JRTC, de Jaegere P, Linker DT, Oomen J, Serruys PW. Limitations of the zero-crossing detector in the analysis of intracoronary Doppler. A comparison with fast Fourier transform of basal, hyperemic and transstenotic blood flow velocity measurements in patients with coronary artery disease. Cathet Cardiovasc Diagn 1992; 28: 56-64.
76. Serruys PW, Di Mario C, Kern MJ. Intracoronary Doppler. In Topol EJ (ed) Textbook of Interventional Cardiology, Saunders, in press.
77. Serruys PW, Di Mario C, Meneveau N, de Jaegere P, Strikwerda S, de Feyter PJ, Emanuelsson H. Intracoronary pressure and flow velocity from sensor tip guidewires. A new methodological comprehensive approach for the assessment of coronary hemodynamics before and after interventions. Am J Cardiol 1993; 71: 41D-53D.
78. Segal J, Kern MJ, Scott NA, King SB, Doucette JW, Heuser RR, Ofili E, Siegel R. Alterations of phasic coronary artery flow velocity in humans during percutaneous coronary angioplasty. J Am Coll Cardiol 1992; 20: 276-86.
79. Ofili EO, Kern MJ, Labovitz AJ, Vrain J, Segal J, Aguirre FV, Castello R. Analysis of coronary blood flow velocity dynamics in angiographically normal and stenosed arteries before and after endolumen enlargement by angioplasty. J Am Coll Cardiol 1993; 21: 308-16.
80. Gould KL, Lipscomb K, Hamilton GW. Physiologic basis for assessing critical coronary stenosis:

instantaneous flow response and regional distribution during coronary hyperemia as measures of coronary flow reserve. Am J Cardiol 1974; 33: 87-94.
81. Klocke FJ. Measurements of coronary flow reserve: defining pathophysiology versus making decisions about patient care. Circulation 1987; 76: 245-53.
82. McGinn Al, White CW, Wilson RF. Interstudy variability of coronary flow reserve: influence of heart rate, arterial pressure and ventricular preload. Circulation 1990; 81: 1319-30.
83. Rossen JD, Winniford MD. Effect of increases in heart rate and arterial pressure on coronary flow reserve in humans. J Am Coll Cardiol 1993; 21: 343-48.
84. Wilson RF, Marcus ML, White CW. Prediction of the physiologic significance of coronary arterial lesions by quantitative lesion geometry in patients with limited coronary artery disease. Circulation 1987; 75: 723-732.
85. Harrison DG, White CW, Hiratzka LF, Eastham CL, Marcus ML. The value of lesional cross-sectional area determined by quantitative coronary angiography in assessing the physiologic significance of proximal left anterior descending coronary artery stenoses. Circulation 1984; 69: 111-19.
86. Zijlstra F, van Ommeren J, Reiber JHC, Serruys PW. Does the quantitative assessment of coronary artery dimensions predict the physiologic significance of a coronary stenosis? Circulation 1986; 75: 1154-62.
87. Laarman GJ, Serruys PW, Suryapranata H. Inability of coronary flow reserve measurements to assess the efficacy of coronary angioplasty in the first 24 hours in unselected patients. Am Heart J 1991; 122: 631-37.
88. Wilson RF, Johnson MR, Marcus ML, Aylward PEG, Skorton DJ, Collins S, White CW. The effect of coronary angioplasty on coronary blood flow reserve. Circulation 1988; 71: 873-885.
89. Serruys PW, Juilliere Y, Zijlstra F, Beatt KJ, De Feyter PJ, Suryapranata H, van den Brand M, Roelandt J. Coronary blood flow velocity during percutaneous transluminal coronary angioplasty as a guide for assessment of the functional result. Am J Cardiol 1988; 61: 253-259.
90. Kern MJ, Deligonul U, Vandormael M, Labovitz A, Gudipati CV, Gabliani G, Bodet J, Shah Y, Kennedy HL. Impaired coronary vasodilator reserve in the immediate postcoronary angioplasty period: analysis of coronary artery flow velocity indexes and regional cardiac venous efflux. J Am Coll Cardiol 1989; 13: 860-72.
91. Uren NG, Crake T, Lefroy DC, de Silva R, Davies GJ, Maseri A. Delayed recovery of coronary resistive vessel function after coronary angioplasty. J Am Coll Cardiol 1993; 21: 612-21.
92. Sabinston D.C. Jr., Gregg D.E. Effect of cardiac contraction on coronary blood flow. Circulation 1957; 15: 14-23.
93. Krams R, Sipkema P, Westerhof N. Varying elastance concept may explain systolic flow impediment. Am J Physiol 1989; 257: H-1471-H1479.
94. Krams R, Sipkema P, Zegers J, Westerhof N. Contractility is the main determinant of coronary systolic flow impediment. Am J Physiol 1989; 257: H1936-H1944.
95. Folts J.D., Gallagher K., Rowe G.G. Blood flow reductions in stenosed canine coronary arteries: vasospasm or platelet aggregation? Circulation 1982; 65: 248-53.
96. Goto M, Flynn AE, Doucette JW, Kimura A, Hiramatsu O, Yamamoto T, Ogasawara Y, Tsujioka K, Hoffman JIE, Kaijwa F. Effect of intracoronary nitroglycerin administration on phasic pattern and transmural distribution of flow during coronary artery stenosis. Circulation 1992: 85: 2296-2304.
97. Kajiya F., Ogasawara Y., Tsujioka K. Evaluation of human coronary blood flow with an 80 channel 20 MHz pulsed Doppler velocimeter and zero-cross and Fourier transform methods during cardiac surgery. Circulation 1986: 74 (suppl III): III-53-59.
98. Kajiya F., Ogasawara Y., Tsujioka K. Analysis of flow characteristics in post-stenotic regions of the human coronary artery during bypass graft surgery. Circulation 1987; 76: 1092-97.
99. Spaan JAE, Breuls NPW, Laird JD. Diastolic-systolic coronary flow differences are caused by intramyocardial pump action in the anesthetized dog. Circ Res 1981; 49: 584-93.
100. Ofili E.O., Labovitz A.J., Kern M.J. Coronary flow dynamics in normal and diseased arteries. Am J Cardiol 1993; 71: 3D-9D.
101. Donohue TJ, Kern MJ, Aguirre FV, Bach RG, Wolford T, Bell CA. Assessing the hemodynamic

significance of coronary artery stenoses: analysis of translesional pressure-flow velocity relations in patients. J Am Coll Cardiol 1993; 22: 449-58.
102. Mancini G.B.J., Mc Gillem M.J., DeBoe S.F., Gallagher K.P. The diastolic hyperemic flow vs pressure relation: a new index of coronary stenosis severity and flow reserve. Circulation 1989; 80: 941-50.
103. Mancini G.B.J., Cleary R.M., DeBoe S.F., et al. Instantaneous hyperemic flow-vs-pressure slope index. Microsphere validation of an alternative to masures of coronary flow reserve. Circulation 1991; 84: 862-70.
104. Di Mario C, Krams R, de Feyter PJ, Serruys PW. The slope of the instantaneous hyperemic diastolic coronary flow-velocity pressure relation. A new index for the assessment of the physiologic severity of coronary stenoses in humans. In: Reiber JHC, Serruys PW (eds): Quantitative coronary arteriography 1993, Kluwer Academic Press, Dordrecht, 1993 (in press).
105. Gould KL. Phasic pressure-flow and fluid-dynamic analysis. In Gould LD (ed) "Coronary Artery Stenosis", Elsevier, New York-Amsterdam-London, 1991: 40-52.
106. Di Mario C, de Feyter PJ, Slager CJ, de Jaegere P, Roelandt JRTC, Serruys PW. Intracoronary blood flow velocity and transstenotic pressure gradient using sensor-tip pressure and Doppler guidewires. Cath Cardiovasc Diagn 1993; 28: 311-19.
107. Di Mario C, de Feyter PJ, Schuurbiers JHC, de Jaegere P, Gil R, Emanuelsson H, Slager CJ, Serruys PW. Assessment of coronary stenosis severity from simultaneous measurement of transstenotic pressure gradient and flow. A comparison with quantitative coronary angiography. In Serruys PW, Foley D, de Feyter PJ: QCA in clinical practice, Kluwer Academic Publisher, Dordrecht, 1993, pp. 284-306.
108. The GUIDE Trial Investigators. Initial report of the GUIDE trial for intravascular ultrasound imaging in coronary interventions (abstr). J Am Coll Cardiol 1992; 19: 223A.

Part 2

Two-dimensional intracoronary ultrasound

CHAPTER 2

INTRAVASCULAR ULTRASOUND: AN EVOLVING RIVAL FOR QUANTITATIVE CORONARY ANGIOGRAPHY

Carlo Di Mario, M.D., Jos R.T.C. Roelandt, M.D., Ph.D., Peter de Jaegere, M.D., Ph.D., Pim J. de Feyter, M.D., Ph.D., Patrick W. Serruys, M.D., Ph.D.

From the Intracoronary Imaging Laboratory and Cardiac Catheterization Laboratory, Thoraxcenter, Rotterdam, The Netherlands

Reprint from Serruys PW, Foley DP, de Feyter PJ (eds): QCA in clinical practice. Dordrecht, Kluwer Academic Publishers, 1993.

37. Intravascular ultrasound: An evolving rival for quantitative coronary angiography

CARLO DI MARIO, JOS R.T.C. ROELANDT, PETER P. DE JAEGERE, PIM J. DE FEYTER and PATRICK W. SERRUYS

Introduction

Quantitative angiography has been used to validate the accuracy of the measurement obtained with the early intravascular ultrasound catheters [1–3]. In more recent reports [4–12] it was suggested that intravascular ultrasound can be superior to quantitative angiography in the assessment of complex lesions (eccentric stenosis, asymmetric lesions, vascular dissections). In this article, advantages and limitations of the two techniques in the assessment of vascular dimensions are discussed based on the results reported in the literature and of our experience in 72 patients with coronary artery disease.

Previous studies comparing cintravascular ultrasound and angiography for the assessment of vascular dimensions

The results of 11 clinical studies in which quantitative angiography and intravascular ultrasound were compared are summarized in Table 1. Differences in equipment and methods of analysis limit the comparison and interpretation of data. Linear regression analysis is most commonly used as a statistical test in these studies. However, a regression coefficient close to 1 is not sufficient to conclude that the two techniques provide similar quantitative measurements [13]. The mean difference of the paired measurements and indexes of dispersion along the line of identity are more meaningful parameters but are not always reported. With the exception of Tobis [6] the results indicate that there is a good correlation between intravascular ultrasound and angiographic measurements in normal or moderatey diseased segments (Fig. 1). In general larger cross-sectional areas were measured with intravascular ultrasound than with angiography [6, 8, 9, 11, 12]. A major limitation for a precise comparison is that the measurement of the same arterial cross-section is difficult. This is especially true when a major change of vascular cross-sectional area occurs along a very short segment. An angiogram of sufficient quality to be quantitatively analyzed can not be obtained

P.W. Serruys, D.P. Foley and P.J. de Feyter (eds.), Quantitative Coronary Angiography in Clinical Practice, 695–715.

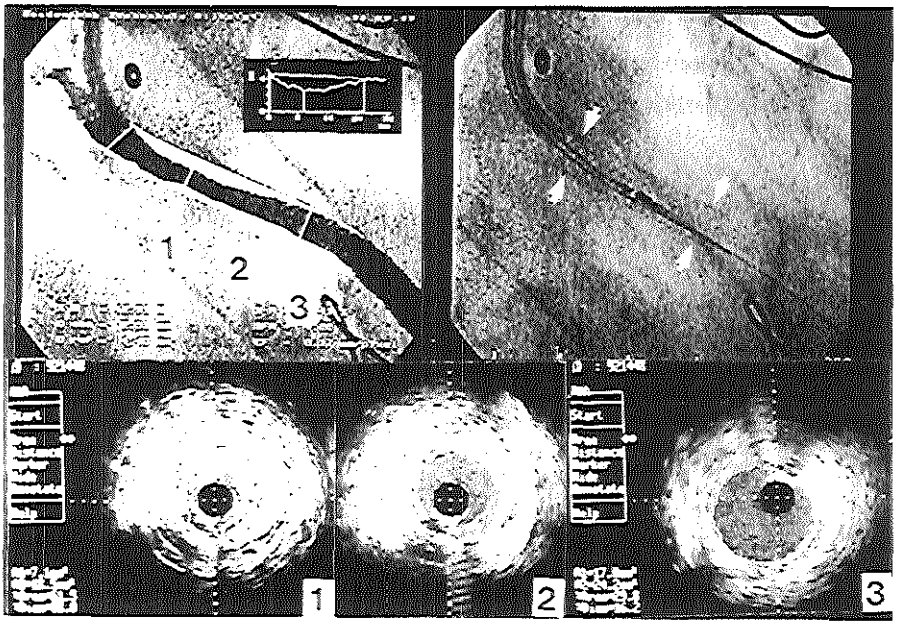

Figure 1. Digital angiogram of a Palmaz-Schatz stent 4 months after implantation in a saphenous vein graft used as aorto-coronary bypass conduit. In the fluoroscopic image the poorly radioopaque stent, indicated with arrows, is examined with a 4.3 rotating mirror ultrasound catheter. The minimal lumen of the moderate (re-)stenosis observed within the stent (position 1) corresponds with ultrasound to a homogeneous area of poorly echogenic intimal thickening. Note that intravascular ultrasound in this case overestimates the minimal luminal cross-sectional area (4.94 mm^2 with angiography vs 7.10 mm^2 with ultrasound). A diffuse area of intimal thickening within the stent is detected also in position 2, a relatively normal segment angiographically. Calibration: 0.5 mm.

during the echographic measurements since the catheter positioned in the stenotic segment partially occludes blood flow and hampers the run-off of contrast medium. In eccentric lesions or lesions treated with balloon angioplasty a poor correlation and a large scatter of the paired measurements was found. After angioplasty, Tobis measured with intravascular ultrasound cross-sectional areas which were up to 50% larger than the corresponding angiographic cross-sectional areas calculated assuming a circular model [6].

Percent diameter and cross sectional area stenosis: Which technique provides the correct measurements?

The use of different reference measurements for the calculation of relative vascular dimensions with quantitative angiography and intravascular ultrasound explains the large discordance of the results obtained with the two

Table 1. Quantitative angiography vs intravascular ultrasound: clinical comparative studies.

Authors	Patients	Examined Arteries	"r"	SEE	Mean Diff.	% Diff
Davidson et al.[2]	21 pts undergoing cardiac cath.	femoroiliac arteries	0.97	1.83		
Sheikh et al.[3]	15 pts undergoing cardiac cath.	femoral arteries	0.95	0.91		
The et al.[4]	8 pts undergoing cardiac cath.	femoroiliac arteries	0.96	0.47		
Bartorelli et al.[5]	8 pts undergoing cardiac cath.	normal common femoral arteries	0.96		0.3 mm	4%
Tobis et al.[6]	27 CAD pts undergoing PTCA	normal sites	0.26		2.1 mm^2	30%
		stenosis post-PTCA	0.18		1.7 mm^2	51%
Nissen et al.[7]	8 normal subjects	normal coronaries	0.92	0.21	−0.05 mm	1%
	43 CAD pts	coron. art. (all les.)	0.86	0.43	0.05 mm−	2%
		eccentric lesions	0.77	0.77	0.06 mm	2%
Werner et al.[8]	14 CAD pts	normal sites	0.86			
		stenosis post-PTCA	0.48			
StGoar et al.[9]	20 cardiac transplant recip.	normal coronaries (angiographially)	0.86	0.07	0.04 mm	12%
Jain et al.[10]	6 CAD patients	SVBG	0.96			
Hodgson et al.[11]	34 CAD patients undergoing PTCA	reference segment	0.77			
		stenosis post-PTCA	0.63			
Haase et al.[12]	20 CAD patients	stenosis post-PTCA	0.53		2.3 mm^2	

CAD: coronary artery disease: PTCA: percutaneous transluminal coronary angioplasty; SVBG: saphenous vein bypass grafts.

techniques (Fig. 2). Reference diameter and cross-sectional area are measured in an angiographically normal segment of the vessel with quantitative angiography. In muscular arteries intravascular ultrasound allows a direct measurement of the area inside the internal elastic lamina, the so called original lumen area which equals to the sum of lumen and plaque area. This area is used as a reference in intravascular ultrasound. Intimal thickening is often present in angiographically normal reference segments (Fig. 3). Furthermore, a compensatory enlargement of the vessel can be present at the stenotic site [14]. These reasons explain why the lumen cross-sectional area used as angiographic reference is smaller than the ultrasonic reference area [15] so that less severe percent diameter and cross-sectional area stenosis will be calculated with quantitative angiography than with intravascular ultrasound. In the diagram of Fig. 2A, in the presence of a 1/2 mm thick intimal lesion in the reference segment, a major difference is observed in percent diameter and cross-sectional area stenosis between quantitative angiography and intravascular ultrasound. The practical occurrence of this phenomenon

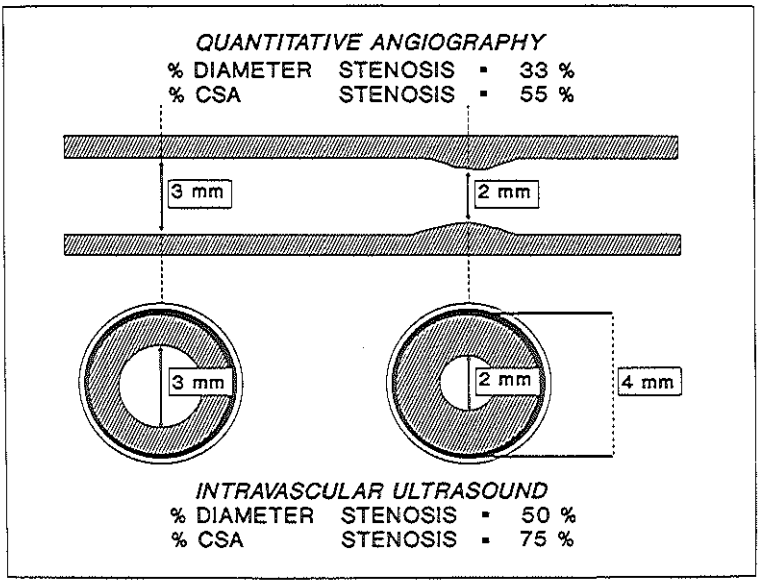

Figure 2. A) Calculation of percent diameter and cross-sectional area stenosis based on intravascular ultrasound and quantitative angiographic measurements. The reference lumen diameter is measured with quantitative angiography in the normal segments of the vessel while intravascular ultrasound directly measures the thickness of the atherosclerotic plaque at the stenosis site. In the presence of compensatory enlargment of the stenotic site or, as in this example, of a diffuse concentric intimal thickening involving also the angiographic reference segment, the intravascular ultrasound reference diameter, traced within the black band representing the muscular media, is larger than the angiographic reference diameter. As a result the angiographically moderate percent stenosis is considered more severe, "significant" according to the normally used criteria (≥50% diameter stenosis and ≥75% cross-sectional area stenosis) with intravascular ultrasound.

is illustrated in the example of Fig. 1B, showing the presence of a large concentric plaque in the angiographic reference segment.

Percent diameter and cross-sectional area stenosis are physiologically important parameters and are major determinants of the pressure drop across a stenosis [16]. However, the results obtained from animal models of acute external constriction of normal vessels [17] can not be simply applied to the percent lumen reduction measured with quantitative angiography. Harrison showed that the stenosis-related impairment of post-occlusion reactive hyperemia can not be predicted based on the coronary angiographic assessment of percent diameter and cross-sectional area stenosis [18]. Awareness of these drawbacks has already contributed to focus the interest in the measurement of absolute rather than relative lumen stenosis in quantitative angiography [19]. Intravascular ultrasound can directly measure plaque area and avoid the use of a reference measurement in a potentially diseased segment of the vessel. However, this reference area does not necessarily reflect the

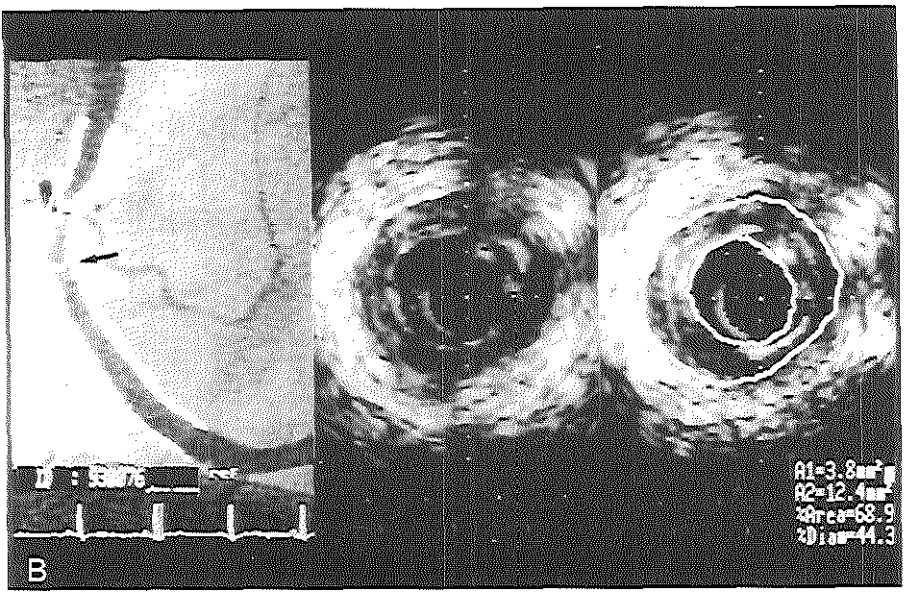

Figure 2. B) Digital angiogram of a right coronary artery with the reference diameter positioned at the site examined with intracoronary ultrasound. Note that in this angiographically normal reference segment intracoronary ultrasound shows the presence of a concentric plaque inducing a 44% diameter stenosis. Calibration: 0.5 mm.

physiologically ideal vascular dimension because of the already mentioned compensatory enlargement. In particular the presence of a crescentic plaque with an outward remodelling of the vessel is likely not to influence the dimension of the vascular lumen. The presence of a reduction of the "ideal" dimension of lumen cross-sectional area is more difficult to be judged in the presence of a diffuse circular ring of intimal thickening (Fig. 3) [20]. Therefore the assessment of the physiologic significance of a vascular stenosis requires different approaches such as the measurement of trans-stenotic velocity increase or of the pressure drop at maximal hyperemia across the stenosis or the calculation of coronary flow reserve based on angiographic or Doppler measurements.

Advantages of intravascular ultrasound

Advantages and disadvantages of intravascular ultrasound vs angiography are summarized in Table 2.

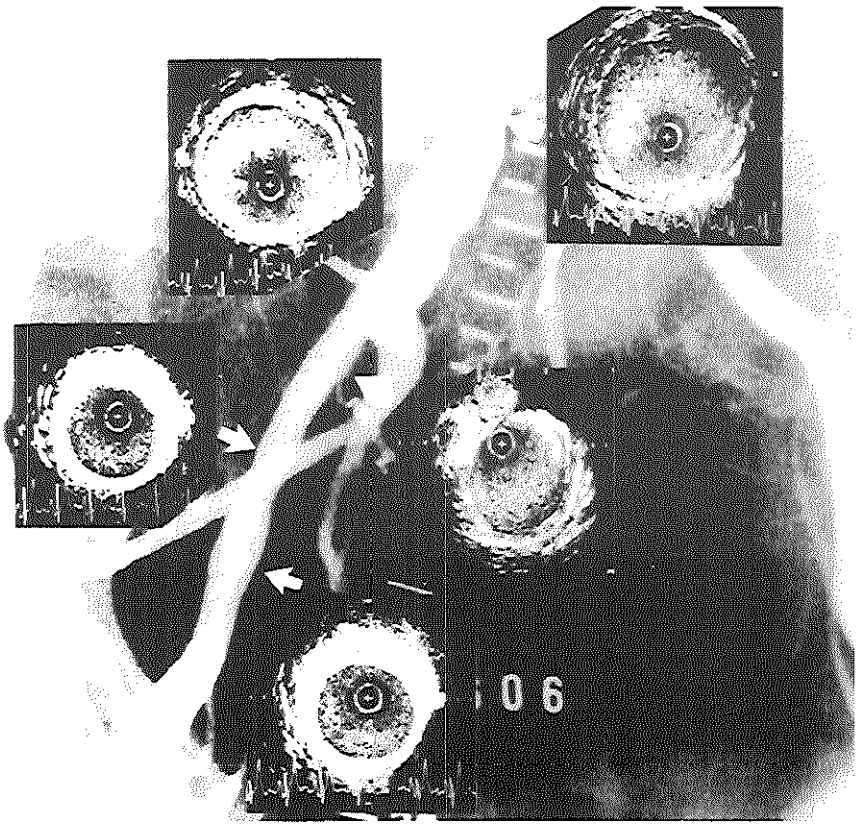

Figure 3. Digital angiogram of a right iliac artery showing multiple edge irregularities and a mild stenosis. The arrowheads indicate the position of the ultrasound transducer during the acquisition of the displayed arterial cross-sectional images. Note the relatively concentric bright ring of intimal thickening in the two upper images, corresponding to an apparently normal circular lumen at angiography. In the following cross-section an eccentric, fibrocalcific plaque is shown in a segment of moderate lumen diameter stenosis with quantitative angiography. Note that the two lowest ultrasonic cross-sections, corresponding to a normal angiographic segment at angiography and showing a semilunar bright eccentric atherosclerotic plaque not protruding inside the regular circular lumen at ultrasound. Calibration: 1 mm.

No calibration is required

For angiography the measurement of a radiopaque structure of known dimension is required for calibration. When the tip of the catheter is used as a scaling device, possible sources of error are off-plane position of the catheter and of the examined vessel, tapering of the catheter at the distal end and discordance between true catheter diameter and the diameter reported by

Table 2. Advantages and limitations of intravascular ultrasound for quantitative assessment of vascular dimensions.

Advantages of intravascular ultrasound	Limitations of intravascular ultrasound
1) No calibration required	1) Introduction of the catheter is necessary
2) Instantaneous and continuous measurements available	2) Potential errors due to catheter malalignment
3) No contrast medium required	3) Artifacts from non-uniform rotation[1], near-field artifacts[2], low sampling rate[2]
4) Independent of lumen eccentricity or complex lumen geometry (dissection)	4) Automatic edge-detection difficult
5) Simultaneous morphometric analysis of wall components	5) Reproducibility of the measurements not yet tested

[1] Single element mechanically rotating systems; [2] multielement synthetic aperture array systems.

the manufacturer [21]. Furthermore, calibration must be repeated for every angiographic view. A potentially more precise but even more cumbersome approach is the geometric correction for beam divergence, based on the measurement of the distances between x-ray source, imaged object and image amplifier (isocenter technique) [22].

The measurement of a distance with ultrasound is based on the wavelength of the ultrasound beam and the velocity of sound in the medium. When the instrument is calibrated for the ultrasound speed in blood (1,560 m/s) a negligible overestimation occurs when saline is injected to replace the more echogenic blood and delineate the intimal contour.

Instantaneous measurements are available

Recently introduced digital angiographic equipment allows the performance of on-line measurements of vascular dimensions. As a consequence, quantitative angiography can be used for guidance and immediate evaluation of interventional procedures. The time required for the analysis, however, is still considerable when compared to the really instantaneous measurement available with ultrasound.

No contrast medium required: A continuous monitoring is possible

Angiography requires the injection of contrast material to delineate the vascular lumen. As a consequence, angiography can not be used for a continuous monitoring of vascular dimension. Other disadvantages of the use of contrast medium are the modification of the intraluminal pressure during the forceful injection of contrast and the vasoactive properties of these agents.

Intravascular ultrasound allows a continuous real-time measurement of vascular dimensions, a great potential advantage for monitoring interventions and assessment of the effects of vasoactive agents on vascular dimensions and dynamics [23].

Morphometric analysis of the vessel wall

Angiography provides only a shadowgram of the vascular lumen, so that the presence of vascular lesions is derived indirectly from irregularities of the luminal contour. The only information on the composition of atherosclerotic plaques concerns the presence of fluoroscopically visible vessel wall calcification. Pathology studies and, more recently, the application of intraoperative and intravascular high-frequency ultrasound have shown that coronary arteries undergo a progressive enlargement in relation with increases in plaque area, so that a reduction of lumen area is delayed until the atherosclerotic lesion occupies more than 40% of the area circumscribed by the internal elastic lamina [14, 24, 25]. These findings explain why angiographically normal arterial segments may show an extensive atherosclerotic involvement at autopsy and upon direct surgical inspection . Several reports have confirmed that intravascular ultrasound detects atherosclerotic changes in angiographically normal segments [4, 9] (Fig. 2). Furthermore, intravascular ultrasound displays the components of the atherosclerotic plaque with a different intensity proportional to their backscatter power [26–28], allowing their qualitative differentiation. In vitro studies have shown that intravascular ultrasound has a high sensitivity and specificity in the detection of intimal lesions and in the differentiation between fibrous, calcific and lipid-containing plaques [29]. Plaque thickness can be measured, especially if the presence of an echographically hypoechoic medial layer facilitates the delineation of plaque contours and if no shadowing or attenuation from plaque components is present [29].

The possibility to provide information on plaque morphology and dimension at the same time makes intravascular ultrasound an ideal technique for the assessment of the mechanism of the different coronary interventions and the modalities of progression/regression of the atherosclerotic plaque. Wall stretching and wall dissection have been reported as the main operative mechanism of balloon angioplasty in both coronary [30] and peripheral arteries [31]. A significant plaque compression (absolute reduction of plaque area) has been more recently reported [32]. Standard methods used in quantitative angiography for the assessment of regression of atherosclerosis are the measurement of mean luminal area and severity of edge irregularities [33] (roughness profile). A long-term follow-up of large cohorts of patients is necessary to show a statistically significant trend towards regression or delayed progression of plaques in peripheral [34, 35] and coronary [36, 37] atherosclerotic disease.

Intravascular ultrasound has the potential of detecting atherosclerotic wall

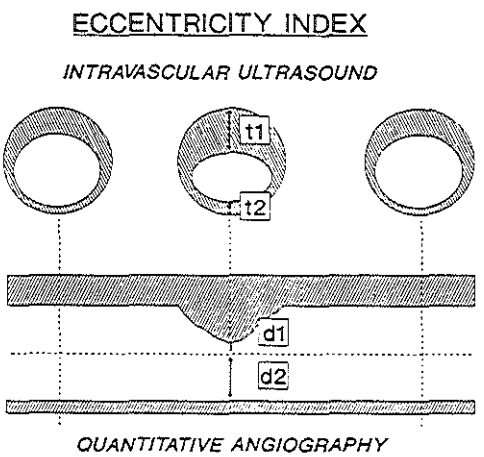

Figure 4. A) Eccentricity index calculated with quantitative angiography and intravascular ultrasound. Intravascular ultrasound allows the direct assessment of the wall thickness (t) so that the eccentricity index is based on the ratio between plaque thickness and thickness of the opposite wall. Quantitative angiography estimates the eccentricity of a plaque from the distance (d) between the center of the lumen and the luminal contours at the site of the stenosis. In this example, however, the presence of a different thickness of the wall also in the angiographically normal segment induces an underestimation of the plaque eccentricity.

disease in the prestenotic phase and allows the measurement of both lumen and plaque area [38]. Dietary and pharmacologic interventions may cause a more rapid and complete regression of the vascular changes in the early "prestenotic" phase of atherosclerosis rather than in the more advanced phases [39]. Animal studies have shown that intravascular ultrasound can detect plaque progression earlier and more accurately than quantitative angiography [40–42]. The possibility to differentiate lipid plaques, potentially amenable to regression after interventions, from fibro-calcific plaques, less likely to respond to such an intervention [43] is of particular interest.

Plaque eccentricity

In most cases, with the use of multiple projections, an angiogram perpendicular to the maximal thickness of the plaque can be obtained. In less than 50% of the cases, however, appropriate orthogonal projections, amenable to quantitative analysis, can be obtained to measure lumen area from its long- and short-axis when an elliptical area is present [44]. Furthermore, angiography determines the eccentricity of a stenosis comparing the proximal and distal segments of the vessel, assumed as "normal" reference segments so that a misinterpretation is possible if the eccentric plaque involves also the reference segments (Fig. 4).

Intravascular ultrasound detects the eccentricity of the lesion from a direct

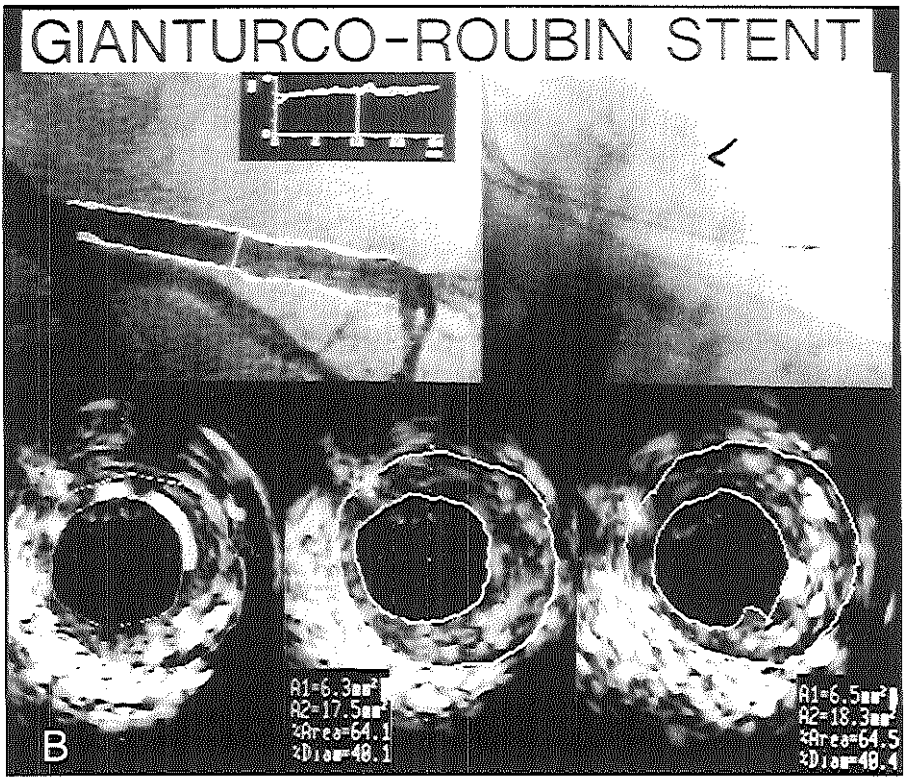

Figure 4. B) Digital angiogram showing a regular lumen after implantation of a Gianturco Roubin stent in a proximal left anterior descending coronary artery. The stent is barely visible in the fluoroscopic image obtained during the ultrasound examination but the circumferentially arranged metallic wires of the stent show a high echogenicity with ultrasound. Note that an eccentric residual plaque is shown despite the regular circular lumen (echographic images on the right), with a small protrusion of the plaque tissue through the wires of the stent. Calibration: 0.5 mm.

measurement of the maximal and minimal thickness of the plaque. The eccentricity index calculated with intravascular ultrasound is independent from the characteristics of the contiguous segments [45]. The advantage of the direct visualization of eccentric plaques is obvious in the guidance of a selective removal of plaque, avoiding a potentially dangerous treatment in areas of thin, normal wall [46].

Complex lumen geometry (wall dissection)

Pathology studies have shown that splitting of the vessel wall is extremely frequent after balloon angioplasty and is one of the major mechanisms of

effective lumen enlargement [47, 48]. Only large dissections are angiographically evident after balloon angioplasty. Several reports [6, 30–32, 49–51] have confirmed that intravascular ultrasound is more sensitive than angiography in the detection of plaque rupture. The absence of echographically evident plaque rupture has been recently reported to increase the risk of restenosis [52]. The quantitative measurement of residual stenosis early after balloon angioplasty is a poor indicator of the functional result of the procedure as assessed by coronary flow reserve [53] and persistence of scintigraphic and electrocardiographic signs of reversible myocardial ischemia. Several reasons may explain this finding but in some cases the comparison between echographic and quantitative angiographic measurements suggests that an overestimation of the lumen really available for blood passage may occur when a geometric technique (edge-detection) is used (Fig. 5). Densitometric measurements have been suggested in order to overcome the limitations of edge-detection in lesions of complex geometry (including stenosis post-angioplasty and eccentric lesions) [54]. Densitometry, however, requires a homogeneous filling of the lumen with contrast and a perfect orthogonality of the x-ray beam to the vessel lumen, is highly dependent on the radiographic setting and modalities of film processing and cannot directly provide absolute measurements [55].

Limitations of intravascular ultrasound (Table 2)

Necessity of catheter insertion

Intravascular ultrasound requires the insertion of the echo-catheter along the entire vascular segments to be studied. Instrumentation of a coronary vessel is the current practice for all the interventional techniques. However, especially in the examination of the coronary arteries, the insertion of the echo-catheter increases the complexity and duration of the procedure and carries out a potential risk of complications. Recent improvements in catheter flexibility and miniaturization allow the examination of the proximal and middle coronary arteries in most patients. A possible limitation, however, concerns the examination of severe coronary stenosis before interventions, one of the most interesting potential applications of intravascular ultrasound. A quantitative angiographic study of large cohorts of candidates to balloon angioplasty [56] has shown that the measured minimal luminal diameter before balloon dilatation (1.02 ± 0.37 mm) is similar to the diameter of the recently introduced second generation of catheters (from 3.5 to 4.3 French, equal to 1.15–1.4 mm), Fig. 6.

The intravascular ultrasound examination after successful therapeutic interventions is facilitated by the increased lumen diameter. However, recrossing large, unstable dissection flaps carries a potential risk of acute occlusion. Furthermore, a correct assessment of the real morphology of a complex

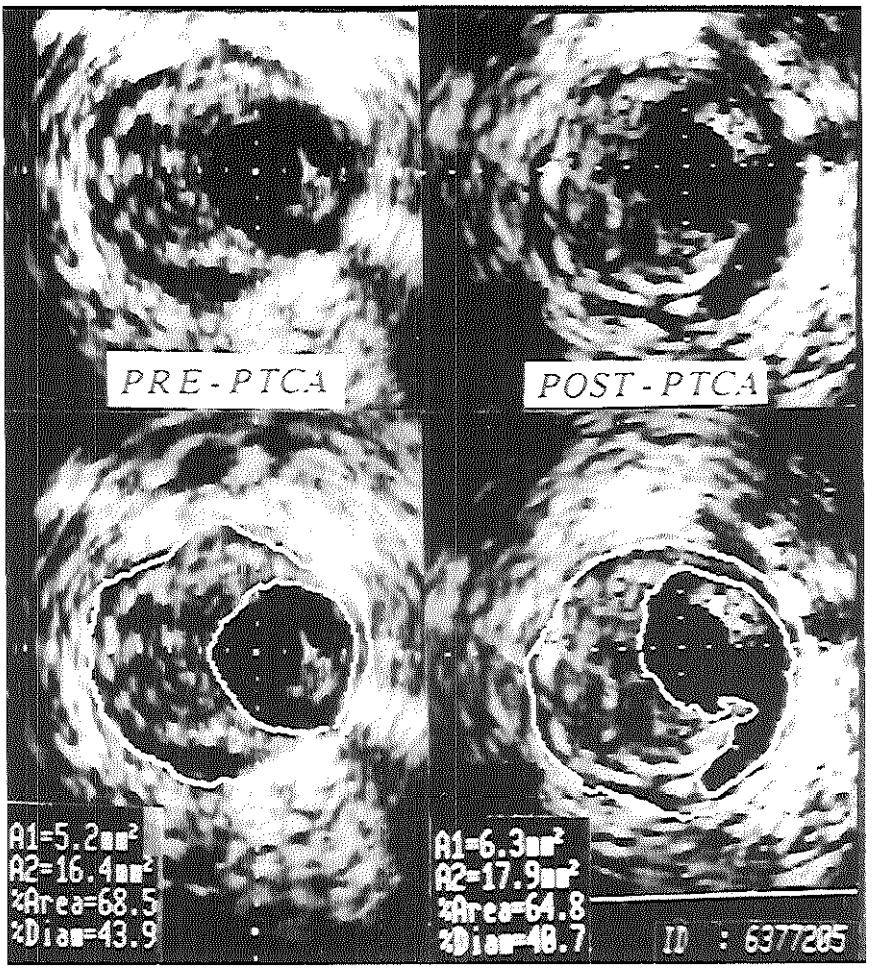

Figure 5. Intravascular ultrasound cross-sections of a severe stenosis in a left circumflex artery before and after balloon dilatation. Note that the eccentric plaque has been dissected at the site of its insertion on the normal wall. The complex lumen after angioplasty can not be correctly measured in any angiographic projection. Note that in this case the increase in lumen area seems to be largely dependent from the induction of a wall dissection and the stretching of the arterial wall, while no significant changes were observed in the plaque dimensions. Calibration: 0.5 mm.

spiral dissection and the consequent impairment to blood passage is difficult because it would require a three-dimensional reconstruction of the ultrasonic cross-sections [57–61] and because the communication between true and false lumen is modified by the physical presence of the catheter. Proximal injection of saline or agitated contrast can help to delineate the lumen and

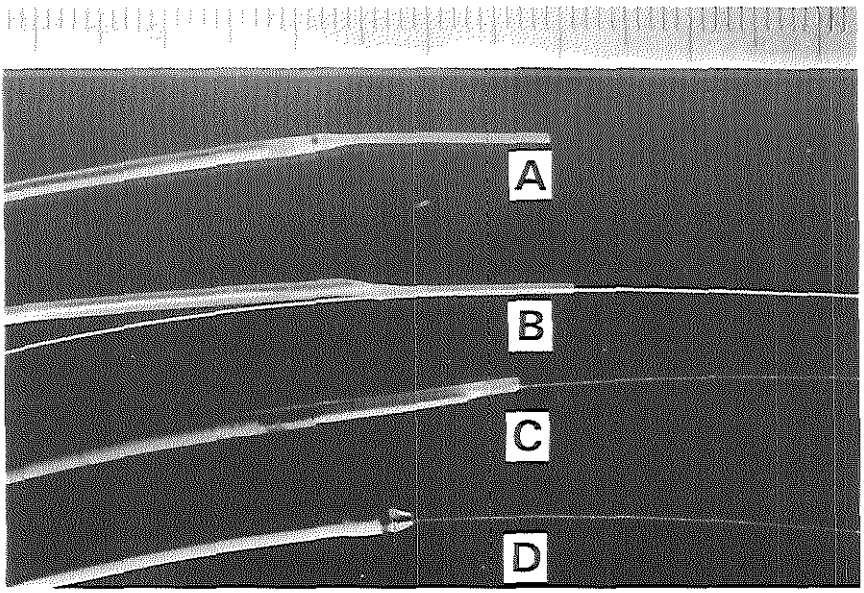

Figure 6. The distal end of four intravascular ultrasound coronary catheters is shown. A) Single element rotating mirror (arrow) catheter characterized by a completely independent external sheath and inner catheter: this system has the potential for an extreme miniaturization (3.5 French catheters are in clinical use) but has the limitation that the insertion of the guidewire requires the removal of the ultrasound catheter; B) rotating element 4.1 French 30 MHz ultrasound catheter, characterized by a very small Monorail lumen at the distal end (DuMed, Rotterdam, The Netherlands); C) Single element rotating mirror intravascular ultrasound catheter (Cvis, Sunnyvale, CA, USA) allowing the continuous use of a guidewire using a Monorail technique (diameter: 4.3 French); D) Multielement dynamic array catheter (a 5 French catheter is shown but 3.5 French catheter and combined balloon/ultrasound catheters are available, Endosonics, Costa Mesa, CA, USA); 64 elements are aligned circumferentially around the tip so that a central lumen is available for catheter insertion and the shaft can be very flexible because no driving cable is required: the small dimension of the elements, however, is responsible for a lower image quality in comparison with the mechanical scanners.

detect the presence of stagnant blood flow but an effective injection through the proximal guiding catheter is not always possible with the relatively large ultrasound catheters in place.

An example of another possible limitation of intravascular ultrasound in the presence of wall dissection is shown in Fig. 7 in which drop-outs occur in segments of dissected wall which are explored with an unfavourable angle of incidence of the ultrasound beam [62]. Furthermore, the underlying structures cannot be imaged. In our experience, these complex artifacts are more frequent in peripheral than in coronary arteries, because in these latter small vessels the physical presence of the ultrasound catheter modifies the orientation of the dissected flap.

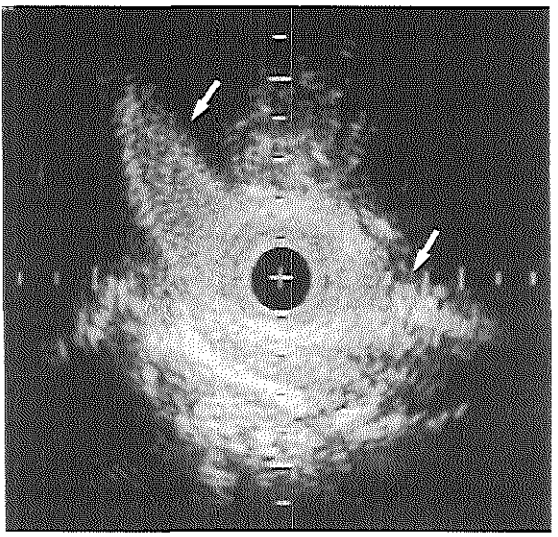

Figure 7. In vivo intravascular ultrasound image of a human femoral artery after balloon dilatation. The echogenic blood clearly delineates the vascular lumen. An almost complete drop-out, however, occurs in the segments in which the vessel wall and the underlying perivascular structures (arrows) are oriented at a narrow angle with the direction of the ultrasound beam. This sudden disappearence of the vessel wall can be clearly distinguished from drop-outs due to attenuation from blood, which would lead to a more progressive reduction in echo-intensity and would mainly affect the wall opposite to the position of the catheter. Courtesy of Dr. Pieterman/Dr. Gussenhoven, Radiology Department, Dijkzigt Academic Hospital, Rotterdam. Calibration = 1 mm.

The combination of intravascular ultrasound imaging and balloon angioplasty or alternative debulking techniques in the same catheter can make the evaluation with intravascular ultrasound before and after interventions easier and more practical and can allow continuous monitoring and guidance during the procedure. At present, however, only prototypes of catheters for directional atherectomy mounting ultrasound crystals are in the phase of preliminary clinical evaluation and in the already available echo-balloon catheters the transducer is mounted proximal to the balloon [63, 64]. This configuration maintains a low profile of the balloon and avoids the artifacts induced by the balloon membrane but precludes the possibility of a continuous assessment before, during and immediately after balloon dilatation.

Catheter malalignment

A central position of the catheter in the vessel lumen is not frequent in intravascular ultrasound. With a simple eccentricity of the catheter position, the echographic cross-section is still perpendicular to the long-axis of the

vessel so that no change in the measured area is expected. When the catheter is not only eccentric but also non-parallel to the long-axis of the vessel the vascular lumen is distorted, with an angle-dependent overestimation of the vascular lumen. In a bending artery, however, despite the centering effect of an over-the-wire system, the ultrasound catheter can frequently assume a non-parallel orientation with the long-axis of the vessel. Fortunately, in coronary arteries the small size of these vessels relative to the catheter diameter limits the practical relevance of this problem [9].

Non-uniform rotation, near field artifact, inadequate sampling rate

With mechanically rotating catheters, a 1:1 rotation of the ultrasound element (or mirror) can be impossible if the catheter is inserted in very tortuous vessels, resulting in a variable distortion of the ultrasound image.

In the multielement systems these artifacts are not present. A limitation of these systems, however, is that the near-field artifact is partially obscuring the structures close to the catheter.

Artifacts can also result from the systo-diastolic changes of vascular dimensions or of the position of the catheter inside the vessel throughout the cardiac cycle if a sufficiently high sampling rate is not obtained.

Application of automatic measurements

Sophisticated techniques of edge-detection or videodensitometry have been developed for quantitative angiography [65]. The difference in brightness between the radiographic contrast filling the vascular lumen and the background facilitates the application of the proposed algorithms for computer-assisted automatic contour detection.

In intravascular ultrasound, on the contrary, the relatively similar echoreflectivity of blood in comparison with the underlying vessel wall is of potential obstacle to fully automatic measurements of lumen area. The frequently necessary manual corrections may increase the subjectivity of the results [66]. In our Center a fully automatic technique, based on the measurement of the vessel wall displacement from a semiautomatic defined template image, is successfully used to measure the systo-diastolic changes of vascular dimensions [67].

Reproducibility of the measurements

Changes in vascular tone, variability of repeated measurements, modifications of radiographic projections and setting, cardiac and respiratory movements influence short- and long-term reproducibility of the angiographic measurements, making the assessment of the development of real changes in vascular dimensions more difficult. Intravascular ultrasound is not limited by some of these factors. A crucial element for reproducibility of repeated

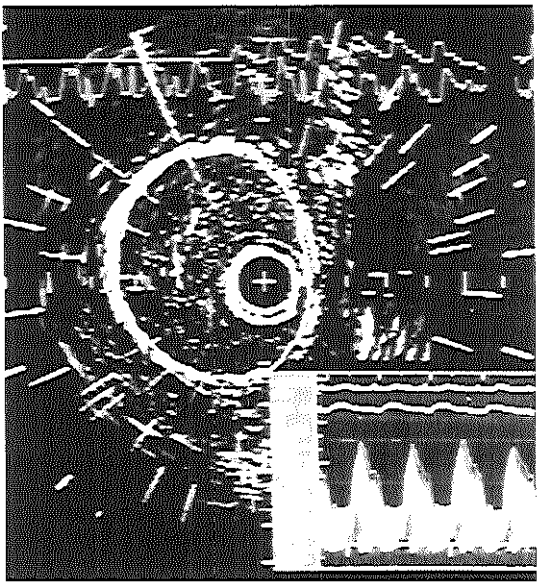

Figure 8. Intravascular ultrasound cross-section of a proximal normal left circumflex artery 6 months after cardiac transplantation. The simultaneous recording in the same position of flow velocity with a Doppler guidewire (Cardiometrics, CA, USA) allows the calculation of the instantaneous absolute flow. Calibrations: intravascular ultrasound = 1 mm; Doppler = 120 cm/s.

measurements, however, is a position of the catheter exactly at the same site in the vessel, a trivial requirement which is practically very difficult to satisfy.

No assessment of blood flow

Various angiographic techniques have been described which use the contrast medium as a marker of flow and calculate relative changes of blood flow based on contrast appearance time and/or on changes in the density of the myocardium [68–70]. This principle is not applicable with the current intravascular ultrasound imaging catheters. An alternative ultrasound-based technique is the measurement of the Doppler shift induced by the motion of the red blood cells to directly calculate blood flow velocity. Prototypes of combined imaging-Doppler catheters have been described [71, 72] and Doppler guidewires which can integrate the ultrasound imaging catheters are in current clinical use [73–75] (Fig. 8).

Conclusions

Intravascular ultrasound can accurately assess luminal dimensions and has potential advantages on quantitative arteriography in the presence of eccentric lesions and lumens of complex geometry. The application of this technique, however, increases duration, risk, complexity and cost of a conventional diagnostic or interventional procedure based on a purely angiographic quantitative assessment. In clinical practice, therefore, it seems unlikely that quantitative arteriography can be replaced by intravascular ultrasound as a routine technique of measurement of luminal dimensions.

Intravascular ultrasound has a potential role as a research tool for the assessment of vessel dynamics and effects of pharmacologic interventions. The information concerning characteristics and composition of the atherosclerotic plaque is not available with angiography and makes intravascular ultrasound potentially more suitable than angiography for the follow-up of interventions aimed at the regression of atherosclerotic lesions. Improvements in catheter technology can make quantitative intravascular ultrasound a valuable tool for the correct planning and guidance of interventional procedures.

Acknowledgments

The authors wish to thank the Medical and Technical Staff of the Cardiac Catheterization Laboratory, University Hospital Dijkzigt, Rotterdam for their contribution to the acquisition of the ultrasonic and angiographic images.

References

1. Nissen SE, Grines CL, Gurley JC, et al. Application of a new phased-array ultrasound imaging catheter in the assessment of vascular dimensions. In vivo comparison to cineangiography. Circulation 1989; 81: 660–666.
2. Davidson CJ, Sheikh KH, Harrison KJ, et al. Intravascular ultrasonography versus digital subtraction angiography: a human in vivo comparison of vessel size and morphology. J Am Coll Cardiol 1990; 16: 633–636.
3. Sheikh KH, Davidson CJ, Kisslo KB, et al. Comparison of intravascular ultrasound, external ultrasound and digital angiography for evaluation of peripheral artery dimensions and morphology. Am J Cardiol 1991; 67: 817–822.
4. The SKH, Gussenhoven EJ, Serruys PW, et al. Quantitative angiography vs intravascular ultrasound for the assessment of vascular dimensions and systo-diastolic changes. J Interven Cardiol 1992; 16: 143–147.
5. Bartorelli AL, Neville RF, Keren G, et al. In vivo and in vitro intravascular ultrasound imaging. Eur Heart J 1992; 13: 102–108.
6. Tobis JM, Mallery J, Mahon D, et al. Intravascular ultrasound imaging of human coronary arteries in vivo. Circulation 1991; 83: 913–926.

7. Nissen SE, Gurley JC, Grines CL, et al. Intravascular ultrasound assessment of lumen size and wall morphology in normal subjects and patients with coronary artery disease. Circulation 1991; 84: 1087–1099.
8. Werner GS, Sold G, Buchwald A, et al. Intravascular ultrasound imaging of human coronary arteries after percutaneous transluminal angioplasty: morphologic and quantitative assessment. Am Heart J 1991; 122: 212–220.
9. StGoar FG, Pinto FJ, Alderman EL, et al. Intravascular ultrasound of angiographically normal coronary arteries: an in-vivo comparison with quantitative angiography. J Am Coll Cardiol 1991; 18: 952–958.
10. Jain SP, Roubin GS, Nanda NC, et al. Intravascular ultrasound imaging of saphenous vein graft stenosis. Am J Cardiol 1992; 69: 133–136.
11. Hodgson McJB, Reddy KG, Suneja R, Nair RN, Lesnefsky EJ, Sheehan HM. Intracoronary ultrasound imaging: correlation of plaque morphology with angiography, clinical syndrome and procedural results in patients undergoing coronary angioplasty. J Am Coll Cardiol 1993; 21: 35–44.
12. Haase J, Ozaki Y, Di Mario C et al. Can intravascular ultrasound correctly assess the luminal dimensions of coronary artery lesions? A comparison with quantitative angiography. Eur Heart J, submitted for publication.
13. Bland JM, Altman DG. Statistical methods for assessing agreement between two methods of clinical measurement. Lancet 1987; Feb 8: 307–310.
14. Stiel GM, Schofer J, Donath K, et al. Impact of compensatory enlargement of atherosclerotic coronary arteries on angiographic assessment of coronary artery disease. Circulation 1989; 80: 1603–1609.
15. Davidson CJ, Tenaglia AN, Buller CE, et al. Coronary angiography underestimates postinterventional lesion stenosis and reference segment (abstr). Circulation 1991; 84: II-437.
16. Young DF, Tsai FY. Flow characteristics in models of arterial stenosis. J Biomech 1973; 6: 395–406.
17. Gould KL. Pressure-flow characteristics of coronary stenoses in unsedated dogs at rest and during coronary vasodilatation. Circ Res 1978; 43: 242–251.
18. Harrison DG, White CW, Marcus ML, et al. The value of lesion cross-sectional area determined by quantitative coronary angiography in assessing the physiologic significance of proximal left anterior descending stenoses. Circulation 1984; 69: 1111–1119.
19. Reiber JHC, Serruys PW. Quantitative coronary angiography. In Marcus ML, Schelbert T, Skorton WA, et al (eds): Cardiac Imaging. A companion to Braunwald's Heart Disease. Philadelphia, W.B. Saunders, 1991: 213–280.
20. Nissen SE, Gurley JC, Booth DC, et al. Mechanisms for false negative coronary angiography: insights from intravascular ultrasound imaging (abstr). J Am Coll Cardiol 1992; 19: 140A.
21. Reiber JHC, Kooijman CJ, Serruys PW, et al. Assessment of dimensions and image quality of coronary contrast catheters from cineangiograms. Cath Cardiovasc Diag 1985; 11: 521–531.
22. Gould LK. Quantitative coronary arteriography. In: Gould LK (editor) Coronary artery stenosis. New York, Amsterdam, London: Elsevier, 1991: 93–107.
23. Wilson R, Di Mario C, Roelandt J, et al. Changes in large arteries compliance measured with intravascular ultrasound (abstr). J Am Coll Cardiol 1992; 19: 140A.
24. McPherson DD, Hiratzka LF, Sirna SJ, et al. Coronary artery remodeling studied by high frequency epicardial echocardiography: an early compensatory mechanism in patients with obstructive coronary atherosclerosis. J Am Coll Cardiol 1991; 17: 79–86.
25. Nissen SE, Booth DC, Gurley JC, et al. Coronary remodelling in coronary artery disease: intravascular ultrasound evidence of vessel expansion (abstr). Circulation 1991; 84: II-437.
26. Gussenhoven EJ, Essed CE, Roelandt J, et al. Arterial wall characteristics determined by intravascular ultrasound imaging: an in vitro study. J Am Coll Cardiol 1989; 14: 947–952.
27. Nishimura RC, Edwards WD, Warnes CA, et al. Intravascular ultrasound imaging: in vitro validation and pathologic correlation. J Am Coll Cardiol 1990; 16, 145–154.

28. Gussenhoven WJ, Frietman P, The SHK et al.. Assessment of medial thinning in atherosclerosis with intravascular ultrasound. Am J Cardiol 1992; 68: 625–632.
29. Di Mario C, Serruys PW, Roelandt JRTC, et al. Detection and characterization of vascular lesions with intravascular ultrasound. J Am Soc Echocardiogr 1992; 5: 135–146.
30. Tenaglia AN, Buller CE, Kisslo KB, Stack RS, Davidson CJ. Mechanisms of balloon angioplasty and directional coronary atherectomy as assessed by intracoronary ultrasound. J Am Coll Cardiol 1992; 20: 685–691.
31. The SHK, Gussenhoven EJ, Zhong Y et al. Effect of balloon angioplasty on femoral artery evaluated with intravascular ultrasound imaging. Circulation 1992; 86: 483–493.
32. Losordo DW, Rosenfield K, Pieczek A, Baker K, Harding M, Isner JM. How does angioplasty work? Serial analysis of human iliac arteries using intravascular ultrasound. Circulation 1992; 86: 1845–1858.
33. de Feyter PJ, Serruys PW, Davies MJ, et al. Quantitative coronary angiography to measure progression and regression of coronary atherosclerosis: value, limitations and implications for clinical trials. Circulation 1991; 84: 412–423.
34. Blackenhorn DH, Azen SP, Crawford DW, et al. Effects of colestipol-niacin therapy on human femoral atherosclerosis. Circulation 1990; 83: 438–447.
35. Olsson AG, Ruhn G, Erikson U. The effect of serum lipid regulation on the development of femoral atherosclerosis in hyperlipidaemia: a non-randomized controlled study. J Int Med 1990; 227: 381–390.
36. Greg Brown B, Albers JJ, Fisher LD, et al. Regression of coronary artery disease as a result of intensive lipid-lowering therapy in men with high levels of apolipoprotein B. N Engl J Med 1980; 323: 1289–1298.
37. Kane JP, Malloy MJ, Ports TA, et al. Regression of coronary atherosclerosis during treatment of familial hypercholesterolemia with combined drug regimens. J Am Med Assoc 1990; 3007–3012.
38. Pinto FJ, StGoar FG, Popp RL, et al. In vivo correlation of intimal proliferation by intracoronary ultrasound with angiographic evidence of coronary artery progression (abstr). J Am Coll Cardiol 1991; 19: 300A.
39. Armstrong ML, Heistad DD, Marcus ML, et al. Structural and hemodynamic responses of peripheral arteries of macaque monkeys to atherogenic diet. Atherosclerosis 1985; 5: 336–346.
40. Lassetter JE, Krall RC, Moddrelle DS, et al. Intravascular ultrasound detects plaque progression earlier and more accurately than quantitative angiography (abstr). J Am Coll Cardiol 1991; 17: 156A.
41. Lassetter JE, Krall RC, Moddrelle DS, Jenkins RD. Morphologic changes of the arterial wall during regression of experimental atherosclerosis (abstr). Circulation 1992; 86: I-518.
42. Gupta M, Connoly AJ, Zhu BQ et al. Quantitative analysis of progression and regression of atherosclerosis by intravascular ultrasound: validation in a rabbit model (abstr). Circulation 1992; 86: I-518.
43. Blackenhorn DH, Krausch DM. Reversal of atherosclerosis and sclerosis: the two components of atherosclerosis. Circulation 1989; 79: 1–7.
44. Lesperance J, Hudon G, White GW, et al. Comparison by quantitative angiographic assessment of coronary stenoses of one view showing the severest narrowing to two orthogonal views. Am J Cardiol 1989; 64: 462–465.
45. Honye J, Ashit J, Tobis JM, et al. Atherosclerotic plaque eccentricity: a comparison of angiography and intravascular ultrasound imaging (abstr). Circulation 1991; 64: II-701.
46. Kimura BJ, Fitzgerald PJ, Sudhir K, Amidon TM, Strunk BL, Yock PG. Guidance of directional coronary atherectomy by intracoronary ultrasound imaging. Am Heart J 1992; 124: 1385–1369.
47. Potkin BN, Roberts WC. Effects of percutaneous transluminal angioplasty on atherosclerotic plaque and relation of plaque composition and arterial size to outcome. Am J Cardiol 1988; 62: 41–50.

48. Waller BF. Coronary balloon artery dissections: "The Good, the Bad and the Ugly". J Am Coll Cardiol 1992; 20: 701–706.
49. Tenaglia AN, Buller CE, Kisslo KB, Phillips HR, Stack RS. Intracoronary ultrasound predictors of adverse outcomes after coronary artery interventions. J Am Coll Cardiol 1992; 20: 1385–1390.
50. Fitzgerald PJ, Ports TA, Yock PG. Contribution of localized calcium deposits to dissection after angioplasty. An observational study using intravascular ultrasound. Circulation 1992; 86: 64–70.
51. Potkin BN, Keren G, Mintz GS et al. Arterial response to balloon coronary angioplasty: an intravascular ultrasound study. J Am Coll Cardiol 1992; 20: 942–951.
52. Honye J, Mahon DJ, Tobis JM, et al. Morphological effects of coronary balloon angioplasty in vivo assessed by intravascular ultrasound imaging. Circulation 1992; 85: 1012–1025.
53. Wilson RF, Johnson MR, Marcus ML, et al. The effect of coronary angioplasty on coronary flow reserve. Circulation 1988; 77: 873–885.
54. Serruys PW, Reiber JHC, Wijins W, et al. Assessment of percutaneous transluminal coronary angioplasty by quantitative coronary arteriography: diameter vs densitometric area measurement. Am J Cardiol 1984; 54: 482–488.
55. Whiting JS, Pfaff JM, Eigler NL. Advantages and limitations of videodensitometry in quantitative coronary angiography. In: Reiber JHC, Serruys PW (editors) Quantitative Coronary Arteriography, Dordrecht, Kluwer Academic Publishers 1991: 43–54.
56. Serruys PW, Rutsch W, Heyndrickx G, et al. Prevention of restenosis after percutaneous transluminal coronary angioplasty with thromboxane A2-receptor blockade: a randomized, double-blind, placebo-controlled study. Circulation 1991; 84: 1568–1580.
57. Rosenfield K, Losordo DW, Isner JM, et al. Three-dimensional reconstruction of human coronary and peripheral arteries from images recorded during two-dimensional intravascular ultrasound examination. Circulation 1991; 84: 1938–1956.
58. Di Mario C, Wenguang L, Linker DT, PJ de Feyter, Bom N, Serruys PW. Three-dimensional intracoronary ultrasound. Goals and practical problems. Int J Cardiac Imaging 1993; 61–73.
59. Rosenfield K, Kaufman J, Pieczek A, Langevin RE, Razvi S, Isner JM. Real-time three-dimensional reconstruction of intravascular ultrasound images of iliac arteries. Am J Cardiol 1992; 70: 412–415.
60. Coy KM, Park JC, Fishbein MC et al. In vitro validation of three-dimensional intravascular ultrasound for the evaluation of arterial injury after balloon angioplasty. J Am Coll Cardiol 1992; 20: 692–700.
61. Cavaye DM, White RA, Lerman RD et al. Usefulness of intravascular ultrasound imaging for detecting experimentally induced aortic dissection in dogs and for determining the effectiveness of endoluminal stenting. Am J Cardiol 1992; 69: 705–707.
62. Di Mario C, de Kroon M, Roelandt JRTC, et al. Angle-dependency in intravascular ultrasound (abstr). Circulation 1991; 64: II-541.
63. Isner JM, Rosenfield K, Losordo DW, et al. Combination balloon-ultrasound imaging catheter for percutaneous transluminal angioplasty. Circulation 1991; 84, 739–754.
64. Hodgson J, Cacchione J, Reddy K, et al. Combined coronary angioplasty balloon and ultrasound catheter: preliminary findings (abstr). Eur Heart J 1991; 12, 381.
65. Reiber JHC. An overview of coronary quantitation techniques as of 1989. In Reiber JHC, Serruys PW (editors) Quantitative Coronary Arteriography, Dordrecht, Kluver Academic Publishers, 1991: 55–132.
66. Wenguang L, Gussenhoven WJ, Di Mario C, et al. Validation of quantitative analysis of intravascular ultrasound images. Int J Cardiac Imag 1991; 6: 247–254.
67. Wenguang L, Gussenhoven EJ, Bom N, et al. Frame-to-frame assessment of arterial distensibility using a computerized semiautomatic program. Proceedings of the XII "Congress on Computers in Cardiology", 1991, Venice, in press.
68. Vogel R, LeFree M, Bates E, et al. Application of digital techniques to selective coronary

arteriography: use of myocardial appearence time to measure coronary flow reserve. Am Heart J 1984; 107: 153–164.
69. Zijlstra F, Reiber JHC, Serruys PW, et al. Which cineangiographically assessed anatomic variable correlates best with functional measurements of stenosis severity? A comparison of quantitative analysis of the coronary angiogram with measured coronary flow reserve and exercise/redistribution Thallium 201 scintigraphy. J Am Coll Cardiol 1988; 12: 686–691.
70. Pijls NHJ, van Leeuwen K, Uijen GJH, et al. The concept of maximal flow ratio for immediate evaluation of percutaneous transluminal coronary angioplasty. Circulation 1991; 83: 854–865.
71. Graynburn PA, Willard JE, Donald RH, et al. Measurement of coronary flow using high-frequency intravascular ultrasound imaging and pulsed Doppler velocimetry (abstr). J Am Coll Cardiol 1991; 6, 234A.
72. Linker DT, Torp H, Angelsen AJ, et al. Instantaneous arterial flow estimated with an ultrasound imaging and Doppler catheter (abstr). Circulation 1989; 80, II-580.
73. Doucette JW, Corl PD, Payne HM, et al. Validation of a Doppler guide-wire for intravascular measurement of coronary artery flow velocity. Circulation 1992; 85: 1899–1911.
74. Kaufman J, Rosenfield K, Isner J, et al. Combined intravascular ultrasound and intravascular Doppler wire provide complementary anatomic and physiologic imaging during percutaneous revascularization (abstr). J Am Coll Cardiol 1992; 19: 293A.
75. Sudhir K, Macgregor JS, Yock PG, et al. Simultaneous intravascular two-dimensional and Doppler ultrasound. a new technique for in vivo assessment of coronary flow and vascular dynamics (abstr). J Am Coll Cardiol 1992; 19: 140A.

CHAPTER 3

THREE-DIMENSIONAL INTRACORONARY ULTRASOUND. GOALS AND PRACTICAL PROBLEMS

Carlo Di Mario, M.D., Li Wenguang, M.Sc., David T. Linker, M.D., Pim J. de Feyter, M.D., Ph.D., Nicolaas Bom, Ph.D., Patrick W. Serruys, M.D., Ph.D., Jos R.T.C. Roelandt, M.D., Ph.D.

From the Intracoronary Imaging Laboratory and Cardiac Catheterization Laboratory, Thoraxcenter, Rotterdam, The Netherlands

Reprinted from: Int J Cardiac Imaging, 1993.

THREE-DIMENSIONAL INTRACORONARY ULTRASOUND. GOALS AND PRACTICAL PROBLEMS.

Carlo Di Mario, Li Wenguang, David T. Linker, Pim J. de Feyter, Nicolaas Bom, Patrick W. Serruys, Jos R.T.C. Roelandt

Introduction

In cardiovascular imaging three-dimensional reconstruction has been applied to well established techniques such as computed tomography, nuclear magnetic resonance, transthoracic and transesophageal echocardiography and digital angiography [1]. Many reasons explain why these sophisticated image processing techniques were so rapidly applied to intravascular ultrasound, a technique which is still under development [2,3]. Consecutive ultrasonic cross-sections may show large differences in luminal area and in dimension and composition of the atherosclerotic plaque (Figure 1).

To obtain a better understanding of the spatial distribution of the wall changes one must be able to mentally reconstruct all these two-dimensional images into the three-dimensional equivalent of the arterial segment. Angiography gives no direct information concerning the presence and characteristics of wall pathology but it has the advantage to immediately display the relation of adjacent segments, thus providing essential information for road-mapping. Three-dimensional reconstruction of tomographic intravascular ultrasound images has the potential for a rapid conceptualization of the spatial relations of these complex structures, thus providing a complete assessment of lumen and wall changes.
In this article we describe the different techniques proposed for three-dimensional reconstruction and review the initial results obtained in the quantification of lumen/wall changes and in the assessment of vascular interventions.

J. Roelandt et al. (eds.), Intravascular Ultrasound, 63–77.

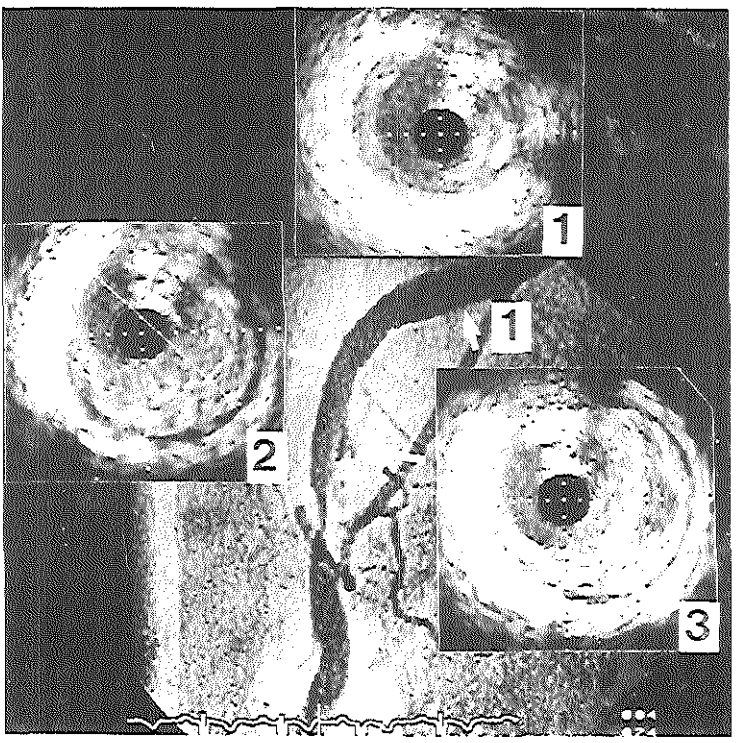

Figure 1 - Digital angiogram of a proximal right coronary artery with a severe stenosis and extraluminal contrast in a patient treated with intracoronary thrombolysis. Intravascular ultrasound shows 1) a diffuse intimal thickening of the proximal artery; 2) a dilatation of the prestenotic artery, filled with inhomogeneous moderately echogenic material; 3) an echofree space in the plaque (at 3.00 o'clock) corresponding to the apparently extravasal contrast. During directional atherectomy thrombotic material at various stages of organization was retrieved.

3-D reconstruction: techniques

Three-dimensional reconstruction requires four basic sequential steps. The sequence of cross-sectional images must be correctly sampled and, after digitization and application of the chosen algorithm, the three-dimensional image can be displayed and the volumetric changes of lumen and wall analyzed.

STEP 1. IMAGE ACQUISITION

The first step is the most crucial. A sequence of cross-sectional images must be sampled in a known and predetermined format and with an optimal constant grey scale. Two techniques can be used: a sequential acquisition of adjacent cross-sections, interspaced by constant intervals, and a continuous pull-back along the examined vascular segment. The latter approach is facilitated by using motorized systems to achieve a

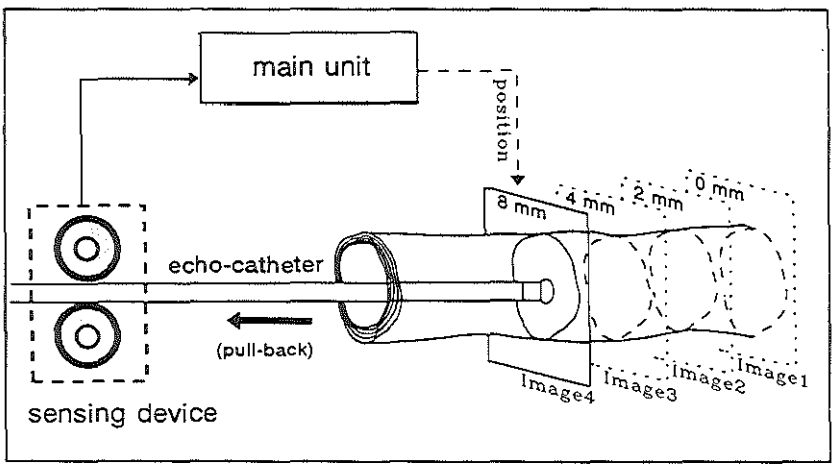

Figure 2 - Diagram showing the acquisition of a series of images from an artery specimen using a dedicated sensor (patent pending). The ultrasound catheter is introduced through a small disposable unit and its movement activates a rotating wheel connected to a potentiometer so that advancement or withdrawal of the catheter is accurately measured. The position of the cross-sections is displayed on-line and can be used to guide the three-dimensional reconstruction.

uniform speed. With these devices accurate measurements of axial displacement are possible [4].

At the Thoraxcentre a dedicated disposable sensor was developed to measure the depth of insertion of the ultrasound catheter and allow a precise definition of the spatial relation of successive cross-sections.

Step 2. Digital conversion and image segmentation

The analog image must be converted into a digital image using an adequately small pixel size for optimal resolution and a sufficiently high number of bits to define the grey level range of each pixel to preserve the dynamic range of the image. There is obviously a trade-off between resolution of the image and speed of computer processing.
Image segmentation is the second step necessary to proceed to the reconstruction of the three-dimensional image. The "threshold method" define a threshold intensity to obtain binary images in which all the voxels with an intensity above or below the threshold are considered as belonging or not belonging to the structure to be reconstructed. The advantage is that this approach allows for a complete automatization but the loss of definition of wall components remains a major limitation.
At the Thoraxcentre research in three-dimensional reconstruction of vascular images has been focused on the automatic detection of the boundaries of the lumen and the media, a preliminary but necessary step for the three-dimensional quantification of lumen and wall changes. After a temporal smoothing of consecutive frames to reduce blood echogenicity and enhance the lumen borders, a semiautomatic method of contour detection is used to define the leading edge of the blood-wall interface. The method is based on the application of a minimum cost algorithm and on the use of dynamic programming techniques to find an optimal contour based on an ellipse model. The media bounded area is defined using a manual tracing as the area included between the intimal contour and the interface between the intima and the hypoechoic media (Figure 3). The contours of this template image are then used as a model to define the search region and resample the rest of the image into a polar coordinate format. For each frame the edge strength of both the lumen border and media is calculated separately in all resampled pixels and used to find the optimal contours through the data representing the strength of the edges.

This method has been extensively validated in vitro [5] and in vivo [6] and has been successfully used for automatic assessment of dynamic systo-diastolic changes of lumen cross-sectional area [7].

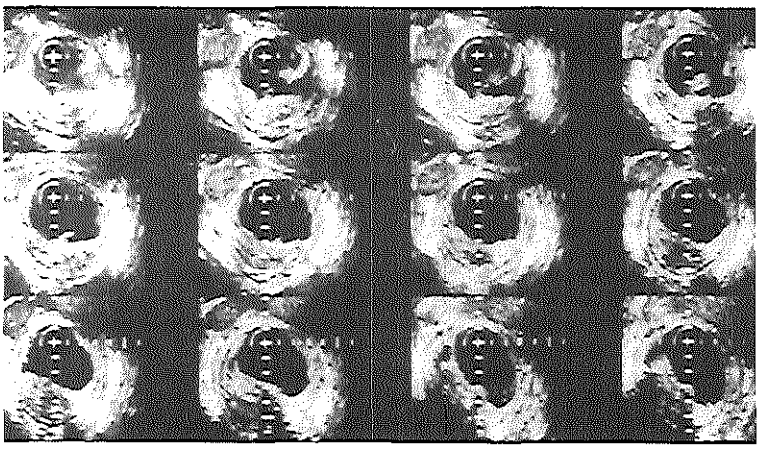

Figure 3 - Consecutive cross-sections obtained at 2 mm intervals in a left coronary artery after balloon angioplasty using a diplacement sensor. The above described method has been used to define the boundaries of the lumen and of the media. A large eccentric plaque, well defined by a thin hypoechoic media, is present along the entire segment examined. An intraluminal dissection flap is also evident in the first 5 cross-sections (from top to bottom). (Courtesy Dr. H. Pieterman).

STEP 3. 3-D RECONSTRUCTION

Table I lists the different algorithms which are presently used for three-dimensional reconstruction.

In the *wire-mesh* model the contours of the objects are manually or automatically defined and their contours on adjacent cross-sections interconnected by straight lines. The polygon representation defines the object surface. This technique is not ideal for representation of structures of complex geometry and has been largely substituted by methods using individual volumetric units (voxels).

TABLE I. ALGORITHMS FOR 3-D RECONSTRUCTION

MODEL	ADVANTAGES	DISADVANTAGES
WIRE-MESH	simple structures require small computer memory	not suitable for objects of complex geometry
BINARY IMAGE	fully automated	no definitions of wall components
FULL GREY SCALE RECONSTRUCTION	visualization of wall components	large computer memory; long processing time

Voxel modelling allows the reconstruction of the image using a categorical cut-off threshold (*binary image*) or maintaining the grey scale of the original ultrasonic cross-sections. The technical development in this field has been so rapid that three-dimensional reconstruction at high resolution and with *full grey scale* range is now possible almost on-line.

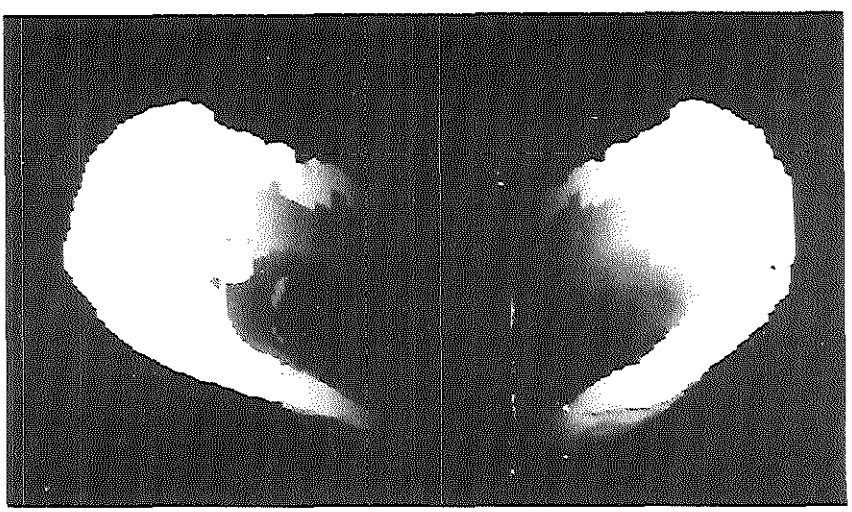

Figure 4 - The resulting reconstructed artery is opened longitudinally to visualize the internal structure of the vessel segment. The brightness of the voxels is computed from both the depth of the voxel, to provide depth perception, and the gradient vector of the voxel.

(Courtesy Dr. H. Pieterman).

At the Thoraxcentre a voxel modelling method is applied to reconstruct three-dimensionally the lumen and plaque from a sequence of cross-sectional images after detection of the lumen and plaque contours [8].

STEP 4. IMAGE DISPLAY

When the three-dimensional reconstruction is complete, many possible formats are available to display the examined arterial segment. The analysis of the intimal surface is facilitated if the artery is opened longitudinally and is appropriately rotated. Two-dimensional cross-sections can be obtained from the reconstructed image along longitudinal, transverse and oblique planes. A longitudinal format, displayed in multiple planes, is particularly convenient to assess the longitudinal extension of wall dissections and to determine the extent of the atherosclerotic involvement along the examined segment. A combination of transverse and longitudinal sections, if available on-line in the interventional suite, gives an ideal guidance to appropriately position and orient the device used.

STEP 5. QUANTITATIVE ANALYSIS

The availability of a cubic matrix allows a direct measurement of volumes after three dimensional reconstruction. The limitation remains, as for two-dimensional intravascular ultrasound, the lack of a sharp definition of the contours of the wall layers. Automatic methods are used to calculate the lumen volume based on the possibility of a reliable automatic detection of the lumen-intima interface in many cases. Plaque volume, on the contrary, requires manual identification of the plaque contours in most cases.

3-D reconstruction: Clinical applications

ASSESSMENT OF LUMEN AND PLAQUE VOLUME

Rosenfield at al [9] have proposed the application of automated edge detection algorithms for the analysis of a three-dimensional lumen cast. With this method a rapid assessment of the minimal cross-sectional area before and after interventions on peripheral arteries was possible on-line in 19 patients.

Matar et al [10] used a motorized pull-back handle to obtain a uniform distance between consecutive cross-sections in the examination of 10 in vitro arterial specimens and of the coronary arteries of 16 patients. The volumes of the reconstructed lumen correlated well with the histology measurements and with the results of biplane quantitative angiography. The measurement of plaque volume opens allows a direct assessment of the changes induced by pharmacologic or dietary interventions aimed at regression of atherosclerosis [11,12] and by interventional procedures. Galli et al [13] compared the true plaque volume of a vessel phantom and the measurements of plaque volume based on planimetry of consecutive cross-sections at a fixed interval and on direct three-dimensional reconstruction. Plaque volumes measured with three- dimensional reconstruction overestimated the true plaque volume of the phantom while more accurate measurements were obtained from direct planimetry of the echographic cross-sections.

ASSESSMENT OF INTERVENTIONS

Rationale: Intracoronary ultrasound has the potential for an accurate detection of plaque dimension and composition, an information of great usefulness to decide type and dimension of the devices to be used and to guide the intervention. Calcification of the target coronary lesion has been reported in 76-83% of the patients undergoing coronary angioplasty [14,15]. An increased incidence, depth and circumferential extension of dissection after balloon dilatation have been reported in calcified than in non-calcified plaques [15,16,17]. In the presence of diffuse subendothelial calcifications a higher incidence of complications and a smaller amount of retrievable material was observed after directional coronary atherectomy [18]. Only with three-dimensional intravascular ultrasound, however, the longitudinal extension and dimension of the calcific plaque components can be assessed along the entire segment to be dilated.

Intravascular ultrasound has been used before and after interventions to identify the mechanism of balloon dilatation. Wall stretching and wall dissection have been reported as the main operative mechanism of balloon angioplasty in both coronary [19] and peripheral arteries [20]. A significant plaque compression (absolute reduction of plaque area) has been more recently reported [21]. A possible reason of these discrepancies is the

unavoidable difference in the examined arterial cross-section before and after interventions. The measurement of plaque volume after three-dimensional reconstruction along the entire dilated segment can provide a more reliable assessment of the plaque changes brought about by the dilatation process.

Pathology studies have shown that diffuse plaque disruption is one of the predominant mechanisms of lumen enlargement after balloon angioplasty [22]. In the presence of complex intraluminal flaps angiography shows the presence of filling defects in a minority of cases. Intravascular ultrasound is more sensitive than angiography in the detection of intraluminal flaps after coronary interventions [23,24,25,26]. The standard cross-sectional display, however, does not show the longitudinal relation of these complex intraluminal flaps. On-line three-dimensional reconstruction would allow an immediate assessment of the wall changes induced by vascular interventions. The prognostic value of these findings in the prediction of immediate outcome and restenosis has been recently reported [27].

Clinical application: From the on- and off-line analysis of the intravascular ultrasound examination of 52 peripheral and 22 coronary arteries Rosenfield et al [28,29] have shown that sagittal reconstructions facilitate the analysis of dissections and the detection of tunnelling of a false lumen in the recanalization of total occlusions. Coy et al. [30] have reported an excellent agreement between three-dimensional reconstruction of intravascular ultrasound images and pathologic findings in the evaluation of length and depth of post-balloon angioplasty dissection in arteries without diffuse intimal calcification.

Recent reports [31,32] have shown the usefulness of computer assisted three-dimensional reconstruction in the identification of the true lumen and of the length of dissection before stenting as bail-out for extensive dissection after coronary angioplasty. After stenting three-dimensional reconstruction allows the measurements of longitudinal and radial dimensions of these poorly radiopacque vascular prostheses [33]. The normal appearance of the stent in contact with the vessel wall has been described and defined as a "cobblestoned" appearance. The technique has been shown to facilitate the detection of an incomplete expansion of the stent. Segments with an incomplete apposition between stent and vessel

wall, a condition with increased risk of acute thrombosis, are more easily identified.

Intravascular ultrasound has been reported as a clinically useful tool in guidance of directional atherectomy [8,34]. Recent reports have shown that three-dimensional reconstruction facilitates the orientation of the cutter in relation to side-branches and the detection of deep cuts or spiral cuts from rotation of the atherectomy catheter during cutting [35]. The clinical utility of intravascular ultrasound in planning and guidance of a variety of transcatheter treatment modalities have been reported in 88 patients. Mintz et al has suggested a specific usefulness in these cases of on-line three-dimensional reconstruction [36]. A more negative experience has been reported by Ferguson et al [37]. The therapeutic strategy was influenced by intravascular ultrasound in 39% of the cases but no changes in the planned strategy were decided based on the results of the three-dimensional reconstruction of the echographic cross-sections.

Limitations

The limitations of three-dimensional reconstruction are listed in Table II.

TABLE II. LIMITATIONS OF 3-D RECONSTRUCTION

IMAGE QUALITY	SEQUENCE OF ACQUISITION
Incomplete definition of the contours of the lumen and plaque (blood echogenicity, calcium shadowing)	Inaccurate longitudinal reconstruction if the adjacent cross-sections are not equidistant
non-coaxial position of the ultrasound catheter inducing an elliptical distortion of the image	curvature of the vessel induces a predictable distortion of the reconstructed image
non-uniform rotation of the transducer (mechanical probes)	twisting of the catheter during pull-back induces a mismatch between orientation of sequential two-dimensional images

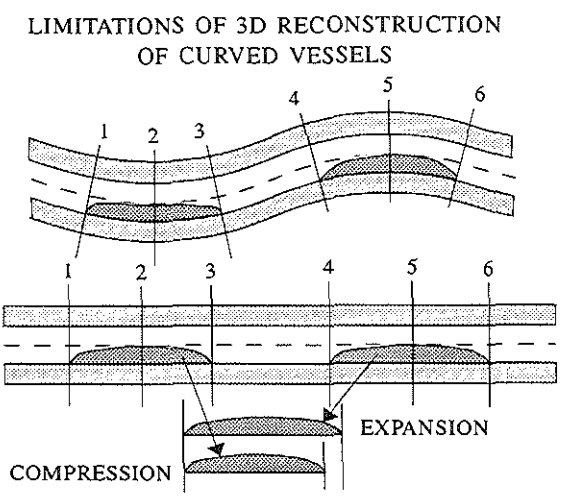

Figure 5 - Diagram showing the principle of image distortion induced by the three-dimensional reconstruction process in the presence of curvatures of the vessel. Upper panel: two plaques of similar thickness and length are present in the convexity and concavity induced by the presence of two opposite curves in the vessel. Lower panel: three-dimensional reconstruction is performed along a straight line, assuming a constant distance of adjacent cross-sections along both the opposite segments of the vessel wall, as indicated by the numbered lines. Consequently, smaller or larger plaque areas are shown according to the location of the plaque in the convexity or concavity of the vessel.

The first critical factor conditioning the results of the three-dimensional reconstruction is the quality of the acquired echographic cross-sections. An insufficient delineation of the intimal border or the absence or incomplete circumferential detection of the hypoechoic media preclude quantitative measurements of lumen and plaque volumes. Calcium shadowing or intraluminal flaps oriented tangentially to the ultrasound beam may also obscure the underlying wall [38]. The use of cross-sectional images distorted by the non-uniform rotation of the echographic transducer or by a non-coaxial position of the catheter inside the lumen may create complex artifacts in the reconstructed image.

The second critical factor is the correct acquisition of the sequence of images. The presence of a fixed difference between adjacent cross-sections is mandatory but difficult to achieve also with sophisticated means such as the use of a motorized pull-back or of sensors measuring catheter displacement. The problem is the possible presence of bends of the ultrasound catheter which may induce a difference between movement of the tip and

of the proximal end of the catheter. Another potential source of error is the rotation of the catheter during pull-back, causing a mismatch between the orientation of sequential images. The use of a miniaturized receiving antenna located at the tip of the ultrasound catheter and of an external electromagnetic transmit antenna in a plane perpendicular to the catheter axis has been proposed as a possible method to measure the orientation of the ultrasound catheter [39]. Curvatures of the vessel may also induce a predictable distortion of the three-dimensional image which is reconstructed along a straight line connecting successive cross-sections (Figure 5).

Expansion or compression of plaques may result in over/underestimation of the volumes measured from the reconstructed image.

Conclusions

In conclusion three-dimensional reconstruction of intravascular ultrasound images is a research tool of potential interest for the assessment of volumetric changes of lumen and plaque. The recent development of techniques of on-line reconstruction may allow the application of this method for guidance and immediate assessment of vascular interventions. High quality intravascular ultrasound cross-sectional images are mandatory to achieve an accurate detection of vessel lumen and plaque. Inaccuracies in image acquisition induce potentially misleading artifacts of the reconstructed image.

References

1. Parker DL, Jiang Wu. 3D reconstruction of the coronary tree from multiview digital angiography: a study of reconstruction accuracy. In: Reiber JHC, Serruys PW, editors. Quantitative coronary angiography. Dordrecht: Kluwer Academic Publishers, 1991:265-94.
2. Kitney RI, Moura L, Straughan K. Three-dimensional intravascular ultrasound. In: Born N, Roelandt JRTC, editors. Intravascular Ultrasound. Dordrecht: Kluwer Academic Publishers, 1989:135-46.

3. Chandrasekaran K, D'Adamo AJ, Segal CM. Three dimensional reconstruction of intravascular ultrasound images. In: Yock PG, Tobis JM, editors. Intravascular Ultrasound Imaging. New York: Churchill-Livingstone, 1992:141-7.
4. Mintz GS, Keller MB, Fay FG. Motorized IVUS transducer pull-back permits accurate quantitative axial measurements. Circulation 1992;86:I-323.
5. Li Wenguang, Gussenhoven WJ, Zhong Y et al. Validation of quantitative analysis of intravascular ultrasound images. Int J Cardiac Imag 1991;6:247-54.
6. Di Mario C, The SHK, Madretsma S et al. Detection and characterization of vascular lesions by intravascular ultrasound. An in-vitro correlative study with histology. J Am Soc Echocardiogr 1992;19:135-46.
7. Di Mario C, Wilson R, Gussenhoven EJ, Serruys PW, Verdouw PD, Roelandt JRTC. Norepinephrine-induced decrease in large artery compliance. Eur Heart J 1992;13:394.
8. Li Wenguang, Bosch JG, Zhong Y et al. Image segmentation and 3D reconstruction of intravascular ultrasound images. Acoustic Imaging 1993; 20: in press.
9. Rosenfield K, Kaufman J, Losordo DW, Isner JM. Lumen cast analysis: a quantitative format to expedite on-line analysis of 3D-intravascular ultrasound images. J Am Coll Cardiol 1992;19:115A.
10. Matar FA, Mintz GS, Douek PC, MB Leon, Popma JJ. Three-dimensional intravascular ultrasound: a new standard for vessel lumen volume measurement? J Am Coll Cardiol 1992;19:382A.
11. Lassetter JE, Krall RC, Moddrelle DS, Jenkins RD. Morphologic changes of the arterial wall during regression of experimental atherosclerosis. Circulation 1992; 86:I-518.
12. Gupta M, Connolly AJ, Zhu BQ et al. Quantitative analysis of progression and regression of atherosclerosis by intravascular ultrasound: validation in a rabbit model. Circulation 1992;86:I-518.
13. Galli FC, Sudhir K, Kao AK, Fitgerald PJ, Yock PG. Direct measurement of plaque volume by three-dimensional ultrasound: potential and pitfalls. J Am Coll Cardiol 1992;19:115A.
14. Mintz GS, Douek P, Pichard AD, Kent KM, Satler LF, Popma JJ, Leon MB. Target lesion calcification in coronary artery disease. J Am Coll Cardiol 1992; 20:1149-55.
15. Honye J, Mahon DJ, White CJ, Ramee SR, Wallis JB, Al-Zarka A, Tobis JM. Morphological effects of coronary balloon angioplasty in vivo assessed by intravascular ultrasound imaging. Circulation 1992;85:1012-25.
16. Fitzgerald PJ, Ports TA, Yock PG. Contribution of localized calcium deposits to dissection after angioplasty. An observational study using intravascular ultrasound. Circulation 1992;86:64-70.
17. Potkin BN, Keren G, Mintz GS et al. Arterial response to balloon coronary angioplasty: an intravascular ultrasound study. J Am Coll Cardiol 1992; 20:942-51.

18. Kimura BJ, Fitzgerald PJ, Sudhir K, Amidon TM, Strunk BL, Yock PG. Guidance of directional coronary atherectomy by intracoronary ultrasound imaging. Am Heart J 1992;124:1385-1369.
19. Tenaglia AN, Buller CE, Kisslo KB, Stack RS, Davidson CJ. Mechanisms of balloon angioplasty and directional coronary atherectomy as assessed by intracoronary ultrasound. J Am Coll Cardiol 1992;20:685-91.
20. The SHK, Gussenhoven EJ, Zhong Y et al. Effect of balloon angioplasty on femoral artery evaluated with intravascular ultrasound imaging. Circulation 1992; 86:483-93.
21. Losordo DW, Rosenfield K, Pieczek A, Baker K, Harding M, Isner JM. How does angioplasty work? Serial analysis of human iliac arteries using intravascular ultrasound. Circulation 1992;86:1845-58.
22. Waller BF. Coronary balloon artery dissections: "The Good, the Bad and the Ugly". J Am Coll Cardiol 1992;20:701-06.
23. Tobis JM, Mallery JA, Mahon D et al. Intravascular ultrasound imaging of human arteries in vivo. Circulation 1991;83:913-26.
24. Nissen SE, Gurley JC, Grines CL et al. Intravascular ultrasound assessment of lumen size and wall morphology in normal subjects and patients with coronary artery disease. Circulation 1991;84:1087-99.
25. Werner GS, Sold G, Buchwald A, Wiegand V. Intravascular ultrasound imaging of human coronary arteries after percutaneous transluminal angioplasty: morphologic and quantitative assessment. Am Heart J 1991; 122:212-20.
26. Gussenhoven WJ, Frietman P, The SHK et al. Assessment of medial thinning in atherosclerosis with intravascular ultrasound. Am J Cardiol 1991; 68:625-32.
27. Tenaglia AN, Buller CE, Kisslo KB, Phillips HR, Stack RS. Intracoronary ultrasound predictors of adverse outcomes after coronary artery interventions. J Am Coll Cardiol 1992;20:1385-90.
28. Rosenfield K, Losordo DW, Ramaswamy K, Isner JM. Three-dimensional reconstruction of human coronary and peripheral arteries from images recorded during two-dimensional intravascular ultrasound examination. Circulation 1991;84:1938-56.
29. Rosenfield K, Kaufman J, Pieczek A, Langevin RE, Razvi S, Isner JM. Real-time three-dimensional reconstruction of intravascular ultrasound images of iliac arteries. Am J Cardiol 1992;70:412-15.
30. Coy KM, Park JC, Fishbein MC et al. In vitro validation of three-dimensional intravascular ultrasound for the evaluation of arterial injury after balloon angioplasty. J Am Coll Cardiol 1992;20:692-700.
31. Cavaye DM, White RA, Lerman RD, Kopchock GE, Tabbara MR, Cormier F, French WJ. Usefulness of intravascular ultrasound imaging for detecting experimentally induced aortic dissection in dogs and for determining the effectiveness of endoluminal stenting. Am J Cardiol 1992;69:705-7.

32. Schryver TE, Popma JJ, Kent KM, Leon MB, Mintz GS. Use of intracoronary ultrasound to identify the true coronary lumen in chronic coronary dissection treated with intracoronary stenting. Am J Cardiol 1992;69:1107-8.
33. Mintz GS, Leon MB, Popma JJ, Kent KM. Three-dimensional reconstruction of endovascular stents. J Am Coll Cardiol 1992;19:224A.
34. Yock PG, Fitzgerald PJ, Linker DT, Angelsen BAJ. Intravascular ultrasound guidance for catheter-based coronary interventions. J Am Coll Cardiol 1991; 17:39B-45B.
35. Smucker ML, Kil D, Sarnat WS, Howard PF. Is three-dimensional reconstruction a gimmick or a useful clinical tool? Experience in coronary atherectomy. J Am Coll Cardiol 1992;19:115A.
36. Mintz GS, Leon MB, Satler LF, Kent KM, Pichard AD. Pre-intervention ultrasound imaging influences transcatheter coronary treatment strategies. Circulation 1992;6:I-323.
37. Ferguson JJ, Krishnaswami A, Turner SA, Kardesch D, Perin EC, Willerson JT, Fish RD. The clinical utility of intravascular ultrasound. Three-dimensional image reconstruction and color mapping of ultrasound images. Circulation 1992;86:I-705.
38. Di Mario C, Madretsma S, Linker D et al. The angle of incidence of the ultrasonic beam: A critical factor for the image quality in intravascular ultrasound. Am Heart J 1993;125:442-8.
39. Aretz HT, Gregory KW, Martinelli MA, Gregg RE, LeDet EG, Haase WC. Ultrasound guidance of laser atherectomy. Int J Cardiac Imag 1991;6:231-7.

CHAPTER 4

DETECTION AND CHARACTERIZATION OF VASCULAR LESIONS BY INTRAVASCULAR ULTRASOUND: AN IN VITRO STUDY CORRELATED WITH HISTOLOGY

Carlo Di Mario, M.D., Salem H.K. The, M.D., Stanley Madrestma, M.D., Robert J. van Suylen, M.D., Richard A. Wilson, M.D., Ph.D., Nicolaas Bom, Ph.D., Patrick W. Serruys, M.D., Ph.D., Elma J. Gussenhoven, M.D., Ph.D., Jos R.T.C. Roelandt, M.D., Ph.D.
With the technical assistance of: Yin Zhong, M.Sc. and Li Wenguang, M.Sc.

From the Department of Cardiology and Pathology, Erasmus University, Rotterdam and the Interuniversity Cardiology Institute, The Netherlands

Reprinted from: J Am Soc Echocardiogr, 1992.

Detection and Characterization of Vascular Lesions by Intravascular Ultrasound: An In Vitro Study Correlated with Histology

Carlo Di Mario, MD,[a] Salem H. K. The, MD, Stanley Madretsma, MD, Robert J. van Suylen, MD, Richard A. Wilson, MD,[b] Nicolaas Bom, PhD, Patrick W. Serruys, MD, Elma J. Gussenhoven, MD, and Jos R.T.C. Roelandt, MD, with the technical assistance of Yin Zhong, MSc, and L. Wenguang, MSc,
Rotterdam, The Netherlands

High-frequency intravascular ultrasound (30 and 40 MHz) was applied to study 112 human vascular specimens. The ultrasound images were compared with histologic cross-sections. In 44 out of 58 of the histologically classified muscular arteries, a hypoechoic middle layer was seen in the vessel wall, giving it a three-layered appearance. In 10 arteries, fibrous degeneration of the muscular media resulted in a homogeneous appearance of the vessel walls, whereas atherosclerotic plaque precluded the visualization of the arterial media in four of the arteries. A three-layered appearance was seen in seven of nine histologically classified transitional arteries, and a homogeneous arterial wall was seen in two of the nine. None of the 33 elastic arteries, veins, venous bypass, and Goretex conduits showed a hypoechoic medial layer. Histologically proved fibrous intimal thickening was echographically detected in 32 of 48 specimens (67%). It was noted that these intimal lesions were easier to detect with 40 MHz than with 30 MHz transducers. Hypoechoic areas of lipid deposition were detected in 32 of 36 specimens (89%) and could be distinguished from fibrous plaques. Histologically evident calcium deposits were detected with intravascular ultrasound in 35 of 36 specimens (97%). Measurement of plaque area was only possible in cross sections with a three-layered appearance. Quantitative analysis showed a significantly larger lumen area measured from ultrasonic images (26.3 ± 21.3 mm^2) than from histologic cross-sections (21.8 ± 16.6 mm^2, $p < 0.001$), probably because of tissue shrinkage during processing for histology. A significant correlation ($r = 0.96$, $p < 0.001$) between ultrasonic and histologic measurements of lumen areas was observed, with and a negligible interobserver and intraobserver variability. Plaque area and medial thickness correlated well with histology ($r = 0.87$, $p < 0.001$ and $r = 0.93$, $p < 0.001$, respectively). It appears from this in vitro study that intravascular ultrasound is an accurate technique for detection and characterization of atherosclerotic lesions. Vessel lumen area can be measured in most instances, whereas plaque area and medial thickness can only be reliably assessed in muscular arteries in which the hypoechoic media serves as a reference, and shadowing by calcium or attenuation by fibrous plaque components is absent. (J Am Soc Echocardiogr 1992;5:135-46.)

From the Department of Cardiology, Thoraxcentre, and Department of Pathology, Erasmus University Rotterdam, and Interuniversity Cardiology Institute.

[a]Dr. C. Di Mario, Div. of Cardiol., Vicenza (Italy), is the recipient of the European Society of Cardiology Research Fellowship 1991.

[b]Dr. R. A. Wilson is the recipient of the NIH Fogarty Senior International Fellowship Grant n. TW0163301.

Reprint requests: Elma J. Gussenhoven, MD, Thoraxcentre, Ee 2312 P.O. Box 1738, 3000 DR Rotterdam, The Netherlands.

27/1/33096

The advantage of intravascular ultrasound over other imaging techniques is its unique capability to combine visualization of the vessel lumen and inspection of composition and extent of the atherosclerotic lesion.[1-3]

For better understanding and interpretation of in vivo images,[4-7] however, in vitro studies comparing ultrasound images with histologic data are of paramount importance.[8-14] The complex morphology of

Table 1a Criteria for histologic classification of arterial specimens (100 arteries) and intimal lesions (111 vessels)

Type of artery	Intimal lesion	Histology	n (%)
Muscular		Prevalence of smooth muscle cells in the medial layer of the artery	58 (58%)
Transitional		Smooth muscle component sandwiched among multiple parallel elastic lamina (internal elastic lamina well defined)	9 (9%)
Elastic		Densely packed multiple elastic lamina in the medial layer (poorly defined internal elastic lamina)	33 (33%)
	Normal intima	Absence of a subendothelial intimal layer, evident at low microscopic magnification (×32), dividing endothelium and internal elastic lamina	7 (6%)
	Fibrous intimal thickening	Diffuse or focal intimal thickening without lipid or calcium deposition	48 (43%)
	Lipid deposits	Focal plaque within the intima having a core of lipids and evident at low microscopic magnification (×32)	36 (31%)
	Calcium deposition	Microscopically evident islands of calcium degeneration	36 (31%)

the atherosclerotic lesions indicates that a large number of arteries must be studied to establish the sensitivity and specificity of the criteria used for both the detection and the characterization of atherosclerotic plaques with intravascular ultrasound.

Therefore, we examined and classified histologically 112 vessel specimens and compared these data with the results of qualitative and quantitative intravascular ultrasonic analyses.

METHODS

Vascular Specimens

Vascular specimens (n = 112) were collected either at surgery or at autopsy from 82 patients (mean age, 66 years; range, 1 to 86 years; 51 men and 31 women) within 8 to 20 hours after death. A vascular segment of 10 mm length was dissected from surrounding tissue and studied with intravascular ultrasound at room temperature immediately or after frozen storage at −20° C and subsequent thawing. In a preliminary study, an intravascular ultrasound examination of five arteries has been performed, showing no changes of the ultrasonic appearance of these specimens after freezing. The following vessels were studied: 10 proximal and middle left and right coronary arteries; 21 internal carotid arteries and one external carotid artery; one subclavian artery; three internal thoracic (mammary) arteries; one brachial artery; four mesenteric, one renal, and four splenic arteries; 33 iliac, 11 femoral, and one popliteal artery; two pulmonary arteries; seven descending aorta; six systemic and pulmonary veins; three coronary and peripheral venous bypass grafts; and three Goretex conduits (Gore & Associates, Inc., Elkton, Maryland).

Histologic Examination

After the ultrasound examination, the proximal site of the vessel was marked with India ink at the twelve o'clock position of the ultrasonic cross section at which ultrasound imaging was started. The vessels were then fixed in 10% buffered formalin for 12 hours, decalcified, and further processed for routine paraffin embedding. Starting at the ink-marked level, two cross sections (thickness, 5 μm) perpendicular to the vascular long axis were cut at 1 mm intervals. One slice was stained with Verhoeff's elastin van Gieson and the other with hematoxylin-azophloxin.

Qualitative analysis. The histologic examination was aimed at the classification of the type of vessel and characterization of the vascular lesions on the basis of criteria presented in Table 1a.

Quantitative analysis. Quantitative analysis of the histologic sections was performed using a commercially available and previously described[16] system (IBAS, Kontron Instruments, Everett, Mass.). This computer-assisted analysis system allows contour tracing and area measurement of the digitized microscopic image. Lumen area was defined as the area surrounded by the most inner vessel contour. Plaque area was defined as the area lying between the lumen and the internal elastic lamina. Finally, the medial

Table 1b Criteria for ultrasonic classification of type of artery (100 arteries) and intimal lesions (111 vessels)

Type of artery	Intimal lesion	Intravascular ultrasound	n (%)
Three-layered appearance		Presence of a hypoechoic middle layer	51 (51%)
Homogeneous appearance		Homogeneous echointensity of the vessel layers	42 (42%)
Nonclassifiable		Outer wall not imaged because of concentric atherosclerotic intimal lesion (shadowing or attenuation)	7 (7%)
	Normal intima	Single echoreflective line between vessel lumen and hypoechoic intermediate layer or, in the absence of a hypoechoic media, homogeneous echointensity of the vessel wall	24 (22%)
	Fibrous intimal thickening	Increased intimal thickness (when defined by a hypoechoic media) or different intimal echointensity, without ultrasonic changes suggestive of lipid or calcium deposition (see below)	32 (29%)
	Lipid deposits	Markedly hypoechoic areas inside the intimal lesion	32 (29%)
	Calcium deposition	Highly echoreflective areas with shadowing and/or reverberations	35 (32%)

area was calculated as the area lying between the internal and external elastic laminae.

Intravascular Ultrasonic Imaging System

Two different systems were used. The first 55 specimens were analyzed using an 8F (diameter, 2.7 mm) catheter with a 40 MHz single-element transducer. Circumferential imaging was realized by motor-driven catheter tip rotation. To complete one cross-sectional image, 20 s were required and a video-scanned memory was used for image reconstruction. The latter 57 specimens were evaluated using a 5F (diameter, 1.6 mm) catheter with a 30 MHz single-crystal transducer mounted on a flexible drive shaft, rotating at speeds between 2 and 16 revolutions/s. This system (DuMed, Rotterdam, The Netherlands) allows real-time acquisition, with a resolution of 512 × 512 pixels and 256 grey levels.

Ultrasonic Examination

The specimens were embedded in a 1.2% agar-agar solution, vertically positioned, and their lumina filled with water. After insertion of the catheter in the proximal part of the vessel lumen, multiple ultrasonic cross sections were sequentially obtained from proximal to distal at 1 mm intervals. Ultrasonic cross sections were independently analyzed by two investigators, without knowledge of the histologic results. One ultrasound cross section from each specimen was selected for comparison with histologic sample on the basis of the most significant lesion thickness.

Qualitative analysis. Type of vessel and presence and characteristics of intimal changes were evaluated on the basis of criteria that are currently used in our laboratory for clinical studies (Table 1b).

Quantitative analysis. From the 57 specimens studied with the real-time ultrasonic system, lumen area, plaque area, and medial area were measured using a computer-assisted analysis system.[16] After digitization of the video-recorded image of interest by a DT 2851 framegrabber (Data Translation, Inc., Marlboro, Mass.) and storage on the hard-disk of an IBM compatible PC, a PC mouse was used to draw the selected boundaries, as shown in Figure 1. To test reproducibility of the measurements, the analysis of the images was repeated in two separate sessions by the same observer and, independently, by a second observer. The average of the three values was used for comparison with histology.

Statistical Analysis

Sensitivity, specificity, and positive and negative predictive values were calculated to compare the histologic with the ultrasonic classification of type of vessel and atherosclerotic lesion.[17] Correlations of the quantitative ultrasonic and histologic measurements were determined by linear regression analysis for two variables. The regression line was compared with the identity line to test the level of significance. Analysis of variance was applied to test the significance of the differences for paired data.

RESULTS

Ultrasonic Patterns of Vessel Wall

Histologic sections showed a ring of parallel smooth muscle cells (muscular type of artery) in 44 of 51 specimens (86%) with a three-layered appearance on the ultrasonic image (Table 2). Mixed muscular and elastic components (transitional type of artery) were present in the remaining seven specimens (14%).

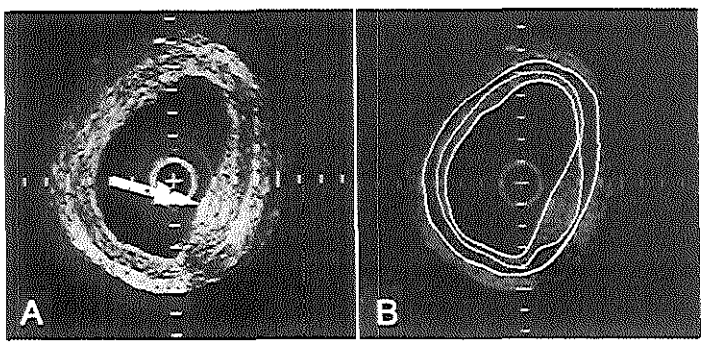

Figure 1 **A,** Echographic cross-section of an iliac artery. Presence of hypoechoic middle band, corresponding to muscular media, allows detection of a moderately echoreflective homogeneous area of intimal thickening *(arrow)*. At histologic examination, this bright area corresponded to an area of dense fibrous intimal thickening, without lipid deposition or microscopically evident calcium degeneration. Thinning of the medial layer underneath the plaque is evident. **B,** The echographic image after digital processing and manual contour of three regions of interest. *Internal circle* marks the lumen area. The *middle circle* is traced at the junction of intimal layer (internal elastic lamina) and hypoechoic muscular media. The *external circle* is traced at the junction of hypoechoic media and the more echoreflective adventitia.

Table 2 Histologic-echographic correlations: type of vessel

Histology	(n)	Intravascular ultrasound	n (%)
Muscular arteries	(58)	Three-layered appearance	44 (76%)
		Homogeneous appearance (medial fibrous degeneration)	10 (17%)
		Concentric atherosclerotic lesions	4 (7%)
Transitional arteries	(9)	Three-layered appearance	7 (78%)
		Homogeneous appearance	2 (22%)
Elastic arteries	(33)	Homogeneous appearance	30 (91%)
		Outer wall not imaged	3 (9%)
Veins and venous bypass	(9)	Homogeneous appearance	9 (100%)
Goretex bypass conduits	(3)	Homogeneous appearance with bright outer ring	3 (100%)

Fourteen specimens were histologically classified as muscular arteries but did not show a three-layered appearance on the ultrasonic image. In 10 specimens the smooth-muscle cells of the media were replaced by collagen (fibrous degeneration of the media), and this layer was indistinguishable from the surrounding wall structures on the ultrasonic images (Figure 2). In four other specimens, the muscular media was not detected on the ultrasonic images because of severe medial thinning from atherosclerotic involvement or diffuse shadowing induced by calcific plaques.

A homogeneous ultrasonic appearance of the vessel wall was observed in 30 of 33 specimens (91%) histologically classified as elastic arteries. Dense fibrous thickening of the intimal layer with marked ultrasound attenuation or diffuse intimal calcification with shadowing prevented ultrasonic evaluation of the outer vessel wall in the remaining three specimens. A homogeneous vessel wall appearance was also observed in two specimens histologically classified as transitional.

All venous bypass grafts as well as systemic and pulmonary veins showed a homogeneous ultrasonic appearance of their walls. Goretex bypass conduits were characterized by an external bright ring on the ultrasonic images.

Ultrasonic Detection of Fibrous Intimal Thickening

Sensitivity, specificity, positive and negative predictive values, and interobserver agreement of intravascular ultrasound in differentiating fibrous intimal thickening from normal arteries or lipid/calcium deposits are reported in Table 3.

Histologically diagnosed fibrous intimal thickening was detected from ultrasonic cross sections in 21

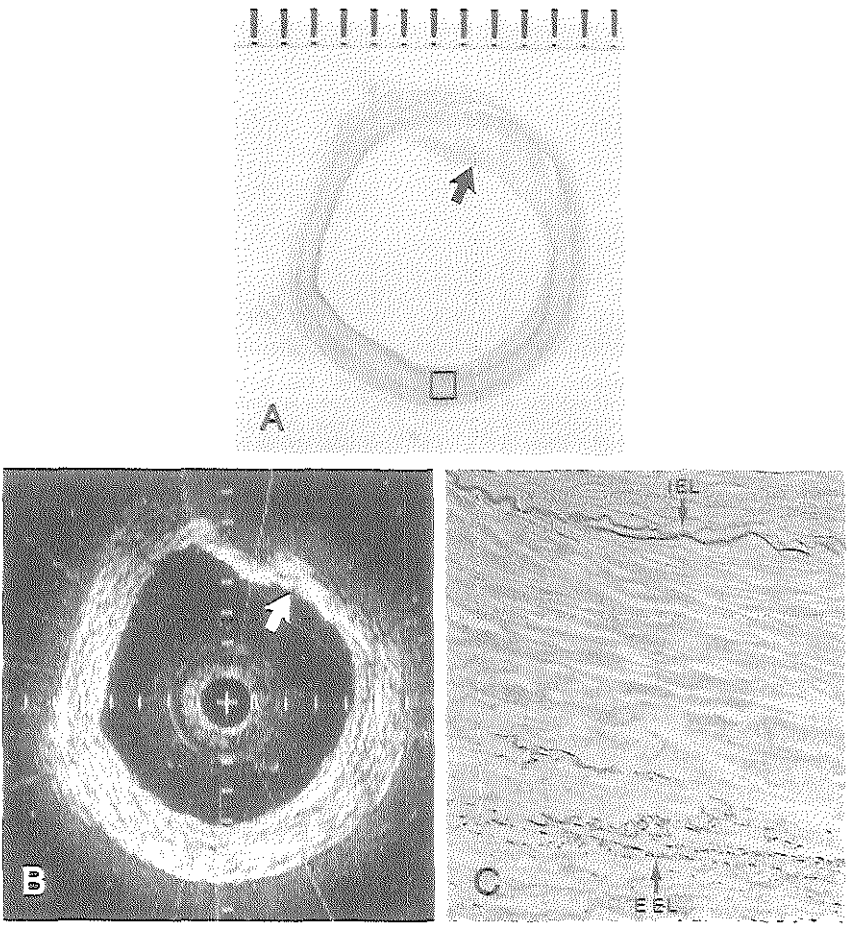

Figure 2 Histologic (**A**) and echographic (**B**) cross-sections of iliac artery. Homogeneous appearance of the vessel wall at ultrasound precludes the detection of a diffuse area of dense fibrous intimal thickening, clearly shown in the magnified histologic cross section. For the major part the muscular media is replaced by dense fibrous tissue. In the magnified histologic image (**C**) the two *arrows* indicate the well preserved, corrugated black lines of the internal elastic lamina *(IEL)* and the fragmented external elastic lamina *(EEL)*. In the enclosed medial layer, the remaining muscular component (yellow-orange) can be distinguished by the prevalent fibrous tissue (pink-purple). *Arrow* in **A** shows a small eccentric plaque in which an area of lipid deposition is surrounded by a fibrocalcific shell. In the echographic image, shadowing precludes evaluation of composition and dimensions of plaque behind bright line of calcification *(arrow)*. (Verhoeff's van Gieson stain, magnification ×6.8 and ×102.)

of 26 (81%) specimens with a three-layered appearance. In the remaining five specimens missed by ultrasound, only minimal thickening was present. Also, large areas of intimal thickening were not recognized in 11 of the 22 specimens (50%) without a three-layered appearance. It is noteworthy that nine of these 11 specimens belonged to the group of 55 specimens studied with a 40 MHz transducer, al-

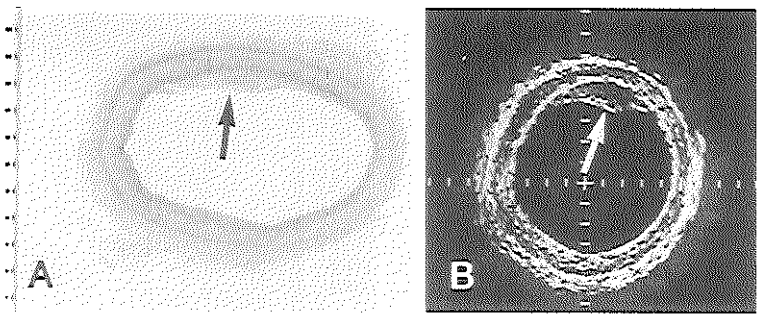

Figure 3 Histologic (A) and echographic (B) cross sections of an iliac artery. The well-preserved muscular media is imaged as a hypoechoic middle layer. The *arrows* in both images indicate a small eccentric plaque, histologically of fibrocellular nature, recognized at ultrasound examination as relatively "soft" area inside the brighter subendothelial line. Note that in the segment of normal or near-normal thin intimal layer, the internal elastic lamina induces a bright and thick echoline. (Verhoeff's van Gieson stain, magnification ×5.1.)

Table 3 Echographic detection of histologically proved vascular lesions

Histology (No. of specimens)	Sensitivity	Specificity	Positive predictive value	Negative predictive value	Interobserver agreement
Fibrous intimal thickening (48)	66.6% (32/48)	100% (64/64)	100% (32/32)	80.0% (64/80)	78.4% (29/37)
Lipid deposits (36)	88.9% (32/36)	100% (76/76)	100% (32/32)	95.0% (76/80)	85.7% (30/35)
Calcium deposition (36)	97.2% (35/36)	98.7% (75/76)	97.2% (35/36)	98.7% (75/76)	97.2% (35/36)

though the 40 and 30 MHz groups had a similar prevalence of fibrous intimal thickening.

The echointensity of the thickened fibrous intima was variable; in 18 instances (56%) a low echointensity was present, corresponding to cellular areas with loose collagen and fibromuscular involvement (Figure 3). Densely packed, almost acellular fibrous connective tissue was present in 14 specimens (44%) and corresponded to areas of high echointensity on ultrasonic cross sections.

Ultrasonic Detection of Lipid Deposits

At histology, large intraplaque lipid deposits were seen in 36 specimens (32%) and consisted mainly of fatty debris or multiple cholesterol needles embedded in areas of loose collagen tissue with diffuse interposition of foamy macrophages. At intravascular ultrasound 32 of 36 (89%) of these intra-plaque lipid deposits were identified (Table 3) and seen as hypoechoic areas covered by bright echoes (fibrous cap) or mixed with bright spots with shadowing (Figure 4). Deposits of calcium were present in 16 of 36 specimens (44%). In four instances (11%), the lipid deposits were not identified from the ultrasonic image (false negative) because of massive calcium deposition in the fibrous cap, masking the underlying lipid pool (Figure 2).

Detection of Calcium Deposition

With intravascular ultrasound the presence of histologically proved calcium deposition was found in 35 of 36 (97%) specimens (Table 3). Calcium deposits were seen as bright areas, lines, or spots producing shadowing and reverberations (Figures 2, 4, and 5). In one specimen, small, diffuse calcium deposits were missed with intravascular ultrasound. In another specimen, shadowing behind a thick, bright intimal band was seen whereas histologic examination showed only densely packed fibrous connective tissue without calcium deposits.

Quantitative Analysis

Lumen area. A total of 40 of 57 lumen areas were analyzed from paired ultrasonic and histologic cross sections. In 13 specimens the vessel dimensions were too large for the histologic analysis sys-

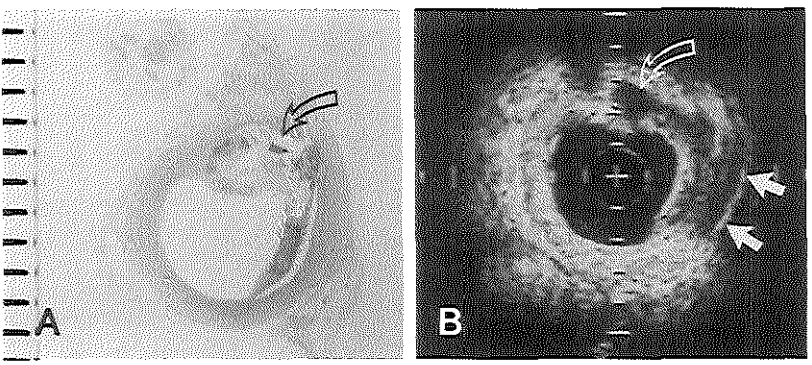

Figure 4 Example of atherosclerotic plaque in an elastic artery (internal carotid artery). The echographic cross section (B) shows an echo-free area *(open arrow)* corresponding in the histology image (A) to diffuse fatty debris *(open arrow)*, partially removed during histologic processing. Calcium deposits induce an intensely bright line with posterior shadowing and duplicate echoes *(arrowheads* in B). (Hematoxylin azophloxin stain, magnification ×6.8.)

tem. Four ultrasonic cross sections could not be analyzed or measured because of incomplete visualization involving more than 20% of the intimal circumference.

Minimal differences were observed in the measurements performed by the same observer in two different sessions (26.1 ± 21.3 mm^2 vs 26.3 ± 21.3 mm^2, NS) and by the two different observers (26.1 ± 21.3 mm^2 vs 26.4 ± 21.4 mm^2, NS), with a correlation coefficient of 0.99 for both comparisons.

Ultrasonic lumen areas were significantly larger than those measured from histologic specimens (26.3 ± 21.3 mm^2 vs 21.8 ± 16.6 mm^2, $p < 0.001$). The regression analysis showed a highly significant correlation ($r = 0.96$, $p < 0.001$, Figure 6, A).

Plaque area. The border between the intimal area and media could be identified in 12 specimens with a three-layered appearance. The middle hypoechoic layer was needed as a landmark for analysis but, when it was thinned or obscured by calcium-containing lesions, the incomplete visualization precluded the quantitative measurements of plaque area. Both intraobserver and interobserver variability of plaque area measurements were slightly larger than the variability of the measurements of lumen area (8.6 ± 5.4 mm^2 vs 9.5 ± 6.9 mm^2, NS, and 8.6 ± 5.4 mm^2 vs 9.5 ± 7.1 mm^2, NS, respectively).

Plaque areas measured from ultrasonic cross-sections were consistently larger than those from histologic examination (9.2 ± 6.3 mm^2 vs 6.2 ± 6.8 mm^2, $p < 0.01$). The regression line is shown in Figure 6, B ($r = 0.87$, $p < 0.001$).

Medial thickness. In two of the 12 analyzable specimens the external border of middle hypoechoic layer could not be identified with certainty. Consequently, medial thickness measurements were available from 10 paired cross sections. A moderate intraobserver and interobserver variability was observed (9.5 ± 6.6 mm^2 vs 8.7 ± 6.3 mm^2, NS, and 9.5 ± 6.6 mm^2 vs 9.6 ± 6.7 mm^2, NS, respectively). Medial thickness was slightly smaller at ultrasound than at histologic examination (9.2 ± 6.5 mm^2 vs 9.5 ± 6.5 mm^2, NS). Figure 6, C shows the corresponding regression line ($r = 0.93$, $p < 0.001$).

DISCUSSION

Ultrasonic Characterization of the Arterial Media

On the basis of the presence or absence of a distinct hypoechoic ring inside the vessel wall, the ultrasonic appearance of the arteries can be classified into two types. Such a simple classification has practical importance because a distinct hypoechoic layer facilitates the identification of the outer boundary of the intimal layer and therefore allows the measurement of intimal thickness. Hypoechoic areas of lipid deposition and bright lines or spots corresponding to calcification are readily detected in elastic type arteries

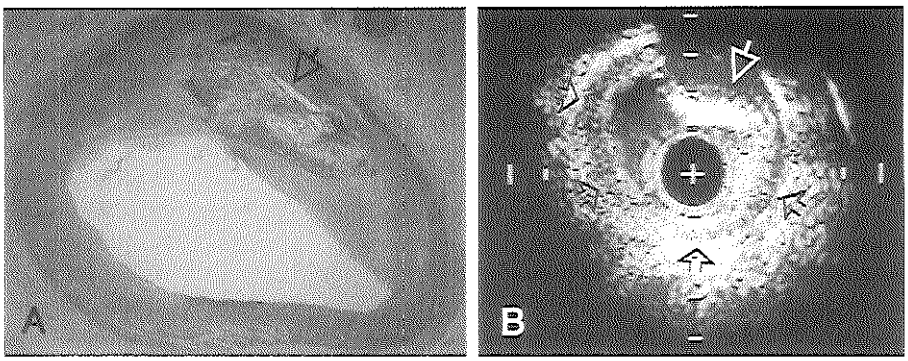

Figure 5 Histologic (A) and echographic (B) cross sections of proximal left anterior descending coronary artery. A discontinuous but clearly defined hypoechoic intermediate layer (*open arrowheads* in B) corresponds to the muscular media. In both images *closed arrows* indicate an area of calcium deposition inside a dense fibrous plaque. Note the marked brightness of the central calcified core of the plaque. Shadowing and duplicate echoes are evident behind the calcified area. (Hematoxylin-azophloxin stain, magnification ×17.)

that otherwise have a homogeneous appearance. However, relatively large areas of fibrous intimal thickening may be missed in some instances because the echointensity of the thickened intima and of the elastic media are similar. A higher ultrasound frequency (40 MHz) may have advantages for this differentiation, but this advantage is outweighed by its reduced penetration, a potential limitation when the catheter is applied in vivo in an echoreflective medium such as blood.

Measurement of plaque area is limited to muscular type arteries with a well-defined hypoechoic media. However, the three-layered structure was not seen in approximately 30% of histologically classified muscular arteries. In some specimens diffuse atherosclerotic intimal changes disrupted the internal elastic lamina with thinning or disappearance of the muscular media, or calcification with shadowing prevented recognition and measurement of both intimal changes and plaque area.[18,19] In most of the specimens diffuse fibrous degeneration of the media obscured the interface between the media and the surrounding intimal and adventitial layers. This fibrous degeneration was found also in arteries relatively free of atherosclerotic intimal changes and may be related to the arterial stiffening connected with the aging process.[20]

Ultrasonic Detection of Fibrous and Atheromatous Intimal Plaques

Fibrous or fibromuscular intimal thickening is a process that begins at young age.[21] However, intimal lesions with predominant fibrous components are present also in atherosclerotic arteries, and most patients have both lipid and fibrous plaques.[22,23] The ultrasonic distinction between hypoechoic areas caused by lipid deposition, loose collagen, or fibromuscular tissue is difficult and will definitely lead to problems of interpretation in the in vivo situation. Typically, lipid deposits are markedly hypoechoic and are seen as black "lakes" in the image. They can be distinguished from fibromuscular plaques which have a weak residual echointensity. However, the differentiation remains difficult and subjective.

Calcification, a marker of pathologic vessel degeneration that is easily recognized from ultrasonic images, occurs in both lipid and fibrous plaques. Dense fibrous tissue may induce a marked ultrasound attenuation and mimic the bright echoes with shadowing that are observed with calcification. In most instances, however, it is possible to distinguish between the abrupt and complete shadowing behind the bright lines caused by calcific tissue and the gradual reduction of echointensity induced by dense fibrous plaques.

Echographic Quantitative Analysis

Free lumen and plaque areas measured histologically were 17% and 33% smaller than the corresponding measurements with ultrasound. Processing tissue for histologic study induces a variable shrinkage mainly dependent on the tissue water content. Siegel et al.[24] compared lumen and plaque areas in fresh arterial specimens and in the same histology-processed ves-

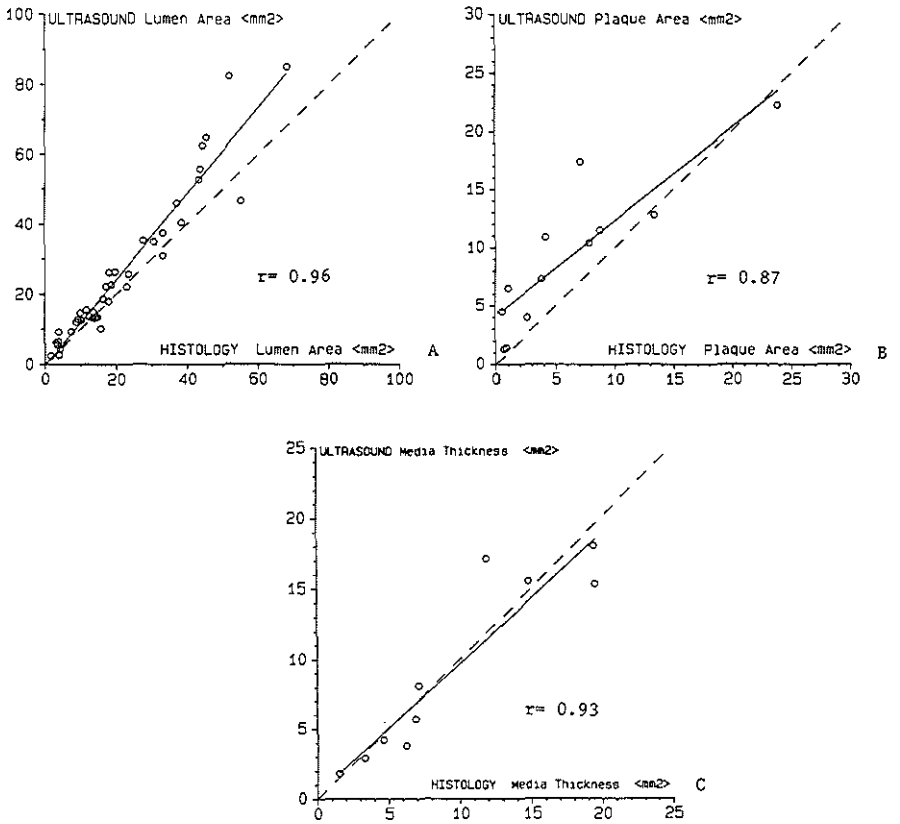

Figure 6 Linear regression analysis of the echographic-histologic measurements of lumen area (graph A), plaque area (graph B) and media thickness (graph C).

sels and observed a 20% to 30% reduction according to the different modalities used for tissue processing for histologic examination. The comparable difference observed in our specimens suggests that fixation, paraffin-embedding, and staining for histology were responsible for the underestimation of the vascular dimensions. The closer values reported in previous studies may be related to the fixation under pressure[11] or to the smaller dimensions (coronary arteries) of the examined vessels.[12]

Angiography can detect atherosclerotic involvement only when distinct changes in vascular lumen occur. Consequently, nonstenosing plaques are observed at histology or high-frequency, intraoperative echography in vascular segments with normal angiographic appearance.[25,26] Intravascular ultrasound makes it possible to measure in vivo the thickness of the diseased intima. Both this study and previous reports[9-12] have shown a satisfactory correlation with histologic measurements. Even though ideal in vitro conditions were used, we were able to detect the external intimal border along most of the circumferential profile of the vessel only in a limited number of specimens and in none of the arteries with homogeneous appearance of the vessel wall.

Although the commonly used definition of media thickness has been maintained, in our study we used a planimetric system for the measurement of the hypoechoic middle layer of arteries with a three-layered appearance. We felt that linear measurement of thick-

ness could be inadequate in the presence of focal areas of medial thinning, as illustrated in Figure 1. Although a satisfactory correspondence between paired histologic and ultrasound measurements and a low intraobserver and interobserver variability were noted, the limited number of measurements suggests that intimal plaque components can mask the medial contours in many atherosclerotic segments. The slight underestimation of media area in the ultrasonic images is probably related to the increased thickness of the internal elastic lamina (Figure 3). This artifactual thickening, caused by the "leading edge" effect, is possibly further magnified by the increased echoreflectivity of the corrugated internal elastic lamina of these undistended specimens.

Limitations of the Study

Histology is the reference method to study aspects of atherosclerotic arterial disease and, therefore, an in vitro ultrasound model was applied in this study. However, several limitations prevent a direct extrapolation of these in vitro observations to the in vivo situation:

1. The specimens were examined at room temperature. Moriuchi et al.[27] found no differences in the qualitative characteristics of the echographic images obtained at 20° C and at 37° C.
2. The specimens were examined without pressure distension. The absence of a distending intraluminal pressure induces an artifactual thickening of the vessel wall and a protrusion of the intimal plaques into the vessel lumen. Thinning of the intermediate hypoechoic layer is observed in vivo when a physiologic pressure is present inside the vascular lumen.[28] In a small preliminary series (nine specimens), the arteries were also examined under application of a fixed pressure of 100 mm Hg. In no cases did the thinning of the medial layer preclude the detection of a three-layered-appearance in the examined specimens. The uncompressibility of the plaque components suggests that significant pressure-related changes of the echographic characteristics of the atherosclerotic plaques are unlikely.
3. The vessels were not examined in a system filled by circulating blood. The acoustic backscatter from the surrounding red blood cells increases with the fourth power of the ultrasound frequency, so that attenuation from blood is of concern with the high-frequency transducers used.[29] Previous in vitro experiences[27] have shown that the attenuation of ultrasound does not preclude the morphologic evaluation of the vessel wall and the quantitative assessment of vascular dimensions. Furthermore, in our clinical experience[30] we observed that circulating blood behaves as a natural echo-contrast agent, delineating complex wall changes as extensive dissections or intraluminal thrombi. If necessary, pressure-injection of saline solution close to the tip of the intravascular ultrasound catheter can induce ideal conditions for the examination in most cases.
4. The examined vessels were fixed, with the catheter in a stable central position. Rapid motion of the arteries, as in the coronary tree, can result in a blurring of the image if an inadequately low sampling rate is used. Furthermore, eccentric, off-axis catheter positions inside the vessel lumen induce a change in the ideally perpendicular angle of incidence of the ultrasound beam with the vessel wall, with possible dropouts of the circumferential image and distortion and incorrect measurement of the luminal dimensions.[11] The experience in peripheral arteries with the 30 MHz intravascular ultrasound system used for the last specimens[30] and recent reports of intracoronary application[7,31] suggest that images of quality comparable to the results of our in vitro study and amenable to quantitative assessment[32,33] can be obtained in vivo.

CONCLUSIONS

Comparison of histologic study with intravascular ultrasound indicates that, in most instances, with ultrasound the morphology of the vessel wall can be studied, the presence of intimal changes and calcification detected, and lesions with large lipid deposits can be differentiated from mainly fibrotic plaques. Although one should be cautious in transferring these in vitro results to the clinical setting, the proposed criteria of classification of the ultrasonic, intravascular image have shown a satisfactory sensitivity and specificity in detection and characterization of histologically proved vascular changes. Problems for ultrasound are (a) degenerative fibrosis of the muscular media concealing the typical three-layered appearance of the muscular arteries, (b) diffuse in-

timal calcification obscuring the vessel wall, and (c) hyporeflective areas of loose collagen or fibromuscular tissue mimicking the presence of lipid deposits.

The highly reproducible measurements of the vessel lumen show a close correlation with histology, although there is a systematic underestimation at histology, probably because of tissue shrinkage during histologic preparation. In most instances plaque calcification and an indistinct border between plaque and underlying wall structures in the absence of a hypoechoic middle layer prevent a quantitative assessment of plaque area. It appears, therefore, that quantitative assessment of atherosclerosis in its advanced stages will be limited.

We thank Mrs. Coby Peekstok for preparing the histologic sections and Mrs. Corrie Eefting for her expert secretarial support.

REFERENCES

1. Roelandt JR, Bom N, Serruys PW, Gussenhoven EJ, Lancée CT, Sutherland GR. Intravascular high-resolution real time cross-sectional echocardiography. Echocardiography 1989; 6:9-16.
2. Yock PG, Johnson EL, Linker DT. Intravascular ultrasound: development and clinical potential. American Journal of Cardiac Imaging 1988;2:185-93.
3. Pandian NG. Intravascular and intracardiac ultrasound imaging: an old concept now on the road to reality. Circulation 1989;80:1091-4.
4. Pandian NG, Kreis A, Brockway B, et al. Ultrasound angioscopy: real-time, two-dimensional, intraluminal ultrasound imaging of blood vessels. Am J Cardiol 1988;62: 493-4.
5. Neville RF, Bartorelli AL, Sidawy AN, Almagor Y, Potkin B, Leon MB. An in vivo feasibility study of intravascular ultrasound imaging. Am J Surg 1989;158:142-5.
6. Pandian NG, Weintraub A, Kreis A, Schwartz SL, Konstam MA, Salem DN. Intracardiac, intravascular, two-dimensional high-frequency ultrasound imaging of pulmonary artery and its branches in humans and animals. Circulation 1990;81:2007-12.
7. Tobis JM, Mallery J, Mahon D, Lehmann K, et al. Intravascular ultrasound imaging of human coronary arteries in vivo. Circulation 1991;83:913-26.
8. Meyer CR, Chiang EH, Fechner KP, Fitting DW, Williams DM, Buda AJ. Feasibility of high-resolution intravascular ultrasound imaging catheters. Radiology 1988;168:113-6.
9. Gussenhoven EJ, Essed CE, Lancée CT, et al. Arterial wall characteristics determined by intravascular ultrasound imaging: an in vitro study. J Am Coll Cardiol 1989;14:947-52.
10. Mallery JA, Tobis JM, Griffith J, et al. Assessment of normal and atherosclerotic arterial wall thickness with an intravascular ultrasound imaging catheter. Am Heart J 1990;119:1392-400.
11. Nishimura RC, Edwards WD, Warnes CA, et al. Intravascular ultrasound imaging: in vitro validation and pathologic correlation. J Am Coll Cardiol 1990;16:145-54.
12. Potkin BN, Bartorelli AL, Gessert JM, et al. Coronary artery imaging with intravascular ultrasound. Circulation 1990; 81:1575-85.
13. Tobis JM, Mallery JA, Gessert J, et al. Intravascular ultrasound cross-sectional arterial imaging before and after balloon angioplasty in vitro. Circulation 1989;80:873-82.
14. Gussenhoven WJ, Essed CE, Frietman P, et al. Intravascular echographic assessment of vessel wall characteristics: a correlation with histology. Int J Card Imaging 1989;4:105-16.
15. Sorber CWJ, De Jong AAW, Den Breejen NJ, De Bruijn WC. Quantitative energy-filtered image analysis in cytochemistry. Ultramicroscopy 1990;32:55-68.
16. Wenguang L, Gussenhoven WJ, Zhong Y, et al. Validation of quantitative analysis of intravascular ultrasound images. Int J Card Imaging 1991;6:247-53.
17. Patton DD. Introduction to clinical decision making. Semin Nucl Med 1978;8:273-84.
18. Crawford T, Levene CI. Medial thinning in atheroma. Journal of Pathology and Bacteriology 1953;66:19-23.
19. Gussenhoven E, Pijl A, Frietman P, et al. Thinning of the media in atherosclerosis: an in vitro/in vivo intravascular ultrasound study [Abstract]. Circulation 1990;82:(suppl III): 458.
20. Lakatta EG, Mitchell JH, Pomerance A, Rowe G. Human aging: changes in structure and function. J Am Coll Cardiol 1987;10:42-7.
21. Haust MD. Atherosclerosis: lesions and sequelae. In: Silver MD, ed. Cardiovascular pathology. New York: Churchill-Livingstone, 1983:191-315.
22. Davies MJ. The pathology of ischemic heart disease. In: Desmond DG, Camm JA, Fox KM, Hall RJC, Poole-Wilson PA, eds. Diseases of the heart. London: Ballière Tindall, 1989:1035-49.
23. Waller BF. Anatomy, histology and pathology of the major epicardial coronary arteries relevant to the echocardiographic imaging techniques. J Am Soc Echocardiogr 1989;2:232-52.
24. Siegel RJ, Swan K, Edwalds G, Fishbein MC. Limitations of postmortem assessment of human coronary artery size and luminal narrowing: differential effects of tissue fixation and processing on vessels with different degrees of atherosclerosis. J Am Coll Cardiol 1985;5:342-6.
25. Glagov S, Weisenberg E, Zatins CK, Stankunavicus R, Kolettis GJ. Compensatory enlargement of human atherosclerotic coronary arteries. N Engl J Med 1987;316:1371-5.
26. McPherson DD, Kerber RE. New insights into the pathophysiology of coronary arteries by epicardial high-frequency echocardiography. J Am Soc Echocardiogr 1989;2:284-95.
27. Moriuchi M, Tobis JM, Mahon D, et al. The reproducibility of intravascular ultrasound imaging in vitro. J Am Soc Echocardiogr 1990;3:444-50.
28. Gurley JC, Nissen SE, Diaz C, Fischer C, O'Connor WN, DeMaria AN. Is the three-layer appearance an artifact? Differences between in vivo and in vitro intravascular ultrasound [Abstract]. J Am Coll Cardiol 1991;17:112A.
29. De Kroon MGM, Gussenhoven WJ, Serruys PW, Roelandt JRTC, Bom N. Varying blood echogenicity over the cardiac

cycle showing dynamics of erythrocyte aggregation. Ultrasound Med Biol 1991;17:121-6.
30. Gussenhoven EJ, The SHK, Serruys PW, et al. Intravascular ultrasound and vascular intervention. Journal of Interventional Cardiology 1991;4:41-8.
31. Nissen SE, Gurley JC, Booth DC, McClure RR, Berk MR, DeMaria AN. Spectrum of intravascular ultrasound findings in atherosclerosis: wall morphology and lumen shape in coronary artery disease patients [Abstract]. J Am Coll Cardiol 1991;17:93A.
32. Davidson CJ, Sheikh KH, Harrison KJ, et al. Intravascular ultrasonography versus digital subtraction angiography: a human in vivo comparison of vessel size and morphology. J Am Coll Cardiol 1990;16:633-6.
33. Sheikh KH, Davidson CJ, Kisslo KB, et al. Comparison of intravascular ultrasound, external ultrasound and digital angiography for evaluation of peripheral artery dimensions and morphology. Am J Cardiol 1991;67:817-22.

CHAPTER 5

PASSIVE AND ACTIVE COMPONENTS OF LARGE ARTERY COMPLIANCE: AN IN-VIVO INTRAVASCULAR ULTRASOUND STUDY

Richard A. Wilson, M.D.; Carlo Di Mario, M.D.; Rob Krams, M.D.;
Anne C. Laird, M.D.; Loe Kie Soei, M.D.; Salem H.K. The, M.D.;
Elma Gussenhoven, M.D.; Pieter Verdouw, Ph.D., Jos RTC Roelandt, M.D.

From The Thoraxcenter, Erasmus University Rotterdam, and The Interuniversity Cardiology Institute, The Netherlands

Supported by: NIH-PHS Fogarty Senior International Fellowship Award #1F06 TWO1633-01 (RAW), the Dutch Heart Foundation Grant (RK), European Society of Cardiology Research Fellowship (CDM), and the Interuniversity Cardiology Institute, The Netherlands.

ABSTRACT

Background: Previous studies have suggested that the compliance of large arteries is a purely passive phenomenon, dependent only on elastin and collagen constituents of the arterial wall. However, the presence of smooth muscle fibers in the wall of these large arteries would suggest that arterial compliance might change in response to vasoactive substances. Thus, the purpose of this study is to determine the basal level of vasomotor tone in these arteries and to determine if the compliance of large conductance arteries can be altered in-vivo by vasoactive agents.
Methods and Results: Proximal iliac arterial compliance was measured in 7 anesthetized pigs, before and during local infusions of adenosine and norepinephrine. Luminal area was measured every 40 ms using a 30 MHz intravascular ultrasound catheter and an automatic edge detection program. Simultaneous high-fidelity pressure measurements were obtained using a catheter-tipped pressure microtransducer positioned at the origin of the iliac artery. Linear regression analysis of the area/pressure relationship in 2 consecutive cardiac cycles (systolic phase only) was performed before and during adenosine and norepinephrine infusions. The slope of the area/pressure regression line was defined as an index of arterial compliance. Measurements after 3 min of infusions of adenosine (5 - 5000 μg/min) and norepinephrine (0.01 - 10 μg/min) were compared with the control measurements. Even at the highest infusion rate, adenosine did not significantly increase arterial compliance compared to baseline (25 ± 7 vs. 19 ± 4 $mm^2/mmHg \times 10^{-3}$, respectively, p=ns). In contrast, norepinephrine decreased arterial compliance compared to the second baseline control (13 ± 3 vs. 20 ± 3 $mm^2/mmHg \times 10^{-3}$, respectively, $p < 0.01$).
Conclusions: Arterial compliance may be modified more by the acute infusion of norepinephrine than of adenosine in large conductance arteries such as the proximal iliac. Thus, in this animal model, smooth muscle tone tends to be minimal and arterial compliance near maximal (i.e., mostly a passive phenomenon). However, arterial compliance does not remain purely passive since smooth muscle tone can be increased by norepinephrine (resulting in decreased arterial compliance). Intravascular ultrasound allows continuous and accurate monitoring of these changes of arterial dimensions, suggesting that this technique can be useful in the evaluation of pharmacologically induced changes in compliance of large arteries.

Key Words: adenosine, norepinephrine, intravascular ultrasound.

INTRODUCTION

Previous studies have suggested that the compliance of large arteries is a purely passive phenomenon - dependent only on elastin and collagen constituents of the arterial wall [1-5] and the arterial distending pressure. However, the presence of smooth muscle cells within the wall of large conductance arteries such as the iliac would suggest that there may be an additive role for active smooth muscle contraction (increased resting tone) modifying arterial diameter and compliance. Early studies of large artery compliance attempted to characterize the compliance

in-vitro, where smooth muscle tone may not have been preserved [3,4,6]. More recent work using external ultrasound in an in-vitro model has demonstrated changes in vascular compliance Neural factors however, are absent in such a preparation [7]. In-vivo studies have demonstrated changes in large artery compliance in response to neural stimulation [8,9] as well as to pharmacologic agents [10-13]. However, these studies used external [8] or intraluminal [10,11] dimension gauges or surgically implanted ultrasonic dimension crystals [9,12,13] which may alter the vascular response to neural or pharmacologic agents and assume a circular shape to calculate luminal area. The development of intravascular ultrasound allows accurate in-vivo measurements of arterial luminal area on a beat-by-beat basis [14-16]. Thus, simultaneous measurement of arterial pressure and luminal area should allow accurate calculation of local compliance without disturbing the artery. Accordingly, the purpose of this study is: 1) to assess the feasibility of serial measurements of local arterial compliance in a large conductance artery, 2) to determine if pharmacologically-induced changes in local compliance occur during in-vivo conditions, and 3) to gain some insight as to the level of resting smooth muscle tone in the artery.

METHODS

Surgical Preparation:

After an overnight fast, cross-bred Landrace x Yorkshire pigs of either sex (n=7, 24-28 kg) were sedated with an intramuscular injection of 500 mg ketamine (A.U.V. Cuijk, The Netherlands), anesthetized with 150 mg metomidate (Janssen Pharmaceutica, Beerse, Belgium) intravenously, intubated and ventilated, using a volume controlled respirator, with a mixture of oxygen and nitrous oxide (1:2). Respiration rate and tidal volume were regulated to maintain arterial blood gases within the physiological range: pH 7.35-7.45, $pC0_2$ 35-45 mmHg, and pO_2 120-180 mmHg. A catheter was placed in the superior vena cava via the left jugular vein for administration of fluids and sodium pentobarbital (Sanofi, Paris, France), 25 mg/kg during the first half hour followed by a continuous infusion of 10 mg/kg/hr. An 8F micromanometer-tipped catheter (Honeywell-Philips, Best, The Netherlands) was placed in the proximal left common iliac artery via the left carotid artery. To calibrate the micromanometer-tipped catheter and to guide placement of the 5F intravascular ultrasound catheter (Du-Med, The Netherlands) an 8F fluid-filled sheath was placed in the left femoral artery. The side arm of the sheath was attached to a pressure transducer. Under fluoroscopic guidance the ultrasound catheter and the micromanometer-tipped catheter were advanced into the left common iliac artery from opposite directions so that the ultrasound catheter was 1-2 cm distal to the micromanometer-tipped pressure catheter. This pressure catheter also had a small distal side-hole which was used for local infusions of adenosine and norepinephrine. To alter venous return and thereby decrease systemic arterial pressure during norepinephrine infusion, a 5F balloon-tipped Swan-Ganz catheter was placed in the inferior vena cava via the

right femoral vein. The balloon was inflated only if systemic pressure rose during the higher doses of norepinephrine.

Data Acquisition:

Simultaneous pressure recordings and ultrasound images were acquired at each study time point. The pressure signal was simultaneously acquired on the ultrasound videotape as well as on a strip chart recorder. Simultaneous pressure calibration was performed on both recordings. End-expiratory heart beats were used for all subsequent data analysis at each drug infusion level. Ultrasound images were acquired using a 30 MHz mechanically rotated transducer providing 16 frames per second.

Experimental Protocol:

After a 20 min. stabilization period, baseline ultrasound and pressure measurements were obtained. These were followed by intra-arterial infusions of increasing concentrations of adenosine and later norepinephrine into the proximal left iliac artery at rates of 1 or 2 ml/min. Infusions of adenosine (0.005, 0.05, 0.5, and 5.0 mg/min) or norepinephrine (0.001, 0.01, 0.1, 1.0, and 10 μg/min) were continued for 3 min. prior to data acquisition. There was a 3-4 min. waiting period between different concentrations of each drug. There was a 15-20 min. washout period between adenosine and norepinephrine infusions. Prior to the infusion of norepinephrine, a second baseline was obtained.

Data Analysis:

Luminal area of the left common iliac artery was measured on the intravascular ultrasound images using a previously described semiautomatic frame-to-frame tracking algorithm [14]. Briefly, this is a template-matching method which allows the measurement of the frame-to-frame changes in the luminal cross-sectional area from ultrasound images through the analysis of the regional wall displacement. The matching is performed by calculating a cross-correlation coefficient between the template image (taken at end-diastole) and the subsequent images throughout the cardiac cycle. The optimal matching is determined using the minimal-cost algorithm. This algorithm finds a path around the inner edge of the arterial wall based on the quality of the match at different radial positions to satisfy the constraints of smoothness and connectivity. This method proved to be more accurate for measuring small changes in arterial lumen area as compared to manual tracing (percent coefficient of variability 1.0% and 2.7%, respectively [14]). For each steady state infusion rate, 2 beats were analyzed and the results averaged. The simultaneous pressure was measured from the videotape to ensure no delays between the pressure and the luminal area measurement. Pressure measurements from the strip chart recorder were used to confirm the accuracy of the pressure measurements derived from the videotape recordings.

Local compliance of the left common iliac artery was calculated from matched area and pressure measurements from 2 consecutive beats as the slope of the area/pressure relationship. To avoid variations in luminal area due to hysteresis, only the end-diastolic and subsequent systolic data points were used. Depending on the heart rate, 8-15 data points were used to calculate the slope of the area/pressure relationship. Luminal area at a given pressure of 80 mmHg was also calculated from the linear regression equation derived from the area/pressure relationship.

Statistical Analysis:

Diffences between baseline and drug infusion values were determined by ANOVA with repeated measures analysis. A p value of < 0.05 was considered significant. Data are expressed as mean ± sem.

RESULTS

Systemic Hemodynamics:

Systemic hemodynamic measurements at baseline and during increasing doses of adenosine and norepinephrine are shown in Table 1. Heart rate did not change significantly with adenosine infusion, but decreased slightly at the highest dose of norepinephrine (10 μg/min). Systolic and mean arterial pressure did not change with either adenosine or norepinephrine infusion. However, diastolic pressure was slightly lower at the highest infusion rate of adenosine (5 mg/min). Baseline heart rates and blood pressures pre-adenosine and pre-norepinephrine were not significantly different.

Arterial Compliance:

Arterial compliance of the iliac artery did not change significantly with increasing doses of adenosine (Table 1). However, with norepinephrine infusion there was a progressive fall in compliance. At a given pressure of 80 mm Hg, the luminal area of the iliac artery did not change in response to increasing concentrations of locally infused adenosine. In contrast, increasing concentrations of norepinephrine resulted in progressively smaller luminal areas (Figure 1). There were no differences between the first and second baseline values for either arterial compliance or luminal area at 80 mmHg.

DISCUSSION

This study demonstrates the ability of intravascular ultrasound to measure arterial compliance in-vivo and to determine the resting tone of the artery by its response to vasodilating and vasoconstricting pharmacologic agents. Arterial compliance of the iliac artery was not significantly altered by the infusion of adenosine but was

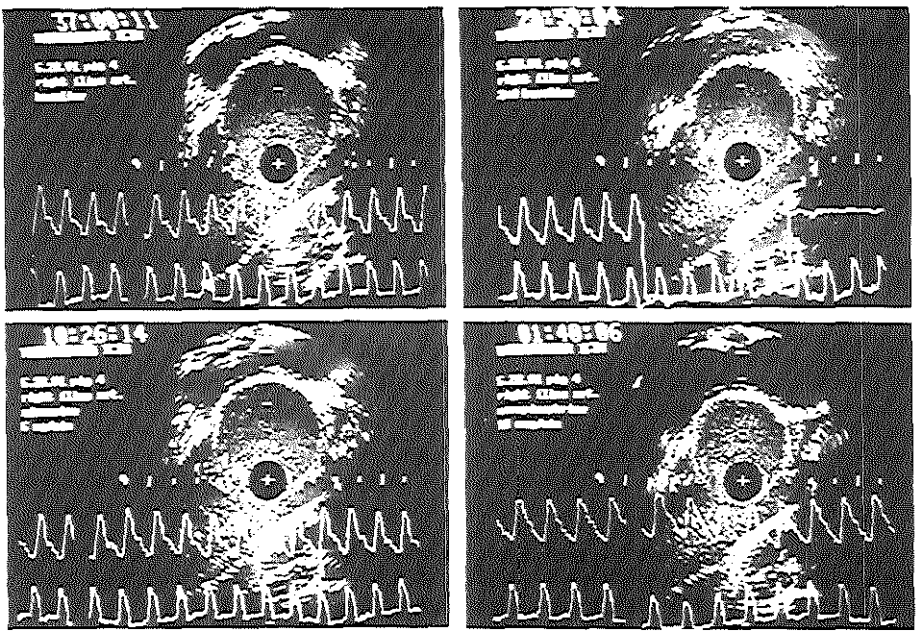

Fig. 1. Intravascular ultrasound end-diastolic images of baseline (upper left panel), during adenosine (lower left panel), second baseline (upper right panel), and during norepinephrine (lower right panel) demonstrate the absence of vasodilation in response to adenosine but the presence of vasoconstriction in response to norepinephrine.

Table 1. Hemodynamic Parameters and Arterial Compliance

	Adenosine (mg/min)					Norepinephrine (μg/min)				
	BL	.005	.05	.5	5	BL	.01	.1	1	10
HR	90	89	90	91	93	89	86	84	84	82*
(1/min)	±4	±4	±3	±3	±3	±4	±3	±3	±3	±2
SBP	110	110	112	109	105	110	103	102	103	106
(mmHg)	±8	±8	±8	±7	±5	±7	±8	±7	±6	±8
MBP	86	85	87	84	77	85	82	83	83	86
(mmHg)	±6	±6	±6	±5	±6	±5	±5	±6	±5	±6
DBP	75	73	76	74	66*	73	71	73	74	76
(mmHg)	±5	±5	±5	±4	±4	±4	±5	±5	±5	±5
LA 80	21	20	21	21	23	21	20	21	19*	13*
(mm^2)	±4	±3	±3	±3	±3	±3	±3	±3	±3	±3
AC	19	25	16	19	25	20	18	15	14	13*
(mm^2/mmHg) x 10^{-3}	±4	±7	±2	±4	±7	±3	±3	±3	±3	±3

Bl = baseline, HR = heart rate, SBP = systolic blood pressure, MBP = mean blood pressure, DBP = diastolic blood pressure, LA 80 = luminal area at 80 mmHg, AC = arterial compliance (the change in area/the change in pressure), * = $p < 0.05$ vs. baseline.

significantly decreased by norepinephrine. Thus, it appears that resting large artery tone in this experimental preparation is low. Previous studies have suggested that the compliance of large arteries is purely a passive phenomenon dependent only on the elastin and collagen constituents of the arterial wall [1-5,17]. The present study suggests that, in the resting state, the compliance of large conductance arteries such as the iliac is indeed mostly a passive phenomenon. However arterial compliance does not remain purely passive since smooth muscle tone can be increased by norepinephrine resulting in decreased arterial compliance. Thus, large conductance arteries are not purely passive conduits under all conditions.

Study limitations:

There are several potential limitations in this study. The method involves the use of 2 catheters, one to measure pressure and the other to measure luminal area. This currently restricts the use of this methodology to large arteries. However, smaller pressure and intravascular ultrasound catheters are being developed to lessen this size limitation.

The invasive nature of the methodology raises the possibility that the catheter itself may affect the accuracy of the measurement of compliance. If the catheters were large relative to the arterial lumen, there could be a pressure gradient in the area of the measurement. For this reason an artery was chosen that had a much larger luminal area (approximately 5 times larger) than the size of the catheters. Arterial spasm induced by the ultrasound catheter could also potentially alter the measurement of arterial compliance. In this study it is unlikely that arterial spasm occurred since the artery did not dilate in response to adenosine but did constrict in response to norepinephrine. If spasm had been present, one would have expected the artery to have dilated in response to adenosine and to have not constricted in response to norepinephrine.

The spatial and temporal resolution of the intravascular ultrasound system could potentially limit the accuracy of the measurement of arterial compliance. The axial resolution of the ultrasound imaging system was 80 μm. The lateral resolution of the ultrasound catheter used in this study was less than 225 μm at a depth of 1 mm. Previous work has documented the ability of the intravascular ultrasound to reproducibly detect changes in arterial area of 1-2% [14]. In the present study the physiologic changes in luminal area exceeded these limits. However in smaller arteries or in atherosclerotic arteries the spatial resolution or variability of the luminal area measurements may not be sufficient to reliably measure changes in luminal area in response to changes in pressure. The temporal resolution of the ultrasound system was limited to 16 frames per second. It is possible that larger changes in luminal area could have been detected if the temporal resolution was better.

Adenosine was chosen as the vasodilator to induce smooth muscle relaxation and thus increase arterial compliance because of its rapid onset of action and its rapid metabolism to allow serial studies in same animal. Adenosine has a major effect on smooth tone at the arteriolar level [18], but it is unclear as to the extent to which adenosine exerts an effect on the smooth muscle in larger vessels. However, previous

work has demonstrated a significant vasorelaxing effect of adenosine on large isolated, precontracted vessels [19-22].

Pentobarbital was used as the anesthetic in this study. In sheep anesthetized with pentobarbital, the aortic smooth muscle response to methoxamine was attenuated compared to the unanesthetized state [12]. Also pentobarbital has been shown to attenuate contractions of rat aorta strips induced by epinephrine, serotonin, and potassium chloride [23]. However, other studies demonstrated changes in characteristic impedance in response to α-adrenergic blockade with phenoxybenzamine in dogs receiving pentobarbital anesthesia [13]. Thus, pentobarbital may have attenuated the α-adrenergic response to norepinephrine by the porcine iliac artery used in this study.

In conclusion, intravascular ultrasound can be used to study the compliance of large conductance arteries in the anesthetized swine. Under these experimental conditions, vasomotor tone appears to be minimal and arterial compliance of the iliac artery near maximal. However, vasoconstriction in response to norepinephrine suggests that even large conductance arteries can alter their compliance and thus influence arterial impedance.

ACKNOWLEDGMENTS

The authors gratefully acknowledge the excellent technical assistance of Li Wenguang, MSc.

REFERENCES

1. Nichols WW, O'Rourke M: McDonald's Blood flow in arteries: theoretic, experimental and clinical principles. Philadelphia, Lea & Febiger, 1990, p 99.
2. Remington JW: The physiology of the aorta and major arteries. In Handbook of Physiology: Circulation. Washington D.C., Am Physiol Soc 1963, II:799-838.
3. Bergel DH: The static elastic properties of the arterial wall. J Physiol 1961;156:445-457.
4. Learoyd BM, Taylor MG: Alterations with age in the viscoelastic properties of human arterial walls. Circ Res 1966;18:278-292.
5. Bader H: Dependence on wall stress in the human thoracic aorta on age and pressure. Circ Res 1967;20:354-361.
6. Hallock P, Benson IC: Studies on the elastic properties of human isolated aorta. J Clin Invest 1937;16:595-602.
7. Fischell TA, Grant G, Johnson DE: Determinants of smooth muscle injury during balloon angioplasty. Circulation 1990;82:2170-2184.
8. Gerova M, Gero J: Range of the sympathetic control of the dog femoral artery. Circ Res 1969;24:349-359.
9. Pagani M, Schwartz PJ, Bishop VS, Malliani A: Reflex sympathetic changes on aortic diastolic pressure-diameter relationship. Am J Physiol 1975;229:286-290.
10. Pieper HP, Paul LT: Responses of aortic smooth muscle studied in intact dogs. Am J Physiol 1969;217:154-160.
11. Nicolosi GR, Pieper HP: Aortic smooth muscle responses to changes in venous return in intact dogs. Am J Physiol 1971;221:1209-1216.

12. Pagani M, Mirsky I, Baig H, Manders WT, Kerkhof P, Vatner SF: Effects of age on aortic pressure-diameter and elastic stiffness-stress relationships in unanesthetized sheep. Circ Res 1979;44:420-429.
13. Stone DN, DuJardin J-PL: Changes in smooth muscle tone influence characteristic impedance of the aorta. Am J Physiol 1984;246:H1-H7.
14. Wenguang L, Gussenhoven WJ, Bosch JG, Mastik F, Reiber JHC, Bom N: A computer-aided analysis for the quantitative assessment of intravascular ultrasound images, in Proceedings of Computers in Cardiology. Los Alanitos, IEEE Computer Society Press, 1990:333-336.
15. Wenguang L, Gussenhoven WJ, Zhong Y, The SHK, DiMario C, Madretsma S, van Egmond F, de Feyter P, Pieterman H, van Urk H, Rijsterborgh H, Bom N: Validation of quantitative analysis of intravascular ultrasound images. Int J Card Imaging 1991;6:247-253.
16. The SHK, Gussenhoven EJ, Wenguang L, de Feyter P, Serruys PW, Wilson RA, Bom K: Intravascular ultrasound assessment of lumen geometry and distensibility of the angiographically normal artery: a correlation with quantitative angiography. Echocardiography 1992;9:133-139.
17. Peterson LH, Jensen RE, Parnell J: Mechanical properties of arteries in vivo. Circ Res 1960;8:622-639.
18. Rubio R, Berne RM: Release of adenosine by the normal myocardium and its relationship to the regulation of coronary resistance. Circ Res 1969;25:407-415.
19. Sabouni MH, Hussain T, Cushing DJ, Mustafa SJ: G proteins subserve relaxations mediated by adenosine receptors in human coronary artery. J Cardiovasc Pharmacol 1991;18:696-702.
20. Brizzolara AL, Burnstock G: Endothelium-dependent and endothelium-independent vasodilatation of the hepatic artery of the rabbit. Br J Pharmacol 1991;103:1206-12.
21. Samson SE, Berezin I, Finkle TJ, Grover AK: Relaxation of coronary artery smooth muscle cells. Arch Intern Pharmacodyn Therap 1991;310:22-34.
22. Merkel LR, Lappe RW, Rivera LM, Cox BF, Perrone MH: Demonstration of vasorelaxant activity with an A1-selective adenosine agonist in porcine coronary artery: involvement of potassium channels. J Pharmacol Exp Therap 1992;260:437-43.
23. Altura BT, Altura BM: Pentobarbital and contraction of vascular smooth muscle. Am J Physiol 1975;229:1635-1640.

CHAPTER 6

THE ANGLE OF INCIDENCE OF THE ULTRASONIC BEAM: A CRITICAL FACTOR FOR IMAGE QUALITY IN INTRAVASCULAR ULTRASONOGRAPHY

Carlo Di Mario, M.D., Stanley Madretsma, M.D., David T. Linker, M.D., Salem H.K. The, M.D., Nicolaas Bom, Ph.D., Patrick W. Serruys, M.D., Ph.D., Elma J. Gussenhoven, M.D., Ph.D., Jos R.T.C. Roelandt, M.D., Ph.D.

From the Department of Cardiology, Thoraxcenter, Rotterdam, and the Interuniversity Cardiology Institute, The Netherlands

Reprinted from: Am Heart J, 1992.

The angle of incidence of the ultrasonic beam: A critical factor for the image quality in intravascular ultrasonography

The effects of the angle of incidence of the ultrasound beam on the image quality were studied in 21 pressurized arterial specimens examined with a 30 MHz intravascular ultrasonographic catheter. When the ultrasonographic catheter was in an eccentric position in the vessel lumen, the videodensity of the segments of the vessel wall with the least favorable angle of interrogation (a shift of 49 ± 6 degrees from the tangent to the tissue surface) was 27% ± 19% lower than the videodensity measured with the catheter in the center of the lumen. When the catheter was placed in a position that was not parallel to the long axis of the vessel, a further decrease was observed, especially in the vessel wall opposite the position of the catheter. An artificial dissection was induced in eight specimens. Dropouts that involved the dissection plane and the underlying structures were produced with positions of the echographic catheter inducing a narrow angle between ultrasound beam and dissection plane. These experimentally induced artifacts were compared with similar findings from the in vivo evaluation of peripheral and coronary arteries. The angle of incidence of the ultrasound beam is a major determinant of the image quality in intravascular ultrasonography. Angle-dependent artifacts occur with eccentric and noncoaxial positions of the ultrasonographic catheter and, in particular, with imaging of large intraluminal dissections. Awareness of this problem may prevent image misinterpretation and has relevance for future improvement of catheter technology and design. (AM HEART J 1993;125:442.)

Carlo Di Mario, MD,[a] Stanley Madretsma, MD,[a] David Linker, MD,[a]
Salem H. K. The, MD,[b] Nicolaas Bom, PhD,[b] Patrick W. Serruys, MD,[b]
Elma J. Gussenhoven, MD,[b] and Jos R. T. C. Roelandt, MD[a]
Rotterdam, The Netherlands

From [a]the Department of Cardiology, Thoraxcenter, Erasmus University Rotterdam and [b]the Interuniversity Cardiology Institute, The Netherlands.

Received for publication Apr. 20, 1992; accepted Aug. 14, 1992.

Reprint requests: Carlo Di Mario, MD, Thoraxcentre, Ee 2332 P.O. Box 1738, 3000 DR Rotterdam, The Netherlands.

Dr. C. Di Mario, Division of Cardiology, Vicenza, Italy, is the recipient of the European Society of Cardiology Research Fellowship 1991.

Images that are obtained with intravascular ultrasonography show great variability in quality and create problems in interpretation.[1-3] An ideal, perpendicular angle of incidence of the ultrasound beam to the vessel wall requires a catheter position in the center of the lumen and parallel to the long axis of the vessel. In practice, several factors (e.g., curvature of

0002-8703/93/$1.00 + .10 4/1/42650

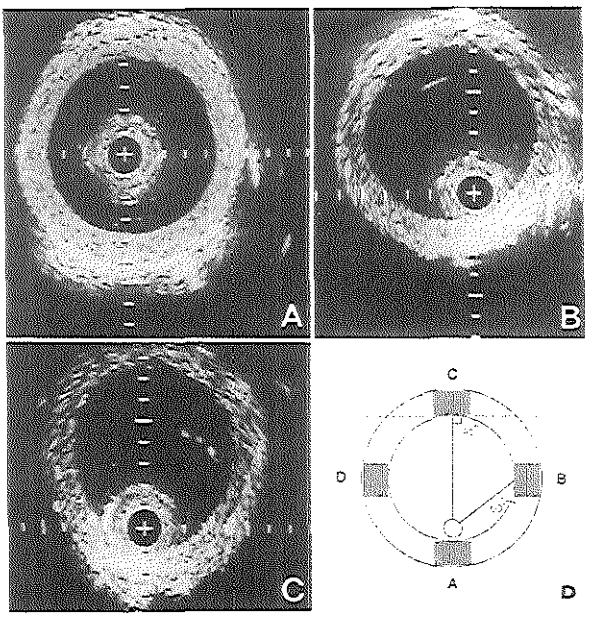

Fig. 1. Three intravascular ultrasonographic images of a common carotid artery (elastic type of artery as determined from histologic studies) examined in vitro, with internal pressure maintained at 100 mm Hg. **A,** The catheter is in the center of the vessel lumen, and the vessel wall shows a uniform intensity. **B,** The catheter is eccentric in the lumen but parallel to the long axis of the vessel. Note the well-preserved circular shape of the lumen, with a maximal videodensity of the vessel wall in the segment beside the catheter and a minimal videodensity in the lateral walls. **C,** When the catheter is not parallel to the long axis of the vessel, the lumen becomes elliptic, with a further decrease in videodensity of the vessel wall and especially of the segment opposite the catheter (calibration = 1 mm). **D,** The drawing shows the position of the regions of interest in which the videodensity has been measured.[4] The angle of incidence of the ultrasound beam is measured as the angle included between the tangent to the midpoint of the intimal surface of the segment of interest and the line joining this point with the center of the catheter.

the vessel, wall irregularities, or dissections) may preclude this optimal situation. In an attempt to improve interpretation of in vivo intravascular ultrasonographic images we reproduced and quantitatively studied angle-dependent artifacts in in vitro pressurized arteries with and without artificially induced arterial wall dissections.

METHODS

Material. Twenty-one arterial specimens of 5 to 6 cm in length were obtained from 13 subjects at autopsy (18 common or external iliac arteries and 3 common carotid arteries). One end of the arterial specimen was closed, and the other was tied to a 7F valved sheath. Saline solution was injected through the side arm of the sheath, and the pressure, which was monitored with a Gould P23ID pressure transducer (Viggo-Spectramed Inc., Critical Care Div., Oxnard, Calif.), was increased to 100 mm Hg and maintained at this level throughout the examination. A 5F 30 MHz rotating element ultrasonographic catheter (DuMed, Rotterdam, The Netherlands)[3] was advanced to the midpoint of the arterial segment through the valved sheath. The internal diameters of the examined vessels were measured at 100 mm Hg with a previously described analysis program[4] and ranged from 6.2 to 8.9 mm (mean, 7.4 ± 1.4 mm).

Intravascular ultrasonographic examination. Cross-sectional imaging was performed with the catheter positioned both in the center of the vessel lumen and close to the vessel wall (Fig. 1, *A* and *B*). The time-gain compensation was unchanged throughout the examination procedure. Subsequently, the closed end of the vessel was raised, which simulated a curvature of 10 to 50 degrees between the proximal segment of the vessel that contained the

echographic catheter and the imaged distal segment of the vessel (Fig. 1, *C*). A previously described computerized system[5] was used to calculate the mean videodensity of four regions of interest, which were situated along the circumference of the vessel wall as shown in Fig. 1, *D*. These measurements were performed with the catheter positioned centrally in the vessel lumen, close to the vessel wall (eccentric position), and noncoaxial with the long axis of the vessel. The angle of interrogation of these regions was measured as the angle between the tangent to the vessel wall and the line that connected the midpoint of the intimal contour of the region of interest with the center of the catheter (Fig. 1, *D*).

In 8 of these 21 specimens an artificial dissection was created by careful separation of the internal and external parts of the vessel wall through half of the circumference of the vessel. The specimens were then embedded in an agar-agar solution with the induced flap largely protruding inside the vessel lumen. Cross-sectional ultrasonic imaging was performed with the ultrasonographic catheter placed in various positions within the true and false lumens of the vessel. The examined positions of the vessel were marked with India ink and corresponding histologic cross-sections (5 μm in thickness) were obtained and stained with hematoxylin azophloxine and Verhoeff's Elastin van Gieson.

Statistical analysis. Analysis of variance (Fisher's exact test) was used to detect the presence of significant differences in videodensity for each position of the transducer. When this test was statistically significant (eccentric and noncoaxial positions) a paired *t* test was used to compare each pair of regions of interest. An unpaired *t* test was used to compare the difference in videodensity of corresponding areas that were examined with different positions of the transducer.

RESULTS

As determined from histologic examination, 13 arteries were classified as muscular, 5 as elastic, and 3 as transitional according to previously reported criteria.[6] A thin layer of diffuse fibrous intimal thickening was observed in 19 arteries. Two arteries showed an atherosclerotic plaque in the studied cross-section. In the eight arteries that were used as a model of wall dissection, the dissected wall was composed of a thickened intimal layer in two cases, intima and the full thickness of the medial layer in three cases, and intima and part of the media in three cases. With the exception of the two arteries with focal atherosclerotic plaques, the videodensity of the four regions of interest (Fig. 1, *D*) was similar when the catheter was in a central position in the vessel lumen (Fig. 2).

Eccentric position of the catheter. When the catheter was positioned close to the vessel wall, the videodensity was higher in the segment close to the ultrasonographic transducer (segment A) and was lower in the opposite vessel segment (segment C) (Fig. 2) ($p < 0.01$). The maximal reduction in videodensity, however, was not observed in the position of maximal distance from the transducer but in the lateral segments (segments B and D in Fig. 2) ($p < 0.01$). For these two areas the angle between the ultrasound beam and the examined vessel segment was 49 ± 6 degrees, and the mean videodensity was 27% ± 19% lower than the videodensity that was measured when the catheter was in a central position ($p < 0.02$).

Noncoaxial orientation of the catheter. In the model that was used in this study, when the catheter was not parallel to the long axis of the imaged vessel, the catheter was also in an eccentric position in the vessel lumen (Fig. 1, *C*). Thus the observed changes in videodensity were the combined result of the changes in two planes of the angle of incidence of the ultrasound beam. In comparison with the measurements in an eccentric but coaxial position, a further decrease in videodensity was observed, especially in the segment opposite the position of the catheter (NS).

Wall dissection. In the presence of a dissected flap inside the vessel lumen, extremely narrow angles between ultrasound beam and plane of dissection could be induced by manipulating the catheter both in the true lumen and the false lumen (Fig. 3). In these positions, the dissected flap could not be visualized with ultrasonography. Furthermore, the dissected flap concealed the underlying lumen and vessel wall so that the identification of dimensions and shape of the true and false lumens became impossible. These effects were dependent only on the angle of incidence of the ultrasound beam. Thickness, severity of intimal fibrosis, and presence or absence of medial layer in the dissected flap did not influence the results.

Atherosclerotic plaques. Fig. 4 shows that the delineation and characterization with intravascular ultrasonography of the atherosclerotic plaque is more difficult when this structure is imaged with an unfavorable angle of incidence.

DISCUSSION

The ratio of the dimensions of the wavelength of the incident beam to the dimensions of the target structure is a major determinant of the backscattered power. If the dimensions of the target are much smaller than those of the beam wavelength, the object behaves as an ideal point scatterer, and its backscatter is similar in all directions. On the contrary, larger structures cause a directional backscatter that depends on the shape of these structures. For a simple flat interface, the backscattered energy decreases if the angle between the ultrasonic beam and the normal to the tissue surface increases. When these basic principles are applied to intravascular ultra-

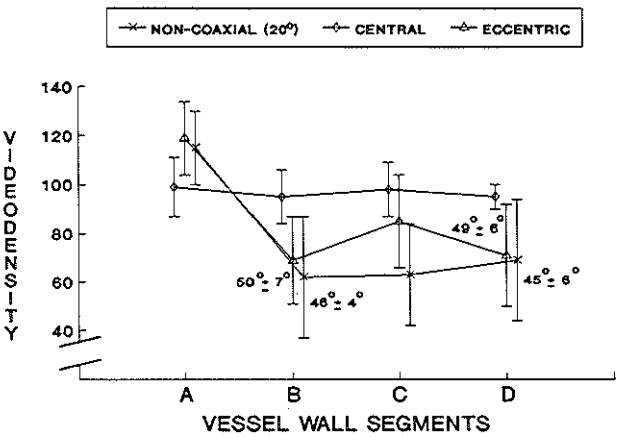

Fig. 2. The graph shows the videodensity of the four selected regions of interest (as indicated in Fig. 1, *D*) of 21 pressurized specimens. The videodensity is measured in arbitrary units. With the catheter in a central position *(upper line)* the regions of interest show a similar videodensity. The eccentricity of the catheter induces *(middle line)* an angle of 49 ± 6 degrees between the ultrasound beam and the tangent to the vessel wall in regions *B* and *D* and a consequent mean reduction of 27% of their videodensity. The noncoaxial position of the catheter, with an angle of 20 degrees with the long axis of the vessel *(lower line)*, induces a further decrease in videodensity, especially in position *C* (opposite wall). The angles between ultrasound beam and tissue surface in segments *B* and *D* (lateral walls) are measured for eccentric positions of the catheter according to the drawing in Fig. 4.

sonographic imaging, red blood cell dimensions are similar to the wavelength of the high-frequency (30 MHz) transducers which are used so that the backscatter of blood can be considered omnidirectional. The behavior of the vessel wall, on the contrary, is inhomogeneous and dependent on the dimension, shape, and orientation of its components, with the presence of various levels of directional backscatter. The uniform directional backscatter of the red blood cells explains why areas of vascular lumen are well delineated in Fig. 5, *A* and *B*, whereas the adjacent vessel walls show large dropouts.

In vitro studies. Picano et al,[7] several years before the development of intravascular ultrasonography, reported that a strongly angle-dependent backscatter is typical of calcific and fibrous plaque components, whereas fatty plaques have a less directive pattern. More recently, de Kroon et al.[8] showed an anisotropic behavior of the muscular and elastic medial layers, with a larger angle-dependent reduction of the integrated backscattered power in planes that are parallel to the long axis of the fibers than in planes that are perpendicular to this axis. In these studies, which were carried out with acoustic microscopes, the focus was on potential interest in these changes for tissue characterization. Nishimura et al.[9] used intravascular ultrasonographic catheters to measure circular wells of known diameter. They observed that the luminal dimensions did not change with the position of the catheter as long as it was parallel to the long axis of the well. A noncoaxial orientation at an angle of 30 degrees, on the contrary, resulted in an increase of 20% of the luminal area, which became elliptical.

Our experience suggests that eccentric or noncoaxial positions of the catheter are not only important for the accuracy of the measurements of the lumen area but also that they also influence the quality of the echographic images of both the normal wall and the atherosclerotic plaques. The lack of steerability of the present generation of ultrasonographic catheters precludes an effective correction of eccentric or noncoaxial catheter positions. Improvement in catheter technology and design (steerability of the catheter, multiplane imaging) is desirable to overcome the present limitations of intravascular ultrasonography. A model of artificial dissection was used to understand the images after balloon angioplasty. The complexity of these images is caused by the very narrow angle between the dissected wall and the ultra-

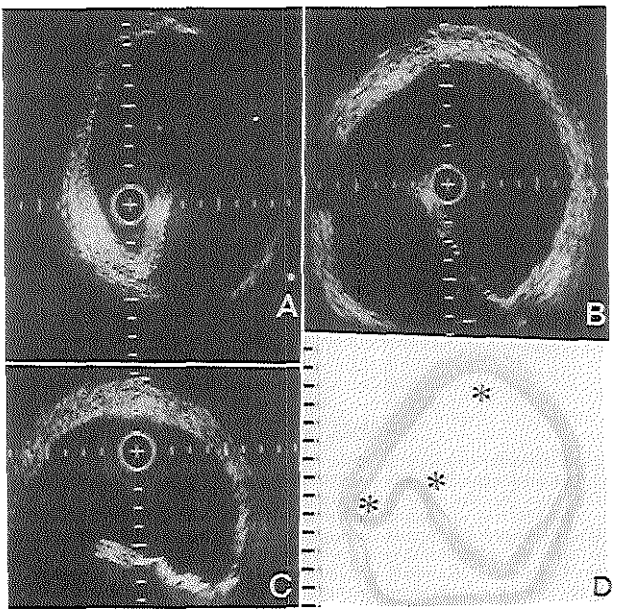

Fig. 3. Panels A-C show three intravascular ultrasonic cross-sections of an iliac artery in which an artificial dissection of the vessel wall is largely protruding inside the lumen. Asterisks mark the positions of the echographic catheter in the corresponding histologic cross-section (**panel D**) for orientation. Complex dropouts of the dissection plane and the underlying vessel wall are induced by narrow angles of incidence of the ultrasound beam on the dissected flap (calibration = 1 mm). **D**, The histologic cross-section shows that the dissection flap consists of a thickened fibrotic intimal layer and part of the degenerated muscular media (Verhoeff's stain; calibration = 1 mm.)

sound beam. The failure to image the vessel wall underlying these dissection flaps is likely to be the result of the decrease in ultrasound energy as it crosses the dissected wall in both directions of the wave propagation (from transducer to underlying structures and vice versa) above a critical angle of incidence of the ultrasound beam.

In vivo studies. An eccentric position of the ultrasonographic catheter, close to the intimal surface of the vessel, is the rule rather than the exception in intravascular ultrasonography. The angle between the ultrasound beam and the vessel wall depends on the dimension of the lumen, and wider angles are observed in larger vessels. The coronary arteries have a small diameter (normally 2 to 4 mm) relative to the diameter of the currently used ultrasonographic catheters (1.0 to 1.6 mm) so that presence and severity of angle-dependent artifacts in these vessels are minimized. In larger vessels, however, partial or complete dropouts of the vessel wall may occur. The echogenicity and the omnidirectional backscatter of blood may allow the tracing of the contour of the vessel lumen despite the presence of relatively large circumferential dropouts of the vessel wall. Complex artifacts, which are due to the presence of large intraluminal dissections, have been common in our experience in patients who were undergoing balloon dilatation of peripheral arteries. Examinations of adjacent cross-sections and knowledge of the principles that underlie the specific features of these images may facilitate their correct interpretation. Unfavorable or eccentric catheter positions have already been reported as a cause of failure or overestimation and distortion of lumen area in intravascular ultrasonographic studies of both peripheral[10-12] and coronary vessels.[13-20] The peculiar characteristics of the artifacts that we observed with large protruding dissections (Fig. 5), however, have not been previ-

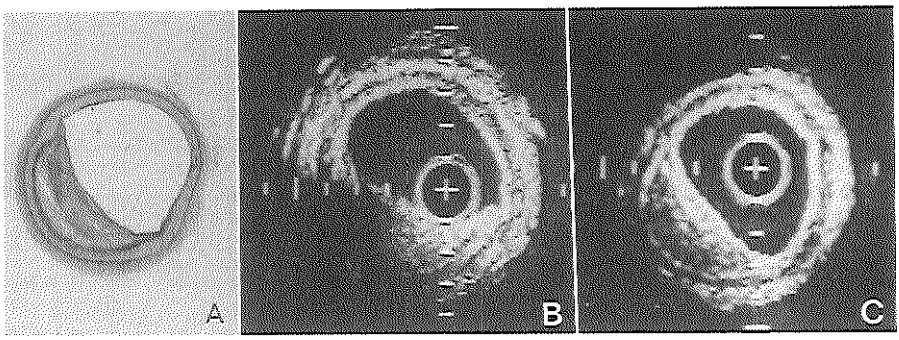

Fig. 4. A, Histologic cross-section of an external iliac artery, with a semicircular plaque composed of stratified lamina of dense fibrous tissue and a well-developed muscular media. (Verhoeff's stain; calibration = 1 mm.) **B,** and **C,** Corresponding intravascular ultrasonographic cross-sections with the catheter adjacent to the vessel wall and in the center of the lumen. The atherosclerotic plaque is well delineated when the ultrasound beam has a perpendicular orientation, whereas identification of the plaque contours becomes impossible with a tangential orientation of the ultrasound beam to the tissue surface. Note the sonolucent band corresponding to the muscular media.

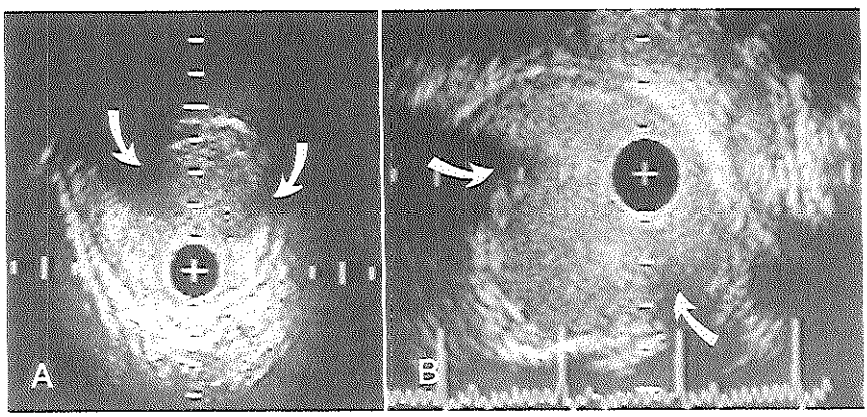

Fig. 5. A, Intravascular ultrasonographic image of a superficial femoral artery after balloon dilatation. The catheter is positioned in a crescent-shaped lumen, which is included between the vessel wall and a large intimal flap. Note that the false lumen and the opposite wall behind the dissection are visualized only in the area of perpendicular orientation to the ultrasound beam. A dropout of the underlying structures is observed in the presence of a narrow angle of incidence of the ultrasound beam on the dissection plane *(arrows).* **B,** Intravascular ultrasonographic image of a superficial femoral artery after balloon dilatation. Large dropouts of the two extremities of the dissected plane *(curved arrows)* and of the underlying vessel wall and lumen cause interpretation problems. Note that the omnidirectional backscatter of blood clearly delineates the half-moon shape of the true lumen.

ously described. We observed these changes only in peripheral vessels, probably because in the smaller coronary vessels the protruding plaques that were dissected from the balloon inflation were pushed against the opposite wall by the ultrasonographic catheter, thus avoiding the development of significant angle-dependent artifacts.

Conclusions. The angle of incidence of the ultra-

sound beam significantly affects the quality of the echographic image in intravascular ultrasonography and explains the image deterioration that occurs with eccentric or noncoaxial positions of the catheter and particularly in the presence of intraluminal dissection flaps that protrude inside the lumen. Awareness of the importance of this phenomenon may improve image acquisition and prevent misinterpretation of intravascular ultrasonographic images. Future developments in design of intravascular ultrasonographic catheters that allow steerability or multiplane imaging may improve image acquisition and circumvent these limitations.

We thank M. G. M. de Kroon, PhD, N. de Jong, PhD, E. Boersma, PhD, C. Lancée, PhD, and J. Oomen, PhD, for help, suggestions, and criticisms in the preparation of this manuscript. The images shown in Fig. 5 were obtained by Dr. H. Pieterman during intravascular ultrasonographic studies, which were carried out in the Radiology Department, Academic Hospital Rotterdam-Dijzigt. We thank Mrs. Coby Peekstok for preparing the histologic sections and Dr. R. J. van Suylen for interpreting them.

REFERENCES

1. Pandian NG. Intravascular and intracardiac ultrasound imaging: an old concept now on the road to reality. Circulation 1989;80:1091-4.
2. Pandian NG, Kreis A, Brockway B, Isner JM, Sacharoff A, Boleza E, Caro R, Muller D. Ultrasound angioscopy: real time, two-dimensional, intraluminal ultrasound imaging of blood vessels. Am J Cardiol 1988;62:493-4.
3. Roelandt JR, Bom N, Serruys PW, Gussenhoven EJ, Lancée CT, Sutherland GR. Intravascular high-resolution real time cross-sectional echocardiography. Echocardiography 1989;6:9-16.
4. Wenguang L, Gussenhoven WJ, Zhong Y, The SHK, Di Mario C, Madretsma S, van Egmond F, de Feyter PJ, Pieterman H, van Urk H, Rijsterborgh H, Bom N. Validation of quantitative analysis of intravascular ultrasound images. Int J Card Imaging 1991;6:247-54.
5. de Jong N, Mittertreiner WH, Ligvoet KM, Ten Cate FJ. A computerized system that uses high-frequency data for analysis of myocardial contrast echocardiograms. J Am Soc Echocardiogr 1990;3:99-105.
6. Di Mario C, The SHK, Madretsma S, van Suylen RJ, Wilson R, Bom N, Serruys PW, Gussenhoven WG, Roelandt JRTC. Detection and characterization of vascular lesions by intravascular ultrasound. An in-vitro correlative study with histology. J Am Soc Echocardiogr 1992;19:135-46.
7. Picano E, Landini L, Distante A, Salvadori M, Lattanzi F, Masini M, L'Abbate A. Angle-dependence of ultrasonic backscatter in arterial tissues. A study in-vitro. Circulation 1985;72:572-6.
8. de Kroon MGM, van der Wal LF, Gussenhoven WJ, Bom N. Angle-dependent backscatter from the arterial wall. Ultrasound Med Biol 1991;17:121-6.
9. Nishimura RA, Edwards WD, Warnes CA, Reeder GS, Holmes DR, Tajik AJ, Yock PG. Intravascular ultrasound imaging: in-vitro validation and pathologic correlation. J Am Coll Cardiol 1990;16:145-54.
10. Isner JM, Rosenfield JO, Losordo DW, Kelly S, Palefski P, Langevin RE, Razvi S, Pastore JO, Kosowsky BD. Percutaneous intravascular ultrasound as adjunct to catheter-based interventions: preliminary experience in patients with peripheral vascular disease. Radiology 1990;175:61-70.
11. Nishimura RA, Welch TJ, Stanson AW, Sheedy PF, Holmes DR. Intravascular ultrasound of the distal aorta and iliac vessels: initial feasibility studies. Radiology 1990;176:523-5.
12. Gussenhoven WJ, Frietman P, The SHK, Egmond van FC, van Suylen F, Lancée CT, Urk van H, Roelandt J, Bom N. Assessment of medial thinning in atherosclerosis with intravascular ultrasound. Am J Cardiol 1991;68:625-32.
13. Tobis JM, Mallery JA, Mahon D, Lehmann K, Zalesky P, Griffith J, Gessert J, Moriuchi M, McRae M, Dwyer ML, Greep N, Henry WL. Intravascular ultrasound imaging of human arteries in vivo. Circulation 1991;83:913-26.
14. Yock PG, Fitzgerald PJ, Linker DT, Angelsen BAJ. Intravascular ultrasound guidance for catheter-based coronary interventions. J Am Coll Cardiol 1991;17:39B-45B.
15. Nissen SE, Gurley JC, Grines CL, Booth DC, McClure R, Berk M, Fisher C, DeMaria AN. Intravascular ultrasound assessment of lumen size and wall morphology in normal subjects and patients with coronary artery disease. Circulation 1991; 84:1087-99.
16. Werner GS, Sold G, Buchwald A, Wiegand V. Intravascular ultrasound imaging of human coronary arteries after percutaneous transluminal angioplasty: morphologic and quantitative assesement. Am Heart J 1991;122:212-20.
17. StGoar FG, Pinto FJ, Alderman EL, Fitzgerald PJ, Stadius ML, Popp RL. Intravascular ultrasound of angiographically normal coronary arteries: an in-vivo comparison with quantitative angiography. J Am Coll Cardiol 1991;18:952-8.
18. Pinto F, StGoar FG, Fischell TA, Stadius ML, Valantine HA, Alderman EL, Popp RL. Nitroglycerin-induced coronary vasodilatation in cardiac transplant recipients. Evaluation with in vivo intracoronary ultrasound. Circulation 1992;85:69-77.
19. Honye J, Mahon DJ, White CJ, Ramee SR, Wallis JB, Al-Zarka A, Tobis JM. Morphological effects of coronary balloon angioplasty in vivo assessed by intravascular ultrasound imaging. Circulation 1992;85:1012-25.
20. StGoar FG, Pinto FJ, Alderman E, Valantine HA, Schroeder JS, Stinson EB, Popp RL. Intracoronary ultrasound in cardiac transplant recipients. In vivo evidence of "angiographically silent" intimal thickening. Circulation 1992;85:979-87.

Part 3

Intracoronary Doppler

CHAPTER 7

INTRACORONARY DOPPLER: INSTRUMENTATION AND PRINCIPLES OF ANALYSIS AND INTERPRETATION

Carlo Di Mario, M.D., Morton J. Kern*, M.D., Ph.D.,
Patrick W. Serruys, M.D., Ph.D.

From the Thoraxcenter, Erasmus University, Rotterdam, Netherlands and *Saint Louis University, Missouri, USA

Modified from: Topol E.J. (ed): Textbook of Interventional Cardiology. Second edition. Saunders W.C., 1993.

PRINCIPLES OF DOPPLER VELOCIMETRY

An observer moving toward a sound source will hear a tone with higher frequency than at rest. An observer moving away from the source, will hear a tone of lower frequency. The same is observed when the source is moving and the observer is at rest. This change in frequency is called the Doppler effect after Christian Johann Doppler (1803-1853), an Austrian physicist who was the first to describe this phenomenon. This principle is applied in practice by mounting a piezoelectric crystal that emits and receives high-frequency sounds on the tip of an intravascular catheter. Changes in the velocity of blood flow velocity alter the return frequency, causing the Doppler shift. Sophisticated electronic circuits precisely determine the Doppler shift and provide a continuous record of blood flow velocity. Coronary flow velocity is calculated from the Doppler frequency shift (which is the difference between the transmitted and returning frequency), using the following Doppler equation:

$$\text{Velocity} = \frac{(F_1 - F_0)\ (C)}{(2F_0)\ (\text{Cos}\ \phi)}$$

Where V = velocity of blood flow
F_0 = transmitting (transducer) frequency
F_1 = returning frequency
C = constant: speed of sound in blood
ϕ = angle of incidence

Maximum velocity can be recorded provided the transducer beam is nearly parallel to blood flow and ϕ is zero so that the cosine ϕ is 1. The waveform of the emitted sound is also important. For example, if continuous sinusoidal waves are employed (continuous wave Doppler), the Doppler signal will reflect all the flow velocities encountered by the exploring ultrasound beam. In contrast, a pulsed wave Doppler permits determination of both magnitude and direction of the flow changes at a predetermined distance from the transducer. Intracoronary Doppler has several advantages for the assessment of the coronary circulation. Doppler flowmeters directly measure the red blood cell velocity so that flow markers are not required, allowing a continuous assessment of flow. Since the catheter can be selectively inserted in epicardial vessels, regional measurements are possible. There is a direct relationship between velocity and volumetric flow, where blood flow = vessel cross-sectional area x mean flow velocity. The differences or changes in Doppler coronary flow velocities, thus, can be used to represent changes in absolute coronary flow provided the cross-sectional area remains constant. Intracoronary Doppler, however, has also several limitations. The method is extremely "space dependent" and may be affected by the stenosis geometry as well as by the intracoronary velocity profile [1]. The angle existing between the piezoelectric crystal and the main stream of the blood is critical for the estimation of flow velocity [2]. In addition, the sampling volume can be rather limited and does not necessarily represent the mean velocity of the bloodstream [3]. These limitations have been partially solved by recent technical

developments, as discussed below briefly, describing the different Doppler transducers available for intracoronary blood flow velocity measurements.

INTRACORONARY DOPPLER PROBES

1. Doppler probes mounted on angiographic catheters

In 1977 Cole and Hartley reported the recording of Doppler tracings at the ostium of the native coronary vessels and of coronary venous bypass grafts using a 20 MHz piezoelectric circular crystal mounted at the tip of a standard 8 Fr Sones catheter [3]. In 58 patients the velocity pattern could be recorded in basal conditions and the hyperemic response to contrast media injection was measured.

Recently, Kern described a left Judkins angiographic catheter with a 20 MHz crystal mounted caudally (6:00 o'clock position) at the tip of the catheter [4].

With these systems, however, no selective measurements can be made in the vessel(s) of interest and a contamination of the coronary flow due to aortic components may be present. Furthermore, the presence of the relatively large catheter in the coronary ostium may, to some extent, obstruct the coronary blood flow, especially during hyperemia.

2. Intracoronary Doppler catheters

Side-mounted probes: At the University of Iowa, special suction mounted epicardial Doppler probes were designed for intraoperative and experimental use [5]. In order to apply Doppler velocimetry during selective coronary catheterization, a Doppler crystal was mounted on one side of a 3 Fr Rentrop perfusion catheter with a flexible guidewire at the tip [6]. The orientation of the beam at 45° from the long axis of the catheter was designed to avoid flow interference from the catheter. Although this design resulted in a reduction of the maximal recorded velocities due to the non parallel orientation of the ultrasonic beam with the maximal flow velocity vector, this limitation was accepted because the main goal of the investigators was the evaluation of relative flow changes [7]. Despite fundamental design limitations, changes in coronary blood flow velocity measured with this intravascular ultrasonic flowmeter correlated well with flow measurement performed with microspheres, timed volume collection of coronary sinus flow, electromagnetic flowmeter measurement and coronary blood flow velocity recorded with epicardial Doppler probes [6,7].

With this system, a selective intracoronary measurement of flow velocities became possible during cardiac catheterization. Further technical development allowed an easier and safer integration of Doppler measurements in the Catheterization Laboratory during coronary interventions due to the availability of an internal lumen for a movable guidewire in the second generation catheters.

End-mounted probes: Sibley et al. [8] obtained subselective Doppler recordings using a circular end-mounted crystal on a flexible 3 Fr catheter amenable to guide-wire insertion. This system was designed to minimize the angle between the ultrasonic

beam and the centerline of the intravascular flow profile (subsequently called "theta" angle), thus allowing the measurement of maximal intravascular velocity. As evident from the Doppler equation (page 2), with an end mounted crystal and a theoretical "theta" angle of 0°, changes of 15° in either direction would induce a negligible reduction (-3.5%) of the measured frequency shift. To contrary, the side-mounted probes with an angle of 45° with the centerline of flow may have a change of the "theta" angle by up to 15%, resulting in a shift of Doppler frequency by as much as 23% from baseline [2].

The flow stream interference due to the presence of the catheter in the bloodstream is of concern if velocities close to the transducer have to be measured. Tadaoka et al [9] reported that in an in-vitro model a blunt or M-shaped velocity profile, depressed at the centerline, is present several mm distal to the catheter tip, resulting in underestimation of flow velocity away from the transducer. A distance of at least 10 catheter diameters was required to have a complete restoration of the flow-velocity profile.

Double side-mounted probes: A possible solution to the angle dependency of the Doppler flow velocity measurements is the use of two piezoelectric crystals located on the side of the Doppler catheter in such a way that a right angle between the transducers is obtained. A prototype of this still experimental system was validated in an in vitro continuous flow model and yielded accurate flow velocity measurements, independent of the catheter position [10].

3. Intracoronary Doppler balloon catheters

A prototype series of coronary balloon-catheters with an end-mounted 20 MHz Doppler crystal have been successfully used at the Thoraxcenter to record intracoronary velocities during and after successive balloon inflations [11]. The system allowed the recording of high quality Doppler tracings distal to the stenosis before, during and after balloon inflation. The maximal hyperemic velocity after balloon inflation was found to be a useful guide for the assessment of the result of angioplasty.

4. Doppler guidewire probes

Although side- and end-mounted Doppler catheters have been extensively used in research cardiac catheterization laboratories, mainly for assessing relative changes of coronary velocities, several limitations have prevented a more widespread clinical application of these devices:

1) Catheters of a diameter of 1 mm are unlikely to be an obstacle to flow in proximal coronary arteries with a diameter of 3-4 mm, as confirmed also at high flow rates in experiments in calves. If, however, the recording is obtained across or distal to a stenotic segment, the obstruction due to the catheter may induce marked reduction or disappearance of the anterograde flow.

2) The catheters must be inserted before and after coronary interventions, resulting in repeated and complex exchange procedures and in the inability to monitor

coronary blood flow velocities during the most critical phases of the procedure.
3) The small sample volume of the current catheters requires an optimal position inside the vessel to record a high quality signal, including the highest blood velocities. The lack of steerability of the present generation of Doppler catheters results in a high number of unsuccessful procedures.
4) The 20 MHz transducers are currently activated with a pulse repetition frequency of 62.5 kHz. Only velocities up to 110 cm/s can be recorded, so that the high velocities across a stenosis can not be accurately measured.
5) Only zero-crossing detectors are commercially available in combination with these Doppler probes.

The *Doppler guidewire* is available as an 0.014" or an 0.018", 175 cm long, flexible and steerable with a 12 MHz piezoelectric ultrasound transducer integrated onto the tip. It has handling characteristics similar to traditional angioplasty guidewires. The wire creates less disturbance of the flow profile distal to its tip when placed within a vessel and can be passed into the smaller coronary arteries without creating significant stenoses. The flexibility and steerability of the Doppler flowire are designed for crossing intracoronary arterial obstructions and maintaining a stable prolonged placement in the distal portion of the coronary artery during coronary angioplasty procedures. Substituting Doppler-tipped guidewire for a standard angioplasty guidewire, phasic coronary flow velocity measurements are easily incorporated into an angioplasty procedure without adding unnecessary technical maneuvers.

The forward directed ultrasound beam diverges at 14° from the Doppler transducer so that the Doppler sample volume is approximately 0.65 mm thick by 2.25 mm in diameter when maintained 5.2 mm beyond the transducer, distal to the area of flow velocity profile distortion induced by the Doppler guidewire [9]. This broad ultrasound beam provides a relatively large area of insonification, sampling a large portion of the flow velocity profile. An adjustable pulse repetition frequency of 16-94 kHz, pulse duration of 0.83 μs and sampling delay of 0.5 μs provides satisfactory parameters for spectral signal analysis. The signal transmitted from the piezoelectric transducer is processed from the quadrature Doppler audio signal by real-time spectral analyzer using on-line fast Fourier transform providing a scrolling gray scale spectral display. The frequency response of this system calculates approximately 90 spectra/second. The spectral analysis of the signal and the Doppler audio-signals are videorecorded for later review. Simultaneous electrocardiogram and blood pressure are displayed with the spectral velocity.

The Doppler guidewire has been validated during intravascular measurement of coronary arterial flow velocity by Doucette et al [12]. The Doppler flow velocity signal was recorded in model tubes with pulsatile blood flow. In four straight tubes with internal diameters varying from 0.79 to 4.76 mm, the peak spectral flow velocity was linearly related to absolute flow velocity measured by on-line electromagnetic flow meters ($r > 0.98$ for each tube). Quantitative volumetric flow was calculated from vessel cross-sectional area and mean flow velocity. The average peak velocity was less accurate in larger tubes (> 7.5 mm) and a slightly reduced correlation with absolute flow was observed in some tortuous model segments. In

four canine circumflex coronary arteries, the electromagnetic flow probe and Doppler flow vessel also demonstrated high correlations in both the proximal and distal segments ($r^2 = 0.93$ to 0.99 in the proximal vessel and 0.86 to 0.99 in the distal vessel). Using quantitative angiography to determine arterial diameter, quantitative flow velocity correlations for the two techniques was $r = 0.95$ in the model cannula and $r = 0.85$ in the proximal coronary artery. These data indicate that the Doppler guidewire accurately measures phasic flow velocity patterns and linearly tracks changes in flow rates in small predominantly straight coronary arteries.

The Doppler guidewire flow velocity signals were not importantly affected by increasing heart rates to 150 beats/minute in the canine model. The motion artifact of rapidly changing heart rate might influence flow velocity, but was not observed in the initial validation studies. Changes of pulsatility intensity examined in the in vitro system demonstrated satisfactory tracking and correlation with electromagnetic flow responses at rapid heart rates. During in vivo pacing experiments, an excellent correlation was found between the average peak velocity of the Doppler guidewire system and flow meter response.

The in vivo studies with the Doppler flowire established several important features applicable to patient use [13]. The Doppler guidewire could be easily steered in the proximal and distal branches of the coronary arterial tree with handling characteristics nearly identical to those of a normal 0.018" angioplasty guidewire. The phasic velocity recordings had a high signal-to-noise ratio and were satisfactory for prolonged monitoring periods in proximal and distal vessels as small as 1.2 mm in diameter. The Doppler spectra provided a precise estimate of forward and reverse flow which were well separated across the zero line [13]. Low frequency wall motion artifact was occasionally encountered, especially at the onset of systole. These artifacts, however, could be minimized by repositioning of the guidewire.

Comparison studies were performed using both an 8 Fr Judkins Doppler catheter with a 20 MHz piezoelectric transducer embedded at its tip and the 12 MHz Doppler guidewire. After the Judkins-style Doppler catheter was positioned in the left main coronary artery, the 0.018" Doppler guidewire was advanced through the 8 French Doppler catheter to sample an identical location within the coronary arteries. Arterial pressure, electrocardiogram, phasic and mean velocity were displayed on a multichannel oscilloscope recorder. Simultaneous flow velocity data were obtained with both Doppler catheter techniques at baseline and following maximal coronary hyperemia with 10 mg of intracoronary papaverine [14]. There was no significant difference between the Doppler guidewire and Doppler catheter mean velocities and coronary vasodilator reserve.

The safety of the instrumentation of normal and mildly diseased coronary arteries with the Dopppler guidewire during diagnostic coronary angiography was assessed in 120 patients. No complications related to the use of the guidewire were observed immediately after the procedure and at a 6 months' follow-up [15].

ANALYSIS OF THE DOPPLER SIGNAL: ADVANTAGES OF THE SPECTRAL ANALYSIS

1. Principles of analysis

Simple straightforward Doppler velocity registrations can be obtained with a zero-crossing (ZC) detector. The interval between each pair of adjacent zero-crossings of the same polarity is measured and the Doppler frequency shift is calculated. Although inexpensive, simple and convenient, this technique is less accurate than spectral signal analysis in areas of disturbed flow and is unable to detect the peak velocities [2]. Coronary blood flow often has regions of varying velocity. The corresponding Doppler signal is the sum of different velocity scatters and is best examined by a full power spectrum provided by fast Fourier transformation. Spectral flow analysis has the advantage in distinguishing laminar from disturbed turbulent flow patterns.

In the presence of composite flow signals, only the analysis of the frequency spectrum of the Doppler signal can detect the maximal Doppler shift and can be used to calculate the mean frequency by averaging the amount of power in the signal for each frequency.

In vitro models: Tadaoka et al [9], using a straight tube perfused with continuous flow, observed that the ZC detector underestimates the true velocities measured with the fast Fourier transform (FFT) analysis. The ZC technique, however, seemed to be sufficiently reliable for the evaluation of relative flow changes.

Animal experience: Kajiya et al [16] have reported that the velocity measured with a ZC detector is consistently lower than the mean velocity obtained with the FFT method in stenotic canine femoral arteries. In a canine model of adjustable coronary flow, Sudhir et al [17] reported that the absolute flow measured with an electromagnetic flowmeter could be successfully estimated using the maximal velocities measured with the FFT. This value, however, was poorly correlated with the velocities measured with a ZC detector. In a separate experiment the same group [18] used stenosis phantoms of known diameter placed in canine coronary arteries and reported that the peak velocity proximal and across the stenosis gave the best estimate of the true cross-sectional area of the stenosis based on the continuity equation. The velocity measured with a conventional ZC detector showed no correlation with this area.

Tanouchi et al [19] reported that the flow velocity measured in the left anterior descending coronary artery with the FFT spectral analysis correlated well with those estimated by electromagnetic flowmeter ($y = .88x + 9.7$, $r = .93$, $p < 0.001$), whereas the velocities measured with a ZC detector significantly underestimated those by electromagnetic flowmeter ($y = .23x + 1.6$, $r = .82$).

Clinical experience: At the Thoraxcenter, a Doppler fast Fourier transform (FFT) system was used to analyze the signal obtained using 20 MHz Doppler catheters [20]. The software of analysis included algorithms for the measurement of the instantaneous maximal and mean velocities and of the standard deviation of the velocity distribution. The maximal velocity was defined as the 90th percentile of the velocity distribution and the mean velocity was calculated as the intensity weighted average

of the velocity spectrum. Time-averaged values over 10 or 20 s of recording were also calculated and displayed. The mean velocity measured with a ZC detector (Millar MVD 20) was compared with the time-averaged maximal and mean velocities easured with the FFT technique in the same period in 19 patients undergoing percutaneous balloon coronary angioplasty [20]. The comparison with the maximal and mean velocities measured with the FFT technique showed large differences among the paired measurements (SD = ±37% in both cases). Also the ratio between maximal hyperemic and basal flow velocity (coronary flow reserve) calculated using the ZC measurements and the maximal or mean FFT velocities showed large individual differences suggesting that the two techniques of analysis are not interchangeable also when relative measurements are required. Furthermore, only the spectral analysis allowed the detection of frequency aliasing when the flow velocity measurements were obtained within the stenosis.

The identification of the maximal velocity and the more accurate measurement of the mean velocity are not the only advantages of the spectral analysis. This system allows also the detection of morphologic modifications of the spectrum of velocity distribution related to physiological flow changes. Denardo et al [21] calculated four indices of coronary blood flow turbulence from FFT analysis of the Doppler signal in 6 patients post-PTCA and 6 patients after coronary atherectomy: spectral broadening index, coefficient of variation, coefficient of skewdness and coefficient of kurtosis. They concluded that flow within post directional coronary atherectomy regions was less turbulent than upstream; flow within post-PTCA lesions was more turbulent.

Large differences between flow velocity measurements obtained with ZC and FFT were also observed by Piek et al [22] in the assessment of collateral flow changes during coronary angioplasty.

In 12 normal subjects, Yamagishi et al [23] used an FFT technique for the analysis of Doppler signals recorded in the proximal left anterior descending coronary artery. The percent variation in flow velocity obtained with cardiac pacing at increasing frequency was compared with the increase of great cardiac vein flow measured with the thermodilution technique. A high correlation of the percent increase measured with the two techniques was observed.

CORONARY BLOOD FLOW VELOCITY PATTERNS

Pulsatile characteristics of coronary flow: The pulsatility of coronary arterial flow was already described by Scaramucci in the late XVIIth century [24]. In contrast with the flow characteristics of most arterial districts, arterial coronary blood flow has a distinctive and unique phasic pattern. Blood flow is higher in diastole and lower in systole. Large differences, however, may be present between the flow pattern in the left and in the right coronary artery (Figure 1). An opposite flow pattern is present in the coronary veins, which are characterized by a predominant systolic component, by flow variations during the cardiac cycle synchronous with the right atrial pressure waves and by large phasic changes due to respiration (Figure 2). These opposite flow

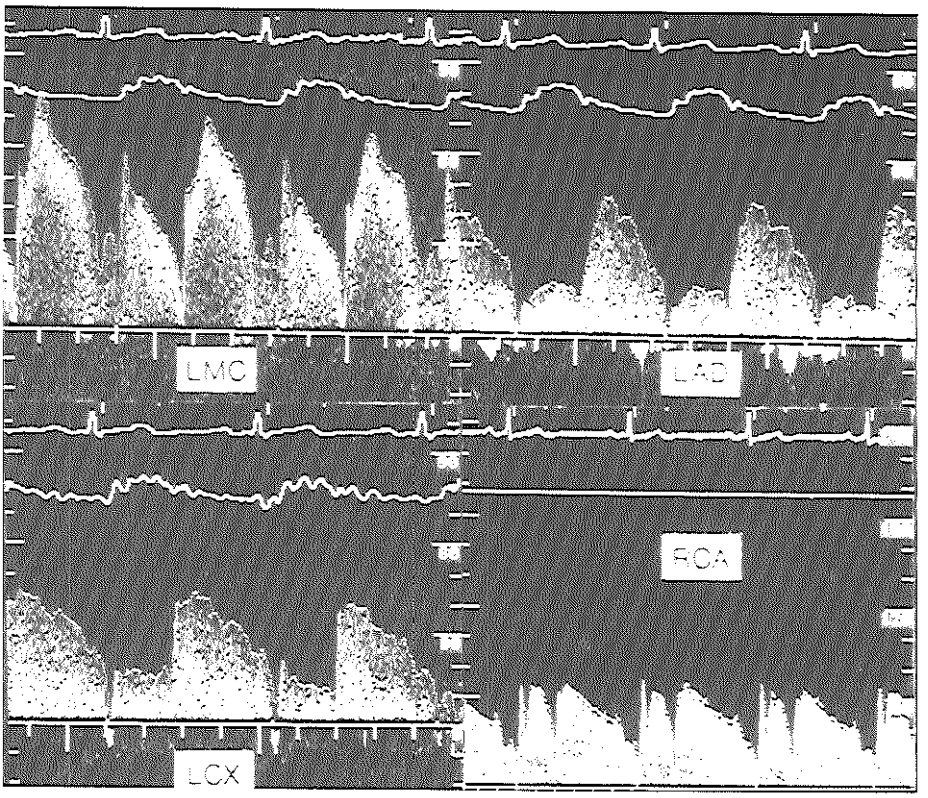

Fig. 1. Flow velocity measurements obtained in the left main coronary artery (LMC) and the proximal segments of the left anterior descending (LAD), left circumflex (LCX) and right coronary artery (RCA) of a patient without epicardial coronary stenoses. Note the prevalent diastolic component and the similar pattern and maximal velocity observed in the left anterior descending and left circumflex arteries.

changes during the cardiac cycle can be explained only assuming the presence of a blood reservoir between the arterial and venous side of the coronary circulation (intramyocardial capacitance). The classical experiments of Sabistorn and Gregg have confirmed that the systolic reduction of arterial coronary flow is due to the contraction of the heart [25]. Squeezing of the capillary network due to the increase in tissue pressure during myocardial compression related to the high systolic intraventricular pressure was considered the cause of the flow changes during the cardiac cycle. More recently, an increased systolic stiffness of the cardiac myocytes has been considered a possible alternative. The different patterns of flow during the cardiac cycle in the right and left coronary arteries is in part attributable to the greater systolic compressive force of the left ventricle or to the higher stiffness of the left ventricular myocytes during the contractile phase. Both theories can then explain the presence of a reversal of flow during systole in some patients with severe aortic valve stenosis or obstructive hypertrophic cardiomyopathy [26,27].

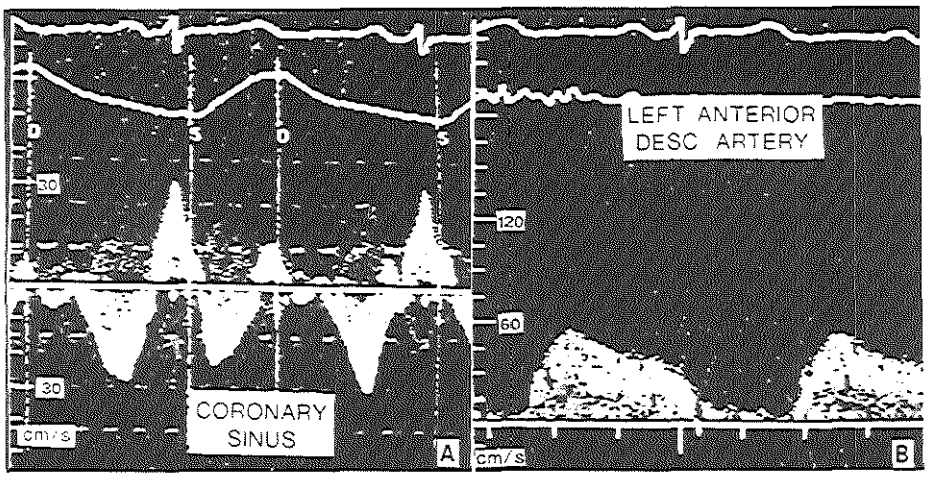

Fig. 2. Flow velocity measurements obtained in the coronary sinus (A) and in the left anterior descending coronary artery (B). Note that the arterial flow is mainly diastolic while the flow in the coronary sinus shows a systolic and a diastolic positive component and two retrograde waves corresponding to the "v" and "a" wave of the right atrial pressure.

Normal blood flow velocity and flow pattern: Knowledge of normal flow velocity range and of signal characteristics in normal proximal and distal coronary arteries is an essential prerequisite for the evaluation of the flow velocity changes in patients with coronary lesions. In order to define the normal range of coronary flow velocity, the time averaged blood flow velocity was measured in 81 proximal mid coronary arteries without hemodynamically significant coronary stenosis (diameter stenosis measured with a computer-assisted automatic quantitative angiographic system < 30)%. A Doppler guidewire was advanced into a straight smooth and regular proximal /middle segment of the studied artery and the flow velocity signal was recorded during spectral velocity analysis. An on-line measurement of time-averaged peak blood flow velocity and mean diastolic-to-systolic velocity ratio is automatically available in the previously described Doppler guidewire system. In order to verify the accuracy of the quantitation of the systo-diastolic components of the velocity signal, the video-recorded Doppler tracing was analyzed after digital conversion using a custom-designed computer analysis system . After calibration, the contours of the Doppler envelope were traced using a digitizing tablet. The systolic and diastolic components were defined based on the simultaneously recorded electrocardiogram (QRS complex), aortic pressure (dicrotic notch) and flow changes. A repeated independent analysis of 10 Doppler tracings from the same observer or from a second observer showed < 5% inter- and intraobserver variability for all the analyzed parameters. The time-averaged peak velocity was 23 ± 11 cm/s (mean ± sd of all the arterial segments). A large range of velocity (9-61 cm/s) was observed. Maximal blood flow velocity was 42 ± 17 cm/s (range 14-82 cm/s). In Figure 3 the time averaged velocity and the diastolic-to-systolic velocity is reported for the left anterior descending, left circumflex and right coronary artery. Significantly higher diastolic-

to-systolic ratios of mean velocity and velocity integrals were measured in both branches of the left coronary artery compared to the right coronary artery ($p < 0.0005$).

Ofili et al [28] have recently reported the results of the analysis of simultaneous flow velocity measurements in 55 angiographically normal, proximal and distal coronary arteries (right coronary artery = 12, left circumflex artery = 19, left anterior descending coronary artery = 24) obtained both in baseline conditions and after the selective injection of 8 - 18 μg of adenosine intracoronary. Proximal and distal velocities in each artery were not different at baseline or hyperemia. Coronary flow reserve (hyperemic/basal flow velocity ratio) was also similar in the proximal and distal guidewire locations in all 3 arteries.

Thus, proximal and distal normal native coronary arteries have similar relative flow velocity parameters and vasodilator reserve with a diastolic predominant pattern, findings which are generally less marked in the right coronary artery.

The minor reduction of flow velocity observed advancing the Doppler probe from proximal to distal is somewhat surprising when the large reduction of the corresponding cross-sectional areas and, consequently, coronary flow is considered. The maintainance of flow velocity across the length of the epicardial artery is due to the gradually diminishing vessel area as volumetric flow is distributed to side branches along the proximal to distal vessel course. Anatomically, the division of the coronary arteries is extremely irregular, with the presence of small transmural arteries directly branching from the major epicardial arteries and of a non symmetrical division of the mother vessels into numerous smaller daughter branches. Stralher ordering and fractal models have been proposed to describe the heterogeneity of the vessel distribution, in analogy of other physiological structures such as the airways of the lung [29].

When only the increase of the total arterial cross-sectional area between mother and daughter vessels in large epicardial arteries is considered, a progressive moderate increase is observed, in accordance with the principle of limited/adaptive vascular shear stress, minimum vascular volume at bifurcations and with the principle of minimum viscous energy loss. After three-dimensional reconstruction of the arterial tree, Seiler et al [30] calculated a ratio between area of the mother vessel and mean of the areas of the daughter vessels of 1.647, similar to the ratio predicted based on the previously mentioned principles (1.588). These considerations explain with only a moderate decrease, inversely proportional to the moderate increase in total cross-sectional area, occurs from proximal to distal in the coronary arterial tree (Figure 4). Flow velocity, therefore, is relatively uniform in the epicardial arteries of the same patient and a rapid decrease indicates redistribution of flow in the lower resistance branches proximal to a flow-limiting coronary stenosis.

The above considerations may explain the poor correlation between cross-sectional area and flow velocity observed in our control population (74 cases). In normal arteries or in arteries with early atherosclerotic changes not modifying the normal arterial cross-section, the variability of the flow velocity measurements seems to be dependent more on the variable basal flow requirements than on the anatomic differences in dimension or distribution of the major epicardial arteries.

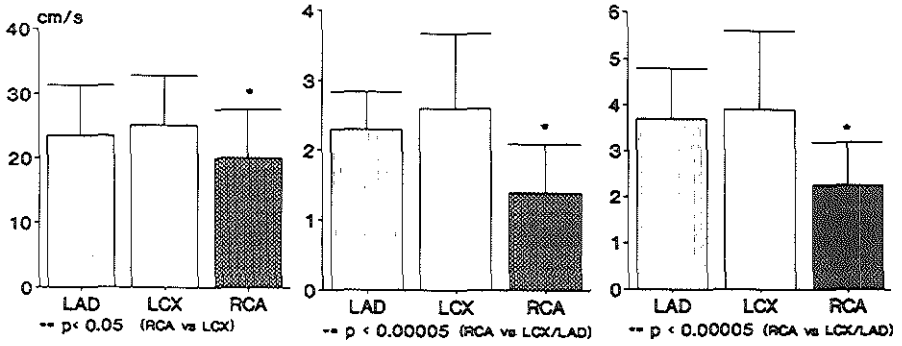

Fig. 3. Time-averaged peak velocity, diastolic to systolic ratio of the mean velocity and of the velocity integrals in the left anterior descending (LAD), left circumflex (LCX) and right coronary artery (RCA).

Flow velocity in saphenous veins and mammary arteries used as coronary conduits: The saphenous vein grafts have a predominantly diastolic flow, similar to the flow in native coronary arteries [31]. In the proximal saphenous veins used as aorto-

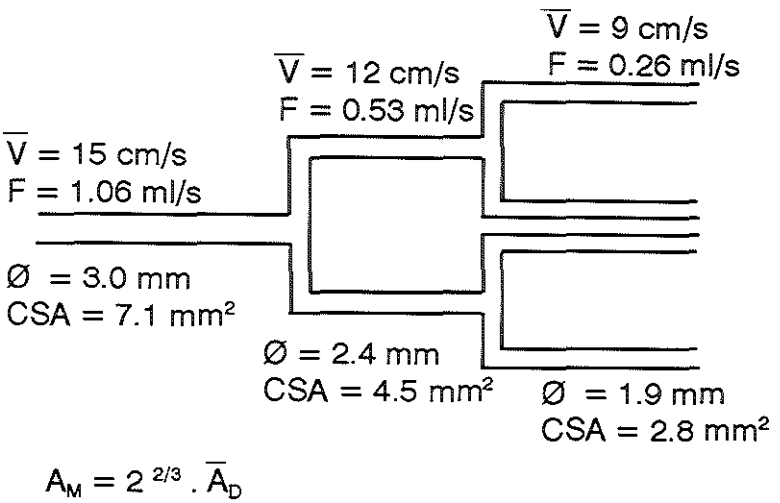

Fig. 4. Diagram showing a schematics of variations of vascular diameter (Ø), cross-sectional area (CSA), flow (F) and flow velocity (V) from proximal to distal in the coronary arteries. In the example, the division between mother artery (A_M) and daughter arteries (A_D) is symmetrical and obeys the principle of limited/adaptive vascular shear stress. Note that the decrease in flow velocity from proximal to distal is much smaller than the decrease in cross-sectional area and volume flow.

coronary bypass, however, large high-peaked systolic waves may be present, probably reflecting the higher distensibility of these long thin-walled vascular conduits, with a higher vascular capacitance than the shorter and smaller native coronary arteries. In the proximal segment of in situ internal thoracic (mammary) arteries anastomosed to coronary arteries, the phasic blood flow velocity resembles the subclavian artery [31,32], with a predominant systolic peak velocity (diastolic-to-systolic mean velocity ratio = 0.6 ± 0.2). The velocity pattern changes in the distal internal mammary with a predominant diastolic flow. Saphenous vein bypass grafts and mammary arteries also show significant differences in the absolute velocity measurements. Diastolic peak velocity of 14 ± 6 cm/s have been reported in venous aorto-coronary bypass grafts. In mammary arteries diastolic velocities similar to those recorded in native coronary arteries were observed (diastolic velocity = 45 ± 16 cm/s) [31]. A peculiar characteristics of saphenous veins used as sequential conduits is the sudden decrease in velocity observed distal to a coronary anastomosis, in contrast with the progressive velocity decrease observed from proximal to distal in native coronary arteries. The low flow velocity consequent to the inability to adjust the caliber according to flow demand may explain why saphenous vein grafts are more prone to accelerated atherosclerosis than native coronary arteries or mammary arteries used as coronary bypass. The low flow velocity and shear rate may facilitate thrombosis and greater interactions between blood elements and intimal surface. With the use of an implantable ultrasonic Doppler miniprobe, the flow velocity in the internal thoracic artery and gastroepiploic artery as measured 2 weeks after implantation. Both grafts showed a significant increase during exercise and dobutamine infusion but no changes after nitroglycerin or nifedipine [33]. Interestingly, the gastroepiploic artery after coronary implantation continued to show a large increase in flow velocity (+83 ± 48%) between 30 and 90 min after the patient taking meals.

CALCULATION OF VOLUME FLOW FROM FLOW VELOCITY MEASUREMENTS

Two crucial steps are required to accurately calculate absolute (volume) flow from flow velocity measurements: the calculation of the mean blood flow velocity in a given vascular cross-section and the accurate measurement of the cross-sectional area at the site of the measurement.

Assessment of mean blood flow velocity: The measurement of the mean blood flow velocity requires an adequate Doppler sampling of the peak flow region within a vessel:

a) the ultrasound beam should be aligned parallel with the centerline of flow. The Doppler guidewire has the piezoelectric crystal mounted at the tip so that a partial malalignment of the probe would only minimally affect the velocity recording, an angle of 30° with the velocity vector producing underestimation of flow of approximately 6%;

b) the entire flow profile or at least a significant proportion which includes the maximal velocity must be insonified;
c) the physical presence of the Doppler probe should not modify the velocity profile at the site of the Doppler sample volume;
d) a spectral analysis of the Doppler frequency should be performed to identify all the different velocities in the sample volume, including the maximal velocity. Theoretically, mean blood flow velocity can be measured from the weighted average of the velocity spectrum [34]. Several technical shortcomings limit the practical usefulness of the measurement of mean blood flow velocity from the velocity spectrum:
1) the filtering process necessary to remove the high intensity/low velocity signals from vessel wall contact artifacts (wall "thumps") affects the accuracy of the measurement of mean velocity;
2) measured from the intensity weighted velocity spectrum mean velocity is more sensitive than the maximal velocity to a variety of noise components of the signal;
3) the mean velocity calculated from the intensity weighted velocity spectrum may be inaccurate, if the entire parabolic profile of the artery is not included in the sample volume. Accurate measurements can still be obtained from the maximal flow velocity. Small changes in the position of the tip of the catheter inside the vessel, are also more likely to change the mean than the maximal velocity;
4) the weighing factors for the different velocities of the velocity spectrum can not be reliably determined as signal intensity is modified by several unknown parameters such as rouleaux formation [35,36].
5) inhomogeneities in the distribution of ultrasonic beam power may cause significant errors in the measurement of mean coronary blood flow velocity [37].

A different approach is based on the use of the maximal blood flow velocity which is less sensitive to the presence of noise and is more easily included in the sample volume based on the above described characteristics of the Doppler system. Mean blood flow velocity can be estimated from the maximal BFV in the presence of a laminar flow field and a fully developed velocity profile (Figure 5).

An important limitation to the applicability of this formula is that the velocity profile is assumed to be parabolic and fully developed. The distance L necessary to allow the full development of a parabolic flow profile is defined by the equation [38]:

$$L = (0.03\ R_e)\ d$$

where R_e is the Reynolds number and d the diameter of the conduit. Consequently, the velocity measurement should be taken at a distance of 4-6 times the vessel diameter to allow a complete development of the velocity profile at the Reynolds numbers present in normal epicardial coronary arteries (150-200 units). The same issues must be considered sampling velocity distal to major bifurcations of the vessel. Also in the presence of changes of the vascular diameter, the measurement of mean blood flow velocity from maximal velocity can be misleading if the stenotic segment is too short to allow a full development of the velocity profile. The non-Newtonian characteristics of blood will induce a flatter than expected velocity profile so that the

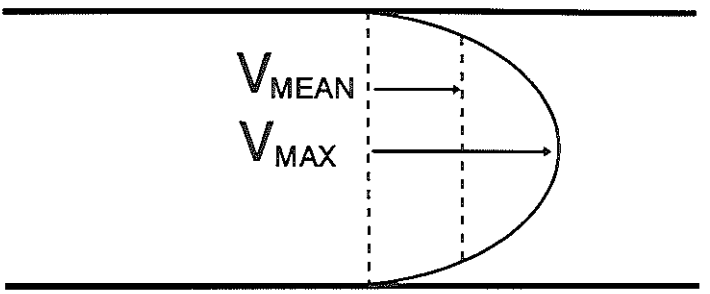

$$V_x = \frac{\Delta P}{4\mu L}(r^2 - x^2)$$

$$V_{MEAN} = (\Delta P \P r^2/8\P L)/\P r^2$$

$$V_{MEAN} = V_{MAX}/2$$

Fig. 5. Diagram showing the fixed relation (2:1) between maximal and mean flow velocity in a conduit with a laminar parabolic velocity profile. The fixed relation between maximal and mean velocity in a conduit with a laminar parabolic velocity profile can be derived from the classical equations describing the velocity of each streamline of flow according to its distance X from the centerline of flow and from the Poiseuille equation.
ΔP = pressure gradient; μ = viscosity; r = conduit radius; L = length of the segment.

mean blood flow velocity may be underestimated deriving this parameter from the maximal flow velocity [39]. These considerations underline the difficulties in obtaining reliable volumetric flow measurements based on blood flow velocity despite the recent progress in Doppler probe technology and signal analysis. Nevertheless, recent validation studies have shown a high correlation both in vitro and in vivo between volumetric flow measured with an electromagnetic flowmeter and flow derived from Doppler measurements obtained with the Doppler guidewire probes [12].

Assessment of the cross-sectional area at the site of the Doppler sample volume: A high quality angiogram, suitable for measurements of the cross-sectional at the site of the Doppler sample volume, can be performed almost simultaneously with the acquisition of the Doppler recording using the 0.018" Doppler guidewire. It must be noted, however, that more accurate measurements are obtained when the probe is positioned in an arterial segment of uniform caliber so that a mean cross-sectional area over a short arterial segment immediately distal to the Doppler probe (approximately 5 mm for the Doppler guidewire) can be obtained.

An alternative method is the combination of intracoronary Doppler and two-dimensional coronary ultrasound imaging. A continuous recording of high-quality echographic cross-sections, suitable for automated quantitative analysis, can be

achieved with the modern ultrasound imaging catheters. Although prototype system of combined Doppler-imaging ultrasound catheters have been tested [40,41], the introduction of the Doppler guidewire allows a simultaneous assessment with ultrasound catheters. The slighty different position of the Doppler sample volume and of the echographic cross-section and the potential electrical interference are minor limitations of this approach.

ASSESSMENT OF CORONARY FLOW RESERVE

Since the original work of Gould, Lipscomb, and Hamilton [58], the assessment of coronary flow reserve has been viewed as a method to establish the severity of a stenosis located in one of the major epicardial vessels. It is assumed that the reduction in hyperemic flow through the stenotic lesion would be an indicator of stenosis severity. This assumption is derived from the complex hemodynamic principles regulating the coronary circulation. At rest, flow is independent from the driving pressure over a wide range (60 - 180 mmHg) of physiological pressures, a phenomenon classically described as autoregulation of the coronary circulation. During maximal vasodilatation, flow becomes linearly related to the driving pressure [59]. The presence of a flow limiting stenosis in a major epicardial vessel generates a pressure drop across the stenotic lesion which is the result of viscous and turbulent resistances, so that the driving pressure distal to the stenosis decreases exponentially in response to the flow increase [60].

The coronary flow reserve concept is appealing to the clinician because it constitutes a functional surrogate to the anatomic description of the lesions located in the epicardial vessels. Many investigators have shown in animal experiments that a decrease in flow reserve may discriminantly detect lesions of increasing severity [61]. Although the concept may be easily and accurately applied in an optimal physiological situation in humans [62,63], it should be recognized that coronary flow reserve is influenced by several factors independent from the hydrodynamic characteristics of the stenotic lesion. Since flow reserve is, by definition a ratio, similar values may be obtained at very different levels of resting and hyperemic flow. Changes in basal resting flow without changes in hyperemic flow will considerably affect the ratio. Furthermore, any factors affecting the hyperemic pressure flow relationship would likewise modify the flow reserve and thereby change the assessment of the severity of the coronary lesion under study. The hyperemic pressure flow relationship is influenced by factors such as heart rate, preload, myocardial hypertrophy or disease of the microvasculature [59,64].

Effects of the pharmacologic agents used to induce maximal hyperemia: An increase in coronary blood flow can be observed either during reactive hyperemia induced by transluminal occlusion or by pharmacologically induced hyperemia. Widely used vasodilator agents are dipyridamole, nitroglycerin, papaverine and adenosine. The hyperosmolar ionic and low osmolar non-ionic contrast media can not be used because they do not produce maximal vasodilatation [65]. Nitrates have a predominant effect on large conductance vessels so that the flow changes due to peripheral

vasodilatation are partially masked by the large simultaneous increase in cross-sectional area in the proximal arterial segments. Continuous infusion of an adequate dose of dipyridamole results in maximal coronary vasodilation, but it has the disadvantage of a long duration of action, which makes the repeated assessment of the coronary hyperemic response of the coronary vascular bed or the assessment of different coronary vascular bed response during the same procedure impossible.

Bookstein & Higgins [65] have shown in dogs that the hyperemic response after an intracoronary bolus injection of adenosine-triphosphate or papaverine is of the same magnitude as that occurring after a 15-second occlusion of the coronary artery. The dose range of intracoronary papaverine needed to produce maximal coronary vasodilation has been established in humans by Wilson & White [66]. Selective intracoronary infusion of papaverine produced a maximal hyperemic response in most (80%) coronary arteries after 8 mg and in all coronary arteries after 12 mg. Papaverine in this dose range (8 to 12 mg) produced a response equal to that of an intravenous infusion of dipyridamole in a dose of 0.56 to 0.84 mg/kg of body weight.

The coronary vasodilation after intravenous or intracoronary adenosine is of a comparable magnitude to that observed after papaverine. The time from intracoronary injection of adenosine to peak hyperemia, as well as the total duration of the hyperemic response, is about four times shorter than that of papaverine (Figure 6) [67]. Furthermore, adenosine does not prolong QT interval and avoids the potentially dangerous ventricular arrhythmias observed after papaverine [68]. Wilson et al [69] recently reported that an intracoronary bolus or infusion of adenosine increases coronary velocity to levels similar to those recorded after papaverine without significant systemic effects or symptoms. Adenosine can also be administered intravenously. Kern et al. have shown that a continuous intravenous infusion of 140 μg/Kg/min induces maximal coronary vasodilation in the vast majority of patients with the presence of mild hypotension and bradycardia [70]. The frequent development of symptoms (flushing: 35%, chest discomfort: 34%, headache; 21%, dyspnea: 19%) and of 1st-2nd degree atrio-ventricular block (< 10%) rarely requires discontinuation of the infusion [71]. In view of the extremely high safety profile of low dose intracoronary adenosine, this agent and route is the pharmacologic stimulus of choice.

Intracoronary papaverine has been reported to increase coronary blood flow velocity to four-six times the resting value in patients with normal coronary arteries [66,72]. In these series, however, a highly selected patient population was studied, with the exclusion of myocardial hypertrophy, previous myocardial infarction or of any other condition known to increase the baseline flow (anemia, hypertyroidism, etc).

Using papaverine 8-12.5 mg and a Doppler guidewire in an unselected series of patients with coronary artery disease, we observed in 81 arteries without hemodynamically significant coronary artery stenosis a coronary flow reserve of 2.9 ± 0.95, with a large individual variability (range 2.1-4.2).

Effect of the pharmacologic agent used to induce hyperemia on stenosis geometry: The ideal vasodilator should dilate exclusively the resistance vessels without affecting the geometry of the flow limiting stenosis in the epicardial coronary artery.

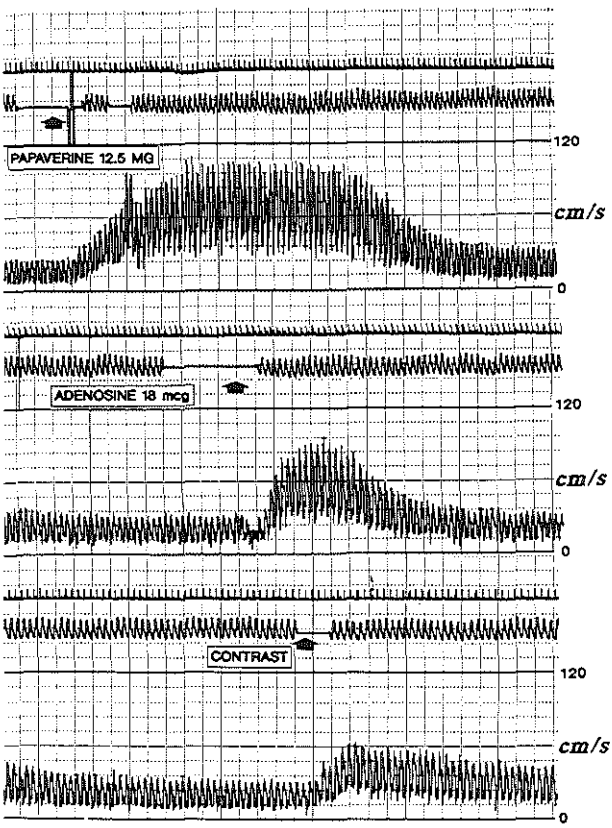

Fig. 6. Flow velocity recording after selective intracoronary injection in the left anterior descending coronary artery of papaverine (12.5 mg), adenosine (18 μg) and Iopamidol (7 ml, 370 μg Iodine/ml). Note that the hyperemic response after contrast injection and adenosine are much shorter than the hyperemic state induced by papaverine. The hyperemic flow velocity after contrast injection is lower than the flow velocity observed after adenosine and papaverine.

Unfortunately, as indicated by our results with intracoronary papaverine [73], the agents used to induce vasodilation of the resistance vessels also influence the epicardial coronary arteries. The hyperemia induced by intracoronary papaverine cannot be solely attributed to a fall in arteriolar resistance but is partially due to changes in the geometry of epicardial stenoses. In other words, the methodologic approach affects the investigated phenomenon, namely the pressure - flow relationship of the flow-limiting stenoses.

Gould & Kelley found important changes in stenosis geometry caused by papaverine induced hyperemia in dogs [74]. However, there are some qualitative differences between their results and ours, due to the different nature of human coronary atherosclerotic lesions and stenoses produced by an external constriction of normal coronary arteries in dogs. In this study an isolated increase in "normal" area

without change in the stenosis lumen area was observed. In our study [73], on the contrary, the most significant change in stenosis geometry was the increase in the cross-sectional area of the stenosis. Since change in vessel caliber caused by the coronary vasodilator (dipyridamole, papaverine or adenosine) may alter the pressure/flow relationship, administration of nitrates before the measurement of coronary flow reserve is strongly advocated to negate the epicardial vasodilator action of the drugs used for the induction of maximal hyperemia [73]

Factors influencing the accuracy of Doppler-based coronary flow reserve as an index of stenosis severity: The coronary flow velocity reserve is estimated by the ratio of peak to resting flow velocity. One of the potential problems of this measurement is that the flow velocity ratio can be affected by a change in resting flow velocity caused either by factors increasing myocardial oxygen consumption (e.g. thyrotoxicosis) or producing a resting high flow state (e.g. anemia). Changes in arterial pressure between measurements of resting and peak flow velocity can also affect this ratio. To address this problem, an index of resistance has been proposed by Wilson et al. [7] calculated as the quotient of:

$$\frac{\text{mean aortic pressure and peak flow}}{\text{peak flow velocity}} \quad \text{and} \quad \frac{\text{resting aortic pressure}}{\text{resting blood flow velocity}}$$

McGinn et al [75] have studied the influence of heart rate, arterial pressure and ventricular preload on the long-term variability of serial coronary flow reserve measurements. In 45 patients with normal left ventricular function (38 cardiac allograft recipients, five patients with normal coronary arteries and two patients with minimal coronary artery disease (< 50% diameter stenosis), coronary flow reserve measurements were highly reproducible in the absence of conditions known to affect resting or hyperemic coronary blood flow. Increases in heart rate or preload reduced coronary flow reserve because resting coronary blood flow velocity was increased while hyperemic coronary blood flow velocity was unchanged. In contrast, changes in mean arterial pressure did not alter coronary flow reserve. Interpretation of coronary flow reserve measurements should account for the variable hemodynamic conditions at which the flow velocity measurements are obtained.

A final technical note concerns the possible induction of flow obstruction due to the large guiding catheter engaged in the ostium. In this case after selective injection of the vasodilator, the catheter should be immediately pulled out from the ostium without moving the Doppler probe. A careful monitoring of the pressure waveform recorded through the guiding catheter can facilitate the detection of damping of velocity. Use of diagnostic coronary catheters (6-7 Fr) is an easier alternative possibility to prevent flow obstruction allowed by the use of the Doppler guide wire.

CONCLUSIONS AND FUTURE DIRECTIONS

The last few years have seen rapid advances in coronary Doppler probe technology and signal analysis and the development of new approaches to the interpretation of the flow velocity measurement. These changes have transformed a complex technique reserved to a few research laboratories into a reliable diagnostic tool which can be used for the assessment of stenosis severity and for the evaluation of the results of coronary interventions. These technical developments have also facilitated and increased the application of the technique in the study of coronary circulation. The availability of smaller Doppler probes (0.014" guidewires) now allows the integration of Doppler flow measurements in all coronary interventions. Combined Doppler and imaging ultrasound systems will be applied for a continuous measurement of absolute coronary flow as well as for the simultaneous study of morphological and functional characteristics of the coronary system. The development of combined Doppler-pressure sensors with guidewire technology can facilitate the assessment of stenosis hemodynamics.

Technical improvements alone, however, are insufficient to establish intracoronary Doppler as the ideal technique for the functional assessment of the coronary circulation. Knowledge of the recent advances in coronary flow physiology is a prerequisite for the interpretation of the flow velocity changes and the development of new methodological approaches mutuated from the experimental animal laboratory. The investigators using this technique in the clinical field, therefore, must remember that a close collaboration with basic scientists and coronary physiologists has been started since the very beginning by the pioneers in this field and is essential for the future development of the technique.

REFERENCES

1. Kilpatrick D., Webber S.B. Intravascular blood velocity in simulated coronary artery stenoses. *Cathet Cardiovasc Diagn* **12**: 317, 1986.
2. Hatle L., Angelsen B. Physics of blood flow. In Hatle L., Angelsen B. (Eds.): Doppler Ultrasound in Cardiology: Chapter 2: Physics of blood flow: 8-31. Lea and Feabiger, Philadelphia, 1982.
3. Hartley C.J., Cole J.S. An ultrasonic pulsed Doppler system for measuring blood flow in small vessels. *J Applied Physiol* **37**: 626, 1974.
4. Kern M.J., Courtois M., Ludbrook P., A simplified method to measure coronary blood flow velocity in patients: validation and application of a new Judkins style Doppler tipped angiographic catheter. *Am Heart J* **120**: 1202, 1990.
5. Wright C.B., Doty D.B., Eastham C.L. Measurement of coronary reactive hyperemia with a Doppler probe: intraoperative guide to hemodynamically significant lesions. *J Thorac Cardiovasc Surg* **80**: 888, 1980.
6. Marcus M.L. The coronary circulation in health and disease. *McGraw-Hill, New York*, 23, 1983.
7. Wilson R.F., Laughlin D.E., Ackell P.H., et al Transluminal, subselective measurement of coronary artery blood flow velocity and vasodilator reserve in man. *Circulation* **72**: 82, 1985.
8. Sibley D.H., Millar H.D., Hartley C.J., Whitlow P.L. Subselective measurement of coronary blood flow velocity using a steerable doppler catheter. *J Am Coll Cardiol* **8**: 1332, 1986.
9. Tadaoka S., Kagiyama M., Hiramatsu O., et al Accuracy of 20 MHz Doppler catheter coronary

artery velocimetry for measurement of coronary blood flow velocity. *Cathet Cardiovasc Diagn* **19**: 205, 1990.

10. Akamatsu S, Kondo Y. Velocity measurement with a new Doppler catheter independent of incident angle. *Ciculation* **86**: I-869, 1992
11. Serruys P.W., Julliere Y., Zijlstra F., et al Coronary blood flow velocity during PTCA: a guide-line for assessment of functional results. *Am J Cardiol* **61**: 253, 1988.
12. Doucette JW, Douglas Corl P, Payne HP, Flynn AE, Goto M, Nassi M, Segal J. Validation of a doppler guide wire for intravascular measurement of coronary artery flow velocity. *Circulation* **85**: 1899, 1992.
13. Ofili E, Kern MJ, Tatineni S, Deligonul U, Aguirre F, Serota H, Labovitz AJ. Detection of coronary collateral flow by a doppler-tipped guide wire during coronary angioplasty. *Am Heart J* **222**: 221, 1991.
14. Ofili E.O., Karim A.M., Kern M.J., Deligonul U., Aguirre F., Serota H., Tatineni S. Simultaneous comparison of intracoronary spectral and zero-cross flow velocity measurements by Doppler guidewire and ctheter techniques. *J Am Coll Cardiol* **17**: 124A, 1991.
15. Mechem C.J., Kern M.J., Aguirre F., Caulev M., Stonner T. Safety and outcome of angioplasty guidewire Doppler instrumentation in patients with normal or mildly diseased coronary arteries. *Circulation* **86**: I-323, 1992.
16. Kajiya F., Ogasawora Y., Nakai M., et al Evaluation of human coronary blood flow with an 80 channel 20 MHz pulsed Doppler velocimeter and zero-cross and Fourier transform methods during cardiac surgery. *Circulation* **74** (suppl III): 53, 1986.
17. Sudhir K., Hargrave V.K., Johnson E.l., Aldea G., Mori H., Ports T.A., Yock P.G. Measurement of absolute coronary blood flow using a Doppler catheter. validation in an animal model. *Am Heart J* **124**: 870, 1992.
18. Johnson E.L., Yock P.G., Hargrave V.K., Srebro J.P., Manubens S.M., Seitz W., Ports T.A. Assessment of severity of coronary stenoses using a Doppler catheter. Validation of a method based on the continuity equation. *Circulation* **80**: 625, 1989.
19. Tanouchi J., Kitabatake A., Ishihara K., et al Experimental validation of Doppler catheter technique using fast Fourier spectrum analysis for measuring coronary flow velocity. *Circulation* **80** (suppl II): 4:II-566, 1989.
20. Di Mario C, Roelandt JRTC, de Jaegere P, Linker DT, Oomen J, Serruys PW. Limitations of the zero-crossing detector in the analysis of intracoronary Doppler. A comparison with fast Fourier analysis of basal, hyperemic and transstenotic blood flow velocity measurements in patients with coronary artery disease. *Cathet Cardiovasc Diagn* **28**: 56, 1993.
21. Denardo S.J., Yock P.G., Screbo J.P., et al Measurement of coronary blood flow turbulence post PTCA and coronary atherectomy. *Circulation* **80** (suppl II): 4:II-371, 1989.
22. Piek J.J., Koolen J.J., Metting van Rijn A.C., Bot H., Hoedemaker G., David G.K., Dunninc A.J., Spaan J.A.E., Visser C.A. Spectral analysis of flow velocity of the contralateral artery during coronary angioplasty: a new method for quantification of collateral flow. *J Am Coll Cardiol*, in press.
23. Yamagishi M., Hotta D., Tamai J., et al Validity of catheter-tip Doppler technique in asessment of coronary flow velocity and application of spectrum analysis method. *Am J Cardiol* **67**: 758, 1991.
24. Scaramucci J. De Motu Cordis, Theorema sextum. In Scaramucci J.: Theoremata familiaria de physico-medicis lucubrationibus iucta leges mecanicas. *Urbino*, pp. 70-81, 1695.
25. Sabinston D.C. Jr., Gregg D.E. Effect of cardiac contraction on coronary blood flow. *Circulation* **15**: 14, 1957.
26. Akasaka T., Yoshikana J., Yoshida K., Maeda K. Systolic coronary flow reversal assocated with abnormal diastolic flow dynamics in patients with aortic stenosis assessed by a coronary Doppler catheter. *Circulation* **84**: II-372, 1991.
27. Memmola C., Iliceto S., Carella L., Saponetti L., Napoli F.V., Franchini P., Rizzon P. Assessment of coronary blood flow velocity characteristics in hypertrophic obstructive cardiomyopathy by transesophageal echo Doppler. *Circulation* **86**: I-725, 1992.
28. Ofili E.O., Labovitz A.J., Kern M.J. Coronary flow dynamics in normal and diseased arteries. *Am J Cardiol* 71: 3D-9D, 1993.

29. Spaan J.A.E. Structure and function of the coronary arterial tree. In: Spaan J.A.E. (ed): "Coronary blood flow". Kluwer Academic Publishers, Dordrecht, pp. 37-64, 1991.
30. Seiler C., Kirkeeise R.L., Gould K.L. Basic structure-function relations of the epicardial coronary vascular tree. *Circulation* **85**: 1987, 1992.
31. Bach R.G., Kern M.J., Donohue T., Aguirre F., Penick D. Comparison of arterial and venous coronary bypass conduits: analysis or intra vessel blood flow velocity characteristics. *Circulation* **86**: I-181, 1992.
32. Pezzano A., Cali G., Cataldo G., Milazzo A., Pabala A. Evaluation of post-operative flow of internal mammery coronary graft by two-dimensional and color-Doppler echocardiography. *J Am Coll Cardiol* **19**: 298A, 1992.
33. Takayama T., Suma J., Wanibuchi Y., et al. Physiological and pharmacological responses of arterial graft flow after coronary artery bypass grafting measured with on implantable ultrasonic Doppler miniprobe. *Circulation* **86**: II-217, 1992.
34. Evans D.H., Schlindwein F.S., Levene M.I. The relationship between time averaged intensity weighted mean velocity and time averaged maximum velocity in neonatal cerebral arteries. *Ultrasound Med Biol* **15**: 429, 1989.
35. De Kroon M.G.M., Slager C.J., Gussenhoven W.J., Serruys P.W., Roelandt J.R.T.C., Bom N. Cyclic changes of blood echogenicity in high-frequency ultrasound. *Ultrasound Med Biol* **17**: 723, 1991.
36. Shung K.K., Cloutier G., Lim C.C. The effects of hematocrit, shear rate and turbulence on ultrasonic blood spectrum from blood. *IEEE Trans Biomed Eng* **39**: 462, 1992.
37. Denardo S.J., Talbot L., Hargrave V., Ports T.A., Yock P.G. Advantage of peak velocity over mean velocity measurements made by Doppler catheters. *Circulation* **86**: I-870, 1992.
38. Caro CG, Pedley TJ, Schroter RC, Seed WA. Flow in pipes and around objects. In Caro CG, Pedley TJ, Schroter RC, Seed WA(eds): "The mechanics of the circulation", Oxford University Press, pp. 44-73, 1978.
39. Ling SC, Atabek HB, Fry DL, Patel DJ, Janicki JS. Application of heated-film velocity and shear probes to hemodynamic studies. *Circ Res* **23**: 789, 1968.
40. Linker D.T., Torp H., Groenningsaether A., et al. Instantaneous arterial flow estimated with an ultrasound imaging and Doppler catheter (abstract). *Circulation* **80**: II-580, 1989.
41. Sudhir K., MacGregor J.S., Brabant S., Gupta M., Yock P.G., Chatterjee K. In vivo demonstration of role for nitric oxide in the regulation of coronary vascular tone by simultaneous intravascular two-dimensional and Doppler ultrasound. *J Am Coll Cardiol* **19**: 211A, 1992.
42. Furuse A., Klopp E.H., Brawley R.K., Gott V.L. Hemodynamic determinations in the assessment of distal coronary artery disease. *J Surg Res* **19**: 25, 1975.
43. Wiesner T.F., Levesque M.J., Rooz E., Nerem R.M. Epicardial coronary blood flow including the presence of stenoses and aorto-coronary bypasses. II. Experimental comparison and parametric investigations. *Trans ASME* **110**: 144, 1988.
44. Kajiya F., Ogasawara Y., Tsujioka K., et al. Evaluation of human coronary blood flow with an 80 channel 20 MHz pulsed Doppler velocimeter and zero-cross and Fourier transform methods during cardiac surgery. *Circulation* **74** (suppl III): III-53, 1986.
45. Kajiya F., Ogasawara Y., Tsujioka K., et al. Analysis of flow characteristics in post-stenotic regions of the human coronary artery during bypass graft surgery. *Circulation* **76**: 1092, 1987.
46. Segal J., Kern M.J., Scott N.A., King S.B.III, Doucette J.W., Heuser R.R., Ofili E., Siegel R. Alterations of phasic coronary artery flow velocity in man during percutaneous coronary angioplasty. *J Am Coll Cardiol* **20**: 276, 1992.
47. Ofili E.O., Kern M.J., Labovitz A.J., St. Vrain J.A., Segal J., Aguirre F., Castello R. Analysis of coronary blood flow velocity dynamics in angiographically normal and stenosed arteries before and after endoluminal enlargement by angioplasty. *J Am Coll Cardiol* **21**: 308, 1992.
48. Serruys P.W., Di Mario C., Meneveau N., de Jaegere P., Strikwerda S., de Feijter P.J., Emanuelsson H. Intracoronary pressure and flow velocity from sensor-tip guidewires. A new methodological comprehensive approach for the assessment of coronary hemodynamics before and after coronary interventions. *Am J Cardiol*, in press, 1993.

49. Dirschinger J., Dennig K., Hall D., Rudolph W. Intracoronary blood flow velocity profile in patients with coronary artery disease. *Circulation* **86**: I-587, 1992.
50. Segal J. Applications of coronary flow velocity during angioplasty and other coronary interventional procedures. *Am J Cardiol*: 71: 17D, 1993.
51. Hatle L., Angelsen B. Pulsed and continuous wave Doppler in diagnosis and assessment of various heart lesions. In Hatle L, Angelsen B (eds): Doppler ultrasound in cardiology, Lea & Feabiger, Philadelphia, 97, 1985.
52. Blasini R., Schad H., Huttl S., Mendler N., Blomer H. Intracoronary Doppler catheter: Determination of the cross-sectional area of coronary artery stenoses by improved frequency analysis (abstr). *Eur Heart J* **13**: 362, 1992.
53. Nakatami S., Yamagishi M., Tamai J., Takaki H., Haze K., Miyatake K. Quantitative assessment of coronary artery stenosis by intravascular Doppler catheter technique. *Circulation* **85**: 1786, 1992.
54. Di Mario C., Slager C.J., Linker D.T., Serruys P.W. Quantitative assessment of coronary artery stenosis by intravascular Doppler catheter technique. *Circulation* **86**: 2016, 1992.
55. Di Mario C., Meneveau N., Gil R., de Jaegere P., de Feyter P.J., Slager C.J., Roelandt J.R.T.C., Serruys P.W. Maximal blood flow velocity in severe coronary stenoses measured with a Doppler guidewire. *Am J Cardiol* 71: 41D, 1993.
56. Nissen S.E., Gurley J.C., Grines C.L., Booth D.C., McClure R., Berk M., Fisher C., DeMaria A.N. Intravascular ultrasound assessment of lumen size and wall morphology in normal subjects and patients with coronary artery disease. *Circulation* **84**: 1087, 1991.
57. StGoar F.G., Pinto F.J., Alderman E.L., Fitzgerald P.J., Stadius M.L., Popp R.L. Intravascular ultrasound of angiographically normal coronary arteries: an in-vivo comparison with quantitative angiography. *J Am Coll Cardiol* **18**: 952, 1991.
58. Gould K.L., Lipscomb K., Hamilton G.W. Physiologic basis for assessing critical coronary stenosis: instantaneous flow response and regional distribution during coronary hyperemia as measures of coronary flow reserve. *Am J Cardiol* **33**: 87, 1974.
59. Klocke F.J. Measurements of coronary flow reserve: defining pathophysiology versus making decisions about patient care. *Circulation* **76**: 245, 1987.
60. Sugawara M. Stenosis: theoretical background. In Sugawara M, Kajiya F, Kitabatake A, Matsuo H (eds) "Blood Flow in the Heart and Large Vessels", Springer-Verlag, Tokyo-Berlin-New York, p.91, 1989.
61. Gould K.L., Kirkeeide R.L., Buchi M. Coronary flow reserve as a physiologic measure of stenosis severity. *J Am Coll Cardiol* **15**: 459, 1990.
62. Wilson R.F., Marcus M.L., White C.W. Prediction of the physiologic significance of coronary arterial lesions by quantitative lesion geometry in patients with limited coronary artery disease. *Circulation* **75**: 723, 1987.
63. Harrison D.G., White C.W., Hiratzka L.F., Eastham C.L., Marcus M.L. The value of lesional cross-sectional area determined by quantitative coronary angiography in assessing the physiologic significance of proximal left antrerior descending coronary artery stenoses. *Circulation* **69**: 111, 1984.
64. Klocke F.J. Cognition in the era of technology: "seeing the shades of gray". *J Am Coll Cardiol* **16**; 763, 1990.
65. Bookstein J.J., Higgins C.B. Comparative efficacy of coronary vasodilatory methods. *Investigational Radiology* **12**: 121, 1977.
66. Wilson R.F., White C.W. Intracoronary papaverine: an ideal coronary vasodilator for studies of the coronary circulation in conscious humans. *Circulation* **73**: 444, 1986.
67. Zijlstra F., Juillière Y., Serruys P.W., Roelandt J.R.T.C. Value and limitations of intracoronary adenosine for the assessment of coronary flow reserve. *Cathet Cardiovasc Diagn* **15**: 76, 1988.
68. Wilson R.F., White C.W. Serious ventricular dysrhythmias after intracoronary papaverine. *Am J Cardiol* **62**: 1301, 1988.
69. Wilson R.F., Wyche K., Christensen B.V., Laxson D.D. Effects of adenosine on human coronary arterial circulation. *Circulation* **82**: 1595, 1990.
70. Kern M.J., Deligonul U., Aguirre F., Hilton T.C. Intravenous adenosine: continuous infusion and

low dose bolus administration for determination of coronary vasodilator reserve in patients with and without coronary artery disease. *J Am Coll Cardiol* **18**: 718, 1991.

71. Abreu A., Mahmarian J.J., Nishimura S., Verani M.S. Tolerance and safety of pharmacologic coronary vasodilatation with adenosine in association with thallium 201 scintigraphy in patients with suspected coronary artery disease. *Am J Cardiol* **18**: 730, 1991.
72. Zijlstra F., Ommeren J. van, Reiber J.H.C., Serruys P.W. Does quantitative assessment of coronary artery dimensions predict the physiologic significance of a coronary stenosis? *Circulation* **75**: 1154, 1987.
73. Zijlstra F., Reiber J.H.C., Serruys P.W., et al. Does intracoronary papaverine dilate epicardial coronary arteries? Implications for assessment of coronary flow reserve. *Cathet Cardiovasc Diagn* **14**: 1, 1988.
74. Gould K.L., Kelley K.O. Physiological significance of coronary flow velocity and changing stenosis geometry during coronary vasodilation in awake dogs. *Circ Res* **50**: 695, 1982.
75. McGinn A.L., White C.W., Wilson R.F. Interstudy variability of coronary flow reserve: influence of heart rate, arterial pressure, and ventricular preload. *Circulation* **81**: 1319, 1990.

CHAPTER 8

LIMITATIONS OF THE ZERO CROSSING DETECTOR IN THE ANALYSIS OF INTRACORONARY DOPPLER

A comparison with fast Fourier transform analysis of basal, hyperemic and transstenotic blood flow velocity measurements in patients with coronary artery disease

Carlo Di Mario, M.D.,* Jos R.T.C. Roelandt, M.D., Ph.D.,
Peter de Jaegere, M.D., Ph.D., David T. Linker, M.D., Jan Oomen, Ph.D.,
Patrick W. Serruys, M.D., Ph.D.

From the Cardiac Catheterization Laboratory, Division of Cardiology,
Thoraxcenter, Erasmus University, Rotterdam

Reprinted from: Cathet Cardiovasc Diagn, 1993.

Catheterization and Cardiovascular Diagnosis 28:56–64 (1993)

Technical Note

Limitations of the Zero Crossing Detector in the Analysis of Intracoronary Doppler: A Comparison With Fast Fourier Transform Analysis of Basal, Hyperemic, and Transstenotic Blood Flow Velocity Measurements in Patients With Coronary Artery Disease

Carlo Di Mario, MD, Jos R.T.C. Roelandt, MD, PhD, Peter de Jaegere, MD, David T. Linker, MD, Jan Oomen, PhD, and Patrick W. Serruys, MD, PhD

The current clinical standard for the analysis of intracoronary Doppler signals is the application of a zero-crossing (ZC) detector. However, the accuracy of the method is questionable, especially in areas of disturbed flow, as confirmed by in vitro studies, animal experiments, and intraoperative observations. The aim of this study is the comparison of a conventional ZC detector and a custom-designed spectral analyzer (fast Fourier transform, FFT) in the analysis of intracoronary Doppler signals obtained in 19 patients undergoing coronary angioplasty.

A 3F catheter with an end-mounted Doppler ceramic crystal was placed over an 0.014" guidewire in a normal or near-normal segment proximal to the lesion to be dilated. The Doppler signal was recorded before and after intracoronary infusion of 12.5 mg of papaverine. In 9 patients high flow velocities could be recorded when the catheter was advanced across the stenosis.

The blood flow velocity measurements obtained with ZC were significantly lower than the maximal FFT flow velocity measurements (16±12 cm/s vs. 29±18 cm/s, $p < .001$). In all the conditions of Doppler signal acquisition (baseline, hyperemia, stenosis) a large scattering of the signed differences between corresponding measurements was observed. The standard deviation of the difference ZC-FFT was ±11 cm/s and ±5 cm/s for the maximal and mean FFT flow velocity, corresponding in both cases to ±37% of the mean of the ZC and FFT measurements. Large differences were also observed in the values of coronary flow reserve (CFR) calculated as the ratio between ZC and FFT flow velocity measurements 30 s after papaverine intracoronary and at baseline. The standard deviation of the difference ZC-FFT based CFR was ±1.3 and ±1.2 for the values derived from the maximal and mean FFT flow velocities (percent difference ±32% and ±37%, respectively).

In conclusion, the measurements obtained from the same intracoronary Doppler signal analyzed with a ZC detector and an FFT technique showed large differences in various conditions of flow and also in the assessment of relative flow velocity derived indices such as CFR. Spectral analysis should replace the current use of a ZC detector for the evaluation of coronary Doppler signals, even for the assessment of relative flow velocity changes.

Key words: blood flow velocity, Doppler ultrasound, coronary stenosis, coronary flow reserve

INTRODUCTION

Spectral analysis has replaced the use of zero-crossing (ZC) detectors in most applications of Doppler ultrasound in cardiology. With a ZC detector the Doppler shift is measured from the interval between each pair of adjacent ZCs of the same polarity. Although this technique is adequate for a simple sinusoidal signal, only a rough approximation of the mean frequency is obtained

From the Cardiac Catheterization Laboratory, Division of Cardiology, Thoraxcenter, Erasmus University, Rotterdam, The Netherlands.

Received March 16, 1992; revision accepted June 1, 1992.

Address reprint requests to Dr. Patrick Serruys, M.D., Ph.D., Cardiac Catheterization Laboratory, Div. Cardiology, Thoraxcenter, Ee 2332, Erasmus University, P.O. Box 1738, 3000 DR Rotterdam, The Netherlands.

Dr. C. Di Mario (Card. Div. Vicenza, Italy) is the recipient of the European Society of Cardiology Research Fellowship 1991.

when ZC is used for the analysis of composite Doppler signals induced by the presence of scatterers of different velocity in the Doppler sample volume [1,2]. The main advantages of the analysis of the full frequency spectrum of the Doppler signal are the detection of the maximal Doppler frequency and the more accurate calculation of the mean Doppler frequency from the weighted intensity of the signal for each frequency. Furthermore, the presence of noise can be more easily detected and distinguished from the physiologic signal. Despite these advantages of spectral analysis, ZC detectors are almost invariably used in recent reports applying intracoronary Doppler [3–5]. The small sample volume of most intracoronary Doppler probes and the use of relative rather than absolute measurements are possible arguments supporting the use of a ZC detector for the analysis of intracoronary signals [6].

Aim of this study is the comparison of a conventional ZC detector and a custom-designed spectral analyzer using a fast Fourier transform (FFT) algorithm for the analysis of intracoronary Doppler recordings. To this purpose intracoronary Doppler signals have been recorded and simultaneously analyzed with the two techniques in baseline conditions, during pharmacologically induced hyperemia, and in areas of disturbed flow (stenosis) in 19 patients undergoing coronary angioplasty.

MATERIALS AND METHODS

Patients

The Doppler studies were performed in 19 patients (age 57 ± 12 years, 11 men and 8 women) undergoing percutaneous treatment of symptomatic high-grade coronary stenosis (14 balloon angioplasty, 5 directional atherectomy). The protocol was approved by the Ethics Committee Erasmus University/Dijkzigt Hospital (protocol #104.975/1990/55). Written informed consent was obtained in all cases. The treated vessel was the left anterior descending artery in 8 cases, the right coronary artery in 6 patients, and the left circumflex artery in 5 patients.

Catheterization Procedure

The Doppler transducer consisted of a 20 MHz annular piezoelectric crystal [7] mounted at the tip of a 3F (diameter = 1 mm) intracoronary catheter (Schneider, Zürich, Switzerland). After systemic heparinization with 10,000 I.U. and intracoronary injection of 2–3 mg of isosorbide-dinitrate, the Doppler catheter was inserted into the proximal coronary artery through the guiding catheter and along an 0.014" guidewire (Monorail technique). The position of the Doppler probe was optimized in order to obtain stable recordings in basal conditions. Afterwards, 12.5 mg of papaverine was injected intracoronarily through the guiding catheter and a new recording was obtained after 30 s [8,9]. The guiding catheter was withdrawn from the coronary ostium to avoid limitations of flow during hyperemia. Based on clinical conditions and severity and characteristics of the stenosis an attempt to advance the Doppler catheter across the stenosis was performed in 14 cases before angioplasty and in 4 cases after angioplasty. In 3 cases the severity of the lesion precluded the passage of the Doppler catheter. No complications related to the use of the Doppler catheters occurred. The entire procedure of acquisition of the Doppler tracings, from insertion to withdrawal of the Doppler catheter, had a mean duration of 12 min (range 7–31 min).

Doppler Recording and Analysis

The Doppler catheter was activated with an MVD pulsed Doppler velocimeter (Millar Instruments, Houston, TX, USA) with a carrier frequency of 20 Mhz and a pulse repetition frequency of 62.5 kHz. The gate control (sample volume of 0.46 mm in depth, movable from 1 to 10 mm from the catheter tip) was adjusted from 2 to 4 mm to optimize the signal intensity and characteristics. Low frequencies (<200 Hz) were partially removed using a high-pass filter. The quadrature audio signal was simultaneously analyzed with an internal ZC detector and transmitted to a spectral analyzer. This system uses an ADSP-2100A signal processor provided with two analog/digital converters (AD 1332). The FFT analysis was performed on 256 samples every 10 ms and transmitted across a parallel interface to an Olivetti M250 PC. With both systems the Doppler frequencies (kHz) were transformed in velocity (cm/s) by multiplying the frequency shift by 3.75 times according to the Doppler equation. After the recording of a calibration signal, the phasic and time-averaged ("mean") ZC velocities were continuously recorded on a strip-chart recorder. When a stable signal was obtained in basal conditions, across the stenosis and 30 s after papaverine injection, the ZC velocities were recorded at 25 mm/s simultaneously to the acquisition and storage of 10 s of signal processed with the FFT analyzer (Fig. 1). The time-averaged ("mean") ZC flow velocity was compared with the time-averaged maximal and mean FFT simultaneously acquired flow velocities automatically calculated as the 90th and 50th percentile of the flow velocity spectrum distribution, respectively.

Coronary flow reserve (CFR) was calculated as the ratio between coronary velocity 30 s after intracoronary papaverine infusion and at baseline (Fig. 2).

Statistical Analysis

The statistical significance of the difference between simultaneously acquired time-averaged ZC and maximal

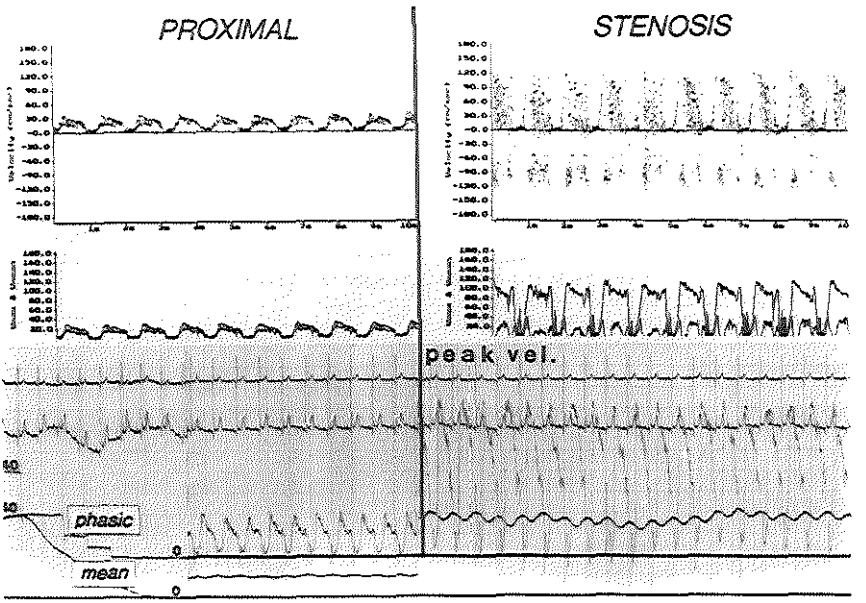

Fig. 1. Example of Doppler blood flow velocity recording in the proximal (PROXIMAL) left anterior descending coronary artery and with the Doppler catheter advanced across the stenosis (STENOSIS). Note that in the right upper tracing, recorded across the stenosis and analyzed with the FFT technique, the flow velocities higher than 120 cm/s are shown as negative because of frequency aliasing. Consequently, the algorithms automatically applied for calculation of maximal (Vmax) and mean (Vmean) blood flow velocity underestimated the true flow velocity. In the ZC tracing (lower part of the illustration, with the calibration signals for both phasic and time-averaged ("mean") flow velocity shown on the left) no clear evidence of the presence of frequency aliasing indicated that the ZC flow velocity measurement was falsely low.

and mean FFT measurements and derived CFRs was evaluated using Student's t-test. The time-averaged ("mean") ZC flow velocity was compared with the corresponding maximal and mean FFT velocities using linear regression analysis. The regression equation was separately calculated for the measurements at baseline, during hyperemia, and across the stenosis. Subsequently, according to the method described by Bland and Altman for the assessment of the agreement between different methods of measurement [10], the signed differences of the corresponding measurements were plotted against the mean of the measurements.

RESULTS

Forty-eight Doppler recordings were available for comparison (23 recordings in baseline conditions, 16 at peak papaverine effect, 9 across the stenosis). Papaverine injection was not performed in 3 patients. In 4 patients the measurements during hyperemia were impossible because of frequency aliasing (2 cases) and of signal deterioration after papaverine infusion (2 cases). In 3 of the 15 recordings across the stenosis a complete obstruction was induced by the Doppler catheter, with the development in 2 cases (excluded from this comparative study) of collateral circulation (reversed flow with very low negative flow velocity). In 3 cases frequency aliasing precluded the analysis of the tracings (Fig. 1). In 4 of the remaining 9 recordings mean FFT velocities could not be measured because of the impossibility to correctly analyze the flow velocity signal in the presence of prominent artifacts from vessel wall movements.

Comparison Between ZC and FFT Flow Velocity Measurements

The blood flow velocities measured with the ZC detector were significantly lower than the maximal FFT velocities (16±12 vs. 29±18 cm/s, $p < .001$). No sig-

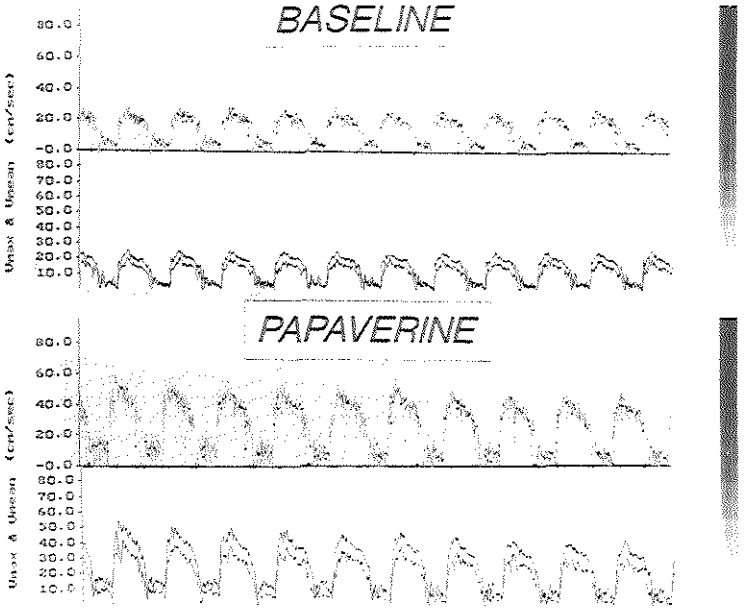

Fig. 2. Example of flow velocity measurement with the FFT analysis system used at the Thoraxcenter. The upper tracing (BASELINE) shows the spectral analysis of 10 s of Doppler flow velocity recording in the left anterior descending artery in basal conditions. The lower lines indicate the automatically calculated maximal flow velocity (Vmax) and mean flow velocity (Vmean). In the lower tracing (PAPAVERINE) the blood flow velocity increase 30 s after intracoronary injection of 12.5 mg of papaverine is shown in the same patient and with the same catheter position.

nificant differences were observed between ZC and mean FFT flow velocity measurements (16±12 vs. 15±9 cm/s, NS).

In Figure 3 linear regression analysis was used to compare ZC flow velocity measurements with the corresponding maximal (A) and mean (B) FFT flow velocity measurements. As evident from the comparison in Figure 3A of the three regression lines with the line of identity (slope of the regression line for the three series of measurement = 0.55), the blood flow velocity measurements obtained with ZC, a technique based on the averaging of the Doppler signal, were lower than the maximal FFT coronary blood flow velocities. The overall regression coefficient for the three series of measurements was 0.80. A better correlation was observed when ZC and mean FFT measurements were compared (Fig. 3B), with a slope of the cumulative regression line of 1.06 and an r value of 0.89.

In Figure 4 the signed percent differences of the corresponding ZC and FFT measurements are plotted against their mean value. As predicted from the principle of analysis of the ZC detector, negative differences were observed in the comparison with the maximal FFT blood flow velocity (mean −58%) while the mean difference with the mean FFT flow velocity measurements was −4%. With both techniques, however, a large scattering of the signed differences was observed (sd of the ZC/FFT difference = ±11 and ±5 cm/s for maximal and mean FFT velocities, equal to 37% of the mean of the ZC+FFT flow velocity measurements in both cases).

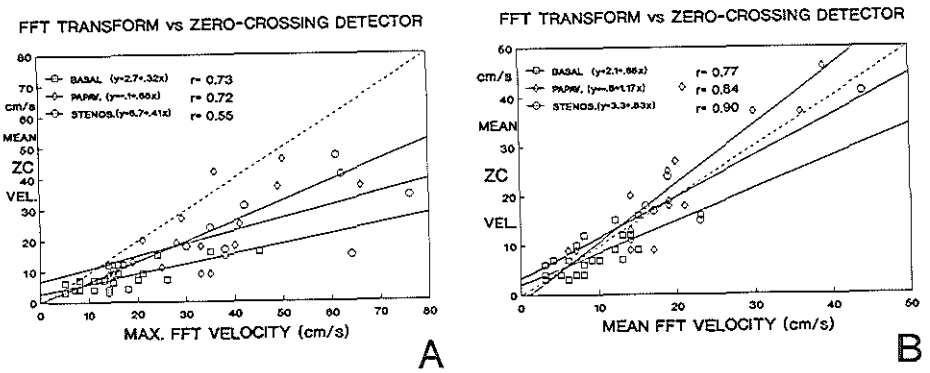

Fig. 3. Linear regression analysis of the 43 paired flow velocity measurements obtained with a ZC detector (y-axis) and the FFT technique (x-axis, maximal (MAX) FFT flow velocity in A, mean FFT flow velocity in B). The open boxes, triangles, and circles indicate the recordings in basal conditions, 30 s after intracoronary papaverine infusion (PAPAV.) and across the stenosis (STENOS.), respectively. For each set of measurements the regression equation and coefficient are reported and the regression line is drawn (basal: lower line; papaverine: intermediate line; stenosis: upper line). The line of identity is also drawn for comparison.

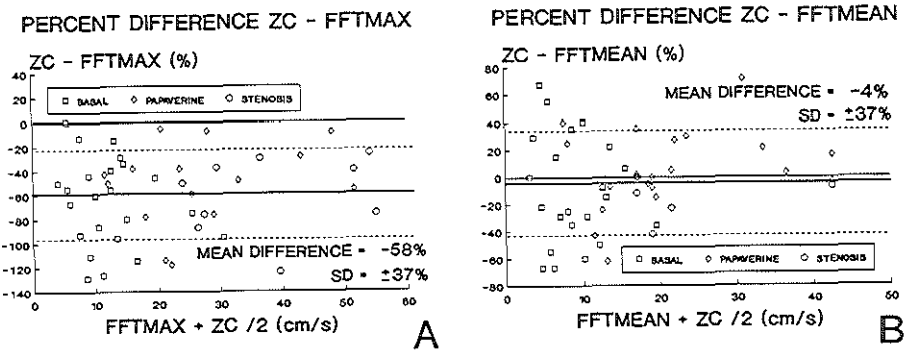

Fig. 4. Comparison of the FFT maximal (MAX, A) and mean (B) flow velocities with the corresponding ZC measurements. The mean of the FFT maximal/mean flow velocity measurement and the ZC flow velocity measurement is plotted on the x-axis. On the y-axis the signed difference between ZC and FFT paired measurements is plotted after normalization for the corresponding value on the x-axis (percent value). The thick continuous line indicates the mean difference and the dashed lines the standard deviation of the difference. Note the underestimation of the maximal FFT velocities and the large scattering of the data-points (SD = ±37% for both maximal and mean FFT velocities) over the wide range of explored velocities and in conditions of basal and hyperemic flow as well as in the recordings across the stenosis.

Comparison of ZC vs. FFT Analysis: Coronary Flow Reserve

Higher values of CFR were calculated from the ZC flow velocity measurements than from the FFT measurements (3.2±3.1 vs. 2.4±1.4 and 3.2±3.1 vs. 2.3±1.4 for maximal and mean FFT CFR measurements, respectively). Both differences, however, were not statistically significant.

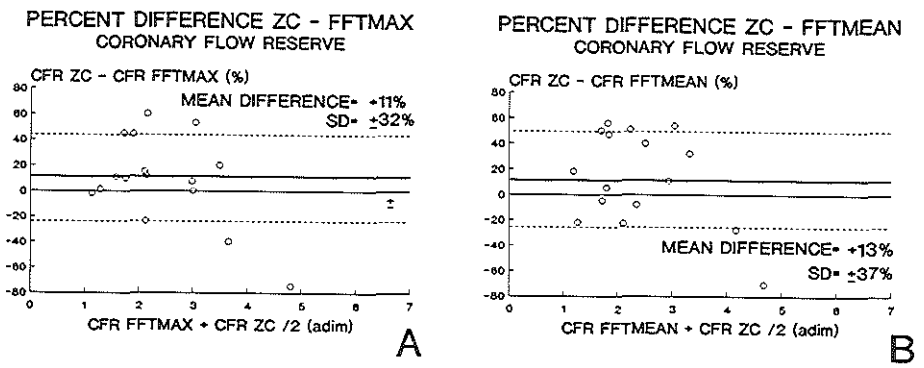

Fig. 5. Comparison of the CFRs calculated from the maximal (MAX, A) and mean (B) flow velocities with the corresponding ZC CFR values. The mean of the FFT maximal/mean flow velocity measurement and the ZC flow velocity measurement is plotted on the x-axis. On the y-axis the difference between ZC and FFT corresponding measurements is displayed after normalization for the corresponding value on the x-axis. The thick continuous line indicates the mean difference and the dashed lines the standard deviation of the difference.

When the difference of CFR calculated with the two techniques is plotted against the mean of the two values (Fig. 5), the presence of a large scattering of the values is evident (SD of the difference between ZC and FFT CFR measurements = ±1.3 (±32%) and ±1.2 (±37%) for maximal and mean FFT CFR measurements, respectively).

Maximal Vs. Mean Fast Fourier Transform Flow Velocities

The mean FFT flow velocity was obviously smaller than the maximal FFT flow velocity (15±9 vs. 29±18 cm/s, $p < .001$).

In Figure 6A linear regression analysis shows that the relation between the paired mean and maximal FFT measurements in basal and hyperemic conditions was defined by a regression equation with an intercept almost equal to 0 and a slope close to 0.5.

Similar values of CFR were calculated from maximal and mean FFT flow velocity measurements (2.4±1.4 vs. 2.3±1.4, NS).

As evident from the linear regression analysis of these data (Fig. 6B), maximal and mean FFT CFR values were highly correlated ($r = 0.95$), with a regression line almost superimposed to the line of identity.

DISCUSSION

The usefulness of the FFT analysis in the evaluation of intravascular Doppler signals is supported by previous in vitro and animal experience. Tadaoka et al. [11], using a straight tube perfused with continuous flow, observed that the ZC detector underestimated the true flow velocities, which were correctly measured with the FFT analysis. The ZC technique, however, seemed to be sufficiently reliable for the evaluation of relative flow velocity changes. Kajiya et al. [12] have reported that the flow velocity measured with a ZC detector is consistently different from the mean flow velocity detected with the FFT method in stenotic canine femoral arteries. In a canine model of adjustable coronary flow, Yock et al. [13] reported that the absolute flow measured with an electromagnetic flowmeter could be successfully estimated using the maximal velocities measured with the FFT but was poorly correlated to the flow velocities measured with a ZC detector. The same group in a separate experiment used stenosis phantoms of known diameter placed in canine coronary arteries and reported that the maximal FFT velocity proximal and across the stenosis gave the best estimate of the true cross-sectional area of the stenosis based on the continuity equation [14]. On the contrary, the corresponding flow velocities measured with a conventional ZC detector were poorly correlated with the cross-sectional areas where the sample volume was located. Tanouchi et al. [15] reported that the flow velocity measured in the left anterior descending coronary artery with the FFT spectral analysis correlated well with those estimated by electromagnetic flowmeter ($y = .88x + 9.7$, $r = .93$), whereas the velocities measured with a ZC detector significantly un-

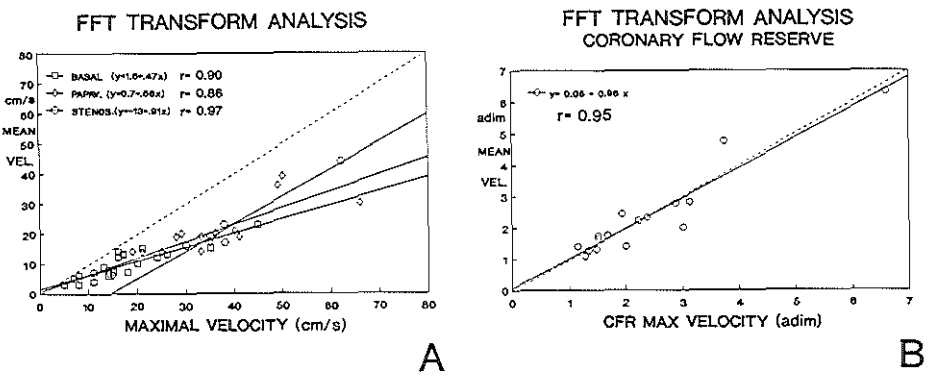

Fig. 6. A: Linear regression analysis of the mean FFT (y-axis) vs. maximal FFT (x-axis) flow velocity measurements. Symbols as in Figure 3. B: Linear regression analysis of the CFR calculated from the mean FFT (y-axis) and the maximal (MAX, X-axis) flow velocity measurements. The regression line (continuous line) is almost superimposed to the line of identity (dashed line).

derestimated those by electromagnetic flowmeter ($y = .23x + 1.6$, $r = .82$). Our study confirms that the agreement between ZC and FFT flow velocity measurements is too poor to allow the use of these techniques interchangeably for the analysis of the coronary signal. In principle ZC is an adequate technique for the assessment of a laminar flow containing only scatterers of the same velocity. In most of our FFT tracings, however, broad velocity spectra were recorded suggesting that the sample volume, despite the relatively small dimensions (longitudinal depth of the three-dimensional volume of 0.46 mm), included various blood flow lamina within the velocity profile of the vessel. Furthermore, the sample volume should be considered not as a spatially well demarcated region outside which no signal is received from the ultrasound transducer but rather as the area of greatest sensitivity [1].

Although a high pass filter was used in all cases, the Doppler signal was often disturbed by the presence of low velocity/high intensity signals induced by the movement of the coronary wall, a condition that further increases the complexity of the recorded Doppler signal. Experienced users of the ZC detector can adjust the position of the probe in order to improve the quality of the Doppler signal based on the careful evaluation of the audio feedback and the absence of "spiking" in the recording. With the use of spectral analysis the wall thumps are clearly distinguished from the flow velocity signal and their presence does not influence the measurements of maximal flow velocity. The ZC tracing, on the contrary, does not directly display these non-flow related signals which are averaged with the blood flow signal resulting in a misinterpretation of the true flow velocity.

The presence of disturbed flow or turbulence is a condition known to greatly impair the accuracy of the ZC detector, as shown by previously reported animal experiences [12]. In this study the scattering of the differences between corresponding ZC and FFT measurements was similar for the signals acquired across the stenosis and in the proximal artery probably because the Doppler system that we used was unable to record the true transstenotic maximal velocity. The relatively large dimensions of the catheter in comparison with the stenosis diameter induced partial or complete obstruction to flow and the high frequency and the pulse repetition rate of the system precluded a reliable measurement of flow velocities > 120 cm/s. The corresponding phasic ZC tracings (Fig. 1) showed no clear changes warning that frequency aliasing had occurred, inducing a falsely low flow velocity measurement.

An argument used to justify the use of the ZC detector is that intracoronary Doppler is a technique already confined to the assessment of relative flow velocity changes, for instance to study the effects of acute infusions of drugs or of coronary interventions, because of its well-known limitations for the measurement of absolute flow velocities (malalignment of the catheter with the maximal flow velocity, inclusion of a limited area of the velocity profile in the sample volume, presence of non-flow related disturbing signals) [16,17]. Our findings,

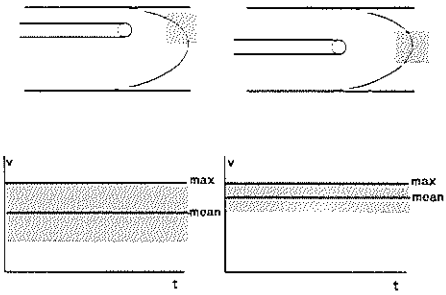

Fig. 7. Artist's representation of the effects of a change of the position of the sample volume (dashed square) across the same parabolic flow profile. A large difference is present in the calculated mean velocity while no changes are observed when the maximal velocity is considered. t = time; v = velocity.

however, do not corroborate the applicability of a ZC detector even for this simple purpose. As previously reported, Tadaoka et al. [11] found ZC reliable for the assessment of relative flow changes. The in vitro conditions of the study, in the presence of a continuous flow and of a stable catheter position, are very different from the more complex in vivo coronary application. In this latter situation the rough averaging process performed by the ZC detector is less likely to be linearly correlated to the true blood flow velocity changes.

The maximal blood flow velocity is detectable only using techniques of spectral analysis. The lower flow velocity measurements obtained with ZC are a predictable result because this technique measures a mean of all the Doppler shifts at a certain time. The use of the maximal flow velocity, however, gives substantial advantages over the Doppler measurements based on signal averaging, including the spectral mean velocity [18]. The average of the flow velocity signal can be modified by the presence of noise or artifacts that frequently occur during the acquisition of intracoronary Doppler recordings due to coronary wall motion and insufficient insulation of the Doppler catheter. The maximal velocity is less influenced by the presence of noise. The use of the maximal velocity, moreover, can partially obviate one of the most important limitations of intracoronary Doppler, the extreme space-dependency of the technique. As shown in Figure 7 changes of the position of the catheter in the vessel and, consequently, of the sample volume across the flow velocity profile can largely modify the measured mean velocity. The maximal velocity, however, does not change as long as the centerline of maximal flow is included in the sample volume. Another disadvantage of the use of averaged Doppler measurements is the different echogenicity in the flow velocity profile induced by the presence of varying conditions of erythrocyte aggregation according to the varying shear rate [19]. In our study when the mean velocity was measured using the FFT analysis, at least for the measurement obtained in the proximal coronary segment, the values were almost half of the corresponding maximal velocity values. This proportion corresponds to the theoretical estimate of the maximal/mean flow velocity ratio in vessels with a fully developed velocity profile.

In this study no attempts were performed to correlate the Doppler flow velocity measurements with an independent method of measurement of coronary flow. Yamagishi et al. [20] have recently reported that the relative changes of coronary flow measured with coronary sinus thermodilution were well correlated to the changes of the measured diastolic Doppler flow velocities measured with an FFT spectral analyzer.

CONCLUSIONS

The results of the analysis of intracoronary Doppler signals recorded in various conditions of flow with a conventional ZC detector and the FFT technique of spectral analysis showed a poor agreement between the two techniques, even in the assessment of relative flow velocity changes. Based on these findings and on the well-known principles of operation of the two techniques, we suggest that spectral analysis should replace the current use of ZC detectors for the analysis of intracoronary Doppler tracings because of its unique capability to detect the maximal flow velocity and more accurately measure mean flow velocity and of the easier detection of frequency aliasing, wall motion artifacts, and other noise components precluding a meaningful interpretation of the Doppler recording or requiring a readjustment of the probe position.

ACKNOWLEDGMENTS

The spectral analyzer used was built through a concerted effort of the Department of Biomedical Technology, Erasmus University-Rotterdam and the Instrumentation Department of the University Hospital of Utrecht. The technical assistance of Mr. R. van den Perk, M.Sc., and Miss E. Montauban van Swijndregt, M.Sc., is gratefully acknowledged.

REFERENCES

1. Hatle L, Angelsen B: Blood flow velocity measurements using the Doppler effect on backscattered ultrasound. In Hatle L, An-

gelsen B (eds): "Doppler Ultrasound in Cardiology." Philadelphia: Lea and Febiger, 1982, pp 32–70.
2. Lunt MJ: Accuracy and limitations of the ultrasonic Doppler blood flow velocimeter and zero crossing detector. Ultrasound Med Biol 2:1–10, 1975.
3. Wilson RF, Wyche K, Christensen BV, Laxson DD: Effects of adenosine on human coronary arterial circulation. Circulation 82: 1595–1606, 1990.
4. Golino P, Piscione F, Willerson JT, Cappelli-Bigazzi M, Focaccio A, Villari B, Condorelli M, Chiariello M: Divergent effects of serotonin on coronary artery dimensions and blood flow in patients with coronary atherosclerosis and control patients. N Engl J Med 324:641–648, 1991.
5. Zeiher AM, Drexler H, Wollschläger H, Just H: Endothelial dysfunction of the coronary microvasculature is associated with impaired coronary blood flow regulation in patients with early atherosclerosis. Circulation 84:1984–1992, 1991.
6. Wilson RF, Laughlin DE, Ackell PH, Chilian WM, Holids MD, Hartley CJ, Armstrong ML, Marcus ML, White CW: Transluminal, subselective measurement of coronary artery blood flow velocity and vasodilator reserve in man. Circulation 72:82–92, 1985.
7. Sibley DH, Millar HD, Hartley CJ, Whitlow PL: Subselective measurement of coronary blood flow velocity using a steerable Doppler catheter. J Am Coll Cardiol 8:1332–1340, 1986.
8. Wilson RF, White CW: Intracoronary papaverine: an ideal coronary vasodilator for studies of the coronary circulation in conscious humans. Circulation 73:444–451, 1986.
9. Zijlstra F, Juillière Y, Serruys PW, Roelandt JRTC: Value and limitations of intracoronary adenosine for the assessment of coronary flow reserve. Cathet Cardiovasc Diagn 15:76–80, 1988.
10. Bland MJ, Altman DG: Statistical methods for assessing agreement between two methods of clinical measurement. Lancet 8: 307–309, 1986.
11. Tadaoka S, Kagiyama M, Hiramatsu O, Ogasawara Y, Tsujioka K, Wada Y, Sawayama T, Kajiya F: Accuracy of 20 MHz Doppler catheter coronary artery velocimetry for measurement of coronary blood flow velocity. Cathet Cardiovasc Diagn 19:205–213, 1990.
12. Kajiya F, Ogasawora Y, Nakai M, Goto M, Wada Y, Tadoka S, Matsuoka S, Mito K, Fuwruora T: Evaluation of human coronary blood flow with an 80 channel 20 MHz pulsed Doppler velocimeter and zero-cross and Fourier transform methods during cardiac surgery. Circulation 74(Suppl III):III-53–III-60, 1986.
13. Yock PG, Hargrave VK, Johnson EI: Measurement of absolute coronary blood flow using a Doppler catheter. Validation in an animal model (abstract). J Am Coll Cardiol 11:45A, 1988.
14. Johnson EL, Yock PG, Hargrave VK, Srebro JP, Manubens SM, Seitz W, Ports TA: Assessment of severity of coronary stenoses using a Doppler catheter. Validation of a method based on the continuity equation. Circulation 80:625–635, 1989.
15. Tanouchi J, Kitabatake A, Ishihara K, Fujii K, Uematsu M, Yoshida Y, Doi Y: Experimental validation of Doppler catheter technique using fast Fourier spectrum analysis for measuring coronary flow velocity. Circulation 80(Suppl II):II-566, 1989.
16. Serruys PW, Hermans WRM, Zijlstra F, De Feyter PJ: Coronary Doppler. In Topol EJ (ed): "Textbook of Interventional Cardiology." Boston: W.B. Saunders Company, 1990, pp 768–798.
17. Serruys PW, Julliere Y, Zijlstra, Roelandt JRTC: Coronary blood flow velocity during PTCA: a guide-line for assessment of functional results. Am J Cardiol 61:253–259, 1988.
18. Evans DH, Schlindwein FS, Levene MI: The relationship between time averaged intensity weighted mean velocity and time averaged maximum velocity in neonatal cerebral arteries. Ultrasound Med Biol 15:429–435, 1989.
19. De Kroon MGM, Slager CJ, Gussenhoven WJ, Serruys PW, Roelandt JRTC, Bom N: Cyclic changes of blood echogenicity in high frequency ultrasound. Ultrasound Med Biol 17:723–728, 1991.
20. Yamagishi M, Hotta D, Tamai J, Nakatani S, Miyatake K, Validity of catheter-tip Doppler technique in assessment of coronary flow velocity and application of spectrum analysis method. Am J Cardiol 67:758–762, 1991.

CHAPTER 9

MAXIMAL BLOOD FLOW VELOCITY IN SEVERE CORONARY STENOSES MEASURED WITH A DOPPLER GUIDEWIRE

Limitations for the application of the continuity equation in the assessment of stenosis severity

Carlo Di Mario, M.D., Nicolas Meneveau, M.D., Robert Gil, M.D., Peter de Jaegere, M.D., Ph.D., Pim J. de Feyter, M.D., Ph.D., Cornelis J. Slager, Ph.D., Jos R.T.C. Roelandt, M.D., Ph.D., Patrick W. Serruys, M.D., Ph.D.

From the Cardiac Catheterization Laboratory, Division of Cardiology, Thoraxcenter, Erasmus University, Rotterdam

Reprinted from: Am J Cardiol, 1993.

Maximal Blood Flow Velocity in Severe Coronary Stenoses Measured with a Doppler Guidewire

LIMITATIONS FOR THE APPLICATION OF THE CONTINUITY EQUATION IN THE ASSESSMENT OF STENOSIS SEVERITY

Carlo Di Mario, MD, Nicolas Meneveau, MD, Robert Gil, MD, Peter de Jaegere, MD, Pim J. de Feyter, MD, PhD, Cornelis J. Slager, PhD, Jos R. T. C. Roelandt, MD, PhD, and Patrick W. Serruys, MD, PhD

In vitro and animal experiments have shown that the severity of coronary stenoses can be assessed using the continuity equation if the maximal blood flow velocity of the stenotic jet is measured. The large diameter and the low range of velocities measurable without frequency aliasing with the conventional intracoronary Doppler catheters precluded the clinical application of this method for hemodynamically significant coronary stenoses in humans. This article reports the results obtained using a 12 MHz steerable angioplasty guidewire in a consecutive series of 52 patients undergoing percutaneous coronary angioplasty (61 coronary stenoses). The ratio between coronary flow velocity in a reference segment and in the stenosis was used to estimate the percent cross-sectional area stenosis. A Doppler recording suitable for quantization was obtained in the stenotic segment in only 10 of 61 arteries (16%). The time-averaged peak velocity increased from 15 ± 5 to 115 ± 26 cm/sec from the reference normal segment to the stenosis. Volumetric coronary flow calculated from the product of mean flow velocity and cross-sectional area was similar in the stenosis and in the reference segment (33.2 ± 14.9 vs 33.5 ± 17.0 mL/min, respectively, difference not significant). The percent cross-sectional area stenosis and minimal luminal cross-sectional area derived from the Doppler velocity measurements using the continuity equation and calculated with quantitative angiography were also similar (Doppler, 86.7 ± 5.1% and 1.00 ± 0.48 mm²; quantitative angiography, 85.9 ± 7.9% and 1.02 ± 0.50 mm²). A significant correlation was observed between Doppler-derived and angiographic measurements (percent cross-sectional area: r = 0.64, p <0.05; minimal cross-sectional area: r = 0.69, p <0.05). Although the percent cross-sectional area stenosis and minimal cross-sectional area derived from the Doppler measurements based on the continuity equation were significantly correlated with the corresponding quantitative angiographic measurements, this determination could be achieved in a minority of cases (16%), limiting the practical application of this approach for the assessment of coronary stenosis severity.

(Am J Cardiol 1993;71:54D–61D)

The principle of the continuity equation is largely applied for the calculation of cardiac valve areas from the integration of Doppler flow velocity measurements and 2-dimensional echocardiography.[1] Miniaturization of the Doppler probes, tip-mounted on flexible catheters 1 mm in diameter, has allowed the application of this equation for the assessment of the severity of coronary artery stenoses.[2] In vitro studies in hydraulic models of coronary stenoses have shown an excellent correlation between true cross-sectional area of the stenosis and stenosis area calculated from the ratio of the flow velocity in a normal segment and in the stenosis.[3] Similar results were obtained also in animal experiments[4] and, more recently, in humans for the assessment of moderate coronary stenoses (<50% diameter stenosis).[5] The intracoronary Doppler catheters, however, cannot be used in very severe coronary stenoses because their relatively large diameter (1 mm) induces an almost complete obstruction to flow when the catheter is

From The Cardiac Catheterization Laboratory, Division of Cardiology, Thoraxcenter, Erasmus University, Rotterdam, The Netherlands.

Address for reprints: Patrick Serruys, MD, PhD, Cardiac Catheterization Laboratory, Division of Cardiology, Thoraxcenter, Ee 2332, Erasmus University, P.O. Box 1738, 3000 DR Rotterdam, The Netherlands.

advanced into the stenosis. Adjustment of the distance of the Doppler sample volume from the catheter tip has been used to investigate the stenotic jet without crossing the stenosis. This technique, however, is applicable only for short stenoses and induces an inaccurate estimation of the velocity ratio if the change of position of the Doppler sample volume is performed within the area of flow distortion distal to the catheter tip (10 times the catheter diameter).[6] Further, frequency aliasing precludes the recording of velocities higher than 110 cm/sec because of the high frequency and relatively low repetition rate of these systems. The ultraminiaturized Doppler probes mounted at the tip of a steerable angioplasty guidewire (0.018 inch) can be introduced through moderate stenoses without generally inducing a significant obstruction to flow. Further, the use of spectral analysis and the lower frequency and higher repetition rate of the Doppler guidewire system allow the recording of velocities as high as 6 m/sec without frequency aliasing.[7]

To assess the feasibility of the measurement of maximal velocity in the stenosis with a Doppler guidewire, velocity data were obtained in 52 consecutive patients during coronary angioplasty. The accuracy of the relative measurements of cross-sectional area reduction based on the ratio of the velocity measurement in a normal arterial segment and in the stenosis was also compared with the corresponding quantitative angiographic measurements.

METHODS

Study patients: The study group consisted of 52 consecutive patients (mean age 57 ± 10 years, 43 men and 9 women) undergoing coronary balloon angioplasty or other nonsurgical revascularization procedures with the use of the Doppler guidewire for the angioplasty. Arteries with complete or functional occlusion (Thrombolysis in Myocardial Infarction [TIMI] flow class 0–1) or arteries with extreme tortuosity were excluded from this study. In 9 patients the Doppler guidewire was used in 2 arteries before dilation, so that a total of 61 arteries were studied. The Doppler guidewire was successfully used to cross the coronary stenosis in 58 arteries (95%). The study angioplasty artery was the left anterior descending coronary artery in 36 cases (59%), the left circumflex in 7 (12%), the right coronary artery in 13 (21%), and a saphenous vein bypass graft in 5 (8%).

Catheterization procedure: After intravenous administration of 10,000 IU of heparin and 250 mg of acetylsalicylic acid, an 8 F guiding catheter was advanced up to the coronary ostium. After isosorbide dinitrate (2–3 mg intracoronary), cineangiograms suitable for quantitative assessment were obtained in 1–3 angiographic views.

The Doppler guidewire was advanced into the artery to be dilated and a baseline flow velocity recording was obtained in a straight angiographically normal or minimally diseased segment of the artery proximal or distal to the lesion. Care was taken to avoid the presence of major side branches between the site of the flow velocity measurement and the stenosis. When prestenotic acceleration and poststenotic deceleration of flow were identified, the guidewire position was readjusted. A new angiogram was obtained with the Doppler guidewire in place in order to locate the position of the Doppler sample volume and measure the corresponding cross-sectional area. When the guidewire approached the stenosis, the probe was slowly advanced and, if a high velocity signal was observed, carefully rotated and/or moved in order to optimize the Doppler recording. The duration of these attempts before crossing the lesion ranged between 50 and 560 sec (mean 140 sec).

Doppler guidewire and flow velocity measurements: The Doppler angioplasty guidewire is a 0.018-in (diameter 0.46 mm), 175-cm long, flexible and steerable guidewire with a floppy distal end mounting a 12 MHz piezoelectric transducer at the tip[7] (Cardiometrics, Mountain View, CA). The sample volume is positioned at a distance of 5.2 mm from the transducer. At this distance, the sample volume has a width of approximately 2 mm due to the divergent ultrasound beam so that a large part of the flow velocity profile is included in the sample volume also in case of eccentric positions of the Doppler guidewire. The pulse repetition frequency (17–96 kHz) varies with the velocity range selected (50–600 cm/sec full scale) so that flow velocities up to 6 m/sec can be recorded without frequency aliasing (Figure 1). In order to increase the reliability of the measurements, a real-time fast Fourier transform algorithm is used for the analysis of the Doppler signal.[8] The flow velocity measurements obtained with this system have been validated in vitro and in an animal model using simultaneous electromagnetic flow measurements for comparison.[7] The Doppler system calculates and displays on-line several spectral variables, including the instantaneous peak velocity and the time-averaged (mean of 2 beats) peak velocity (APV). Mean blood flow velocity was estimated 50% of the time-averaged peak velocity

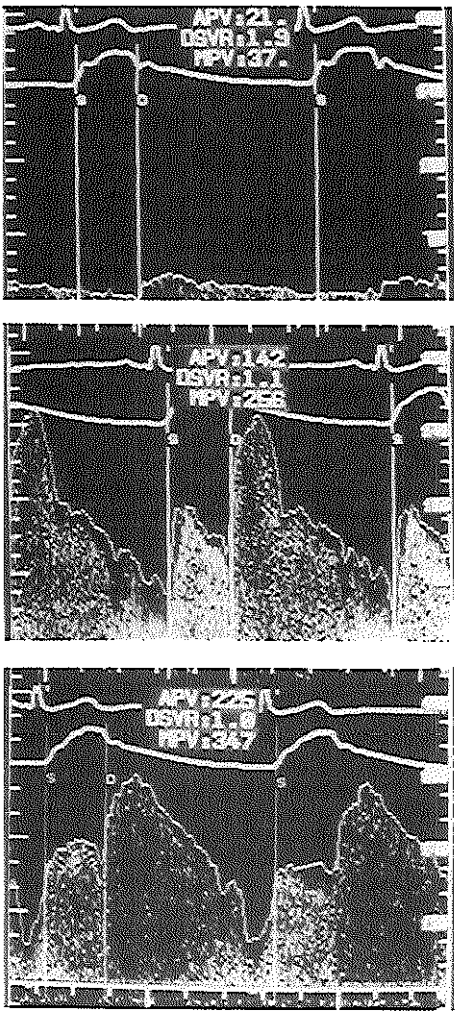

FIGURE 1. ***Upper panel:*** **Doppler flow velocity tracing proximal to a 70% cross-sectional area stenosis of the left anterior descending coronary artery (scale, 0–400 cm/sec).** ***Middle panel:*** **when the Doppler probe is advanced into the stenosis, the flow velocity shows a large increase of the average peak velocity and especially of the systolic flow velocity component (decrease of the diastolic/systolic velocity ratio from 1.9 to 1.1; scale, 0–400 cm/sec).** ***Lower panel:*** **a further increase is observed after contrast-induced hyperemia. Note the perfectly defined Doppler envelope despite the presence of flow velocities of 3.5 m/sec (scale, 0–480 cm/sec). APV = time-averaged peak flow velocity (cm/sec); DSVR = ratio of the time-averaged diastolic and systolic flow velocity components; MPV: maximal peak velocity (cm/sec). All these measurements were automatically performed after spectral analysis of the Doppler signal (FloMap, Cardiometrics).**

(APV), assuming a fully developed velocity profile.[9,10] Coronary flow (CoBF) was calculated from the corresponding mean blood flow velocity and cross-sectional area (CSA) as:

$$\text{CoBF (mL/min)} = 0.6 \times \text{CSA (mm}^2\text{)} \times \frac{\text{APV}}{2}\text{ (cm/sec)}$$

where 0.6 is the conversion factor for mm^2/cm^2 and min/sec (Figures 2 and 3). The Doppler-derived percent cross-sectional area stenosis (CSA_{St}) is calculated from the following:

$$\%CSA_{St} = (1 - APV_{Ref}/APV_{St}) \times 100$$

where APV_{Ref} is the reference APV and APV_{St} is the stenosis APV. Absolute minimal cross-sectional area (MICSA) of the stenosis was calculated as:

$$\text{Doppler MICSA} = CSA_{Ref} \times APV_{Ref}/APV_{St}$$

with the reference cross-sectional area (CSA_{Ref}) measured with quantitative angiography from the corresponding diameter at the site of the Doppler sample volume assuming a circular cross-section.[11]

Quantitative angiographic measurements: The guiding catheter, filmed without contrast medium, was used as a scaling device.[12] A previously validated on-line analysis system operating on digital images[13] (ACA-DCI; Philips, Eindhoven, The Netherlands) and a cine-film based off-line system[14] (CAAS System; Pie Medical Data, Maastricht, The Netherlands) were used. After automatic detection of the vessel centerline, a weighted first and second derivative function with predetermined continuity constraints was applied to the brightness profile on each scan line perpendicular to the vessel centerline to determine the contours of the lumen.[11] From the measured minimal luminal diameter (MLD), the minimal luminal cross-sectional area was calculated assuming a circular cross-section (average of the measurements in the 8 patients in whom multiple views were acquired). Percent cross-sectional area stenosis was calculated using the cross-sectional area at the site of the Doppler measurement as reference using the following formula:

$$\%CSA_{St} = (1 - CSA_{St}/CSA_{Ref}) \times 100$$

Statistical analysis: A two-tailed paired Student's *t* test was used to compare the difference between the coronary flow calculated in the stenosis and in the reference segment and between the Doppler-derived and the angiographic percent

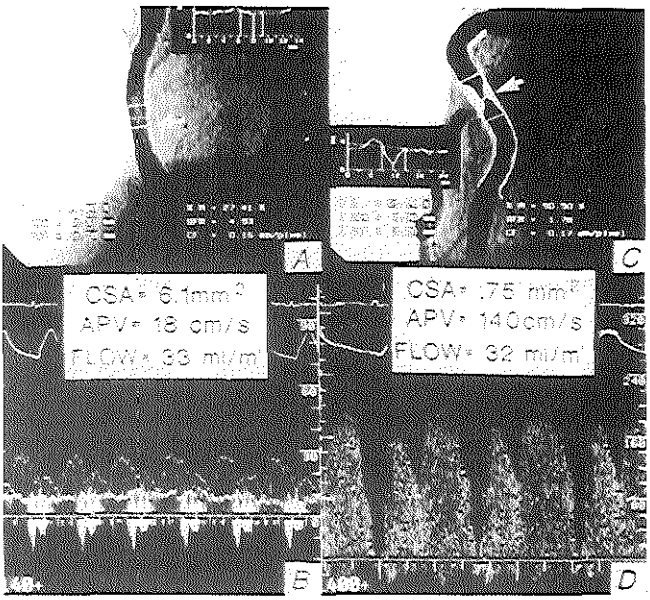

FIGURE 2. ***Upper panels:*** **magnified digital angiogram of the middle segment of a right coronary artery with a severe coronary stenosis. *A*, measurement at the site of the Doppler sample volume, distal to the stenosis; *C*, minimal luminal diameter (Philips DCI-ACA analysis package).** ***Lower panels:*** **flow velocity recordings distal to the stenosis *(B)* and in the stenosis *(D)*. Note the large velocity increase (maximal velocity of 210 cm/sec). APV = average peak velocity; CSA = cross-sectional area (mm^2). Note that the scale is changed from 0–90 cm/sec in *B* to 0–320 cm/sec in *D* for jet analysis.**

cross-sectional area stenosis and minimal luminal cross-sectional area stenosis. Linear regression analysis was used to compare percent cross-sectional area stenosis and minimal luminal cross-sectional area measured with quantitative angiography with the corresponding values derived from the Doppler flow velocity measurements. The difference between Doppler-derived and measured stenosis minimal luminal cross-sectional area was plotted versus the stenosis minimal luminal cross-

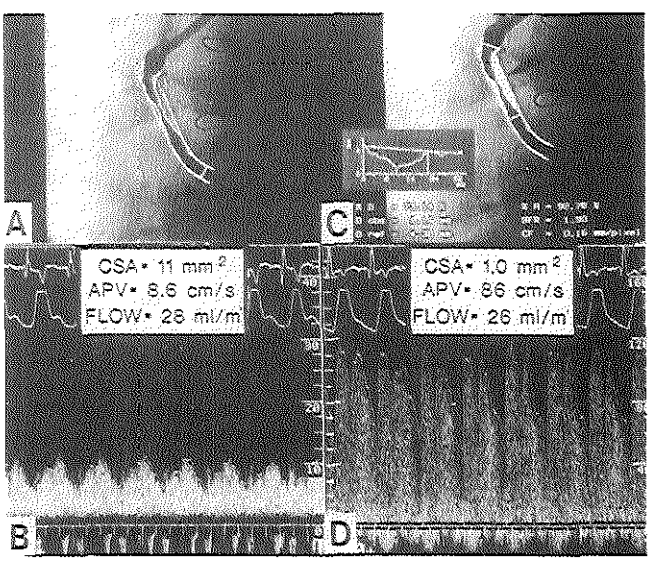

FIGURE 3. ***A, C,*** **magnified digital angiogram of a saphenous vein bypass graft with a severe proximal stenosis (92% area stenosis).** ***B, D,*** **corresponding Doppler flow velocity tracings and automatic measurements of a severe proximal stenosis and of the site of the flow velocity measurement in the reference segment (in this particular example, necessarily distal to the very proximal stenosis). Note that the scale is changed from 0–40 to 0–320 cm/sec for jet analysis.**

TABLE I Detection of High Transstenotic Flow Velocities in the Study Population

Examined Vessel	LAD	LCX	RCA	SVBG	Total
Vessels examined (n)	36	7	13	5	61
Detection of velocity increase in the stenosis	8 (22%)	2 (29%)	4 (31%)	3 (60%)	17 (28%)
Doppler recordings suitable for quantization	4 (11%)	1 (14%)	3 (23%)	2 (40%)	10 (16%)

LAD = left anterior descending; LCX = left circumflex; RCA = right coronary artery; SVBG = saphenous vein bypass graft.

TABLE II Flow Velocity and Cross-Sectional Area Measurements and Estimated Coronary Blood Flow in a Reference Normal Segment and in the Stenosis

	Reference			Stenosis		
Patients	CSA mm²	BFV cm/sec	Flow mL/min	CSA mm²	BFV cm/sec	Flow mL/min
CE (92/275)	12.10	21	76	0.97	138	40
KD (92/239)	9.10	9	25	0.75	90	20
ME (92/339)	6.30	18	34	1.27	77	29
HR (91/1,838)	10.90	9	28	1.00	86	26
WD (92/1,132)	6.29	11	21	0.66	118	24
MV (92/1,065)	7.06	11	23	0.59	137	24
SM (92/822)	5.06	12	18	0.50	130	19
GF (91/1,860)	6.10	18	33	0.75	140	32
RA (92/1,792)	8.75	18	47	2.06	90	56
GF (92/1,504)	4.77	21	30	1.46	142	62
Mean	7.64	15	33.5	1.00	115	33.2
± SD	2.47	5	17.0	0.48	26	14.9

BFV = blood flow velocity; CSA = cross-sectional area.

sectional area according to the method proposed by Bland and Altman.[15] Statistical significance was defined as $p < 0.05$. All data were expressed as mean ± SD.

RESULTS

The minimal luminal diameter of the 61 studied arteries was 1.07 ± 0.32 mm (percent diameter stenosis 62 ± 6.8%). A Doppler signal could be obtained in the stenosis in 17 arteries (28%). In only 10 cases (16%), however, was the quality of the Doppler recording satisfactory to allow the measurement of the time-averaged peak velocity (Table I). The flow velocity and the cross-sectional area measurements in the reference segment and in the stenosis are reported in Table II for the 10 arteries in which recordings suitable for quantitative analysis were obtained. The time-averaged peak velocity increased from 15 ± 5 to 115 ± 26 cm/sec from the reference normal segment to the stenosis. An inverse change was observed in the corresponding angiographically measured cross-sectional areas (7.75 ± 2.55 vs 1.05 ± 0.61 mm² for the reference and stenosis areas, respectively). Consequently, the coronary flow in the stenosis and in the reference segment showed no significant

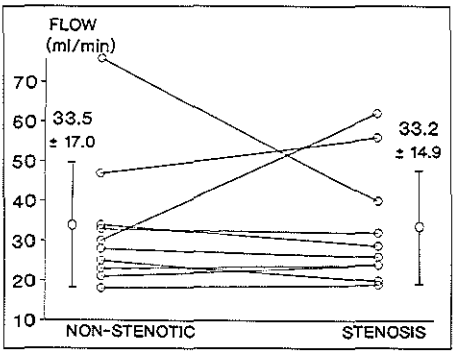

FIGURE 4. Diagram illustrating the individual measurements of coronary flow from the Doppler flow velocity and angiographic cross-sectional area measurements in a nonstenotic reference segment and in the stenosis.

difference (33.2 ± 14.9 vs 33.5 ± 17.0 mL/min, respectively, Table II). Figure 4 illustrates the individual differences between coronary flow calculated from Doppler velocity and cross-sectional area measurements in the stenosis and in the reference segment.

The percent reduction of cross-sectional area calculated from the quantitative angiographic measurements and from the Doppler flow velocity measurements is plotted in Figure 5. The Doppler-derived percent cross-sectional area stenosis showed a significant correlation with the angiographic percent cross-sectional area stenosis (86.7 ± 5.1 vs 85.9 ± 7.9%; $r = 0.64$, $p < 0.05$). Similar minimal luminal cross-sectional areas were calculated from the stenotic velocity ratio and from quantitative angiography (mean difference, 0.0–0.005 ± 0.37 mm², difference not significant; Figure 6).

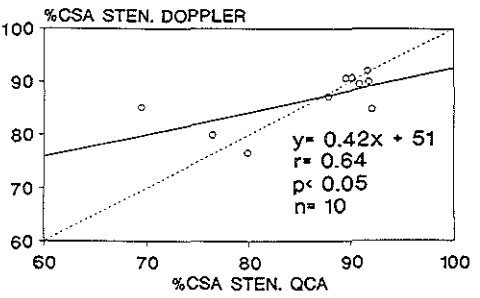

FIGURE 5. Linear regression analysis of the percent cross-sectional area stenosis measurements obtained from quantitative angiography and derived from the Doppler stenotic velocity ratio. CSA = cross-sectional area (mm²); QCA = quantitative coronary angiography; STEN. = stenosis.

DISCUSSION

Application of the continuity equation in the assessment of stenosis severity: These results demonstrate the ability of intracoronary Doppler to obtain accurate flow velocity data in the normal segment of the artery and, in conjunction, to measure higher jet velocity within a severe stenosis. In the first study consistently applying the principle of the continuity of flow in the human coronary circulation, Nakatami et al[5] used 20 MHz Doppler catheters with a pulse repetition frequency of 62.5 kHz. With this system, unfortunately, flow velocities > 115 cm/sec were not recorded because of the development of frequency aliasing. As a result of this technical limitation, all the flow velocity measurements were obtained only in mild-to-moderate coronary stenosis, with a percent cross-sectional area reduction < 75% (diameter stenosis < 50%).

In the current study, patients with significant coronary stenoses undergoing coronary balloon angioplasty were studied. The use of steerable Doppler guidewires with smaller diameter and cross-sectional area (0.17 mm^2), larger sample volume, lower carrier frequency (12 MHz), and higher pulse repetition rate (up to 96 kHz) allowed the recording of higher jet velocities within severe coronary stenoses. With these Doppler probes the continuity equation can be applied also in severely stenotic coronary arteries, providing a measurement of percent cross-sectional area reduction independent of angiography.

This approach, however, has practical and theoretical limitations. The first problem is the choice of the reference "normal" segment. Epicardial and intravascular ultrasound has confirmed pathologic findings showing that diffuse or focal intimal thickening is present in angiographically normal arterial segments.[16,17] An abnormally high flow velocity measurement is obtained in a segment already narrowed by atherosclerotic wall encroachment. In this case, the percent cross-sectional area stenosis calculated from the velocity measurements will underestimate the true hemodynamic severity of the stenosis. The hemodynamic significance of a coronary stenosis is influenced by all the elements defining lesion geometry, including length of the narrowed segment and inflow–outflow angles. The stenotic velocity ratio, however, can calculate only the percent reduction in cross-sectional area.

An additional problem with the use of the continuity equation is the interposition of major side branches between the site of the measurement and the stenosis. In particular, experience obtained

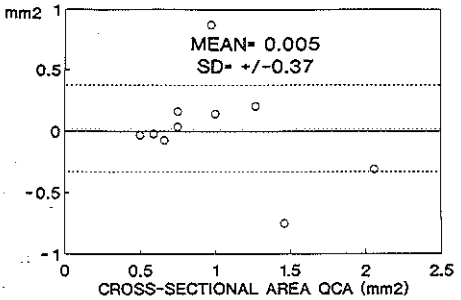

FIGURE 6. The difference between minimal luminal cross-sectional area calculated from the Doppler measurements and from quantitative angiography is plotted against the angiographic minimal luminal cross-sectional area. CSA = minimal luminal cross-sectional area (mm^2); QCA = quantitative coronary angiography.

with the Doppler guidewire in intermediate stenoses has shown that in branching arteries the ratio between the flow velocity recorded proximal and distal to a stenosis can be used as an indirect index of stenosis severity.[18] In the presence of severe stenoses, the flow will be preferentially directed to the prestenotic branches so that high proximal-to-distal flow velocity ratios will be obtained. Proximal flow velocity was used when possible, assuming minimal redistribution by intervening branches and avoiding the segment of proximal lesion acceleration in the zone of convergence. In practice, however, we were forced to record the reference flow velocity in a segment distal to the stenosis in 7 of our 10 cases, possibly inducing a further obstruction to flow due to the guidewire.[19]

A more important limitation is related to the measurement of the flow velocity in the stenosis. The comparison of the time-averaged peak flow velocities in the stenosis and in the reference segment is based on the assumption that maximal and mean velocities are linked by a fixed ratio in the presence of a fully developed parabolic flow velocity profile (2:1 for a perfect Newtonian fluid). In the presence of abrupt changes of vascular diameter, however, a vascular segment several times longer than the vascular diameter is required to obtain a fully developed parabolic profile, as predicted from classic models and confirmed experimentally.[10] It is obvious, therefore, that for a short stenosis the use of the maximal velocity will lead to a predictable underestimation of the percent cross-sectional area stenosis. A possible alternative is the direct measurement of the mean flow velocity from the Doppler spectrum. This measurement, however, is unreliable because of the unavoidable presence of nonflow-related signals (wall thumps,

artifacts), the inability to include the entire velocity profile of the artery in the sample volume, and the different signal intensity induced by the higher density of scatterers in the central flow lamina.[20,21]

Despite all these theoretical limitations, in our experience the percent cross-sectional area stenosis measured with quantitative angiography and estimated from the ratio of stenosis/reference velocity showed a significant correlation, with closer values being obtained in the most severe coronary stenoses. The accuracy of the Doppler-derived measurements in these cases cannot obscure the fact that Doppler recordings suitable for quantization were obtained within the stenosis only in a minority of the study population. The inability to record the flow velocity in severe stenoses is the most important practical limitation to the applicability of the continuity equation from Doppler measurements obtained with guidewire-type intracoronary probes. The failure to record the intrastenotic velocities is in contrast with the high acquisition rate of adequate Doppler signals in normal or near-normal arterial segments, proximal or distal to the lesion.

Yuan and Shung[22] have shown that the ultrasonic backscatter from flowing whole blood is dependent on the shear rate. The ultrasonic backscatter of porcine whole blood measured at a shear rate of 22 sec^{-1} was 15 dB lower than the ultrasonic backscatter measured at a shear rate of 2 sec^{-1}, probably as a consequence of a reduced rouleaux formation. In the stenoses evaluated in this study a much higher shear rate can be expected: a shear rate of 2,600 sec^{-1} can be estimated in the presence of a peak velocity of 100 cm/sec in a lumen of 1 mm. Consequently, the amount of intact rouleax in the stenosis can be minimal and explain the reduced echointensity of the stenotic jet. An alternative possible explanation of this difference is the greater difficulty in orientating the Doppler sample volume in the narrowed tapering segment immediately proximal to the lesion and the very small dimension of the stenotic jet in comparison to the Doppler sample volume, leading to an unfavorable signal-to-noise ratio. A more extensive manipulation of the Doppler guidewire in front of the stenotic lesion, reshaping the distal end of the guidewire if necessary, might have resulted in a higher success rate in the acquisition of high-velocity signals in the stenosis. The potential risk to induce flow-limiting intimal lesions while the access to the distal vessel has not been secured makes this approach hazardous and of limited clinical applicability. The low success rate obtained in the assessment of flow velocity within the stenosis in patients undergoing coronary angioplasty cannot be extrapolated to the assessment of less severe stenoses. The clinical applicability of the use of flow velocity measurements obtained with a Doppler guidewire in moderate or intermediate coronary stenoses as well as after coronary interventions remains to be tested.

Additional application of intracoronary Doppler flow velocity for the assessment of stenosis severity: Other indices than the coronary flow reserve and the intrastenotic/normal segment velocity ratio can be obtained from the measurements of flow velocity distal to the stenosis. An abnormal phasic flow velocity pattern recorded during individual cardiac cycles and, in particular, a low diastolic-to-systolic velocity ratio has been proposed as an index of stenosis severity that can be easily obtained in almost all the cases using the Doppler guidewire.[18,23,24] In addition, in severely stenotic arteries the velocity in the proximal segment is much higher than the distal velocity, because of preferential flow toward the prestenotic branches of lower resistance. The presence of a high proximal-to-distal velocity ratio appears to differentiate arteries with flow-limiting stenoses from normal arteries.[24] More sophisticated indices, based on the instantaneous hyperemic diastolic pressure–flow velocity relation and implemented in animal experimental laboratories[25,26] can be applied in the catheterization laboratory with this intracoronary Doppler guidewire technology.[27] Further, the combined simultaneous assessment of the transstenotic pressure gradient and flow velocity using Doppler and pressure microsensors with guidewire technology provides all the elements required for a complete hemodynamic characterization of the stenosis severity.

CONCLUSION

The measurement of blood flow velocity in the stenotic jet in patients with severe coronary stenoses is possible with ultraminiaturized Doppler probes tip-mounted on angioplasty guidewires. High-quality Doppler recordings, suitable for quantization, can be obtained only in a small subset of the studied vessels. When measurable, however, the percent cross-sectional area stenosis derived from the stenosis velocity shows a significant correlation with the angiographic percent cross-sectional area stenosis. In summary, although accurate for quantification of lesion significance, use of the continuity equation employing intrastenotic jet velocity recordings is difficult and impractical for

clinical application even when using flow velocity spectra obtained with a Doppler guidewire.

Acknowledgment: The contribution to the acquisition of the data of the medical, technical, and nursing staff of the Catheterization Laboratory, Thoraxcenter, Dijkzigt University Hospital, is gratefully acknowledged.

REFERENCES

1. Hatle L, Angelsen B. Pulsed and continuous wave Doppler in diagnosis and assessment of various heart lesions. In: Hatle L, Angelsen B, eds. Doppler ultrasound in cardiology. Philadelphia: Lea & Febiger, 1985:97–282.

2. Sibley DH, Millar HD, Hartley CJ, Whitlow PL. Subselective measurement of coronary blood flow velocity using a steerable Doppler catheter. *J Am Coll Cardiol* 1986;8:1332–1340.

3. Biasini R, Schad H, Huttl S, Mendler N, Blomer H. Intracoronary Doppler catheter: determination of the cross-sectional area of coronary artery stenoses by improved frequency analysis. (Abstr.) *Eur Heart J* 1992;13:362.

4. Johnson EL, Yock PG, Hargrave VK, Manubens SM, Seitz W, Ports TA. Assessment of severity of coronary stenoses using a Doppler catheter. Validation of a method based on the continuity equation. *Circulation* 1989;80:625–635.

5. Nakatani S, Yamagishi M, Tamai J, Takaki H, Haze K, Miyatake K. Quantitative assessment of coronary artery stenosis by intravascular Doppler catheter technique. *Circulation* 1992;85:1786–1791.

6. Taduoka S, Kagiyama M, Hiramatsu O. Accuracy of 20 MHz Doppler catheter coronary artery velocimetry for measurement of coronary blood flow velocity. *Cathet Cardiovasc Diagn* 1990;19:205–213.

7. Doucette JW, Corl PD, Payne HM, Flynn AE, Goto M, Nassi M, Segal J. Validation of a Doppler guidewire for intravascular measurement of coronary artery flow velocity. *Circulation* 1992;85:1899–1911.

8. Di Mario C, Roelandt JRTC, de Jaegere P, Linker DT, Oomen J, Serruys PW. Limitations of the zero-crossing detector in the analysis of intracoronary Doppler. A comparison with fast Fourier analysis of basal, hyperemic and transstenotic blood flow velocity measurements in patients with coronary artery disease. *Cathet Cardiovasc Diagn* 1992;27:28:56–64.

9. Di Mario C, de Feyter PJ, Slager CJ, de Jaegere P, Roelandt JRTC, Serruys PW. Intracoronary blood flow velocity and transstenotic pressure gradient using sensor-tip pressure and Doppler guidewires. *Cathet Cardiovasc Diagn* 1993;28: (in press).

10. Caro CG, Pedley TJ, Schroter RC, Seed WA. The mechanics of the circulation. Oxford: Oxford University Press, 1978:53.

11. Reiber JHC, Serruys PW, Kooijman CJ, Wijns W, Slager CJ, Gerbrands JJ, Schumblers JCH, den Boer A, Hugenholtz PG. Assessment of short-, medium-, and long-term variations in arterial dimensions from computer-assisted quantization of coronary cineangiograms. *Circulation* 1985;71:280–288.

12. Di Mario C, Hermans WRM, Rensing BJ, Serruys PW. Calibration using angiographic catheters as sealing devices. Importance of filming the catheters not filled with contrast medium. *Am J Cardiol* 1992;69:1377–1378.

13. Haase J, Di Mario C, Slager CJ, van der Giessen WJ, den Boer A, de Feyter PJ, Reiber JHC, Verdouw PD, Serruys PW. In-vivo validation of on-line and off-line geometric coronary measurements using insertion of stenosis phantoms in porcine coronary arteries. *Cathet Cardiovasc Diagn* 1992;27:16–27.

14. Di Mario C, Haase J, den Boer A, Reiber JHC, Serruys PW. Videodensitometry versus edge detection for the assessment of in vivo intracoronary phantoms. *Am Heart J* 1992;124:1181–1189.

15. Bland JM, Altman DG. Statistical methods for assessing agreement between two methods of clinical measurement. *Lancet* 1986;ii:307–310.

16. Nissen SE, Gurley JC, Grines CL, Booth DC, McClure R, Berk M, Fisher C, DeMaria AN. Intravascular ultrasound assessment of lumen size and wall morphology in normal subjects and patients with coronary artery disease. *Circulation* 1991;84:1087–1099.

17. StGoar FG, Pinto FJ, Alderman EL, Fitzgerald PJ, Stadius ML, Popp RL. Intravascular ultrasound of angiographically normal coronary arteries: an in-vivo comparison with quantitative angiography. *J Am Coll Cardiol* 1991;18:952–958.

18. Donohue TJ, Kern MJ, Bach RG, Aguirre F, Bell C, Wolford T, Penick D. Transstenotic pressure-gradient-flow velocity relationships in patients with coronary artery disease. *Circulation* 1992;86:I-855.

19. De Bruyne B, Vantrimpont P, Stockbroekx J, Demoor D, Heyndrickx GR. Influence of a PTCA wire on stenosis dynamics. *Circulation* 1992;86:I-322.

20. Evans DH, Schlindwein FS, Levene ML. The relationship between time averaged intensity weighted mean velocity and time averaged maximum velocity in neonatal cerebral arteries. *Ultrasound Med Biol* 1989;15:429–435.

21. De Kroon MGM, Slager CJ, Gussenhoven WJ, Serruys PW, Roelandt JRTC, Born N. Cyclic changes of blood echogenicity in high-frequency ultrasound. *Ultrasound Med Biol* 1991;17:723–728.

22. Yuan YW, Shung KK. Ultrasonic backscatter from flowing whole blood. I: Dependence on shear rate and hematocrit. *J Acoust Soc Am* 1988;84:52–58.

23. Ofili E, Kern MJ, Tatineni S, Deligonul U, Aguirre F, Serota H, Labovitz AJ. Detection of coronary collateral flow by a Doppler-tipped guide wire during coronary angioplasty. *Am Heart J* 1991;222:221–225.

24. Segal J, Kern MJ, Scott NA, King SB, Doucette JW, Heuser RR, Ofili E, Siegel R. Alterations of phasic coronary artery flow velocity in humans during percutaneous coronary angioplasty. *J Am Coll Cardiol* 1992;20:276–286.

25. Mancini GBJ, Cleary RM, DeBoe SF, Moore NB, Gallagher KP. Instantaneous hyperemic flow-versus-pressure slope index: microsphere validation of an alternative to measures of coronary reserve. *Circulation* 1991;84:862–870.

26. Mancini GBJ, McGillem MJ, DeBoe SF, Gallagher KP. The diastolic hyperemic flow versus pressure relation: a new index of coronary stenosis severity and flow reserve. *Circulation* 1989;80:941–950.

27. Serruys PW, Di Mario C, Meneveau N, de Jaegere P, Strikwerda S, de Feyter PJ, Emanuelsson H. Intracoronary pressure and flow velocity from sensor-tip guidewires. A new methodological comprehensive approach for the assessment of coronary hemodynamics before and after coronary interventions. *Am J Cardiol* 1993;71:41–53.

CHAPTER 10

INTRACORONARY BLOOD FLOW VELOCITY AND TRANSSTENOTIC PRESSURE GRADIENT USING SENSOR-TIP PRESSURE AND DOPPLER GUIDEWIRES

A new technology for the assessment of stenosis severity in the Catheterization Laboratory

Carlo Di Mario, M.D., Pim J. de Feyter, M.D., Ph.D., Cornelis J. Slager, Ph.D.,
Peter de Jaegere, M.D., Ph.D., Jos R.T.C. Roelandt, M.D., Ph.D.,
Patrick W. Serruys, M.D., Ph.D.

From the Cardiac Catheterization Laboratory, Division of Cardiology,
Thoraxcenter, Erasmus University, Rotterdam

Reprinted from: Cathet Cardiovasc Diagn, 1993.

Catheterization and Cardiovascular Diagnosis 28:311–319 (1993)

Intracoronary Blood Flow Velocity and Transstenotic Pressure Gradient Using Sensor-Tip Pressure and Doppler Guidewires: A New Technology for the Assessment of Stenosis Severity in the Catheterization Laboratory

Carlo Di Mario, MD, Pim J. de Feyter, MD, Cornelis J. Slager, PhD, Peter de Jaegere, MD, Jos R.T.C. Roelandt, MD and Patrick W. Serruys, MD

In a patient undergoing percutaneous balloon angioplasty of a stenotic proximal right coronary artery the transstenotic pressure gradient was measured using a 0.018" guidewire with a distal optical microsensor. Blood flow velocity was measured proximal to the stenosis using a 0.018" Doppler guidewire. Transstenotic pressure gradient and blood flow velocity were measured in baseline conditions and after intracoronary injection of 12.5 mg of papaverine. Coronary blood flow was calculated from the measured blood flow velocity and the corresponding cross-sectional area. The measured pressure gradients were compared with the values derived from the stenosis geometry assessed with quantitative coronary angiography (automated edge detection measurements in two orthogonal views, assuming an elliptical cross-sectional area).

The measured transstenotic pressure gradient was 15 mm Hg in baseline conditions and 42 mm Hg at the peak effect of the papaverine injection. A 50% flow velocity increase was observed at peak hyperemia (time-averaged maximal flow velocity = 30 cm/s before and 45 cm/s after papaverine). The transstenotic pressure gradient calculated from the measured stenosis geometry was 20 mm Hg and 42 mm Hg in baseline and hyperemic conditions, respectively.

The combined use of a pressure and a Doppler guidewire provides a complete assessment of the transstenotic pressure/coronary flow velocity relation at rest and after pharmacologically induced hyperemia and allows the characterization of stenosis hemodynamics and functional severity.

Key words: quantitative coronary angiography, coronary blood flow, intravascular ultrasound

INTRODUCTION

A 58 year-old man was referred to our Hospital because of disabling effort angina and presence during a maximal bicycle stress test of horizontal ST-segment depression at 125 Watts in the infero-lateral leads despite a tailored maximal medical therapy. Selective coronary angiography of the native coronary arteries showed a severe proximal stenosis of the right coronary artery without visible collateral circulation from the left coronary artery which was free from significant narrowings. Left ventricular function was normal. An 8F soft-tip Judkins guiding catheter was used to selectively cannulate the right coronary artery. Two coronary angiograms were performed after intracoronary injection of 3 mg of isosorbide dinitrate in a 30° RAO view and a 60° LAO view. The catheter was filmed not filled with contrast medium in the same projections for calibration [1] and cineangiography was performed at 25 frames/s with a 5" field of view. A previously described and validated [2–4] computer-assisted automatic quantitative coronary angiographic analysis system (CAAS) was used for the analysis of the selected end-diastolic cineframe using a geometric technique (Fig. 1A,B). The automatic mea-

From the Cardiac Catheterization Laboratory, Division of Cardiology, Thoraxcenter, Erasmus University, Rotterdam, The Netherlands.

Received June 24, 1992; revision accepted October 22, 1992.

Address reprint requests to Dr. P.W. Serruys, Cardiac Catheterization Laboratory, Div. Cardiology, Thoraxcenter, Erasmus University, P.O. Box 1738, 3000 DR Rotterdam, The Netherlands.

Dr. C. Di Mario (Div. Cardiol. Vicenza, Italy) is the recipient of the European Society of Cardiology Research Fellowship 1991.

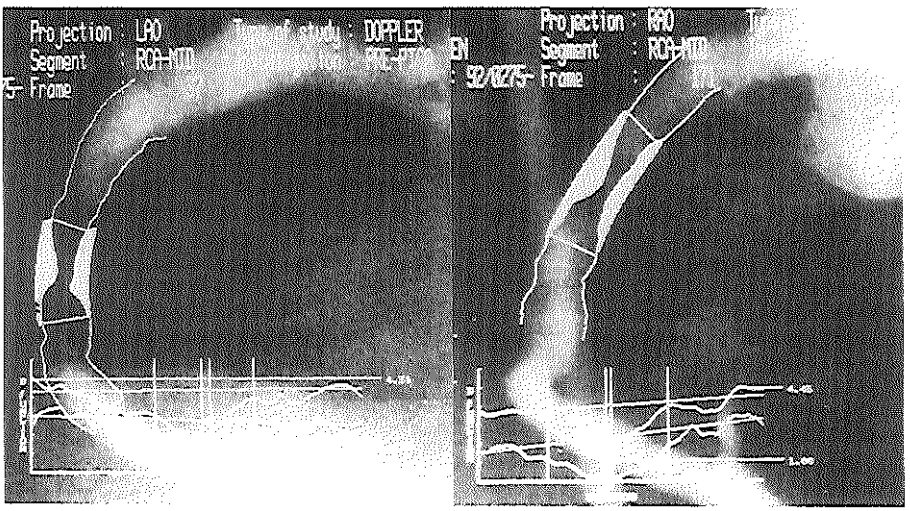

Fig. 1. Biplane orthogonal cineangiograms (A: LAO, B: RAO) of a right coronary artery showing the presence of a significant concentric stenosis of the middle segment. The magnified image has been digitized into a 512 × 512 pixel matrix corresponding to < 0.1 mm/pixel with the 5" field of view of the image intensifier used. The diagram shows the measured diameter of the examined segment after automatic contour detection and the filled white areas outside the stenosis lumen represent the automatically reconstructed (interpolated technique) original lumen profile where the diameter of the reference segment is measured.

surement of the reference diameter was performed with an interpolated technique and was used for the calculation of percent diameter and cross-sectional area (CSA) stenosis. Based on the measured stenosis geometry the hemodynamic parameters were calculated according to Appendix A.

After intravenous injection of heparin 10,000 I.U. and acetylsalicylic acid 250 mg a 12 MHz 0.018" (diameter = 0.46 mm) Doppler guidewire [5] (Cardiometrics, Mountain View, CA, USA) was introduced into the proximal right coronary artery and blood flow velocity (BFV) was measured in the first segment of the right coronary artery (arrow in Fig. 2A). No major side-branches were interposed between Doppler measurement site and the stenosis. Cineangiography (LAO 60°, Fig. 2A) was repeated with the Doppler guidewire in place in order to measure the vascular diameter at the site of the Doppler sample volume (5.2 mm distance from the guidewire tip). A constant CSA was assumed throughout the procedure as a result of the pretreatment with intracoronary nitrates [6]. From the time-averaged maximal BFV, automatically calculated for two consecutive beats from the spectral Doppler envelope (Fig. 3), mean BFV was calculated as described in Appendix B. Coronary blood flow was then calculated as the product of CSA at the site of the Doppler measurement times mean BFV. A 0.018" (diameter 0.46 mm) guidewire with a fiber optic pressure microsensor 3 cm from its tip (RadiMedical Systems, Uppsala, Sweden) was calibrated immediately before insertion and subsequently introduced into the proximal right coronary artery [7]. After recording of the proximal intracoronary pressure for comparison with the measurements obtained in the same position through the guiding catheter (Fig. 2C) the pressure guidewire was advanced across the stenosis (Fig. 2B) and the transstenotic pressure gradient was measured (Fig. 2D). The signals received simultaneously from the control unit of the fiber optic pressure sensor and from a Statham-Gould pressure transducer connected to the guiding catheter were transmitted to a computer-assisted central work station. Systolic, diastolic, mean pressures, and mean pressure gradient were automatically measured from 4 sinus beats selected from a continuous recording of 16 s [8] (Fig. 2C,D).

After intracoronary injection of 12.5 mg of papaverine through the guiding catheter, the transstenotic pressure gradient and BFV were continuously measured up to the

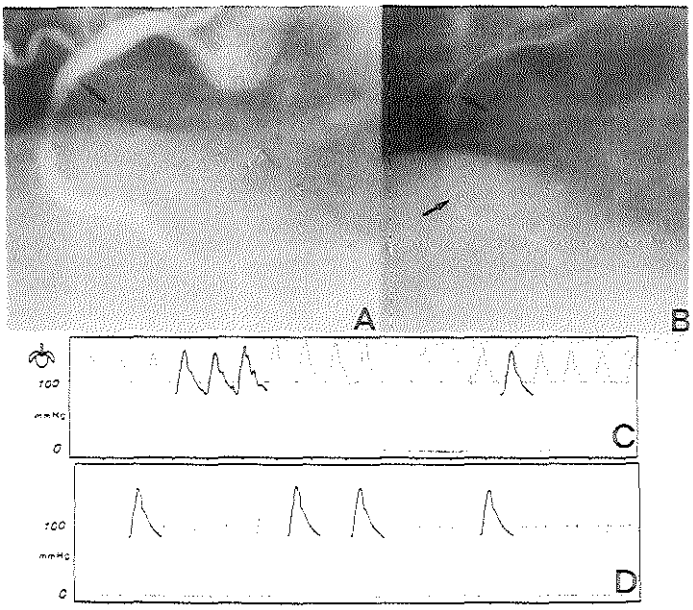

Fig. 2. A: Cineangiogram of the right coronary artery showing the position of the Doppler guidewire, proximal to the stenosis (arrow). The position of the pressure sensor, at the junction between more radioopaque floppy distal tip and body of the guidewire, is better appreciated in the image without contrast (B, arrow). In C and D the almost complete superimposition of proximal and distal coronary pressures with the pressure transducer proximal to the stenosis (C) can be compared with the moderate pressure gradient observed in baseline conditions when the guidewire was advanced distal to the stenosis (D).

end of the papaverine effect (return to baseline around 3 min after injection). An off-line beat-to-beat program of analysis of the pressure signal was used to measure proximal and post-stenotic coronary pressures corresponding to the video-recorded on-line measurements during the pharmacologically induced hyperemic reaction [8] (Fig. 3). Thirty-five minutes was necessary for the complete acquisition of the pressure and BFV signals and the quantitative angiographic procedure. The patient subsequently underwent successful coronary balloon angioplasty.

ANALYSIS OF THE RESULTS

The results of the QCA, Doppler, and pressure measurements and derived parameters in baseline conditions and at the peak effect of the papaverine injection are summarized in Table I. Table II compares the transstenotic pressure gradient measured with the micromachined pressure optical sensor and the pressure gradient estimated from the QCA geometric measurements and the measured BFV. For this last calculation the CSA of the pressure guidewire (0.17 mm^2) was subtracted from the CSA of the reference segment and of the stenosis.

The injection of papaverine 12.5 mg induced a prolonged increase of BFV and transstenotic pressure gradient (maximal values reported in Table I and shown in Fig. 3). In Figure 4 the proximal and post-stenotic coronary pressures recorded following the injection of papaverine (peak effect-restoration of baseline conditions) are plotted against the corresponding BFVs (measurement of two consecutive beats every 8 s).

In Figure 5 the distal coronary pressure measurements after papaverine injection are plotted against the measured coronary flow, shown as a ratio to baseline flow at rest according to the method proposed by Kirkeeide et al. [9]. With this method coronary blood flow is normally cal-

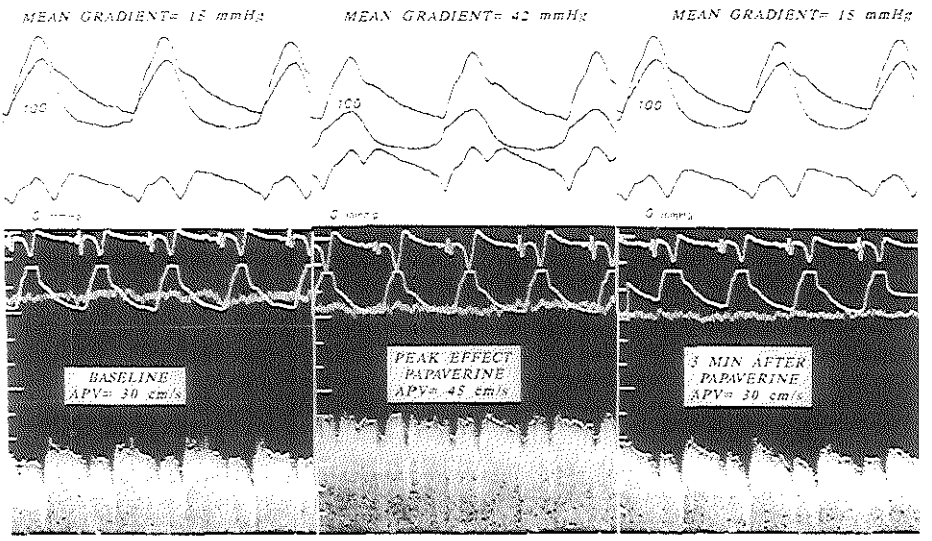

Fig. 3. Simultaneous recording of proximal and distal coronary pressures and derived transstenotic pressure gradient (lower line) immediately before injection of papaverine (baseline, on the left), at peak hyperemia (middle), and 3 min after restoration of baseline conditions (on the right). The corresponding Doppler tracings are shown in the lower images. Note the automatic detection of the maximal BFV (dotted line tracking the Doppler envelope obtained from the spectral analysis of the signal). The indicated time averaged maximal BFV (APV, cm/s) is automatically calculated in the last 2 displayed beats.

culated assuming a mean BFV at rest of 15 cm/s, a value exactly coincident with the measured mean BFV in this patient, and the pressure gradient is calculated from the stenosis geometry assuming a fixed mean proximal coronary blood pressure of 100 mm Hg modified in this case to 110 mm Hg to use a value closer to the true measurement. The lower continuous line plots the relation between coronary perfusion pressure and coronary flow under conditions of maximal vasodilatation. A coronary closing pressure of 10 mm Hg and a coronary flow reserve of 5.5 were assumed [10]. Note that the point of maximal measured flow reserve increase (1.50 times baseline flow) is not aligned on the theoretical relation distal coronary pressure/coronary flow at maximal vasodilatation so that a second line can be drawn to describe the measured pressure/flow relation at maximal vasodilation.

DISCUSSION

An example of simultaneous measurement of BFV and transstenotic pressure gradient was previously reported by our group using a combined Doppler-balloon catheter after PTCA [11–12]. The obstruction to flow due to the relatively large diameter of the balloon catheter (0.64 mm^2) precluded the application of this method to the evaluation of a severe coronary stenosis before coronary interventions. In a recent multicenter trial [13] quantitative analysis of 636 stenoses before coronary angioplasty showed a minimal CSA of 0.82 ± 0.11 mm^2. In moderate or intermediate stenosis and after coronary angioplasty the measurement of the transstenotic gradient can be obtained with conventional fluid-filled catheters with a less severe obstruction to flow. Also in these conditions, however, when the measured transstenotic gradient is essential in the decision-making process, the higher accuracy of the measurements allowed by the use of smaller high-fidelity pressure transducers is desirable.

The introduction of miniaturized pressure transducers mounted at the tip of a flexible soft-tip guidewire of 0.17 mm^2 of CSA potentially allows the direct measurement of the pressure gradient with a minor further reduction of the stenosis CSA [14]. The use of miniaturized Doppler

TABLE I. Angiographic and Hemodynamic Parameters

Quantitative coronary angiography	LAO	RAO	MEAN
Length stenosis (mm)	1.55	1.10	1.32
Reference diameter (interpolated technique) (mm)	3.75	3.58	3.66
Minimal lumen diameter (mm)	1.23	1.00	1.11
Diameter at the site of the Doppler sampling volume (mm)	3.92	*	3.92
Percent diameter stenosis (%)	67%	72%	70%
Reference cross-sectional area (mm^2)	11.07	10.08	10.57
Minimal cross-sectional area (mm^2)	1.20	0.79	0.97[b]
CSA at the site of the Doppler sampling volume (mm^2)	12.10	*	12.10
Percent cross-sectional area stenosis (%)	89%	94%	91%

Doppler blood flow velocity (cm/s)	BAS	PAP
Average peak blood flow velocity	30	45
Mean blood flow velocity	15	22.5

Coronary blood flow (ml/s)	BAS	PAP
Mean coronary blood flow	1.81	2.72

Pressure Measurements (mm Hg)	BAS	PAP
Proximal systolic coronary blood pressure	157	143
Proximal diastolic coronary blood pressure	87	82
Proximal mean coronary blood pressure	112	106
Post-stenotic systolic coronary blood pressure	137	89
Post-stenotic diastolic coronary blood pressure	73	51
Post-stenotic mean coronary blood pressure	97	64
Transstenotic mean pressure gradient	15	42

*Not measured because of significant foreshortening.
[b]Calculated from the minimal lumen diameter in the two orthogonal projections assuming an elliptical model.

TABLE II. Measured and Estimated Mean Predicted Transstenotic Pressure Gradients (mm Hg)

Baseline			Papaverine		
Measured	Estimated (QCA)	% diff	Measured	Estimated (QCA)	% diff
15	20	+33	42	42	0

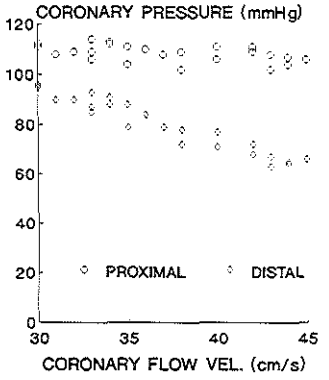

Fig. 4. Plotting of the measured proximal and distal coronary mean pressures vs. the simultaneous coronary BFV during the effect of the papaverine injection. The data-points indicate simultaneous measurements over two cardiac cycles every 8 s.

transducers with a larger sample volume than the conventional Doppler catheters and the spectral analysis of the Doppler signal allow a reliable BFV measurement without any further obstruction to flow if the velocity probe is positioned proximal to the stenosis. The pressure and BFV measurements are complementary parameters in the characterization of stenosis hemodynamics. A low increase in BFV may occur in a variety of conditions including modifications of basal flow or impairment of the vasodilatory mechanisms of the distal vasculature [15]. The simultaneous measurement of a major increase of transstenotic pressure gradient confirms that the flow limiting factor is the high resistance across the stenosis. Conversely, the measurement of a rapidly increasing transstenotic pressure gradient during vasodilatation does not fully define the functional severity of a stenosis if the level of flow increase is not simultaneously measured. In the model of Kirkeeide et al. [9] it is assumed for the purpose of the assessment of the hemodynamic effects of the stenosis that the vasodilatory capacity of the distal bed is intact and that collateral circulation is absent. These reasons may explain why the measured coronary flow reserve was lower and the poststenotic coronary pressure higher than predicted from the assumed theoretical model. The coronary distal pressure and blood flow at maximal hyperemia are ultimately determined by factors unrelated to the stenosis geometry such as the vasodilatory capacity of the distal coronary arteries and the resistance in parallel to the stenosis resistance offered by the collateral vessels.

The trajectory of the distal pressure/BFV curve, how-

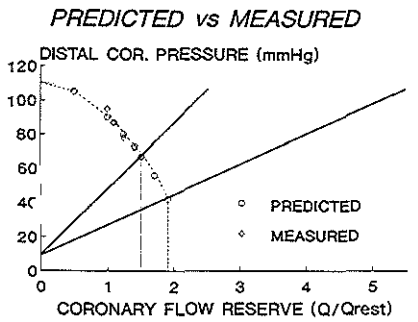

Fig. 5. Plotting of distal post-stenotic coronary mean pressure after papaverine injection vs. the ratio to baseline coronary flow, as proposed by Kirkeeide et al. [9]. Five measured data points (diamond-shaped markers) are shown to indicate the trend of the relation from baseline flow (ratio = 1) to maximal hyperemia (ratio = 1.50). The calculation of mean coronary distal pressure was performed assuming a fixed aortic pressure of 110 mm Hg and over a wider range of coronary flow, from a value corresponding to a ratio to baseline flow of 0.5 to the maximal predicted coronary flow (ratio to baseline = 1.91), corresponding to the point in which the calculated distal pressure intercepts the theoretical relation coronary flow/distal coronary pressure (lower continuous line) [10]. The trajectories of the two curves (dashed line = predicted, dotted line = measured) are almost superimposed. Note that the maximal increase in coronary flow is less than predicted from the theoretical relation coronary flow/distal coronary pressure and is consistent with a shift to the left of this relation (upper continuous line).

ever, is characteristic of the stenosis geometry and the slope of this relation is an index of stenosis severity independent of the values reached at maximal vasodilatation. The prediction of the pressure gradient under different regimens of flow is routinely provided by many systems of computer-assisted quantitative analysis based on the measurements of stenosis geometry [3,9,10,16]. The calculation of the transstenotic pressure gradients based on coronary blood flows calculated from BFV and CSA at the site of the Doppler measurement overestimated the measured values in baseline conditions while, during maximal hyperemia, the predicted pressure gradient and the measured pressure gradient were identical. Inaccuracies in the measurement of stenosis geometry or in the calculation of coronary flow as well as modifications of stenosis geometry in different flow conditions can explain the small differences observed.

A possible limitation of this case-report is the recording of the BFV proximal instead than distal to the lesion. This approach, used in order to avoid the obstruction to flow induced by the passage of two separate guidewires across the stenosis precludes the possibility of the assessment of alterations of the flow velocity pattern distal to the stenosis such as a decrease of the diastolic/systolic velocity ratio [28]. A solution to this problem and a great advantage in terms of practical applicability would be the incorporation of both the Doppler and the pressure sensors in a single guidewire system.

In conclusion, this first report of the combined use of miniaturized coronary pressure and Doppler probes shows that the characterization of stenosis severity can be obtained using a direct simultaneous measurement of the transstenotic pressure gradient and BFV in baseline and in hyperemic conditions. With this approach, the relation between transstenotic pressure gradient/distal coronary pressure and coronary flow reserve can be fully ascertained, allowing a complete assessment of stenosis hemodynamics and the validation of the models proposed for the estimation of these parameters based on QCA measurements of stenosis geometry. The usefulness of this approach in the detection of the functional significance of individual coronary stenoses, however, must be studied in comparison with standard objective tests of myocardial ischemia in a large series of stenoses of different angiographic severity.

ACKNOWLEDGMENTS

The technical assistance of Ronald van den Perk, B.Sc., Eline Montauban van Swijndregt, B.Sc., and Jaap Pameyer, B.Sc. is gratefully acknowledged. The comments and suggestions of Dr. Brian E. Jaski (UCSD, San Diego, CA) and of Dr. Håkan Emanuelsson (University of Göteborg, Sweden) are gratefully acknowledged.

REFERENCES

1. Di Mario C, Hermans W, Rensing B, Serruys PW: Calibration using angiographic catheters as scaling devices. The importance of filming the catheters after flushing with saline. Am J Cardiol 69:1377–1378, 1992.
2. Reiber JHC, Serruys PW, Koojman CJ, Wijns W, Slager CJ, Gerbrands JJ, Schuurbiers JCH, den Boer A, Hugenholtz PG: Assessment of short-, medium- and long-term variations in arterial dimensions from computer-assisted quantitation of coronary cineangiograms. Circulation 71:280–288, 1985.
3. Serruys PW, Juilliere Y, Bertrand ME, Puel J, Rickards AF, Sigwart U: Additional improvement of stenosis geometry in human coronary arteries by stenting after balloon dilatation. Am J Cardiol 61:71G–76G, 1987.
4. Di Mario C, Haase J, den Boer A, Reiber JHC, Serruys PW: Videodensitometry vs edge detection for the assessment of in vivo intracoronary phantoms. Am Heart J 124:1181–1189, 1992. in press.
5. Doucette JW, Corl PD, Payne HM, Flynn AE, Goto M, Nassi M, Segal J: Validation of a Doppler guide wire for intravascular measurement of coronary artery flow velocity. Circulation 85: 1899–1911, 1992.

6. Zijlstra F, Reiber JHC, Serruys PW: Does intracoronary papaverine dilate epicardial coronary arteries? Implications for assessment of coronary flow reserve. Cathet Cardiovasc Diagn 14:1–6, 1988.
7. Emanuelsson H, Dohnal M, Lamm C, Tenerz L: Initial experiences with a miniaturized pressure transducer during coronary artery angioplasty. Cathet Cardiovasc Diagn 24:137–143, 1991.
8. Meester GT, Bernard N, Zeelenberg C, Brower RW, Hugenholtz PG: A computer-system for real-time analysis of cardiac catheterization data. Cathet Cardiovasc Diagn 1:113–132, 1975.
9. Kirkeeide RL, Gould KL, Parsel L: Assessment of coronary stenoses by myocardial perfusion imaging during pharmacologic coronary vasodilatation. Validation of coronary flow reserve as a single integrated functional measure of stenosis severity reflecting all its geometric dimensions. J Am Coll Cardiol 7:103–113, 1986.
10. Bache RJ, Schwartz JS: Effect of perfusion pressure distal to a coronary stenosis on transmural myocardial blood flow. Circulation 65:928–935, 1982.
11. Zijlstra F, Serruys PW: Intracoronary blood flow velocity and transstenotic pressure gradient in an awake human being during coronary vasodilatation. J Interven Cardiol 1:1–8, 1988.
12. Serruys PW, Julliere Y, Zijlstra F, Beatt K, de Feyter PJ, Suryapranata H, van der Brand M, Roelandt JRTC: Coronary blood flow velocity during percutaneous transluminal coronary angioplasty as a guide for assessment of functional result. Am J Cardiol 61:253–259, 1988.
13. De Bruyne B, Pijls NHJ, Paulus WJ, van Trimpont PJ, Sys SU, Heyndrickx GR: Transstenotic coronary pressure gradient measurement in man: in vitro and in vivo evaluation of a new pressure monitoring PTCA guide-wire. Circulation 86:I–322(abstr), 1992.
14. Serruys PW, Rutsch W, Heyndrickx GR, Danchin N, Mast G, Wijns W, Rensing BJ, Vos J, Stibbe J: Prevention of restenosis after percutaneous transluminal coronary angioplasty with thromboxane A_2-receptor blockade. A randomized double-blind placebo-controlled trial. Circulation 84:1568–1580, 1991.
15. Wilson RF, Johnson MR, Marcus ML, Aylward PEG, Skorton DJ, Collins S, White CW: The effect of coronary angioplasty on coronary blood flow reserve. Circulation 77:873–885, 1988.
16. Brown GB, Bolson E, Frimer M, Dodge HT: Quantitative coronary arteriography. Estimation of dimensions, hemodynamic resistance and atheroma mass of coronary artery lesions using the arteriogram and digital computation. Circulation 55:329–337, 1977.
17. Young DF, Tsai FY: Flow characteristics in models of arterial stenoses—II. Unsteady flow. J Biomech 6:547–559, 1973.
18. Young DF, Tsai FY: Flow characteristics in models of arterial stenoses—I. Steady flow. J Biomech 6:395–410, 1973.
19. Seeley BD, Young DF: Effect of geometry on pressure losses across models of arterial stenoses. J Biomech 9:439–448, 1976.
20. Young DF, Cholvin NR, Roth AC: Pressure drop across artificially induced stenoses in the femoral arteries of dogs. Circ Res 36:735–743, 1975.
21. Tadaoka S, Kagiyama M, Hiramatsu O, Ogasawara Y, Tsujioka K, Wada Y, Sawayama T, Kajiwa F: Accuracy of 20 MHz Doppler velocimetry for measurement of coronary blood flow velocity. Cathet Cardiovasc Diagn 19:205–213, 1990.
22. DI Mario C, Roelandt JRTC, de Jaegere P, Linker DT, Oomen J, Serruys PW: Limitations of the zero-crossing detector in the analysis of intracoronary Doppler. A comparison with fast Fourier transform analysis of basal, hyperemic and transstenotic blood flow velocity measurements in patients with coronary artery disease. Cathet Cardiovasc Diagn 28:56–64, 1993.
23. Evans DH, Schlindwein FS, Levene MI: The relationship between time averaged intensity weighted mean velocity and time averaged maximum velocity in neonatal cerebral arteries. Ultrasound Med Biol 15:429–435, 1989.
24. De Kroon MGM, Slager CJ, Gussenhoven WJ, Serruys PW, Roelandt JRTC, Born N: Cyclic changes of blood echogenicity in high-frequency ultrasound. Ultrasound Med Biol 17:723–728, 1991.
25. Shung KK, Cloutier G, Lim CC: The effects of hematocrit, shear rate and turbulence on ultrasonic blood spectrum from blood. IEEE Trans Biomed Eng 39:462–469, 1992.
26. Caro CG, Pedley TJ, Schroter RC, Seed WA: Flow in pipes and around objects. In Caro CG, Pedley TJ, Schroter RC, Seed WA (eds): "The Mechanics of the Circulation." Oxford: Oxford University Press, 1978, pp 44–73.
27. Ling SC, Atabek HB, Fry DL, Patel DJ, Janicki JS: Application of heated-film velocity and shear probes to hemodynamic studies. Circ Res 23:789–801, 1968.
28. Gould KL: Collapsing stenoses. In Gould KL (ed): "Coronary Artery Stenosis." New York: Elsevier 1991, pp 64–76.
29. Segal J, Kern MJ, Scott NA, King SB, Doucette JW, Heuser RR, Ofili E, Siegel R: Alterations of phasic coronary artery flow velocity in humans during percutaneous coronary angioplasty. J Am Coll Cardiol 20:276–286, 1992.

APPENDIX A

Computation of Hemodynamic Parameters From Quantitative Coronary Angiography

The effects of changes in stenosis geometry on transstenotic pressure losses were extensively studied by Young et al. [17–20] using models of stenosis of different length, shape, and percent diameter reduction, under conditions of steady and pulsatile flow. The equation validated by these authors, based on classic Newtonian fluid dynamics, was adapted for tapering stenosis and X-ray analysis by Brown et al. [16]. The algorithm implemented in the software package of the CAAS system uses the following formula:

$$\Delta P = \frac{8\pi\mu L}{1.33\ A_s^2} Q + \frac{\rho}{0.266}\left(\frac{1}{A_s} - \frac{1}{A_n}\right)^2 Q^2 \quad (1)$$

where ΔP is the transstenotic pressure gradient in mm Hg, μ is dynamic blood viscosity in Poise (assumed equal to 0.03), L is the length of the stenosis in mm, A_n is the CSA of the reference normal segment in mm^2, A_s is the minimal CSA of the stenotic segment in mm^2, Q is the mean coronary blood flow in ml/s, and ρ is the blood density in g/ml (assumed equal to 1.05).

This equation assumes that at the exit of the stenosis flow completely separates from the streamline contours so that large eddies develop in the divergent segment distal to the stenosis. An exit half-angle of 15° has been shown to be sufficient to induce a complete separation of flow and this condition seems fulfilled in the examined artery in which exit angles of 31° and 34° were measured with quantitative angiography from the diameter profile

in the LAO and RAO projections. The calculated pressure gradient, therefore, is described as the sum of the losses due to viscous components and the losses due to separation of flow at the exit of the stenosis and can be written in the simplified form

$$\Delta P = K_p Q + K_s Q^2 \quad (2)$$

where K_P and K_S are the coefficient of pressure losses due to, respectively, viscous friction and separation of flow. In the hemodynamic report of the quantitative angiographic analysis using the CAAS system the pressure gradients are calculated for volume flow ranging from 1 to 3 ml/s. In this case the volume flow was derived from the mean Doppler BFV (see Appendix B) and the CSA at the site of the Doppler measurement, calculated from the angiographic diameter assuming a circular cross-section.

APPENDIX B

Doppler Measurements of Coronary Blood Flow Velocity

The measurement of the mean BFV requires an adequate sampling of the Doppler signal:

1. The ultrasound beam probe must be aligned with the centerline of flow; the guidewire has the piezoelectric crystal mounted at the tip so that a partial malalignment of the probe would minimally affect the velocity recording (underestimation of flow of 6% in the presence of an angle of 30° with the velocity vector).
2. The entire flow profile or at least a large part of it including the maximal velocity must be included in the Doppler sample volume; the ultrasound beam opens at 15° from each side from the transducer so that even in the presence of a non-ideal position of the Doppler guidewire (eccentric, off-axis) a large part of the velocity profile will be examined.
3. The presence of the Doppler probe must not modify the velocity profile at the site of the sample volume. In in vitro models Tadaoka et al. [21] has shown a complete restoration of the flow profile at a distance equal to 10 times the diameter of the Doppler probe (the diameter of the Doppler probe is 0.46 mm and the distance of the sample volume was kept constant at 5.2 mm).
4. A spectral analysis of the Doppler frequency must be performed to identify all the different velocities in the sample volume, including the maximal velocity [22]. The frequency spectrum can then be easily converted in the velocity spectrum based only on the knowledge of the ultrasound frequency and the velocity of sound in blood. Theoretically, mean BFV can be measured from the weighted average of the velocity spectrum. This method, however, requires a complete insonification of the velocity profile of the examined vessel and is influenced by the presence of non-flow related signals [23] such as the high intensity-low velocity signals from vessel wall movements during the cardiac cycle (wall thumps). The final measurement, therefore, is critically dependent on the modalities of signal processing. Also the weighing factors for the different velocities cannot be reliably determined as signal intensity is modified by several unknown parameters such as rouleaux formation [24,25].

A different approach is based on the use of the maximal BFV which is less sensitive to the presence of noise and is more easily included in the sample volume based on the above-described characteristics of the Doppler system. Mean BFV can be estimated from the maximal BFV assuming Poiseuille flow using the equation describing the velocity of a laminar flow field:

$$V_x = \frac{\Delta P}{4\mu L}(a^2 - x^2) \quad (1)$$

in which V_x is the velocity of the flow lamina x, ΔP is the pressure gradient in the vascular segment of length L, is blood flow viscosity, a is the radius L is the length in mm of the considered segment. X is the distance of the lamina x from the vessel centerline. This last value is 0 for the centerline of flow so that equation 1 can be rewritten:

$$V_{max} = \frac{\Delta P}{4\mu L} a^2 \quad (2)$$

Under the assumed conditions and if mean velocity times CSA (A) equals blood flow (Q), from the Poiseuille equation follows that

$$V_{mean} = \frac{Q}{A} = \frac{\frac{(\Delta P \pi a^4)}{8\mu L}}{A} \quad (3)$$

with $A = \pi r^2$, equation 3 can be simplified using (2) to

$$V_{mean} = \frac{\Delta P a^2}{8\mu L} = \frac{V_{max}}{2} \quad (4)$$

An important limitation to the applicability of this formula is that the velocity profile is assumed to be parabolic and fully developed. The distance L necessary to allow the full development of a parabolic flow profile is defined by the equation [26]

$$L = (0.03\ R_e)\ d$$

where R_e is the Reynolds number and d the diameter of

the conduit. Consequently, the velocity measurement should be taken not too close to the origin of the vessel because a vascular segment of a length of 4–6 times the vessel diameter is necessary for a complete development of the velocity profile at the Reynolds numbers present in normal epicardial coronary arteries (150–200). The same problem must be considered sampling distal to major bifurcations of the vessel and, more importantly, in the presence of changes of the vascular diameter so that the measurement of mean BFV from maximal BFV can be misleading across short stenotic segments. Also the non-Newtonian characteristics of blood will induce a flatter velocity profile than expected based on the vascular diameter and mean blood viscosity so that an underestimation of the mean BFV can be expected deriving this parameter from the maximal BFV [27]. These considerations underline the difficulties to obtain reliable volume flow measurements based on BFV measurements despite the recent progress in Doppler probe technology and signal analysis. Nevertheless, recent validation studies have shown a high correlation between flow measured with an electromagnetic flowmeter and flow derived from Doppler measurements obtained with the probe used in this study both in vitro and in vivo [5].

CHAPTER 11

ASSESSMENT OF CORONARY STENOSIS SEVERITY FROM SIMULTANEOUS MEASUREMENT OF TRANSSTENOTIC PRESSURE GRADIENT AND FLOW. A COMPARISON WITH QUANTITATIVE CORONARY ANGIOGRAPHY

Carlo Di Mario, M.D., Pim J. de Feyter, M.D., Ph.D., Johan C.H. Schuurbiers, B.Sc., Peter de Jaegere, M.D., Ph.D., Robert Gil, M.D., Håkan Emanuelsson, M.D., Ph.D., Cornelis J. Slager, Ph.D., Patrick W. Serruys, M.D., Ph.D.

From the Intracoronary Imaging Laboratory and Cardiac Catheterization Laboratory, Division of Cardiology, Thoraxcenter, Erasmus University, Rotterdam

From: Serruys PW, Foley D, de Feyter PJ (eds): QCA in clinical practice, Kluwer Academic Publishers, 1993.

16. Assessment of coronary stenosis severity from simultaneous measurement of transstenotic pressure gradient and flow. A comparison with quantitative coronary angiography

CARLO DI MARIO, PIM J. DE FEYTER, JOHAN C.H. SCHUURBIERS, PETER DE JAEGERE, ROBERT GIL, HÅKAN EMANUELSSON, CORNELIS J. SLAGER and PATRICK W. SERRUYS

Introduction

Visual interpretation of the coronary angiogram is the method routinely used to assess the severity of a coronary stenosis and to plan, monitor and judge the results of coronary interventions. Quantitative arteriography allows accurate and reproducible measurements of absolute and relative vascular dimensions but, despite the progressive refinements of computer-assisted analysis in the last years, eccentricity, diffuse atherosclerotic involvement and vessel tortuosity remain major obstacles to a correct assessment. In addition, following interventions, the damage to the vessel wall greatly impairs the accuracy of quantitative angiography inducing haziness of the contours and intraluminal filling defects [1, 2]. Under these circumstances, videodensitometry was a promising alternative [3] but its application has been precluded so far by the presence of basic methodological limitations, requiring further refinement of the technique [4, 5]. Intracoronary ultrasound has the potential for a more accurate assessment of lumen dimensions in the presence of luminal cross-sectional area of complex geometry [6, 7]. The dimension of the currently available ultrasound catheters (diameter 1.0–1.45 mm), however, limits the application of intravascular ultrasound to the assessment of severe coronary stenoses. In addition, an accurate evaluation of all the geometric characteristics of a coronary stenosis (diameter of a normal reference segment, length of inlet-outlet segments and of the stenosis and minimal luminal cross-sectional area) can be obtained only with an automatic three-dimensional reconstruction of multiple ultrasonic cross-sections, a technology still in phase of development and requiring extensive clinical validation [8]. A method alternative to the morphologic study of the lesion is the use of the hemodynamic parameters which characterize the severity of a stenosis, blood flow velocity and transstenotic pressure gradient. A major technical development facilitating the acquisition of these measurements in the Catheterization Laboratory was the introduction of miniaturized pressure and Doppler sensors with guidewire technology, allowing a simultaneous measurement of post-stenotic flow velocity and pressure with only a

P.W. Serruys, D.P. Foley and P.J. de Feyter (eds.), Quantitative Coronary Angiography in Clinical Practice, 283–306.

moderate further obstruction to flow [9, 10]. Aim of this study is the assessment of the clinical applicability and usefulness of indexes of stenosis severity based on the simultaneous transstenotic pressure gradient and flow velocity measurements and in particular on the instantaneous relationship between pressure gradient and flow velocity.

Methods

Patient population

Twenty-one patients (age: 62±10 years, 17 males and 4 females) undergoing elective coronary angioplasty (n = 14) or scheduled for a possible angioplasty procedure but with a stenosis angiographically of intermediate severity (> 40% and < 60% diameter stenosis; n = 7) were studied with a simultaneous measurement of flow velocity and post-stenotic coronary pressure. Patients with acute myocardial infarction, arterial occlusion/subocclusion {Thrombolysis in Myocardial Infarction (TIMI) flow class 0–1}, valvular heart disease, extreme tortuosity of the vessel to be dilated or the presence of an open aorto-coronary bypass graft on the vessel to be treated were not included in the study. Systemic arterial hypertension was present in 5 cases (23%). Previous myocardial infarction in the territory of distribution of the studied artery was present in 7 cases (33%). All patients were under antianginal treatment at the time of the study.

Catheterization procedure

After intravenous administration of 10,000 I.U. of heparin and 250 mg of acetylsalicylic acid, an 8 French guiding catheter was advanced up to the coronary ostium. After isosorbide-dinitrate (2–3 mg intracoronary), cineangiograms suitable for quantitative assessment were obtained in one/three angiographic views.

The pressure guidewire was advanced into the artery to be dilated and the pressure sensor was positioned 1–3 cm distal to the stenosis (Fig. 1). The Doppler guidewire was maintained proximal to the stenosis, avoiding the presence of major side-branches between the site of the measurement and the stenosis and the segment of pre-stenotic acceleration of flow. In 5 patients, due to presence of side-branches immediately proximal to the stenosis, only the flow velocity recordings distal to the stenosis were used for analysis. The proximal coronary pressure, the post-stenotic pressure and the proximal flow velocity were recorded both in baseline conditions and after an intracoronary bolus injection of papaverine (8 mg: right coronary; 12.5 mg: left coronary, saphenous vein bypass graft) [11]. Intracoronary nitrates (isosorbide dinitrate 2–3 mg) were used before the injection of papaverine in order to induce a maximal coronary vasodilatation and avoid changes in cross-

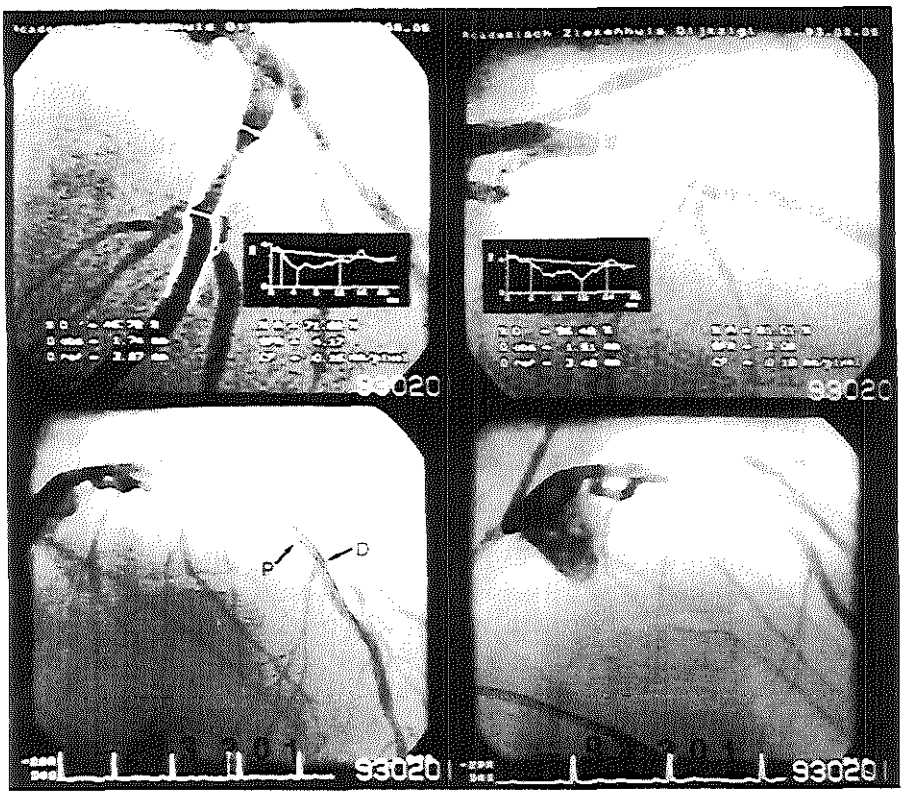

Figure 1. Upper panel: biplane orthogonal digital angiograms (left: LSO, right: RSO) of a left anterior descending coronary artery showing the presence of a significant concentric stenosis of the mid-segment. The diagrams show the diameter function of the examined segment after automatic contour detection. Bottom panels: the positions of the tip-mounted Doppler sensor (D) and of the sensor of the pressure guidewire (P) are indicated with arrows.

sectional area between baseline and post-papaverine assessment [12]. Care was taken to avoid impairment of flow during maximal hyperemia due to the presence of the guiding catheter in the coronary ostium. If damping occurred, the guiding catheter was withdrawn from the coronary ostium immediately after the injection of papaverine. The Doppler guidewire was then advanced distal to the stenosis and a new basal and post-papaverine acquisition was obtained (Fig. 1).

Quantitative angiographic measurements

The guiding catheter, filmed not filled with contrast medium, was used as a scaling device. A previously validated [13] on-line analysis system operating

on digital images (ACA-DCI, Philips, Eindhoven, The Netherlands) was used during the catheterization procedure. In this system, after automatic detection of the vessel centerline, a weighted first and second derivative function with predetermined continuity constraints is applied to the brightness profile on each scan line perpendicular to the vessel centerline [14]. From the measured minimal luminal diameter (MLD) the minimal luminal cross-sectional area was calculated assuming a circular cross-section (in 15 patients (71%) as the average of the measurements in multiple views). An interpolated technique was used to define the reference diameter. Percent diameter and cross-sectional area stenosis were also calculated. A user-defined diameter was measured at the site of the Doppler sample volume in order to calculate coronary blood flow as the product of mean blood flow velocity and cross-sectional area.

Doppler guidewire and flow velocity measurements

The Doppler angioplasty guidewire is a 0.018″ (diameter 0.45 mm, cross-sectional area 0.17 mm^2) 175 cm long flexible and steerable guidewire with a floppy shapable distal end mounting a 12 MHz piezoelectric transducer at the tip (Cardiometrics Inc., Mountain View, CA) [9]. The sample volume is positioned at a distance of 5.2 mm from the transducer in order to avoid the area of distortion of the flow profile due to the presence of the Doppler guidewire [15]. At this distance the sample volume has a width of approximately 2.25 mm due to the divergent ultrasound beam so that a large part of the flow velocity profile is included in the sample volume also in case of eccentric positions of the Doppler guidewire. The pulse repetition frequency (17 to 96 kHz) varies with the velocity range selected. After real-time processing of the quadrature audio signal a fast-Fourier transform algorithm is used to increase the reliability of the analysis [16], the Doppler system calculates and displays on-line several spectral variables including the instantaneous peak velocity and the time-averaged (mean of 2 beats) peak velocity. The flow velocity measurements obtained with this system have been validated in vitro and in an animal model using simultaneous electromagnetic flow measurements for comparison [9]. Mean flow velocity was calculated as time-averaged peak velocity/2, assuming a fully developed flow velocity profile [17]. Coronary flow reserve was defined as the ratio between maximal flow velocity at the peak effect of the papaverine injection and in baseline conditions.

Pressure guidewire and transstenotic pressure gradient measurements

The pressure sensor is located 3 cm proximal to the flexible tip of a 0.018″ guidewire (Radi Medical Systems, Uppsala, Sweden). Light is emitted from a control unit through a beam splitter and is transmitted to the sensor element along an optical fiber integrated in the guidewire. The sensor element consists

of a silicon cantilever with a mirror integrated into its free end. Deflection of the mirror induced by the elastic movement of the sensor in response to changes in the external pressure modulates the reflected light. The signal is then transmitted back through the same optical fiber and is detected by a photo diode in the control unit. The system has already been validated in vitro with regard to signal transfer characteristics, linearity and frequency response [10]. The pressure signal was calibrated immediately before insertion and the accuracy of the measurement was checked by superimposing the pre-stenotic coronary pressure measured with the pressure guidewire and the proximal coronary pressure measured with the guiding catheter. The mean transstenotic gradient was calculated as the difference of mean proximal and mean distal coronary pressure over 4 consecutive beats in baseline conditions and at peak papaverine effect (Fig. 2). The coronary flow measurements derived from the quantitative angiographic and Doppler measurements and the pressure measurements were used to calculate the hyperemic flow velocity-pressure gradient ratio and the delta flow-delta gradient ratio, calculated as the ratio of the differences of measurements of coronary flow and transstenotic gradient at the peak effect of papaverine and in baseline conditions.

Comparison with physiological parameters derived from QCA measurements

Stenosis flow reserve has been proposed by Kirkeeide et al. [18] as a single integrated index of stenosis severity and is based on the calculation derived from the measurements of stenosis geometry, of the transstenotic maximal pressure gradient and maximal flow increase under standardized conditions. These authors validated in vivo [19] flow dynamic equations developed in in vitro models by Young et al. [20, 21] and adapted for tapering stenoses and X-ray analysis by Brown et al. [22]. The algorithm, implemented also in the software package of the Philips DCI analysis system, uses the formula:

$$\Delta P = \frac{8\pi\mu L}{1.33\, A_s^2} Q + \frac{k_e \rho}{0.266} \left(\frac{1}{A_s} - \frac{1}{A_n} \right)^2 Q^2 \qquad (1)$$

where ΔP is the transstenotic pressure gradient in mmHg, μ is dynamic blood viscosity in Poise (assumed equal to 0.03), L is the length of the stenosis in mm, A_n is the cross-sectional area of the reference normal segment in mm^2, A_s is the minimal cross-sectional area of the stenotic segment in mm^2, Q is the mean coronary blood flow in ml/s, ρ is blood density in g/ml (assumed equal to 1.05) and k_e is the expansion coefficient used to correct for the entrance effect in order to apply the above equation in short stenoses as:

$$k_e = 1.21 + 0.08 \frac{Lprox}{RefD} \qquad (2)$$

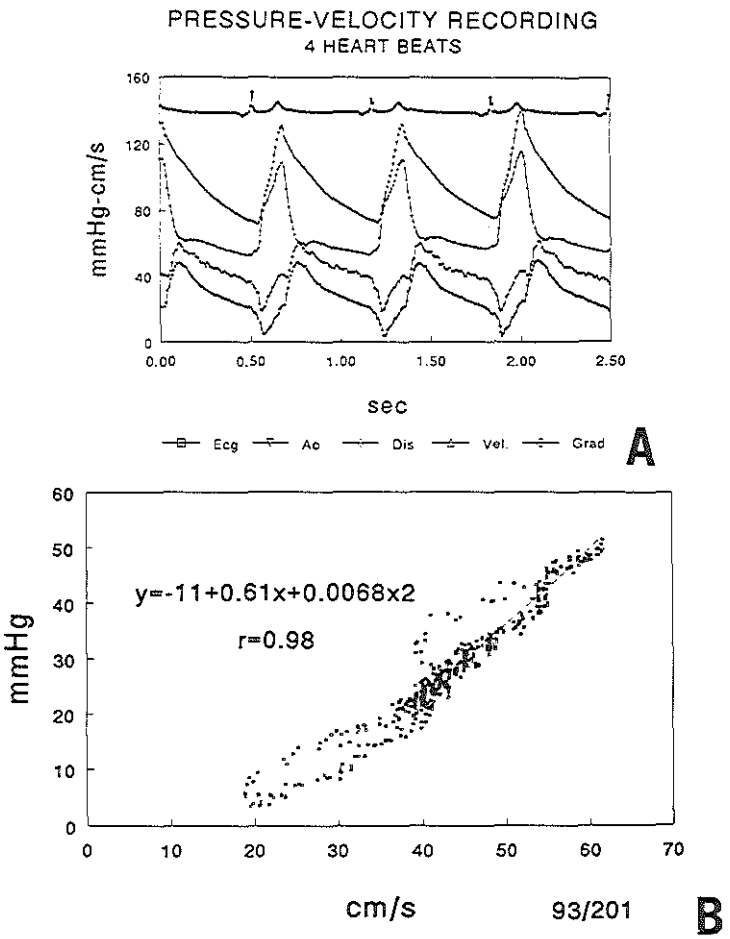

Figure 2. A) Simultaneous recording of electrocardiogram, proximal and distal (post-stenotic) coronary pressures, instantaneous peak flow velocity and transstenotic pressure gradient during four consecutive cardiac cycles at the peak effect of papaverine.

B) Pressure gradient and flow velocity relationship of the same 4 cardiac cycles. The data points corresponding to the phase of early diastolic relaxation and of early systolic contraction and the remaining systolic data-points (empty squares) are not considered for analysis. The dashed line is drawn from the exponential equation showing the best fitting for the mid-late diastolic data-points (filled squares).

where Lprox is the length of the entrance segment, approximated as lesion length divided by 2, and RefD is the diameter of the reference segment [23, 24]. Based on the post-stenotic pressure calculated from the above equations and the measurements of stenosis geometry, stenosis flow reserve was calculated assuming a maximal increase in coronary flow of 5 times at a mean

aortic pressure of 100 mmHg [25], a coronary venous pressure of 10 mmHg and a mean blood flow velocity of 15 cm/s [18, 19].

Stenosis flow reserve was compared both with the measured coronary flow reserve and, to allow a comparison under more standardized conditions, with the ratio between measured hyperemic mean velocity and basal mean velocity assumed in the above equation (15 cm/s).

Equation (1) was used to calculate the baseline and maximal hyperemic transstenotic pressure gradient using the real baseline and hyperemic flow velocities to calculate the corresponding coronary flow so that estimated and measured pressure gradient could be then compared at the same level of flow.

Instantaneous assessment of the pressure gradient-flow velocity relation

In 15 patients (71%) a continuous acquisition of the data was performed with a 12 bits analog-to-digital converter (DataQ Instr., Akron, OH) connected to a PC. Electrocardiogram, pre- and post-stenotic coronary pressure and peak coronary blood flow velocity were continuously sampled at 125 Hz per channel and stored on the hard-disk for off-line analysis (Fig. 2A). Positive or negative drifts of the 0–pressure level of the fiber optic pressure sensor, present in 7 patients (33%), and the phase delay of the pressure signal recorded through the fluid-filled guiding catheter were corrected by superimposing the pressure recorded through the guiding catheter and the prestenotic coronary pressure recorded through the pressure guidewire. Afterwards, the instantaneous transstenotic pressure gradient was calculated and plotted against the corresponding coronary flow velocity using dedicated software (AdvCodas, DataQ, Akron, Ohio), (Fig. 2B). Therefore, the transstenotic pressure gradient/flow velocity relation was analyzed from the digitized pressure and flow velocity during mid-diastole (start-point: maximal diastolic flow velocity, end-point: rapid deceleration of flow due to the begining of myocardial contraction). The phases of rapid acceleration/deceleration of flow were not considered for analysis, as suggested by Gould et al. [26], because the flow changes in these phases are dissociated from the transstenotic pressure gradient changes and are also conditioned by factors not related to the severity of the lesion (myocardial contractility, heart rate, etc.). The systolic phase of the cardiac cycle was not considered in order to avoid possible artifacts of the flow velocity signal, frequent during cardiac contraction (wall thumps, motion artifacts). Four consecutive beats were analyzed at the peak effect of the injection of papaverine.

Statistical analysis

Regression analysis was used to compare the measurements of pressure gradient and coronary flow and derived indexes with the minimal luminal cross-sectional area of the explored stenosis and with transstenotic pressure

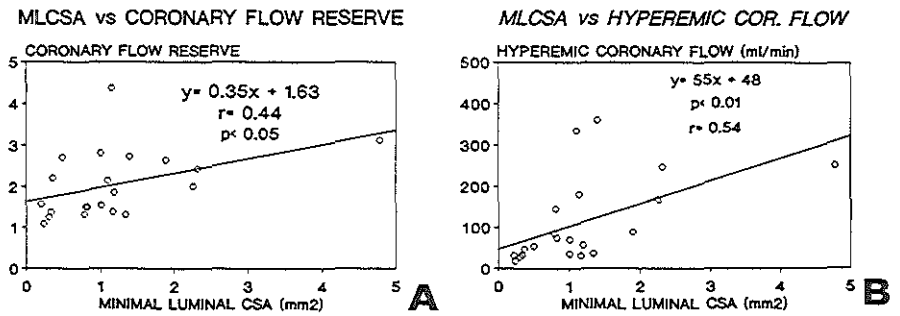

Figure 3. Linear regression analysis of coronary flow reserve (A) and hyperemic coronary flow (B) vs minimal cross-sectional area (MLCSA).

gradients and stenosis flow reserve. A best-fit analysis was used to assess the relationship between instantaneous pressure gradient and flow velocity (BmDP statistical package).Statistical significance was defined as $p < 0.05$. All data were expressed as mean±SD.

Results

Flow velocity and transstenotic pressure gradient measurements

The quantitative angiographic, flow velocity, pressure gradient and flow measurements of the 21 patients studied are reported in Table 1. Coronary flow reserve showed a partial but statistically significant correlation with minimal luminal cross-sectional area (Fig. 3A, $r = 0.44$, $p < 0.05$). Baseline coronary flow showed no significant correlation with the minimal luminal cross-sectional area ($r = 0.37$, NS). Coronary flow during maximal hyperemia, on the contrary, was significantly correlated with the minimal luminal cross-sectional area ($r = 0.54$, $p < 0.01$), (Fig. 3B). The baseline and hyperemic transstenotic pressure gradient showed a significant inverse correlation with the minimal luminal cross-sectional area ($r = -0.66$ and $r = -0.60$, respectively), (Fig. 4). An exponential increase in pressure gradient with the decrease in minimal luminal area was observed.

The maximal hyperemic transstenotic gradient showed a significant inverse correlation with the simultaneously measured hyperemic coronary flow, with a trend towards an exponential increase in transstenotic pressure gradient in the cases with the lowest maximal flow ($r = 0.61$, Fig. 5A). The non-significant stenoses were identified by the presence of hyperemic transstenotic gradients < 20 mmHg associated with a maximal coronary flow > 150 ml/min. At the other extreme, the presence of large transstenotic gradients during hyperemia associated with a low maximal hyperemic flow

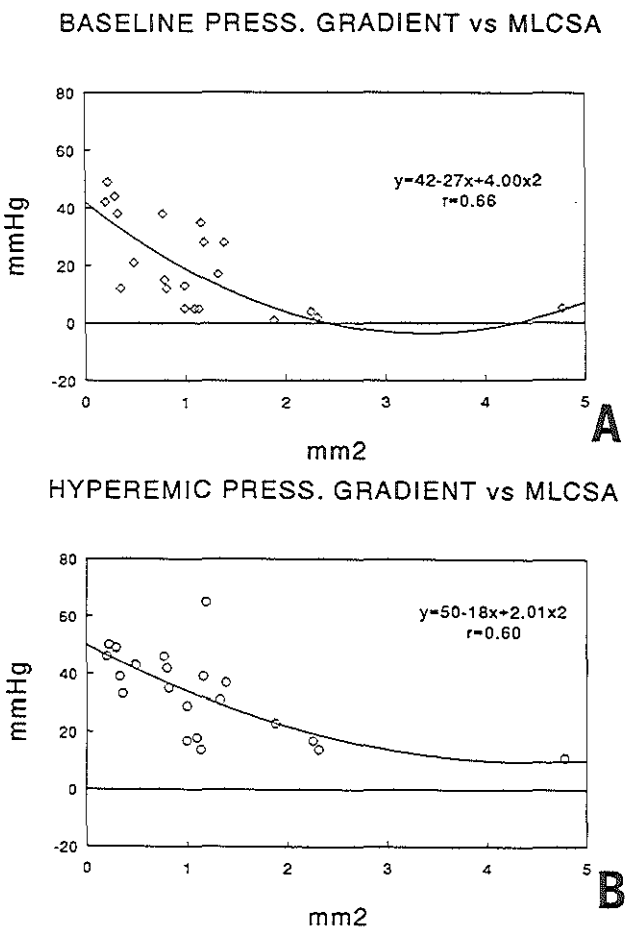

Figure 4. Baseline (A) and hyperemic (B) transstenotic pressure gradient plotted vs minimal luminal cross-sectional area (MLCSA). An exponential gradient increase is observed with decreasing cross-sectional areas.

identified the most severe stenoses. Similarly, when the pressure gradients from baseline to maximal hyperemia were plotted against coronary flow reserve, patients with moderate stenoses could be distinguished from patients with severe coronary stenoses (Fig. 5B).

Combined flow velocity and pressure gradient measurements

The hyperemic flow velocity-pressure gradient ratio and, in particular, the delta flow-delta gradient ratio, derived as previously described from the integration of flow and pressure gradient changes from baseline to hyperemia,

Table 1. Clinical and hemodynamic characteristics of the patients studied with a simultaneous recording of transstenotic pressure gradient and flow velocity.

INIT	AGE (yrs)	SEX	VES	MLCSA mm^2	CSA %	BAPV cm/s	HAPV cm/s	CFR	SFR	BAS GRAD mmHg	HYP GRAD mmHg	BAS FLOW ml/min	HYP FLOW ml/min	FLOW/ GRAD I ml/min/ mmHg
WA	60	m	rca	0.49	0.92	10	27	2.70	1.25	21	43	20	53	1.53
BJL	73	m	svbg	0.21	0.98	7	11	1.57	0.30	42	46	20	31	2.85
FB	70	f	rca	2.26	0.74	31	62	2.00	3.13	4	17	84	167	6.44
BKJ	59	m	rca	0.82	0.95	10	15	1.50	1.0	12	35	50	74	1.08
BJ	62	m	lad	0.78	0.87	34	45	1.32	2.21	38	46	65	86	2.61
RTR	69	m	rca	0.33	0.97	8	11	1.37	0.49	38	39	24	33	9.00
SA	73	m	svbg	4.78	0.68	18	56	3.11	3.14	5	11	81	252	28.50
WC	59	m	lad	1.14	0.84	19	83	4.37	2.24	5	14	41	181	15.53
BJ	55	m	lad	1.10	0.86	66	141	2.14	2.66	5	18	157	336	13.74
DHTA	80	m	rca	0.30	0.97	8	10	1.25	0.46	44	49	23	28	1.13
SEA	74	m	rca	0.23	0.95	11	12	1.09	0.66	49	50	17	18	1.60
OMV	81	f	rca	1.39	0.85	48	131	2.73	2.89	28	37	132	361	25.39
EC	57	m	rca	0.80	0.92	30	45	1.50	1.92	15	42	97	146	1.80
BW	67	m	svbg	1.16	0.87	8	11	1.37	2.31	35	39	21	29	1.99
JB	63	f	rca	1.00	0.82	13	20	1.54	2.87	13	29	23	35	0.77
LTW	50	m	lad	1.19	0.71	21	39	1.86	4.24	28	65	33	56	2.05
WHP	41	m	lcx	1.89	0.77	14	37	2.64	3.92	1	23	34	89	2.50
DAG	52	m	rca	1.00	0.81	10	28	2.80	2.87	5	17	25	70	3.75
JKF	52	m	lcx	1.33	0.88	13	17	1.31	2.50	17	31	27	36	0.60
GMJP	60	f	lad	2.32	0.80	61	148	2.43	3.99	2	41	102	247	12.10
JAK	52	m	rca	0.36	0.93	15	33	2.20	1.31	12	33	21	46	1.19
AVG	62			1.18	0.86	22	47	2.04	2.21	20	33	52	113	6.48
± SD	10			1.02	0.09	17	44	0.81	1.20	16	15	41	105	8.15

BAPV = Baseline time-averaged peak blood flow velocity; CSA = cross-sectional area; CFR = coronary flow reserve; FLOW/GRAD I = (hyperemic flow – baseline flow)/(hyperemic gradient – baseline gradient); HAPV = hyperemic time-averaged peak blood flow velocity; LAD = left anterior descending; LCX = left circumflex; MI = myocardial infarction; MLCSA = minimal luminal cross-sectional area (angiographic measurement minus cross-sectional area of the pressure and (5 cases) Doppler guidewire); NORM BASG = normalized baseline gradient; NORM HYPG = normalized hyperemic gradient; RCA = right coronary artery; SFR = stenosis flow reserve; SVBG = saphenous vein bypass graft.

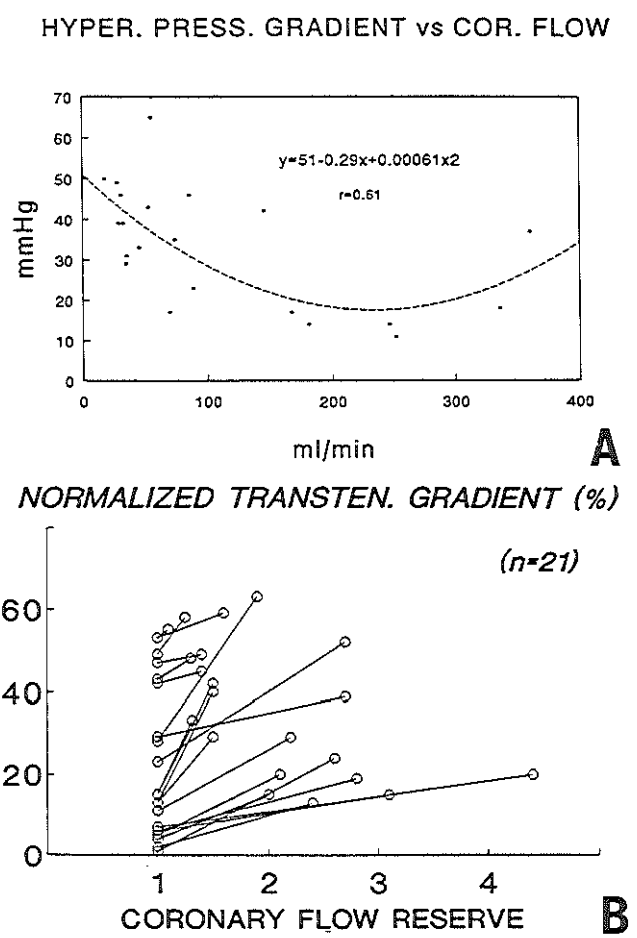

Figure 5. A) Relationship between hyperemic transstenotic pressure gradient and flow.
B) Baseline and hyperemic transstenotic pressure gradient, normalized for the corresponding aortic pressure, are plotted against coronary flow reserve. Higher hyperemic flow or flow reserve and low gradients indicate the least severe stenoses and viceversa.

showed a more strict correlation with minimal luminal cross-sectional area than the other flow velocity and pressure gradient measurements (Fig. 6, $r = 0.54$, $p < 0.02$ and $r = 0.66$, $p < 0.001$, respectively). In particular a delta flow-delta gradient ratio < 3 ml/min/mmHg identified 14 out of 17 cases with a minimal cross-sectional area < 1.5 mm^2.

Measured and estimated flow reserve and transstenotic pressure gradients

No correlation was present between coronary flow reserve and stenosis flow reserve (Fig. 7A). Despite a statistically significant correlation, measured and

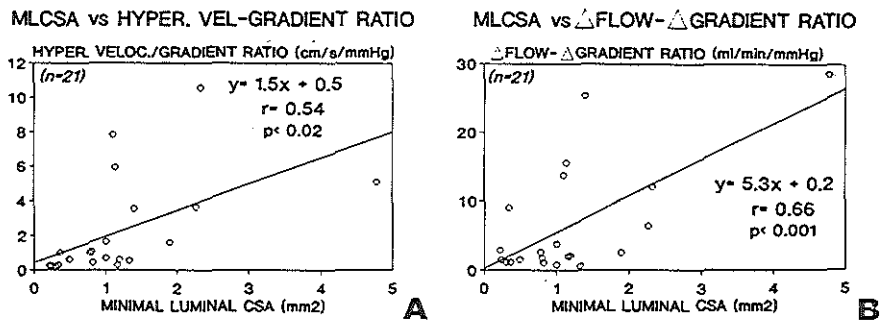

Figure 6. Linear regression analysis of the relationship between minimal luminal cross-sectional area (MLCSA) and (A) ratio between hyperemic flow velocity and pressure gradient and (B) ratio between the difference hyperemic-baseline coronary flow and pressure gradient. The latter index showed a higher correlation with MLCSA than all the other flow velocity and pressure gradient measurements.

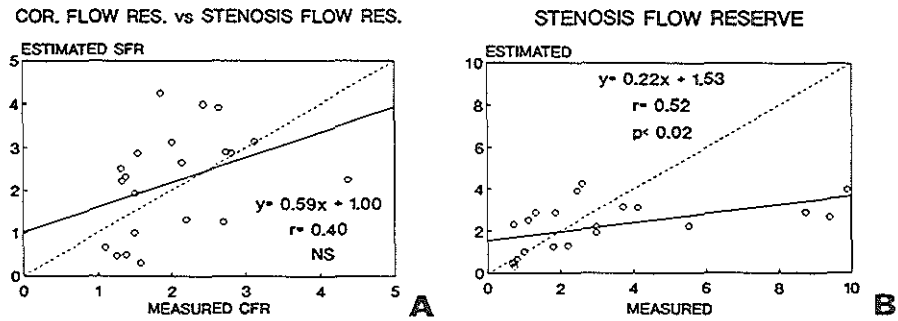

Figure 7. The stenosis flow reserve estimated from the angiographic stenosis geometry is plotted against the measured coronary flow reserve (A) and the ratio between measured maximal hyperemic flow velocity and mean velocity assumed for the calculation of stenosis flow reserve (15 mmHg). The dashed lines indicate the identity lines. The continuous lines indicate the regression lines.

estimated stenosis flow reserve showed a large dispersion of the individual measurements ($r = 0.52$, Fig. 7B). A better correlation was observed between estimated and measured transstenotic pressure gradient in baseline condition ($r = 0.65$, $p < 0.002$, Fig. 8A). During maximal hyperemia, however, no significant correlation was observed between estimated and measured transstenotic pressure gradients ($r = 0.13$, Fig. 8B).

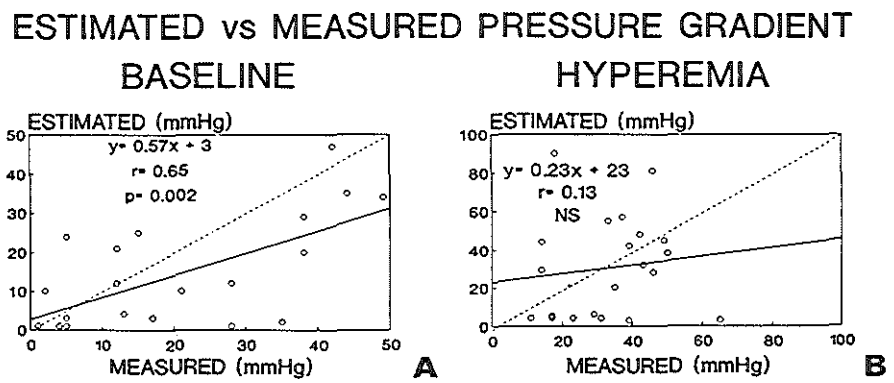

Figure 8. Estimated and measured transstenotic pressure gradients in baseline conditions (A) and at peak hyperemia (B). Dashed lines: identity lines; continuous lines: regression lines.

Instantaneous assessment of the hyperemic coronary pressure/flow velocity relation

A clear Doppler envelope allowing a reliable automatic detection of the hyperemic diastolic peak velocity during four consecutive beats was obtained in 12/15 cases (80%) (Fig. 9). A linear relationship between transstenotic gradient and flow velocity was observed in 5/12 patients (42%). In the remaining patients a quadratic equation had the best fitting for the data obtained (7/12, 58%). In all but 3 cases an intercept close to 0 (± 10 mmHg) was observed. Steeper increases of the transstenotic pressure gradient at a given flow increase were measured in the arteries with the most severe reduction in luminal cross-sectional area.

Discussion

The identification of a single hemodynamic parameter, immediately measurable in the Catheterization Laboratory and predictive of the functional severity of a coronary stenosis would constitute an extraordinary diagnostic tool, especially for the assessment of the immediate results of coronary interventions.

Coronary flow reserve

Experimental reports have shown that a decrease in flow reserve may discriminantly detect a lesion of increasing severity [27]. Although the concept may be easily and accurately applied in an optimal physiological situation [28, 29], it must be recognized that coronary flow reserve is influenced by factors independent from the hydrodynamic characteristics of the stenotic lesion

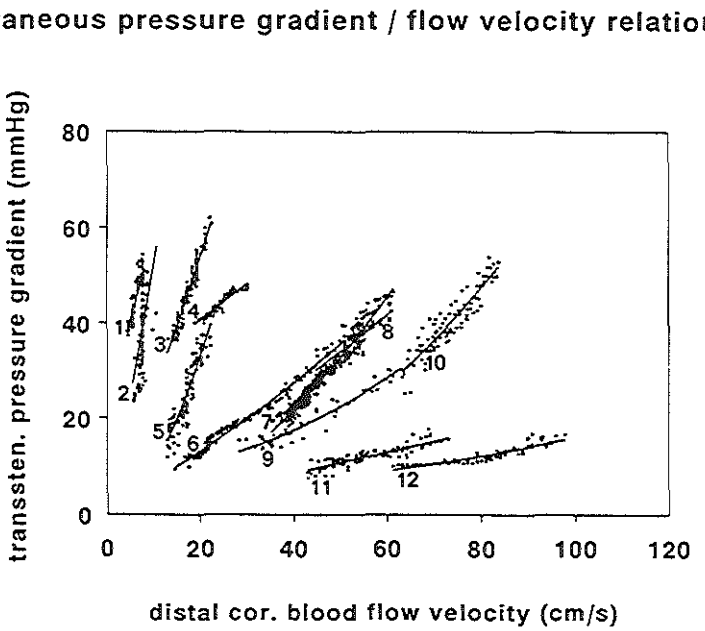

Figure 9. Instantaneous hyperemic diastolic pressure gradient/flow velocity relationship for 12 stenoses of increasing hemodynamic severity (from left to right and from bottom to top). The corresponding minimal luminal cross-sectional area (MLCSA) is reported after subtraction of the cross-sectional areas of the pressure and Doppler guidewires.

Nb/INIT.	CATH.Nb	MLCSA(mm^2)	EQUATION
1 BJL	92707	0.21	$y = 21 + 2.72x$
2 RTR	92999	0.33	$y = -6 + 5.76x$
3 JKF	921858	1.16	$y = 2 + 2.01x + 0.0275x^2$
4 WA	921132	0.49	$y = 25 + 0.79x$
5 BKJ	920922	0.82	$y = 2 + 0.11x + 0.073x^2$
6 DAG	922047	0.83	$y = 1.6 + 0.50x + 0.0035x^2$
7 WHP	930201	1.72	$y = -4 + 0.28x + 0.009x^2$
8 JB	920908	0.83	$y = -4 + 0.76x$
9 JAK	921502	0.36	$y = 9 + 0.0055x^2$
10 LTW	921504	1.19	$y = -0.1 + 0.0074x^2$
11 SA	921448	4.61	$y = -1 + 0.23x$
12 FB	921330	2.09	$y = 5 + 0.0011x^2$

such as heart rate, aortic pressure, presence of collateral circulation, integrity of the distal resistance coronary vessels [30, 31]. Several pathological conditions (cardiac hypertrophy, myocardial scarring, hypercholesterolemia, systemic hypertension, etc) have been reported to alter the normal reactivity and impair the vasodilatory capacity of the distal coronary vasculature. In these conditions, therefore, the severity of the stenosis would be overesti-

mated if the low flow during maximal vasodilatation is attributed to the high resistance across the stenosis. Similarly, the presence of a well-developed collateral flow would lead to an overestimation of stenosis severity because of the decreased maximal flow through the stenosis. Coronary flow reserve is by definition a ratio, so that similar ratios may be obtained at very different levels of resting and maximal flow. Following coronary interventions, acute changes in resting blood flow together with changes in the anatomy of the stenotic lesion and concomitant persistent modifications of the hyperemic pressure-velocity relationship considerably hamper the clinical usefulness of coronary flow reserve for the assessment of the functional results. Our recently reported results with the use of a Doppler guidewire during coronary angioplasty [32] confirmed previous observations [33–36] that an increase in resting and maximal flow velocity occurs following angioplasty so that the usefulness of coronary flow reserve is limited in this clinical setting. Similar observations have been made by our group in the past, using Doppler tip balloon angioplasty catheters [37].

Stenosis flow reserve

Stenosis flow reserve is an alternative approach, based only on quantitative angiographic measurements, to evaluate in standardized conditions the severity of a coronary stenosis, regardless of the individual variability of physiologic conditions [18, 19]. As clearly pointed out by the proposers of this index [18, 19], stenosis flow reserve can not be considered as an estimate of the real coronary flow reserve, determined also by the hemodynamic conditions at the time of assessment, the presence of collateral flow and the properties of the microcirculation. In this respect, the use of standardized conditions assumed in the calculation of this index has the advantage that only flow limitations induced by the stenosis studied are considered. The assumption of hemodynamic conditions not necessarily present in the studied patients is sufficient to explain the poor correlation observed in this study between estimated stenosis flow reserve and measured coronary flow reserve also when a baseline velocity equal to the velocity assumed for the calculation of stenosis flow reserve was used. A more consistent methodology to test whether hemodynamic parameters calculated from quantitative angiographic measurements reflect the real measurements is the comparison of the transstenotic pressure gradient, assuming a coronary flow velocity and an aortic pressure equal to the measured velocity and aortic pressure. This comparison, however, showed large individual differences between measured and estimated transstenotic pressure gradients, possibly as a consequence of the unavoidable inaccuracies in the measurement of the multiple geometric factors which determine stenosis severity and of the limitations to the applicability of the proposed equations, especially at high flows.

Transstenotic pressure gradient

The importance of the dimensions of the pressure sensor used for the measurement of the transstenotic pressure gradient has been reported and extensively studied in the years following the introduction of coronary angioplasty, when the pressure gradient recorded through the central lumen of the balloon catheter was used for the immediate assessment of the results of the procedure [38–40]. More recently, using a pressure guidewire as the angioplasty guidewire, the large increase in pressure gradient observed with the balloon catheter positioned in the lesion has been confirmed [10]. Despite these limitations, the clinical relevance of the residual transstenotic pressure gradient after coronary interventions has been confirmed by the presence of a significant correlation between residual pressure gradient > 20 mmHg after balloon angioplasty and development of restenosis [41]. The correlation observed in this study between transstenotic pressure gradient and angiographic lesion severity has been confirmed in a larger series of patients by Emanuelsson et al. [42]. The dependancy of the pressure gradient on flow, however, precludes a complete understanding of this parameter when the flow level is not simultaneously assessed.

Simultaneous measurement of pressure gradient and flow velocity

The simultaneous measurement of transstenotic pressure gradient and flow velocity avoids a possible misinterpretation of the changes of both these indexes during maximal vasodilatation. When a low maximal flow is present due to factors not dependent from the stenosis resistance, the measurement of a low transstenotic pressure gradient can be misleading, falsely suggesting the presence of a non-significant stenosis. Conversely, only the simultaneous measurement of the pressure gradient can discriminate a low flow increase during maximal vasodilatation due to a hemodynamically severe stenosis (high pressure gradient) from a reduction of the maximal transstenotic flow increase due to an impairment of the distal vasodilatory mechanisms or to competition of flow through a well-developed collateral circulation (low pressure gradient). Although the maximal flow and, consequently, the maximal transstenotic gradient are determined also by factors independent from the stenosis resistance, the transstenotic pressure gradient-flow relationship is intimately correlated with the stenosis hemodynamics. Two alternative approaches have been used to assess the slope of the pressure gradient-flow velocity relation. The first is based on the ratio of the differences of transstenotic pressure gradient and flow velocity from baseline conditions to maximal hyperemia. This index has the dimensions of flow conductance (ml/min/mmHg) and, in this study, showed a higher correlation with the angiographic minimal luminal cross-sectional area than all the single pressure gradient and flow velocity measurements. A technically more complex but promising approach is based on the assessment of the instantaneous pressure

gradient/flow velocity relationship during the progressive flow decrease in mid-late diastole. The advantage of an index based on instantaneous instead of mean gradient/flow changes during the cardiac cycle is that the phases of acceleration of flow in early diastole and deceleration of flow at the beginning of myocardial contraction can be excluded from analysis. In early systole, cardiac contraction induces an increase of the distal coronary pressure, with the possibility of a short reversed pressure gradient and a transient dissociation between transstenotic pressure gradient and flow [26]. An inverse phenomenon is observed in early diastole, when a sudden decrease of distal coronary pressure occurs during the phase of rapid cardiac relaxation, preceding the rapid increase in flow (Fig. 2). When only the passive, post-accelerative diastolic data-points are used for analysis, pressure gradient and flow velocity showed a high correlation in all cases, described by an exponential (58%) or linear (42%) relationship. This approach can also detect sudden changes in stenosis geometry from baseline to maximal hyperemia such as those due to a partial collapse of the vessel wall consequent to a critical reduction of the intrastenotic pressure [43]. In the presence of a fixed stenosis and when a premedication with nitrates intracoronary is used to negate diameter changes of the reference segments, the pressure gradient/flow velocity relationship is independent from the hemodynamic conditions of assessment (baseline or maximal hyperemia). In this study, however, the assessment was performed during maximal hyperemia so that the pressure gradient-flow relationship could be evaluated over a larger range of measurements. A possibility that we has been explored to evaluate the pressure gradient-flow velocity relationship over a large range of flow velocities and up to very low flow velocity levels is the induction of a prolonged cardiac arrest with the use of an extra-bolus of adenosine during post-papaverine maximal hyperemia (Fig. 10).

Potential alternative analysis of the flow velocity-proximal and post-stenotic pressure relationship

A more easily applicable method to assess the severity of a coronary stenosis, based only on the simultaneous assessment of aortic pressure and coronary flow (or flow velocity), has been proposed by Mancini et al. [44]. The slope of the instantaneous coronary flow and pressure relationship was measured during diastole in 43 dogs at 5 different levels of arterial pressure and inducing coronary stenoses of increasing severity. The measured instantaneous diastolic pressure/flow slopes were then compared with a microsphere derived index of myocardial conductance. The instantaneous hyperemic flow vs pressure index demonstrated no dependance on heart rate, left ventricular end-diastolic pressure, mean aortic pressure or inotropic changes [45, 46]. The decrease in flow/pressure slope with the presence of stenoses of increasing severity correlated well with the transmural and the subendocardial microsphere-derived measurements.

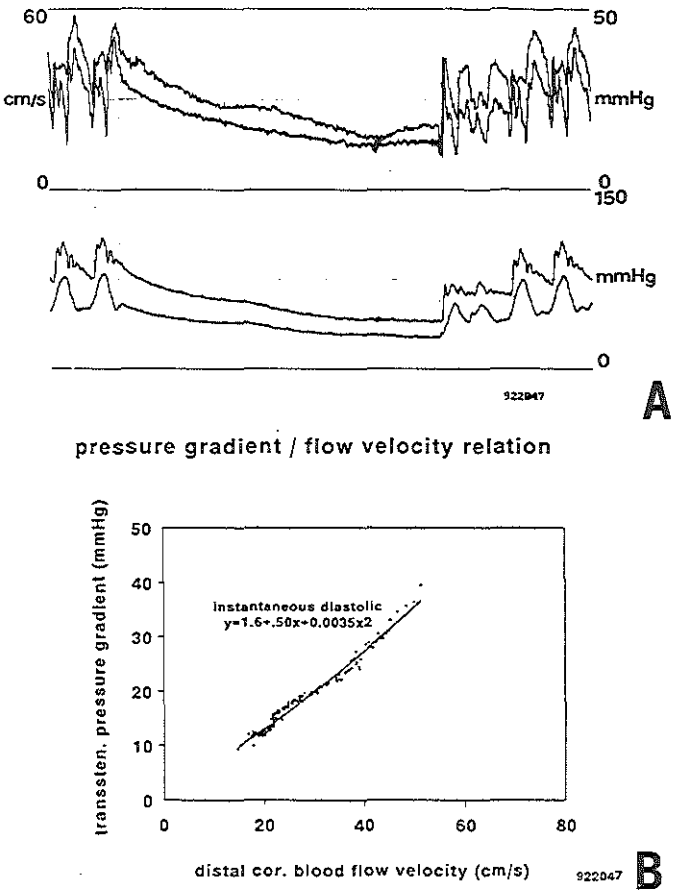

Figure 10. A) Long diastolic pause induced by the infusion of adenosine 3 mg intracoronary. From top to bottom peak flow velocity, instantaneous transstenotic pressure gradient and proximal and post-stenotic coronary pressure. B) Instantaneous hyperemic diastolic pressure gradient/flow velocity relationship of the previously shown diastolic pause.

Feasibility and beat-to-beat variability of the assessment of the instantaneous flow velocity-pressure relationship in humans was assessed in normal and stenotic coronary arteries using a Doppler guidewire [32, 47] (Fig. 11A). A significant difference was observed between velocity-pressure slopes measured in stenotic and normal coronary vessels, with the presence, however, of a partial overlap between the two groups. The measurement of a high fidelity post-stenotic pressure allows a direct assessment of the resistive properties of the distal coronary bed, not taking into account the resistance offered by the coronary stenosis. The integration of this approach with the assessment of the pressure gradient-flow velocity relationship has the poten-

tial for a complete characterization of the two resistances in series given by the epicardial stenosis and by the distal vasculature. After normalization with ballon dilatation or stent implantation of the epicardial arteries, the slope of the post-stenotic flow velocity-pressure relationship before the intervention can be compared with the flow velocity-proximal pressure slope after the interventions, to assess possible acute changes of the vasodilatory capacity of the distal coronary arteries. As evident from the example of Fig. 11B, however, the flow velocity/post-stenotic pressure relationship can be assessed only over a narrow pressure range in the presence of a severe coronary stenosis. An exponential decrease of pressure for any given flow velocity decrease seems to be present, possibly because of the rapid reduction in cross-sectional area in the low pressure range, resulting in an overestimation of flow using the corresponding flow velocity measurements. The consequent reduction of arterial cross-sectional area induces an underestimation of the true flow changes calculated only from the flow velocity measurements.

Limitations of the pressure gradient-flow velocity relationship for assessment of stenosis severity

The pressure gradient-velocity relationship has great advantages for the assessment of the hemodynamic severity of a stenosis but a precise characterization of stenosis hemodynamics does not necesserily provide sufficient elements to confirm or rule out the presence of myocardial ischemia in the territory of distribution of the examined artery. In particular, in the presence of stenoses of similar hemodynamic severity, the development of myocardial ischemia is influenced by the amount of recruitable collateral flow and by the mass of viable myocardium perfused.

The presence and development of the collateral circulation can not be determined based on conventional pressure-flow velocity measurements. Recently, Pijls et al. [48] has proposed a model using the post-stenotic pressure during occlusion (wedge pressure) to estimate maximal flow. This approach, experimentally validated, requires a balloon occlusion at the site of the stenosis so that its application is possible only during balloon dilatation.

Knowledge of the dimension of the perfused myocardial bed is essential to detect a possible mismatch between maximal flow achievable through the studied stenosis at a given aortic pressure and maximal blood flow requirement of the studied artery. The automatic measurement of the length of the angiographically visible coronary branches has been successfully used in animals to estimate the perfused myocardial mass [49]. This method, however, seems not easily applicable for routine diagnostic purposes. It must be noted that the pressure gradient-flow velocity relationship shows a steeper increase in smaller arteries than in larger arteries for a given severity of the coronary stenosis [50]. The use of velocity instead of flow can be considered a correction to this limitation because the characteristics of the coronary branching system result in a moderate reduction of flow velocity from proxi-

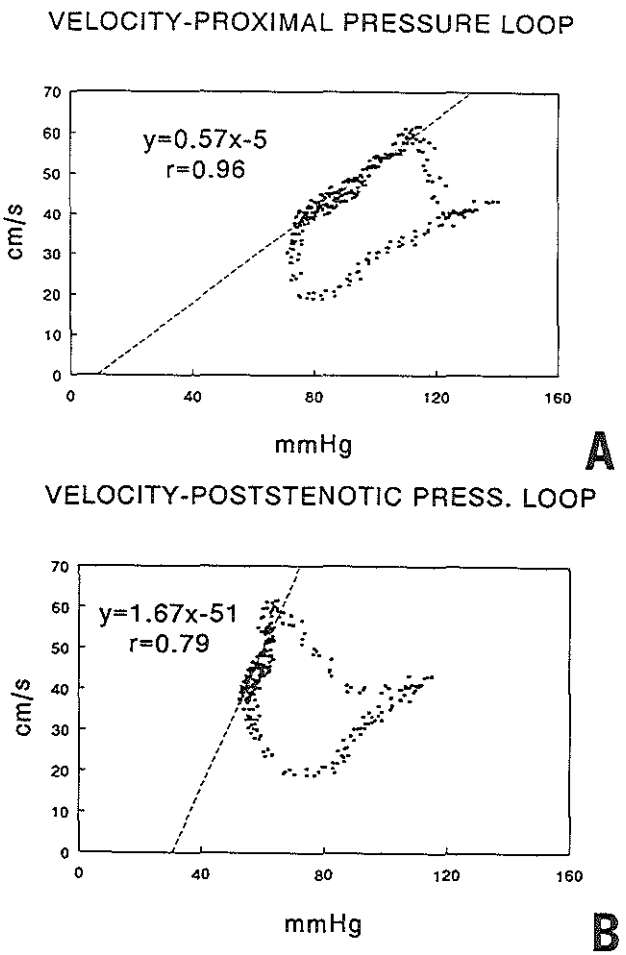

Figure 11. Flow velocity-pressure loop for the same cardiac cycles of Fig. 2. On the Y-axis proximal (pre-stenotic) and distal (post-stenotic) coronary pressure in A) and B), respectively. Linear regression analysis is used in both cases to analyze the flow velocity-pressure relationship in mid-late diastole.

mal to distal coronary segments despite the presence of large changes in coronary flow.

The most important limitation of the proposed approach, however, remains the complexity of the instrumentation required for the measurements. The passage of two separate guidewires with a cross-sectional area of 0.17 mm^2 can induce a significant additional obstruction in the presence of severe coronary stenoses [51]. Further, after coronary interventions the guidewires can prevent a complete collapse of the wall in the presence of large dissection

flaps, precluding a correct assessment of the obstruction to flow. Whenever possible, flow velocity was measured proximal to the stenosis to avoid the simultaneous presence of two guidewires across the lesion. This approach, however, precludes the possibility to take advantage of the availability, with the Doppler guidewire, of a flow velocity signal distal to the stenosis, certainly reflecting the flow limitations induced by the stenosis. Crossing of the lesion with the Doppler guidewire was required in the cases with large side-branches immediately proximal to the lesion and was felt to be mandatory for the recording of the velocity waveform used for the assessment of the instantaneous pressure gradient-flow velocity relationship. Prototypes of 0.014″ Doppler and pressure guidewires are available but a real solution can be obtained only with the combination of the two sensors in the same guidewire system. The ingenious system used to obtain a high fidelity pressure in the pressure guidewires has still practical limitations concerning the rigidity of the segment mounting the sensor and the possibility of a shift of the 0–pressure when this segment is positioned in a sharp vascular bend.

Conclusion

Miniaturization of flow velocity and pressure sensors with guidewire technology now permits the application in conscious humans of a methodological approach to the assessment of stenosis severity previously limited to the animal laboratory. This initial experience suggests that the simultaneous measurement of pressure and flow velocity can reproducibly and accurately characterize the physiologic significance of coronary stenoses.

Acknowledgements

The contribution to the acquisition of the data of the medical, technical and nursing staff of the Cath Lab and in particular of Mr. R.van den Perk and Mr. N. Bruining is gratefully acknowledged. Dr. R.L. Kirkeeide, Dr. R. Krams, and Dr. C.J. Slager are also acknowledged for their contribution and suggestions for the analysis of the data.

References

1. Serruys PW, Foley DP, de Feyter PJ. Restenosis after coronary angioplasty: a proposal of new comparative approaches based on quantitative angiography. Br Heart J 1992; 68: 417–424.
2. De Cesare NB, Williamson PR, Moore NB, DeBoe SF, Mancini GBJ. Establishing comprehensive, quantitative criteria for detection of restenosis and remodelling after percutaneous transluminal coronary angioplasty. Am J Cardiol 1992; 69: 77–83.
3. Serruys PW, Reiber JHC, Wijns W, van den Brand M, Kooljman CJ, Katen ten HJ,

Hugenholtz PG. Assessment of percutaneous transluminal coronary angioplasty by quantitative coronary angiography; diameter versus densitometric area measurements. Am J Cardiol 1984; 54: 482–488.
4. Sanz ML, Mancini GBJ, Lefree MT, Mickelson JK, Starling MR, Vogel RA, Topol EJ. Variability of quantitative digital substraction coronary angiography before and after percutaneous transluminal coronary angioplasty. Am J Cardiol 1987; 60: 55–60.
5. Whiting JS, Pfaff JM, Eigler NL. Advantages and limitations of videodensitometry in quantitative coronary angiography. In: Reiber JHC, Serruys PW (editors) Quantitative coronary arteriography, Dordrecht-Boston-London, Kluwer Academic Publisher, 1991: 43–54.
6. Tenaglia AN, Buller CE, Kisslo KB, Stack RS, Davidson CJ. Mechanisms of balloon angioplasty in vivo assesed by intravascular ultrasound imaging. J Am Coll Cardiol 1992; 20: 685–691.
7. Honye J, Mahon DJ, White CJ, Ramee SR, Tobis JM. Morphological effects of coronary balloon angioplasty in vivo assessed by intravascular ultrasound imaging. Circulation 1992; 85: 1012–1025.
8. Di Mario C, Wenguang L, Linker DT, Gussenhoven EJ, Serruys PW, Roelandt JRTC. Three-dimensional reconstruction in intravascular ultrasound. Promises and practical problems. Int J Cardiac Imag 1993; 66–77.
9. Doucette JW, Corl DP, Payne HP, Flynn AE, Goto M, Nassi M, Segal J. Validation of a Doppler guide wire for intravascular measurement of coronary artery flow velocity. Circulation 1992; 85: 1899–1911.
10. Emanuelsson H, Dohnal M, Lamm C, Tenerz L. Initial experiences with a miniaturized pressure transducer during coronay angioplasty. Cath Cardiovasc Diagn 1991; 24: 137–143.
11. Zijlstra F, Serruys PW, Hugenholtz PG. Papaverine: the ideal coronary vasodilator for investigating coronary flow reserve? A study of timing, magnitude, reproducibility and safety of the coronary hyperemic response after intracoronary papaverine. Cathet Cardiovasc Diagn 1986; 12: 298–303.
12. Zijlstra F, Reiber JHC, Serruys PW. Does intracoronary papaverine dilate epicardial coronary arteries? Implications for the assessment of coronary flow reserve. Cathet Cardiovasc Diagn 1988; 14: 1–6.
13. Haase J, Di Mario C, Slager CJ, van der Giessen WJ, den Boer A, de Feyter PJ, Reiber JHC, Verdouw PD, Serruys PW. In-vivo validation of on-line and off-line geometric coronary measurements using insertion of stenosis phantoms in porcine coronary arteries. Cathet Cardiovasc Diagn 1992; 27: 16–27.
14. Reiber JHC, Serruys PW, Koojman CJ, Wijns W, Slager CJ, Gerbrands JJ, Schumbiers JCH, den Boer A, Hugenholtz PG. Assessment of short-, medium-, and long-term variations in arterial dimensions from computer-assisted quantitation of coronary cineangiograms. Circulation 1985; 71: 280–288.
15. Tadaoka S, Kagiyama M, Hiramatsu O. Accuracy of 20 MHz Doppler catheter coronary artery velocimetry for measurement of coronary blood flow velocity. Cath Cardiovasc Diag 1990; 19: 205–213.
16. Di Mario C, Roelandt JRTC, de Jaegere P, Linker DT, Oomen J, Serruys PW. Limitations of the zero-crossing detector in the analysis of intracoronary Doppler. A comparison with fast Fourier transform of basal, hyperemic and transstenotic blood flow velocity measurements in patients with coronary artery disease. Cathet Cardiovasc Diagn 1992; 28: 56–64.
17. Di Mario C, de Feyter PJ, Slager CJ, de Jaegere P, Roelandt JRTC, Serruys PW. Intracoronary blood flow velocity and transstenotic pressure gradient using sensor-tip pressure and Doppler guidewires. Cath Cardiovasc Diagn 1993; 28: 311–19.
18. Kirkeeide RL, Gould KL, Parsel L. Assessment of coronary stenoses by myocardial perfusion imaging during pharmacologic coronary vasodilatation. Validation of coronary flow reserve as a single integrated functional measure of stenosis severity reflecting all its geometric dimensions. J Am Coll Cardiol 1986; 7: 103–113.

19. Gould KL, Kirkeeide RL, Buchi M. Coronary flow reserve as a physiologic measure of stenosis severity. J Am Coll Cardiol 1990; 15: 459–474.
20. Young DF, Tsai FY. Flow characteristics in models of arterial stenoses-II. Unsteady flow. J Biomechanics 1973; 6: 547–559.
21. Young DF, Cholvin NR, Roth AC. Pressure drop across artificially induced stenoses in the femoral arteries of dogs. Circ Res 1975; 36: 735–743.
22. Brown GB, Bolson E, Frimer M, Dodge HT. Quantitative coronary arteriography. Estimation of dimensions, hemodynamic resistance and atheroma mass of coronary artery lesions using the arteriogram and digital computation. Circulation 1977; 55: 329–337.
23. Lipscomb K, Hooten S. Effect of stenotic dimensions and blood flow on the hemodynamic significance of model coronary arterial stenoses. Am J Cardiol 1978; 42; 781–792.
24. Siebes M, Gottwik M, Schlepper M. Quantitative and qualitative experimental studies in the evaluation of model coronary arteries from angiograms. Computers Cardiol 1982; 211–214.
25. Bache RJ, Schwartz JS. Effect of perfusion pressure distal to a coronary stenosis on transmural myocardial blood flow. Circulation 1982; 65: 928–935.
26. Gould KL. Phasic pressure-flow and fluid-dynamic analysis. In: Gould LD (editor) "Coronary Artery Stenosis", Elsevier, New York-Amsterdam-London, 1991: 40–52.
27. Gould KL, Lipscomb K, Hamilton GW. Physiologic basis for assessing critical coronary stenosis: instantaneous flow response and regional distribution during coronary hyperemia as measures of coronary flow reserve. Am J Cardiol 1974; 33: 87–94.
28. Wilson RF, Marcus ML, White CW. Prediction of the physiologic significance of coronary arterial lesions by quantitative lesion geometry in patients with limited coronary artery disease. Circulation 1987; 75: 723–732.
29. Harrison DG, White CW, Hiratzka LF, Eastham CL, Marcus ML. The value of lesional cross-sectional area determined by quantitative coronary angiography in assessing the physiologic significance of proximal left anterior descending coronary artery stenoses. Circulation 1984; 69: 111–119.
30. Klocke FJ. Measurements of coronary flow reserve: defining pathophysiology versus making decisions about patient care. Circulation 1987; 76: 245–253.
31. McGinn Al, White CW, Wilson RF. Interstudy variability of coronary flow reserve: influence of heart rate, arterial pressure and ventricular preload. Circulation 1990; 81: 1319–1330.
32. Serruys PW, Di Mario C, Meneveau N, de Jaegere P, Strikwerda S, de Feyter PJ, Emanuelsson H. Intracoronary pressure and flow velocity from sensor tip guidewires. A new methodological comprehensive approach for the assessment of coronary hemodynamics before and after interventions. Am J Cardiol 1993; 71: 41D–53D.
33. Wilson RF, Johnson MR, Marcus ML, Aylward PEG, Skorton DJ, Collins S, White CW. The effect of coronary angioplasty on coronary blood flow reserve. Circulation 1988; 71: 873–885.
34. Kern MJ, Deligonul U, Vandormael M, Labovitz A, Gudipati CV, Gabliani G, Bodet J, Shah Y, Kennedy HL. Impaired coronary vasodilator reserve in the immediate postcoronary angioplasty period: analysis of coronary artery flow velocity indexes and regional cardiac venous efflux. J Am Coll Cardiol 1989; 13: 860–872.
35. Segal J, Kern MJ, Scott NA, King SB, Doucette JW, Heuser RR, Ofili E, Siegel R. Alterations of phasic coronary artery flow velocity in humans during percutaneous coronary angioplasty. J Am Coll Cardiol 1992; 20: 276–286.
36. Ofili EO, Kern MJ, Labovitz AJ, Vrain J, Segal J, Aguirre FV, Castello R. Analysis of coronary blood flow velocity dynamics in angiographically normal and stenosed arteries before and after endolumen enlargment by angioplasty. J Am Coll Cardiol 1993; 21: 308–316.
37. Serruys PW, Juilliere Y, Zijlstra F, Beatt KJ, De Feyter PJ, Suryapranata H, van den Brand M, Roelandt J. Coronary blood flow velocity during percutaneous transluminal coronary angioplasty as a guide for assessment of the functional result. Am J Cardiol 1988; 61: 253–259.

38. Grüntzig AR, Senning A, Siegenthaler WE. Nonoperative dilatation of coronary-artery stenosis: percutaneous transluminal coronary angioplasty. N Engl J Med 1979; 301: 61–68.
39. Serruys PW, Wijns W, Reiber JHC, de Feyter PJ, van den Brand M, Piscione F, Hugenholtz PG. Values and limitations of transstenotic pressure gradients measured during percutaneous coronary angioplasty. Herz 1985; 10: 337–342.
40. Leiboff R, Bren G, Katz R, Korhegi R, Katzen B, Ross A. Determinants of transstenotic gradients observed during angioplasty: an experimental model. Am J Cardiol 1983; 52: 1311–1317.
41. Leimgruber PP, Roubin GS, Hollman J. Restenosis after successful coronary angioplasty in patients with single vessel disease. Circulation 1986; 73: 710–717.
42. Emanuelsson H, Lamm C, Di Mario C, Serruys PW. Measurements of coronary artery pressure and stenosis gradients. Clinical applications and comparison with quantitative angiography. In: Serruys PW, Foley DL, de Feyter PJ (editors) QCA in clinical practice, Kluwer Academic Publishers, Dordrecht, 1993 (in press).
43. Walinsky P, Santamore WP, Wiener L. Dynamic changes in the hemodynamic severity of a coronary arterial stenosis in a canine model. Cardiovasc Res 1979; 13: 113–118.
44. Mancini GBJ, Mc Gillem MJ, DeBoe SF, Gallagher KP. The diastolic hyperemic flow vs pressure relation: a new index of coronary stenosis severity and flow reserve. Circulation 1989; 80: 941–950.
45. Mancini GBJ, Cleary RM, DeBoe SF, et al. Instantaneous hyperemic flow-vs-pressure slope index. Microsphere validation of an alternative to masures of coronary flow reserve. Circulation 1991; 84: 862–870.
46. Cleary RM, Aron D, Moore NB, DeBoe SF, Mancini GBJ. Tachycardia, contractility and volume loading alter conventional indexes of coronary flow reserve, but nog the instantenous hyperemic flow versus pressure slope index. J Am Coll Cardiol 1992; 20: 1261–1269.
47. Di Mario C, Meneveau N, De Feyter P, Gil R, Serruys PW. Assessment of the pressure-flow velocity relation using an intracoronary Doppler guidewire (abstr). J Am Coll Cardiol 1993; 21: 348A.
48. Pijls N, Kirkeeide RL, Gould KL et al. Quantitation of relative coronary flow reserve and collateral flow by pressure measurements duting maximal hyperemia: a rapid accurate method for assessing functional stenosis severity at PTCA. Circulation 1993; 86: 1354–61.
49. Seiler C, Kirkeeise RL, Gould KL. Basic structure-function relations of the epicardial coronary vascular tree. Circulation 1992; 85: 1987–2001.
50. Gould KL. Interactions with the distal coronary vascular bed. In: Gould KL (editor) Coronary artery stenosis. Elsevier, New York-Amsterdam-London, 1991; 31–39.
51. De Bruyne B, Pijls NHJ, Paulus WJ, van Trimpont PJ, Sys SU, Heyndrickx GR. Transstenotic coronary pressure gradient measurement in man: in vitro and in vivo evaluation of a new pressure monitoring PTCA guide-wire. J Am Coll Cardiol 1993; 22: 119–26.

CHAPTER 12

INTRACORONARY PRESSURE AND FLOW VELOCITY WITH SENSOR-TIP GUIDEWIRES. A NEW METHODOLOGIC APPROACH FOR ASSESSMENT OF CORONARY HEMODYNAMICS BEFORE AND AFTER CORONARY INTERVENTIONS

Patrick W. Serruys, M.D., Ph.D., Carlo Di Mario, M.D., Nicolas Meneveau, M.D., Peter de Jaegere, M.D., Ph.D., Sipke Strikwerda, M.D., Ph.D., Pim J. de Feyter, M.D., Ph.D., Håkan Emanuelsson, M.D., Ph.D.*

From the Cardiac Catheterization Laboratory, Division of Cardiology, Thoraxcenter, Erasmus University, Rotterdam

Reprinted from: Am J Cardiol, 1993.

Intracoronary Pressure and Flow Velocity with Sensor-Tip Guidewires: A New Methodologic Approach for Assessment of Coronary Hemodynamics Before and After Coronary Interventions

Patrick W. Serruys, MD, PhD, Carlo Di Mario, MD, Nicolas Meneveau, MD, Peter de Jaegere, MD, Sipke Strikwerda, MD, PhD, Pim J. de Feyter, MD, PhD, and Håkan Emanuelsson, MD, PhD

The use of miniaturized pressure and velocity sensors mounted on angioplasty guidewires allows the simultaneous measurement of coronary blood flow velocity and transstenotic pressure gradient, 2 parameters that, combined, should perfectly characterize stenosis hemodynamics. The aim of this article is assessment of the changes in coronary blood flow velocity observed with a Doppler-tipped angioplasty guidewire in 35 patients undergoing balloon angioplasty. We also report our initial experience in 16 patients with the combined use of sensor-tip pressure and Doppler guidewires, and we discuss the application of new methodologic approaches for the study of the coronary circulation allowed by these techniques, such as the instantaneous assessment of the flow velocity/pressure and pressure gradient/flow velocity relations. Before and after angioplasty, flow velocity measurements were obtained distal to the stenosis, both in baseline conditions and after intracoronary injection of 8–12.5 mg of papaverine. The Doppler guidewire was left in place during the dilation procedure and the Doppler signal was continuously recorded during balloon inflation and after deflation to monitor the development of collateral flow, the restoration of flow after balloon deflation, the phase of postocclusive reactive hyperemia, and, incidently, the development of flow-limiting complications. Merits and pitfalls of several flow velocity parameters (average peak velocity, coronary flow velocity reserve, diastolic/systolic velocity ratio), as well as of parameters derived from the combination of pressure and velocity measurements (transstenotic pressure gradient/flow velocity relation and instantaneous diastolic hyperemic flow velocity/pressure relation) were evaluated in 35 patients with, and 37 without, significant coronary stenoses. Miniaturization of flow velocity and pressure sensors has made these methodologic approaches applicable in the interventional suite, yielding reproducible and accurate assessments of parameters previously measured only in experimental animal models.

(Am J Cardiol 1993;71:41D–53D)

Since the advent of coronary angioplasty, assessment of the acute results of interventions has been a source of debate and discussion. Several methodologic approaches have been considered and explored in the past.[1] Andreas Grüntzig, the inventor of the technique, made use of the transstenotic pressure gradient to guide the progression of the balloon catheter in the coronary tree beyond the targeted stenotic lesion and to demonstrate the severity of the stenosis.[2] Following dilation, the transstenotic gradient was used to assess the hemodynamic change brought about by the dilating process, but no attempt in those early days was made to assess the pressure drop across the lesion during hyperemia. Subsequently, pressure recording was progressively disregarded because it was demonstrated that the measurement was not always reliable.[3]

The physiologic value of these measurements, even those obtained with the smallest catheters, must be questioned, since the catheter impedes flow by its presence. Experimental data obtained in

From the Cardiac Catheterization Laboratory, Division of Cardiology, Thoraxcenter, Erasmus University, Rotterdam, The Netherlands, and Department of Cardiology, Sahlgrenska Hospital of Göteborg, Sweden (H.E.).

Address for reprints: Patrick Serruys, MD, PhD, Cardiac Catheterization Laboratory, Division of Cardiology, Thoraxcenter, Ee 2332, Erasmus University, P.O. Box 1738, 3000 DR Rotterdam, The Netherlands.

dog femoral arteries suggest that the "true" stenosis gradient is overestimated in a predictable manner, dependent on the ratio of the catheter diameter over the stenosis diameter.[4] In addition, further miniaturization of the balloon catheter and introduction of the movable guidewire and of the monorail technique soon rendered measurement of pressure gradient less applicable.

In recent years, major efforts were made to obtain accurate measurements of the lumen area of the stenotic lesion, before and after coronary angioplasty, using quantitative angiography with computer-based automatic edge detection.[5] However, for the evaluation of the angioplasty results, this technique has inherent limitations. The disruption of the internal wall of the vessel following the barotrauma of angioplasty cannot be easily delineated by contour detection of the shadowgram obtained with coronary angiography.[6] Videodensitometry was a possible promising alternative, but this method did not fulfill the expectations and critical methodologic problems remained unresolved.[7,8] These limitations have prompted investigators to use blood flow measurement for the functional assessment of angioplasty results. Various digital angiographic techniques and Doppler catheters were introduced and tested.[9–12] The recent miniaturization of pressure and velocity sensors[13,14] has allowed the simultaneous measurement of intracoronary flow velocity and transstenotic pressure gradient, the 2 parameters that characterize the stenosis hemodynamics.

In this article we report the results obtained in 35 patients with a Doppler guidewire during coronary interventions, as well as our initial experience in 16 patients with the combined use of sensor-tip pressure and Doppler guidewires. New methodologic approaches allowed by these techniques include the instantaneous assessment of the flow velocity/pressure and pressure gradient/flow velocity relations.

METHODS

Doppler guidewire during coronary interventions: In 35 patients (31 men, 4 women, mean age 57 ± 10 years) undergoing coronary angioplasty because of symptomatic coronary artery disease, a Doppler angioplasty guidewire was used. Patients who had acute myocardial infarction, arterial occlusion or subocclusion (Thrombolysis in Myocardial Infarction [TIMI] flow class 0–1), valvular heart disease, extreme tortuosity of the vessel to be dilated, and the presence of an open aortocoronary bypass graft on the vessel to be treated were not included for study. Systemic arterial hypertension was present in 9 cases (26%). Seven patients (20%) had a previous myocardial infarction in the territory of distribution of the dilated vessel (Q wave in 2 patients, nontransmural in 5 patients). Antianginal treatment, including in 21 patients (60%) β-adrenergic blocking agents, calcium antagonists, long-acting nitrates, or a combination of these 3 drugs, was not withheld. In 1 patient the Doppler guidewire was used for a 2-vessel angioplasty procedure. The left anterior descending artery was the treated artery in 20 cases (56%), the left circumflex in 4 cases (11%), and the right coronary artery in 8 cases (22%). Four stenoses of a saphenous vein bypass graft were treated using the Doppler guidewire as the angioplasty guidewire (11%).

Catheterization procedure: After intravenous administration of 10,000 IU of heparin and 250 mg of acetylsalicylic acid, an 8 F guiding catheter was advanced up to the coronary ostium. After isosorbide dinitrate (2–3 mg intracoronary), cineangiograms suitable for quantitative assessment were obtained in 1–3 angiographic views.

The Doppler guidewire was advanced into the artery to be dilated and a flow velocity recording was obtained distal to the stenosis, both in baseline conditions and after intracoronary bolus injection of papaverine (8 mg, right coronary; 12.5 mg, left coronary, saphenous vein bypass graft).[15] Intracoronary nitrates were used before the injection of papaverine in order to induce a maximal coronary vasodilation and avoid changes in cross-sectional area between baseline and post-papaverine assessment.[16] Care was taken to avoid the presence of impairment of flow during maximal hyperemia due to the presence of the guiding catheter in the coronary ostium. If damping occurred (Figure 1), the guiding catheter was withdrawn from the coronary ostium immediately after the injection of papaverine. An appropriately sized balloon catheter (2–4 mm) was then introduced, using a monorail technique in most cases. The Doppler guidewire was left in place distal to the lesion during the dilation procedure. The Doppler signal was continuously acquired during balloon inflation and after deflation to monitor the development of collateral flow, the restoration of flow after balloon deflation, the phase of postocclusive reactive hyperemia, and, incidently, the development of flow-limiting complications. Immediately after the end of the inflation, the balloon was withdrawn in the guiding catheter in order to avoid the residual obstruction of flow due to the presence of the deflated balloon across

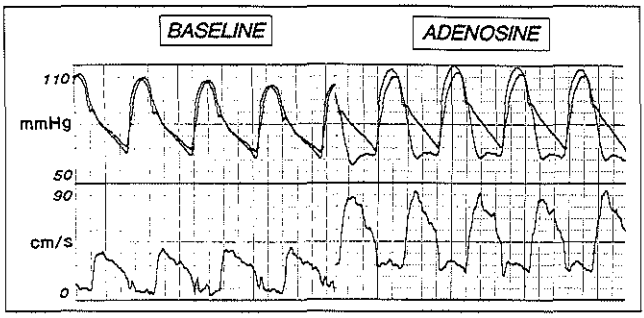

FIGURE 1. ***Top,*** **simultaneous recordings of the pressure in the ascending aorta (tip manometry) and of the aortic pressure recorded with a fluid-filled 8 F guiding catheter at the ostium of the left coronary artery. At baseline the 2 tracings are superimposed, indicating that the voluminous guiding catheter does not impede the flow in the main stem. The intracoronary administration of 18 μg of adenosine induces the development of a pressure gradient between aorta and left main coronary artery, generated by the presence of the guiding catheter. Note the ventricularization of the proximal coronary pressure.** ***Bottom,*** **the simultaneous changes in flow velocity are recorded using a Doppler guidewire positioned in the proximal left anterior descending artery.**

the lesion. When the dilation was judged successful (angiographic percent diameter stenosis <50%), new baseline and post-papaverine flow velocity measurements were obtained distal and proximal to the lesion, taking care that flow velocity measurements were repeated in the same positions as before angioplasty.

Doppler guidewire and flow velocity measurements: The Doppler angioplasty guidewire, a 0.018-in (diameter = 0.46 mm), 175-cm long flexible and steerable guidewire with a floppy shapable distal end mounting a 12 MHz piezoelectric transducer at the tip (Flowire; Cardiometrics, Mountain View, CA), has been described previously.[17] The flow velocity measurements obtained with this system have been validated in vitro and in an animal model using simultaneous electromagnetic flow measurements for comparison.[17] The Doppler system performs a real-time spectral analysis of the Doppler signal[18] and calculates and displays on-line several spectral variables, including the instantaneous peak velocity and the time-averaged (mean of 2 beats) peak velocity. The time-averaged systolic and diastolic flow velocity components were analyzed off-line based on the flow pattern and on the simultaneous recordings of electrocardiogram and aortic pressure (Figure 2). Coronary flow reserve was defined as the ratio between maximal flow velocity at the peak effect of the papaverine injection and in baseline conditions.

Quantitative angiographic measurements: The guiding catheter, filmed without contrast medium, was used as a scaling device.[19] A previously validated on-line analysis system operating on digital images (ACA-DCI; Philips, Eindhoven, The Netherlands[20]; n = 24) and a cinefilm-based off-line system (CAAS System; Pie Medical Data, Maastricht, The Netherlands[21]; n = 11) were used. After automatic detection of the vessel centerline, a weighted first and second derivative function with predetermined continuity constraints was applied to the brightness profile on each scan line perpendicular to the vessel centerline.[22] From the measured minimal luminal diameter (MLD), the minimal luminal cross-sectional area was calculated, assuming a circular cross-section (average of the measurements if multiple views were acquired). An interpolated technique was used to define the reference diameter. Percent diameter and cross-sectional area stenosis were also calculated. A user-defined reference diameter was measured at the site of the Doppler sample volume in order to detect changes of the position of the transducer before and after angioplasty and to calculate the maximal and mean coronary flow.[18,23]

Combination with transstenotic pressure measurements: A total of 16 patients undergoing

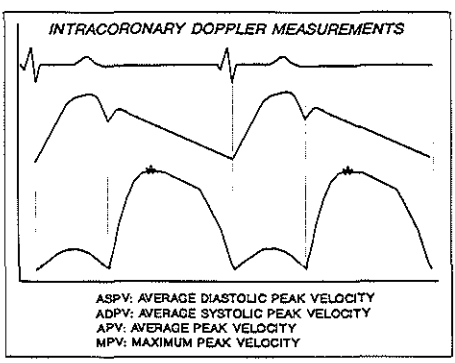

FIGURE 2. Diagram of a simultaneous recording of electrocardiogram, aortic pressure, and flow velocity. The systolic and diastolic phases of the cardiac cycle are identified by vertical bars on the diagram. The R wave of the electrocardiogram and the dicrotic notch of the aortic pressure serve as landmarks of the systolic and diastolic phases. The asterisks indicate the maximum peak flow velocity.

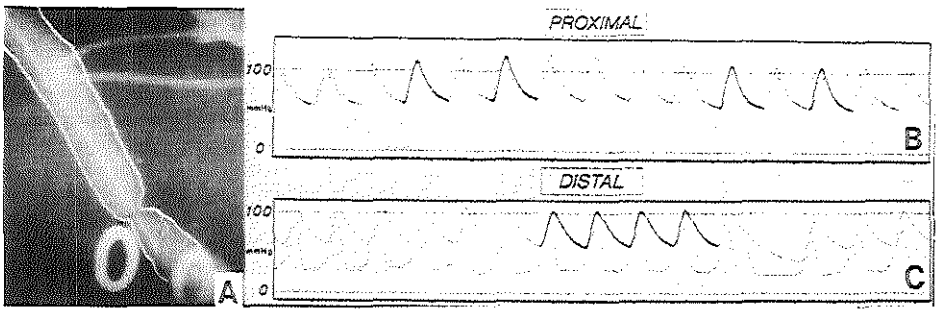

FIGURE 3. *A*, cineangiogram of a saphenous vein bypass graft; automatic edge detection of the contours delineates the stenotic lesion while the radiopaque structure of the pressure guidewire (diameter: 0.46 mm) is seen inside the lumen of the vessel. *B*, pressure recording with the pressure sensor located immediately proximal to the stenotic lesion. Note the almost complete superimposition of the 2 pressure curves. *C*, a significant transstenotic gradient is recorded with the sensor advanced distal to the stenotic lesion.

elective coronary angioplasty (n = 9) or scheduled for a possible angioplasty procedure but with a stenosis angiographically of intermediate severity (>40% and <60% diameter stenosis; n = 7) were studied with a simultaneous measurement of flow velocity and poststenotic coronary pressure. The measurements were obtained in baseline conditions and after papaverine using the Doppler guidewire positioned *proximal* to the stenosis and a fiberoptic pressure microsensor advanced *distal* to the stenosis. This pressure sensor is incorporated in the flexible distal segment of a 0.018-in guidewire (diameter 0.45 mm, cross-sectional area 0.17 mm^2; Radi Medical Systems, Uppsala, Sweden). This system has already been validated in vitro with regard to signal transfer characteristics, linearity, and frequency response.[13] The pressure signal was calibrated immediately before insertion and the accuracy of the measurement was checked by superimposing the prestenotic coronary pressure measured with the pressure guidewire and the proximal coronary pressure measured with the guiding catheter (Figure 3). A correction of a 5/15 mm Hg drift of the 0 pressure was necessary in 4 cases (25%). The mean transstenotic gradient was calculated as the difference of mean proximal and mean distal coronary pressure over 8 consecutive beats in baseline conditions and at peak papaverine effect (Figure 4). In order to facilitate the comparison of patients with different hemodynamic characteristics at the time of the study, the transstenotic pressure gradient was normalized for the corresponding coronary proximal pressure. The coronary flow measurements derived from the quantitative angiographic and Doppler measurements were used to calculate a flow/gradient index, defined as the ratio between the difference of the peak papaverine and baseline measurements of coronary flow and transstenotic gradient.

Instantaneous assessment of the flow velocity/pressure relation: Feasibility and reproducibility of the assessment of the relationship between coronary blood flow velocity and aortic pressure were evaluated in 31 patients with significant coronary artery disease in a nontreated coronary artery without diameter stenosis >30% and in 6

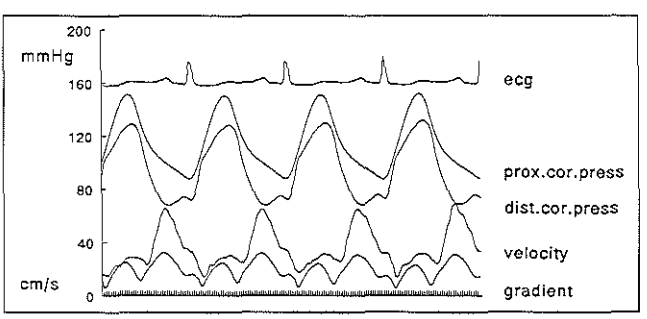

FIGURE 4. From top to bottom: electrocardiogram (ecg), proximal coronary pressure (prox. cor. press) recorded through the guiding catheter (mm Hg), distal coronary pressure (dist. cor. press) recorded with a tip-mounted pressure guidewire (mm Hg), coronary flow velocity recorded with a Doppler guidewire (cm/sec), and transstenotic pressure gradient (mm Hg). Note that the systolic/diastolic changes in flow velocity correspond to the phasic variations of the transstenotic gradient, with the maximal velocity and gradient in proto-mid-diastole.

patients (8 angiographically normal arteries) 1–5 years after cardiac transplantation. The measurement was performed in a proximal–middle segment of the studied artery (left anterior descending in 18 cases [46%], left circumflex in 9 [23%], right coronary artery in 12 [31%] cases) in baseline condition and after papaverine-induced hyperemia. The proximal coronary pressure, measured through the guiding catheter, and the instantaneous peak velocity were continuously acquired using a 12-bit analog-to-digital converter at a sampling frequency of 125 Hz (Data-Q Instruments, Akron, OH). Linear regression analysis was used to assess the slope of the velocity/pressure relation ($cm \cdot s^{-1} \cdot mm\ Hg^{-1}$) in 4 consecutive cardiac cycles during maximal coronary vasodilation. The analyzed mid-to-late diastolic intervals were defined using as start- and endpoints the maximal diastolic peak velocity and the acceleration of the slope of the velocity decrease induced by the myocardial contraction (Figure 5). In 6 cardiac transplant recipients left ventricular and aortic high fidelity pressures were measured simultaneously using a double-sensor pigtail catheter (Sentron, Roden, The Netherlands). In these cases the analysis was performed using the digitized pressure and flow velocity data obtained in the time interval originally proposed by Mancini et al[24,25] (20 msec after the peak negative left ventricular *dP/dt*-upstroke of the positive left ventricular *dP/dt*). In the 8 arteries studied in cardiac transplant recipients a bolus of 3 mg of adenosine was also rapidly injected intracoronary during the maximal papaverine effect so that the velocity/pressure relation could be studied also during a series of long diastolic pauses (up to 11 seconds). Right ventricular pacing was used to restore a normal cardiac contraction when necessary.

Statistical analysis: The differences between flow velocity measurements and derived indexes before and after angioplasty were compared using a paired Student's *t* test. The differences between diastolic/systolic flow velocity ratio in the angioplasty patients and in the control group without significant coronary stenosis of the studied vessel were compared using an unpaired Student's *t* test. The beat-to-beat variability of the slope of the velocity/pressure relation was defined as the ratio between the standard deviation and the average of the slopes measured over 4 consecutive cardiac cycles. In the 8 arteries of cardiac transplant recipients studied during a normal sinus beat and during pharmacologically induced cardiac arrest, the difference between the slopes of the velocity/pressure relation in normal cardiac cycles and prolonged diastolic pauses was compared using a

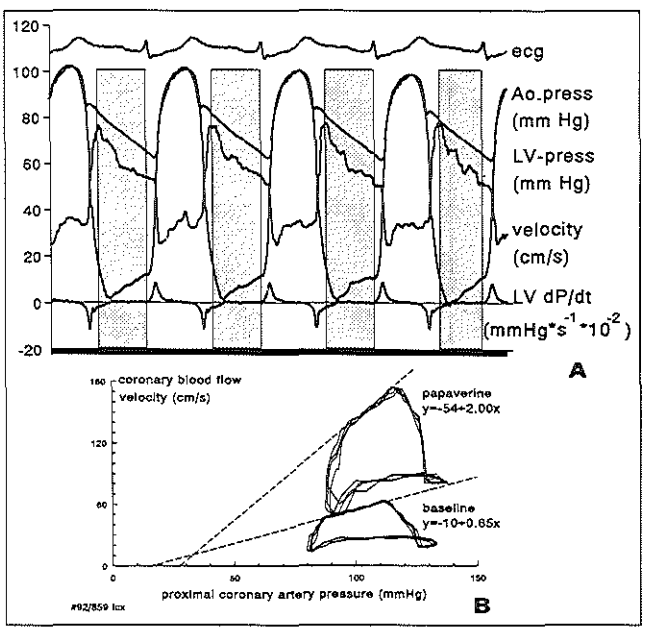

FIGURE 5. ***A*, from top to bottom: electrocardiogram (ecg), aortic pressure (Ao. press; tip manometry), left ventricular pressure (LV-press; tip manometry), coronary blood flow velocity (Doppler guidewire), and first derivative of the left ventricular pressure (*dP/dt*). The *dotted areas* indicate the intervals used for the analysis of the pressure/flow velocity relation from the digitized pressure and flow velocity (starting point, 20 msec after peak negative *dP/dt*, endpoint: left ventricular end-diastolic pressure/upstroke of the positive left ventricular *dP/dt*). *B*, Velocity/pressure loops of 4 consecutive cardiac cycles superimposed (clockwise rotation) in baseline conditions and at the peak effect of papaverine. The regression lines calculated in the mid–late diastolic phases are displayed and extrapolated up to the zero-flow pressure.**

nonparametric (Wilcoxon) test. Statistical significance was defined as $p < 0.05$. All data were expressed as mean ± SD.

RESULTS

Monitoring of the angioplasty procedure with the Doppler guidewire: The angioplasty guidewire was successfully used to cross the stenosis in 32 of 36 arteries (89%). Stable Doppler recordings distal to the lesion were acquired in all these cases. During balloon inflation, a complete disappearance of flow was observed in 26 arteries (81%). In the remaining 6 cases (19%) the flow velocity progressively increased during inflation (in 5 cases with inverted flow velocity signal), presumably indicating recruitment of collateral coronary flow. The restoration of anterograde flow could be immediately detected during the deflation of the balloon, before the disappearance of the electrocardiographic changes or of the symptoms. In 3 cases (9%) a sudden decrease of blood flow velocity was the first warning signal of the development of a flow-limiting wall dissection after angioplasty (Figure 6). Two of these cases were successfully treated with stent implantation and 1 patient required emergency bypass surgery. Coronary angioplasty was judged angiographically successful in all the 29 remaining cases. Minimal luminal diameter increased from 1.02 ± 0.72 mm before coronary angioplasty to 2.12 ± 1.69 mm after angioplasty ($p < 0.001$). Minimal luminal cross-sectional area stenosis increased after percutaneous transluminal coronary angioplasty (PTCA) from 0.84 ± 0.41 to 3.45 ± 2.25 mm^2 ($p < 0.001$). Percent cross-sectional area stenosis decreased from 80 ± 9% to 46 ± 19% after PTCA ($p < 0.001$).

Baseline and hyperemic average peak velocity changes after angioplasty: Baseline and post-papaverine flow velocity signals were obtained before and after dilation in 29 coronary arteries (81%; Figure 7). Baseline average peak velocity increased from 16 ± 9 to 27 ± 14 cm/sec post-PTCA ($p < 0.001$). A >2-fold increase was observed for the average peak velocity recorded at the maximal effect of papaverine (27 ± 17 and 60 ± 28 cm/sec before and after PTCA, respectively; $p < 0.001$). The cross-sectional area at the site of the Doppler recording showed a nonsignificant change before and after PTCA (from 6.08 ± 3.73 to 5.74 ± 3.68 mm^2, difference not significant), suggesting that the velocity changes reflect a true flow increase after PTCA in baseline and hyperemic conditions. Coronary flow reserve, as a ratio of the hyperemic/baseline flow velocity measurements, showed a moderate but significant increase after PTCA (from 1.75 ± 0.55 to

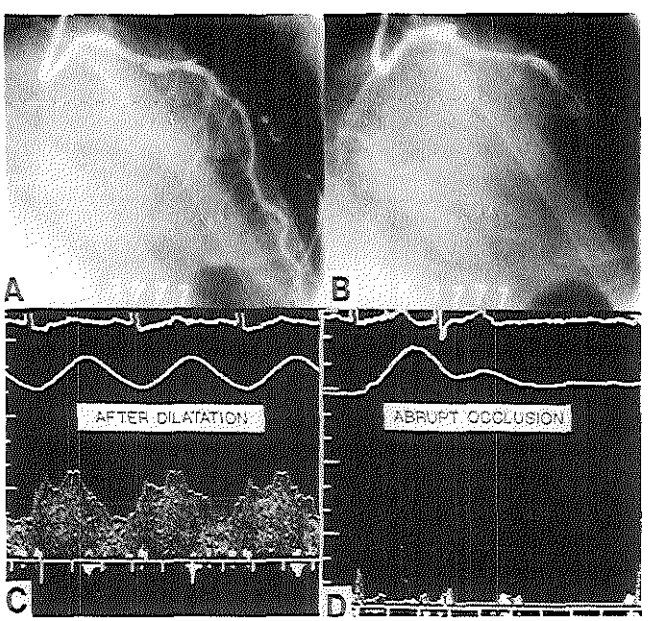

FIGURE 6. Coronary angiogram before *(A)* and after *(B)* abrupt occlusion following balloon dilation. The position of the Doppler guidewire is indicated by an arrow. *C*, simultaneous recordings of the flow velocity signals. *D*, the disappearance of the flow velocity signal consequent to the flow-limiting dissection, a warning signal preceding the electrocardiographic changes and the development of symptoms.

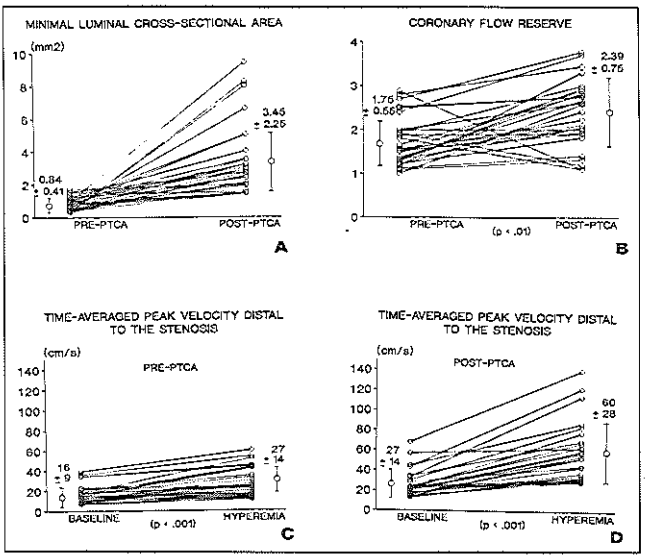

FIGURE 7. *A, B*, Individual changes in minimal luminal cross-sectional area *(A)* and coronary flow reserve *(B)* are shown before and after percutaneous transluminal coronary angioplasty (PTCA). Individual changes in time-averaged peak velocity distal to the stenosis PTCA *(C)* and post-PTCA *(D)*. Both the baseline and the maximal hyperemic flow velocity showed a significant increase post-PTCA ($p < 0.001$).

2.39 ± 0.75; $p < 0.005$). Comparable flow velocity increases were observed after PTCA at the peak effect of the papaverine injection and in the phase of the maximal reactive hyperemia recorded following balloon dilation in 14 patients (45 ± 22 cm/sec peak reactive hyperemia vs 47 ± 20 cm/sec after papaverine, difference not significant). Figure 8 illustrates the relation observed between minimal luminal diameter, before and after PTCA, and maximal hyperemic flow velocity.

Changes in the diastolic/systolic flow velocity ratio after angioplasty: The ratio between mean diastolic and mean systolic flow velocity measured in baseline conditions distal to the stenosis was 1.51 ± 0.58 before PTCA, significantly lower than the ratio measured in the 39 normal or near-normal arteries (2.09 ± 0.90; $p < 0.001$). After angioplasty, the diastolic/systolic flow velocity ratio increased from 1.51 ± 0.58 to 2.16 ± 0.98 ($p < 0.001$) and did not differ from the control group.

Flow velocity/transstenotic pressure gradient measurements: The quantitative angiographic, flow velocity, and pressure measurements of the 16 patients studied with the combined use of Doppler and pressure guidewires are reported in Table I. The maximal (post-papaverine) transstenotic pressure gradient showed a significant inverse correlation with the minimal luminal cross-sectional area ($y = -8.4x + 45$; $r = -0.62$; $p < 0.01$). Coronary flow reserve had only a borderline significant correlation with the minimal cross-sectional area ($y = 0.36x + 1.55$; $r = 0.46$; $p < 0.1$). A parameter derived from the integration of flow and pressure gradient changes from baseline to hyperemia (flow/gradient index) showed a more strict correlation with the minimal cross-sectional area ($y = 5.6x + 0.6$; $r = 0.70$; $p < 0.002$). In particular, a flow/gradient index <3 mL/min/mm Hg was able to identify 10 of 14 cases with a minimal cross-sectional area <1.5 mm^2 (Figure 9B). When the normalized transstenotic gradients were plotted against the coronary flow reserve (Figure 9A),

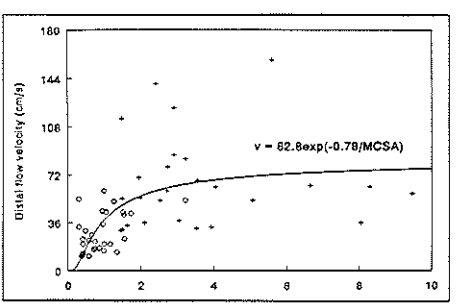

FIGURE 8. Relation between minimal cross-sectional area (MCSA, mm^2) and hyperemic distal flow velocity. The data points obtained before and after percutaneous transluminal coronary angioplasty are indicated with open circles and crosses, respectively. A curvilinear relation was observed between these 2 parameters, with a plateau above the value of cross-sectional area of 2.5 mm^2.

TABLE I Clinical and Hemodynamic Characteristics of the Patients Studied by a Simultaneous Recording of Transstenotic Pressure Gradient and Flow Velocity

Pt	Age (yr)	Sex	MI	Vessel	MLCSA (mm^2)	CSA (%)	BAPV (cm/sec)	HAPV (cm/sec)	CFR	BAS Grad (mm Hg)	HYP Grad (mm Hg)	Norm BASG (%)	Norm HYPG (%)	BAS Flow (mL/min)	HYP Flow (mL/min)	ΔFlow/Δ Grad (mL/min/mm Hg)
WA	60	M	No	RCA	0.49	0.92	10	27	2.70	21	43	23	51	20	53	1.53
BJL	73	M	No	SVBG	0.21	0.98	7	11	1.57	42	46	53	58	20	31	2.85
FB	70	F	No	RCA	2.26	0.74	31	62	2.00	4	17	3	15	84	167	6.44
BKJ	59	M	No	RCA	0.82	0.95	10	15	1.50	12	35	14	41	50	74	1.08
BJ	62	M	No	LAD	0.78	0.87	34	45	1.32	38	46	43	47	65	86	2.61
RTR	69	M	No	RCA	0.33	0.97	8	11	1.37	38	39	46	49	24	33	9.00
SA	73	M	No	SVBG	4.78	0.68	18	56	3.11	5	11	6	14	81	252	28.50
WC	59	M	No	LAD	1.14	0.84	19	83	4.37	5	14	6	19	41	181	15.53
BJ	55	M	No	LAD	1.1	0.86	66	141	2.14	5	18	5	19	157	336	13.74
DHTA	80	M	Yes	RCA	0.30	0.97	8	10	1.25	44	49	49	57	23	28	1.13
SEA	74	M	No	RCA	0.23	0.95	11	12	1.09	49	50	52	54	17	18	1.60
OMV	81	F	No	RCA	1.39	0.85	48	131	2.73	28	37	28	39	132	361	25.39
EC	57	M	Non Q	RCA	0.80	0.92	30	45	1.50	15	42	13	39	97	146	1.80
BW	67	M	Yes	SVBG	1.16	0.87	8	11	1.37	35	39	42	45	21	29	1.99
JB	63	F	Yes	RCA	1.00	0.82	13	20	1.54	13	29	13	29	23	35	0.77
LTW	50	M	No	LAD	1.19	0.71	21	39	1.86	28	65	28	63	33	56	2.05
Mean	66				1.12	0.87	21	45	1.96	23	36	27	40	55	118	7.24
± SD	9				1.07	0.09	16	40	0.84	15	14	18	16	42	109	8.67

BAPV = baseline time-averaged peak blood flow velocity; BAS = baseline; CSA = cross-sectional area; CFR = coronary flow reserve; ΔFLOW/ΔGRAD = (hyperemic flow—baseline flow)/(hyperemic gradient—baseline gradient); HAPV = hyperemic time-averaged peak blood flow velocity; HYP = hyperemic; LAD = left anterior descending; MI = myocardial infarction; MLCSA = minimal luminal cross-sectional area; NORM BASG = normalized baseline gradient; NORM HYPG = normalized hyperemic gradient; RCA = right coronary artery; SVBG = saphenous vein bypass graft.

3 subgroups of patients were identified. At one extreme, the presence of large transstenotic gradients in baseline conditions and during hyperemia (>40% of the corresponding aortic pressure), associated with a minimal increase of flow during hyperemia (<2 times baseline), identified the most severe stenoses. At the other extreme, normalized hyperemic transstenotic pressure gradients <20% with an increase of 2–4 times the baseline flow after papaverine characterized a group with non-flow-limiting lesions. The intermediate group of hemodynamically significant stenoses exhibited variable pressure gradient/flow responses. Coronary flow reserve and maximal (post-papaverine) transstenotic pressure gradient showed a significant inverse correlation ($p < 0.02$; $r = -0.56$).

Instantaneous assessment of the hyperemic flow velocity/coronary pressure relation: A clear Doppler envelope allowing a reliable automatic detection of the hyperemic diastolic peak velocity during 4 consecutive beats was obtained in 31 of 39 cases (79%). The slope of the regression line was 1.86 ± 0.84 mm Hg $\cdot$ $cm^{-1} \cdot s^{-1}$. Negative intercepts on the y-axis were calculated in 27 cases so that a positive pressure at zero flow was estimated in most cases, with a mean value of 34 ± 16 mm Hg. The applicability of linear regression analysis to the study of the flow velocity/pressure relation in the range of measurements obtained during a diastolic interval of a normal cardiac cycle is confirmed by the high correlation coefficients observed ($r = 0.95 \pm 0.03$).

Table II reports the zero-flow pressure and the slope of the hyperemic diastolic flow velocity/pressure relation during sinus beats and during long diastolic pauses induced by the injection of adenosine in 8 angiographically normal arteries of cardiac transplant recipients. The lower slope and x-intercept of the long diastolic pauses as well as the shape of individual curves (Figure 10) suggest that the linearity of the pressure/flow velocity relation observed during normal sinus beats cannot be extrapolated over a larger range of pressures and flow velocity, and cannot be used for an accurate estimation of the zero-flow pressure.

DISCUSSION

Practical and theoretical concerns of using coronary flow reserve: Since the original work of Gould et al,[26] the assessment of coronary flow reserve has been viewed as a method of establishing indirectly the severity of a coronary stenosis. It is assumed that the reduction in flow reserve through the stenotic lesion would be an indicator of stenosis severity. In fact, this simple assumption is derived from the complex hemodynamic principles regulating the coronary circulation. In the schematic description by Klocke[27] (Figure 11A),

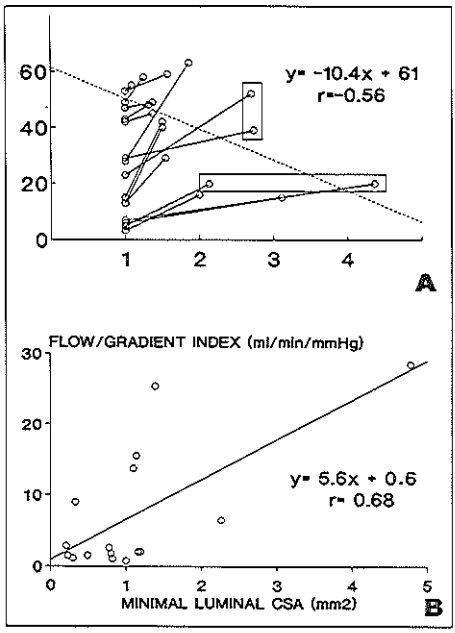

FIGURE 9. *A*, **relation between normalized transstenotic pressure gradient and coronary flow reserve as described in the text. Three subgroups of patients can be identified, each of them with specific pressure gradient flow response. The framed data points indicate either stenotic lesions having similar transstenotic gradients during hyperemia in the presence of different increases in flow reserve or stenotic lesions having similar increases in coronary flow reserve with different increases in transstenotic gradient during maximal hyperemia.** *B*, **relation between minimal cross-sectional area (CSA) and the flow/gradient index, defined as the ratio between the difference of the hyperemic versus baseline flow and the difference of the corresponding transstenotic pressure gradients. Transstenotic flow/gradient indexes of <10 mL/min/mm Hg identify the majority of the lesions with minimal cross-sectional area of <1.5 mm².**

flow reserve at a certain level of pressure is defined by the ratio between flow measured during maximal hyperemia and flow in baseline conditions. At rest, flow is independent of the driving pressure over a wide range of physiologic pressures (60–180 mm Hg), a phenomenon classically described as autoregulation of the coronary circulation. During maximal vasodilation, flow becomes linearly related to the driving pressure. The presence of a flow-limiting stenosis in a major epicardial vessel generates a pressure drop across the stenotic lesion, which is the result of viscous and turbulent resistances, so that the driving pressure distal to the stenosis decreases exponentially with the velocity of blood.[28]

TABLE II Instantaneous Hyperemic Diastolic Flow Velocity/Pressure Relation in Normal Sinus Beats Versus Prolonged Diastolic Pauses

	Sinus Beats	Pauses
Analyzed time interval (msec)	266 ± 187	1,852 ± 1,100
Minimal aortic pressure (mm Hg)	64 ± 4	38 ± 9
Minimal blood flow velocity (cm · sec⁻¹)	41 ± 14	14 ± 8
Zero-flow pressure (mm Hg)	38 ± 9	20 ± 9
Slope (cm · sec⁻¹ · mm Hg⁻¹)	1.9 ± 0.9	1.2 ± 0.6

The coronary flow reserve concept is mainly appealing to the clinician because it constitutes a functional surrogate to the anatomic description of the lesions located in the epicardial vessels, and many authors have shown that a decrease in flow reserve may discriminantly detect a lesion of increasing severity.[28,29] Although the concept may be easily and accurately applied in an optimal physiologic situation,[30,31] it must be recognized that coronary flow reserve is influenced by factors independent of the hydrodynamic characteristics of the stenotic lesion. Since flow reserve is by definition a ratio, similar ratios may be obtained at very different levels of resting and hyperemic flow. Changes in basal resting flow without changes in hyperemic flow will considerably affect the ratio so that knowledge of the absolute flow values is a prerequisite to the interpretation of a relative measurement such as coronary flow reserve. Any factors affecting the hyperemic pressure flow relation would likewise modify the flow reserve and thereby change the assessment of the severity of the coronary lesion under study. The hyperemic flow/pressure relation is influenced by factors such as heart rate,

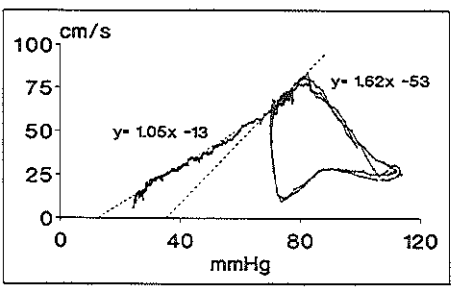

FIGURE 10. Flow velocity/pressure loops during maximal hyperemia in 3 consecutive sinus beats. During mid–late diastole, a linear relation is observed, with an extrapolated zero-flow pressure of 37 mm Hg. However, during a long diastolic pause (cardiac arrest induced by the intracoronary injection of 3 mg of adenosine), the pressure/flow velocity/pressure relation deviates considerably from the extrapolated curve.

preload, myocardial hypertrophy, or disease of the microvasculature.[27,32] Following coronary intervention, acute changes in resting blood flow together with changes in the anatomy of the stenotic lesion and concomitant persistent modifications of the hyperemic flow/pressure relation considerably hamper the clinical usefulness of coronary flow reserve for the assessment of the functional results. The aforementioned considerations are schematically illustrated in Figure 11. Our present results confirmed the observations made by other investigators,[9,11,12,33] namely that an increase in resting and hyperemic flow velocity occurs following angioplasty so that the usefulness of coronary flow reserve is limited in this clinical setting. Similar observations have been made by our group in the past, using Doppler tip balloon angioplasty catheters.[10]

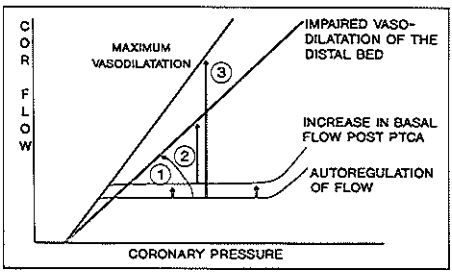

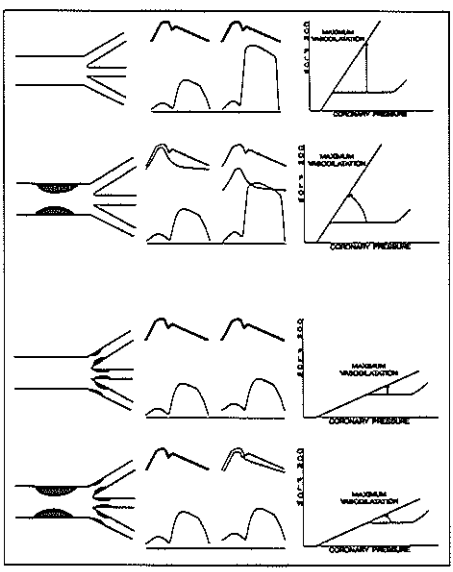

FIGURE 11. ***Upper part,*** **flow/pressure relation in resting and hyperemic conditions according to the description of Klocke.[37] Three confounding factors may obscure the interpretation of the change in coronary flow reserve following a PTCA procedure: (1) an increase in resting blood flow; (2) acute or chronic changes in the flow/pressure relation during hyperemia; (3) alteration of the severity of the stenotic lesion treated by balloon angioplasty.** ***Lower part,*** **from top to *bottom,* an example of normal epicardial artery with normal distal vascular response and of a significant epicardial stenosis inducing a pressure gradient in baseline and hyperemic conditions and an impaired coronary (COR) flow reserve. The presence of an abnormal distal vascular response (last 2 series of diagrams) minimizes the changes in the transstenotic pressure gradient and in maximal flow observed with and without an epicardial stenosis.**

Flow velocity/pressure relation: As previously demonstrated, the determination in absolute terms (cm/sec) of the maximal hyperemic velocity may be more indicative of the increase in coronary conductance achieved with balloon angioplasty. It must be realized, however, that the interpretation of this change in hyperemic response remains ambiguous, since the limiting factor to its increase may be either the persistence of a residual stenosis or an impaired distal vasodilatory response. The simultaneous measurement of a pressure gradient across a stenotic lesion may clarify the situation and indicate the reason why flow does not increase or increases abnormally (see algorithm in Figure 11B). Conversely, the sole measurement of the pressure gradient during hyperemia has also inherent limitations. The absence of a significant transstenotic gradient, for instance, may be related either to the absence of a flow-limiting stenosis or to the presence of a low flow across the stenosis due to either an impaired distal vasodilation or a well-developed collateral circulation.

A more accurate characterization of the severity of a stenotic lesion may be defined by the slope of the relation between mean gradient and coronary flow.[34] The slope of this relation is inversely correlated with the resistance of the stenotic lesion. However, this simplified assessment is only a limited estimation of the true physiologic phenomenon because mean gradient and flow velocities instead of instantaneous values are employed and because only 2 points (baseline and maximal hyperemia) are analyzed. A more complex but more complete and accurate analysis of the pressure gradient/flow velocity relation requires a continuous assessment of the instantaneous pressure gradient/flow velocity changes during the cardiac cycle in a beat-to-beat analysis.[34–36] The combined measurement of transstenotic gradient and flow velocity may provide a comprehensive interpretation of the fluid dynamics across the stenotic lesion, as well as of the myocardial capillary circulation. The

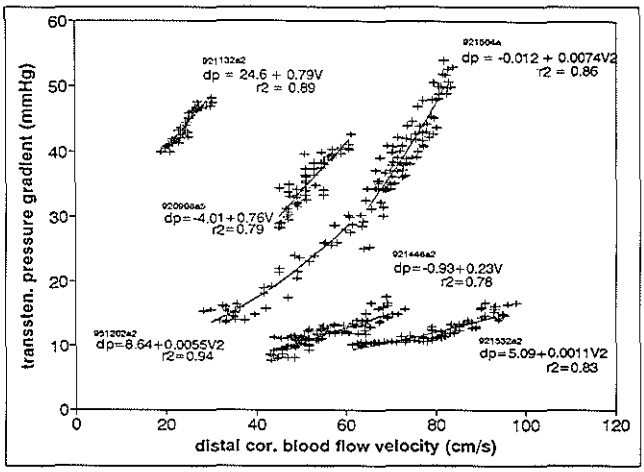

FIGURE 12. Instantaneous hyperemic diastolic pressure gradient/flow velocity relation for 6 stenoses of increasing hemodynamic severity (from *left* to *right* and from *bottom* to *top*). The corresponding best fit equation and curve are also indicated for each set of data. cor = coronary; transsten. = transstenotic.

simultaneous measurement of the instantaneous pressure gradient and flow velocity yields a unique relation that characterizes the hemodynamic properties of the stenosis (Figure 12). On the other hand, the instantaneous hyperemic flow velocity/driving pressure relation allows the analysis of the characteristics and functional integrity of the microcirculation, the other determinant of coronary flow resistance (Figure 13). A prerequisite for a widespread clinical application of these indexes is the assessment of the reproducibility and the identification of the normal and pathologic range in a large patient population.[35] Our preliminary results indicate that measurement of the slope of the flow velocity/pressure relation extrapolated from measurements obtained during normal sinus beats is feasible and reproducible. The slope measurement during a prolonged diastole, however, shows a curvilinear profile deviating substantially from the slope extrapolated during a normal cardiac cycle, an observation previously reported in the experimental literature.[37,38] The necessity to induce a short asystole to obtain a complete assessment of the instantaneous hyperemic flow velocity/pressure relation is a condition that may considerably hamper its clinical applicability. However, for practical purposes, the relation determined only in the physiologic range of pressure and flow velocity appears sufficient to characterize the conductance of the studied vessel.

Phasic alterations of flow velocity after interventions: An alternative approach to the assessment of the acute change after coronary intervention is measurement of the diastolic/systolic flow

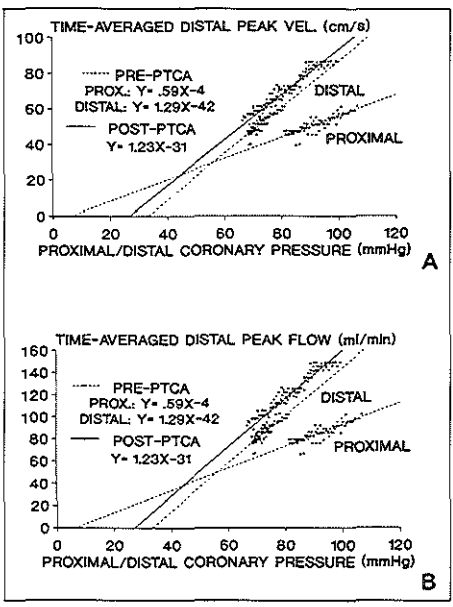

FIGURE 13. Instantaneous hyperemic diastolic flow velocity/pressure relation (*A*) and flow/pressure relation (*B*) before and after coronary angioplasty. The dashed lines indicate the relation observed before percutaneous transluminal coronary angioplasty (PTCA) using the proximal coronary pressure (*lower line*) and the true driving pressure (poststenotic coronary pressure measured with the pressure microsensor, *upper dashed line*). After PTCA (*continuous line*), despite the increase in flow velocity and the absence of transstenotic gradient, the slope of the instantaneous flow velocity/pressure relation was similar to the slope observed before PTCA (*upper dashed line*).

velocity ratio.[11] As previously reported,[12] a normalization of this index occurs in the minutes following a successful angioplasty. The physiologic explanation of this phenomenon remains controversial. The normalization of the diastolic/systolic flow velocity ratio after angioplasty may be intimately related to a rapid modification of the vasodilatory capacity of the capillary bed after angioplasty, possibly reflected by the slope of the instantaneous hyperemic flow velocity/pressure relation. Nevertheless, the clinical applicability of the diastolic/systolic flow velocity ratio, as an index capable of describing the results of coronary angioplasty in individual patients, requires a complete investigation of the factors that can modify this index independently of the stenosis severity (heart rate, contractility, type of studied vessel, etc.).

CONCLUSION

Miniaturization of flow velocity and pressure sensors with guidewire technology now permits the application in conscious humans of methodologic approaches previously limited to the experimental animal laboratory. The initial results based on the slope of the instantaneous hyperemic flow velocity/pressure relation and of the pressure gradient/velocity relation suggest that these techniques can yield a reproducible and accurate assessment of parameters that more precisely characterize the physiologic significance of coronary stenoses before and after interventions.

Acknowledgment: The contribution to the acquisition and analysis of the data of the medical, technical, and nursing staff of the Catheterization Laboratory and in particular of R. van den Perk, N. Bruining, and P. P. Kint is gratefully acknowledged. Dr. R. Gil, Dr. C. J. Slager, and Dr. R. Krams are also acknowledged for their contribution and suggestions in the analysis of the data.

REFERENCES

1. Serruys PW, Zijlstra F, Juilliere Y, de Feyter PJ, van den Brand M. How to assess the immediate results of PTCA. Should we use pressure gradient, flow reserve or minimal luminal cross-sectional area? In: Reiber JC, Serruys PW, eds. New developments in quantitative coronary arteriography. Dordrecht: Kluwer Academic Publishers, 1988;181–206.

2. Grüntzig AR, Senning A, Siegenthaler WE. Nonoperative dilatation of coronary-artery stenosis: percutaneous transluminal coronary angioplasty. *N Engl J Med* 1979;301:61–68.

3. Serruys PW, Wijns W, Reiber JHC, de Feyter PJ, van den Brand M, Piscione F, Hugenholtz PG. Values and limitations of transstenotic pressure gradients measured during percutaneous coronary angioplasty. *Herz* 1985;10:337–342.

4. Leiboff R, Bren G, Katz R, Korhegi R, Katzen B, Ross A. Determinants of transstenotic gradients observed during angioplasty: an experimental model. *Am J Cardiol* 1983;52:1311–1317.

5. De Cesare NB, Williamson PR, Moore NB, DeBoe SF, Mancini GBJ. Establishing comprehensive, quantitative criteria for detection of restenosis and remodelling after percutaneous transluminal coronary angioplasty. *Am J Cardiol* 1992;69:77–83.

6. Serruys PW, Foley DP, de Feyter PJ. Assessment of restenosis after coronary angioplasty: new comparative approaches based on quantitative angiography. *Br Heart J* 1992;68:417–424.

7. Serruys PW, Reiber JHC, Wijns W, van den Brand M, Kooijman CJ, Katen ten HJ, Hugenholtz PG. Assessment of percutaneous transluminal coronary angioplasty by quantitative coronary angiography: diameter versus densitometric area measurements. *Am J Cardiol* 1984;54:482–488.

8. Sanz ML, Mancini GBJ, Lefree MT, Mickelson JK, Starling MR, Vogel RA, Topol EJ. Variability of quantitative digital substraction coronary angiography before and after percutaneous transluminal coronary angioplasty. *Am J Cardiol* 1987;60:55–60.

9. Wilson RF, Johnson MR, Marcus ML, Aylward PEG, Skorton DJ, Collins S, White CW. The effect of coronary angioplasty on coronary blood flow reserve. *Circulation* 1988;71:873–885.

10. Serruys PW, Juilliere Y, Zijlstra F, Beatt KJ, De Feyter PJ, Suryapranata H, van den Brand M, Roelandt J. Coronary blood flow velocity during percutaneous transluminal coronary angioplasty as a guide for assessment of the functional result. *Am J Cardiol* 1988;61:253–259.

11. Kern MJ, Deligonul U, Vandormael M, Labovitz A, Gudipati CV, Gubliani G, Bodet J, Shah Y, Kennedy HL. Impaired coronary vasodilator reserve in the immediate postcoronary angioplasty period: analysis of coronary artery flow velocity indexes and regional cardiac venous efflux. *J Am Coll Cardiol* 1989;13:860–872.

12. Segal J, Kern MJ, Scott NA, King SB, Doucette JW, Heuser RR, Ofili E, Siegel R. Alterations of phasic coronary artery flow velocity in humans during percutaneous coronary angioplasty. *J Am Coll Cardiol* 1992;20:276–286.

13. Emanuelsson H, Dohnal M, Lamm C, Tenerz L. Initial experiences with a miniaturized pressure transducer during coronary angioplasty. *Cathet Cardiovasc Diagn* 1991;24:137–143.

14. Ofili E, Kern MJ, Tatineni S, Deligonul U, Aguirre F, Serota H, Labovitz AJ. Detection of coronary collateral flow by a Doppler-tipped guide wire during coronary angioplasty. *Am Heart J* 1991;222:221–225.

15. Zijlstra F, Serruys PW, Hugenholtz PG. Papaverine: the ideal coronary vasodilator for investigating coronary flow reserve? A study of timing, magnitude, reproducibility and safety of the coronary hyperemic response after intracoronary papaverine. *Cathet Cardiovasc Diagn* 1986;12:298–303.

16. Zijlstra F, Reiber JHC, Serruys PW. Does intracoronary papaverine dilate epicardial coronary arteries? Implications for the assessment of coronary flow reserve. *Cathet Cardiovasc Diagn* 1988;14:1–6.

17. Doucette JW, Douglas Corl P, Payne HP, Flynn AE, Goto M, Nassi M, Segal J. Validation of a Doppler guide wire for intravascular measurement of coronary artery flow velocity. *Circulation* 1992;85:1899–1911.

18. Di Mario C, Roelandt JRTC, de Jaegere P, Linker DT, Oomen J, Serruys PW. Limitations of the zero-crossing detector in the analysis of intracoronary Doppler. A comparison with fast Fourier transform of basal, hyperemic and transstenotic blood flow velocity measurements in patients with coronary artery disease. *Cathet Cardiovasc Diagn* 1992;27:56–64.

19. Di Mario C, Hermans WRM, Rensing BJ, Serruys PW. Calibration using angiographic catheters as scaling devices. Importance of filming the catheters not filled with contrast medium. *Am J Cardiol* 1992;69:1377–1378.

20. Haase J, Di Mario C, Slager CJ, van der Giessen WJ, den Boer A, de Feyter PJ, Reiber JHC, Verdouw PD, Serruys PW. In-vivo validation of on-line and off-line geometric coronary measurements using insertion of stenosis phantoms in porcine coronary arteries. *Cathet Cardiovasc Diagn* 1992;27:16–27.

21. Di Mario C, Haase J, den Boer A, Reiber JHC, Serruys PW. Videodensitometry versus edge detection for the assessment of in vivo intracoronary phantoms. *Am Heart J* 1992;124:1181–1189.

22. Reiber JHC, Serruys PW, Kooijman CJ, Wijns W, Slager CJ, Gerbrands JJ, Schumbiers JCH, den Boer A, Hugenholtz PG. Assessment of short-, medium-, and long-term variations in arterial dimensions from computer-assisted quantitation of coronary cineangiograms. *Circulation* 1985;71:280–288.

23. Di Mario C, de Feyter PJ, Slager CJ, de Jaegere P, Roelandt JRTC, Serruys PW. Intracoronary blood flow velocity and transstenotic pressure gradient using sensor-tip pressure and Doppler guidewires. *Cathet Cardiovasc Diagn* 1993;28:(in press).

24. Mancini GBJ, Cleary RM, DeBoe SF, Moore NB, Gallagher KP. Instantaneous hyperemic flow-versus-pressure slope index: microsphere validation of an alternative to measures of coronary reserve. *Circulation* 1991;84:862–870.

25. Mancini GBJ, McGillem MJ, DeBoe SF, Gallagher KP. The diastolic hyperemic flow versus pressure relation: a new index of coronary stenosis severity and flow reserve. *Circulation* 1989;80:941–950.

26. Gould KL, Lipscomb K, Hamilton GW. Physiologic basis for assessing critical coronary stenosis: instantaneous flow response and regional distribution during coronary hyperemia as measures of coronary flow reserve. *Am J Cardiol* 1974;33:87–94.
27. Klocke FJ. Measurements of coronary flow reserve: defining pathophysiology versus making decisions about patient care. *Circulation* 1987;76:245–253.
28. Sugawara M. Stenosis: theoretical background. In: Sugawara M, Kajiya F, Kitabatake A, Matsuo H, eds. Blood flow in the heart and large vessels. Tokyo: Springer-Verlag, 1989:91.
29. Gould KL, Kirkeeide RL, Buchi M. Coronary flow reserve as a physiologic measure of stenosis severity. *J Am Coll Cardiol* 1990;15:459–474.
30. Wilson RF, Marcus ML, White CW. Prediction of the physiologic significance of coronary arterial lesions by quantitative lesion geometry in patients with limited coronary artery disease. *Circulation* 1987;75:723–732.
31. Harrison DG, White CW, Hiratzka LF, Eastham CL, Marcus ML. The value of lesional cross-sectional area determined by quantitative coronary angiography in assessing the physiologic significance of proximal left anterior descending coronary artery stenoses. *Circulation* 1984;69:111–119.
32. Klocke FJ. Cognition in the era of technology: "seeing the shades of gray." *J Am Coll Cardiol* 1990;16:763–769.
33. Nanto S, Kodama K, Hori M, Mishima M, Hirayama A, Inoue M, Kamada T. Temporal increase in resting coronary blood flow causes an impairment of coronary flow reserve after coronary angioplasty. *Am Heart J* 1992;123:28–36.
34. Gould KL. Interactions with the distal coronary vascular bed. In: Gould KL, ed. Coronary artery stenosis. New York: Elsevier, 1991:31–39.
35. Gould KL. Phasic pressure-flow and fluid-dynamic analysis. In: Gould KL, ed. Coronary artery stenosis. New York: Elsevier, 1991:40–52.
36. Dole WP, Richards KL, Alexander GM, Campbell AB, Hartley CG, Bishop VS. Diastolic coronary artery pressure-flow relationship in conscious man. *Cardiovasc Res* 1984;18:548–554.
37. Bellamy RF. Calculation of coronary vascular resistance. *Cardiovasc Res* 1980;14:261–269.
38. Klocke FJ, Mates RE, Canty JM, Ellis AK. Coronary pressure-flow relationships. Controversial issues and probable implications. *Circ Res* 1985;56:311–323.

CHAPTER 13

THE INSTANTANEOUS HYPEREMIC CORONARY PRESSURE - FLOW VELOCITY RELATIONSHIP IN CONSCIOUS HUMANS

Carlo Di Mario, M.D., Rob Krams*, M.D., Ph.D., Robert Gil, M.D., Nicolas Meneveau, M.D., Patrick W. Serruys, M.D., Ph.D.

From the Intracoronary Imaging Laboratory, Cardiac Catheterization Laboratory and *Experimental Animal Laboratory, Division of Cardiology, Thoraxcenter, Erasmus University, Rotterdam

From Reiber JHC, Serruys PW (eds). Quantitative coronary arteriography 1993. Dordrecht, Kluwer Academic Publishers, 1994 (in press).

SUMMARY

Background: The limitations and inaccuracies in the measurement of stenosis geometry, especially after coronary interventions, have prompted investigators to use functional indexes of stenosis severity, assessing the reduction of flow induced by the stenosis under study. Coronary flow reserve is greatly affected by the hemodynamic conditions at the time of the measurement and can not be applied for the immediate assessment of the results of coronary interventions.

Aim of the study: In this study the instantaneous relation between coronary flow velocity and pressure in the diastolic phase has been assessed during maximal hyperemia in normal or near-normal coronary arteries (< 30% diameter stenosis) in 52 patients and in arteries with ≥ 30% diameter stenosis in 24 patients.

Methods: The instantaneous peak coronary flow velocity measured with a Doppler guidewire was plotted against the simultaneously measured proximal coronary pressure, recorded through the guiding catheter. The phase of progressive flow reduction in mid-late diastole was selected in 4 consecutive cardiac cycles at the maximal effect of 8-12.5 mg of papaverine intracoronary. To study the possibility to determine the zero-flow pressure from the intercept of the velocity-pressure relation on the pressure axis, a controlled diastolic cardiac arrest was induced by an intracoronary bolus injection of 3 mg of adenosine in 9 cardiac transplant recipients.

Results: The slope of the instantaneous hyperemic diastolic flow velocity-pressure relation (IHDVPS) could be assessed in 44/52 patients with < 30% diameter stenosis (85%) and in 15/24 patients with ≥30% diameter stenosis (62%). The presence of a flat diastolic flow velocity curve precluded the assessment of the IHDVPS in the patients with the most severe stenoses. The measurement of IHDVPS was highly reproducible (interobserver difference = 2 ± 1%) and showed a moderate beat-to-beat variability (15 ± 7%) The IHDVPS showed no significant correlation with heart rate, mean diastolic aortic pressure, left ventricular +dP/dt, V_{max}, −dP/dt and τ_1, type of vessel studied and cross-sectional area at the site of the velocity recording. The IHDVPS was significantly lower in arteries with ≥30% diameter stenosis than in normal arteries (0.77 ± 0.52 versus 1.65 ± 0.71 cm s^{-1} $mmHg^{-1}$, $p < 0.0001$).

The study of the velocity-pressure relation during long diastolic pauses showed a curvilinear relation in the lower pressure range between velocity and pressure, with an upwards concavity to the velocity axis and no intercept with the pressure axis in most cases.

Conclusion: The instantaneous flow velocity-pressure relation during maximal hyperemia can be reliably assessed using intracoronary Doppler in the Catheterization Laboratory, has a low inter-observer variability and a moderate beat-to-beat variability, is independent from heart rate, aortic pressure or indexes of left ventricular contractility-relaxation at the time of the assessment. The slope of this relation can distinguish arteries with and without significant coronary stenoses, suggesting that this index is a potential alternative to coronary flow reserve for the assessment of stenosis severity before and after coronary interventions. The curvilinearity of the velocity-pressure relation during long diastolic pauses, possibly due to a significant reduction of luminal cross-sectional area at low pressures,

precludes the use of the flow velocity-pressure relation for the assessment of the zero-flow pressure.

Key words: Coronary flow; Doppler ultrasound, Coronary circulation.

In the cardiac catheterization laboratory the severity of a coronary stenosis before and after coronary interventions is assessed using morphological techniques to measure absolute and relative dimensions of the stenotic segment. Computer-assisted quantitative angiography has greatly increased the accuracy of these measurements [1] and new techniques, such as intracoronary ultrasound, have the potential to further improve this accuracy in the presence of a lumen of complex geometry such as after coronary interventions [2]. However, multiple geometric characteristics of the stenotic segment (minimal luminal cross-sectional area, length, entrance and exit angles, etc.) must be determined to estimate the stenosis hemodynamics [3,4]. A complete three-dimensional reconstruction of the stenosis geometry is beyond the possibility of the techniques currently applied to study stenosis morphology, and larger inaccuracies can be expected in the assessment of the results of coronary interventions which induce a severe disruption of the vessel wall [5]. Furthermore, the measurements in the reference segment for the assessment of percent diameter and cross-sectional area reduction are often misleading due to the presence of a relative stenosis due to diffuse atherosclerosis or of pre- or post-stenotic ectasia. The use of physiological indexes of stenosis severity, assessing the reduction of flow induced by the stenosis under study, may overcome these limitations. Baseline flow, however, is reduced only in the presence of very severe stenoses, inducing a resistance to flow exceeding the high basal resistance of the distal coronary vasculature. An increase of myocardial metabolic demand or the use of pharmacologic agents inducing a maximal reduction of the distal coronary resistance is required to assess the limitation to the maximal coronary conductance induced by less severe stenoses. The measurement of absolute coronary flow, normalized per unit of viable myocardial mass, is an unequivocal indicator of the adequacy of the maximal myocardial perfusion in the territory of distribution of the artery under study. This measurement, however, can be obtained only with techniques not applicable in humans (radiolabeled microspheres) or not immediately applicable in the interventional laboratory due to their inherent technical complexity (positron emission tomography) [6,7,8]. The ratio of maximal flow to baseline flow (coronary flow reserve, CFR) is a well-established alternative, well correlated in previous experimental work with the severity of coronary stenoses [9]. As a ratio. however, CFR is influenced by changes in resting myocardial flow and by factors modifying the slope of the flow-pressure relation during maximal hyperemia such as the presence of myocardial hypertrophy and changes in pre-load, heart rate and myocardial contractility [10-12]. Furthermore, the ratio between maximal hyperemic flow, linearly related to changes of driving pressure, and baseline flow, relatively independent from pressure changes in the autoregulatory range, is necessarily variable with the level of aortic pressure at the time of the measurement [10]. Coronary flow reserve, measured in clinical studies using Doppler or videodensitometry, correlated well with the angiographically measured stenosis severity only in very selected

subsets of patients [13-15], but this index could not be successfully applied in a large population of patients with coronary artery disease [16]. Furthermore, after coronary interventions the increase in baseline flow and/or the persistence of an impaired vasodilatory response of the distal vasculature, precludes the use of CFR for the immediate assessment of the results of this treatment in the interventional suite [17-23].

To overcome these limitations, Mancini et al. [24] proposed the assessment of the instantaneous relation between aortic pressure and coronary flow during maximal hyperemia in the phase of progressive flow decrease in mid- and end-diastole. In their experimental preparation, electromagnetic flowmeters were used to measure coronary flow and left ventricular pressure was used to define the start- and end-points for the measurement, avoiding the phase of rapid cardiac relaxation and the phase of isovolumetric myocardial contraction. In four separate series of experiments [24-27], the slope of the instantaneous hyperemic diastolic flow-pressure relation (IHDFPS) was shown to be independent from changes in heart rate, preload, aortic pressure and cardiac contractility. The IHDFPS was well correlated with the severity of coronary stenoses, showing larger decrements than CFR with increasing stenosis. The measurement of coronary conductance obtained with this index was best correlated with maximal subendocardial conductance measured using radiolabelled microspheres. In humans, selective measurements of instantaneous coronary flow can not easily be performed in the cardiac catheterization laboratory. Intracoronary Doppler, however, can accurately measure instantaneous flow velocities during the cardiac cycle [28,29]. Using Doppler-tipped guidewires the velocity measurements can be obtained distal to the stenosis, so that the flow changes will certainly reflect the severity of the lesion under study.

Aim of the study: feasibility, reproducibility and independency from the hemodynamic parameters at the time of the assessment of the slope of the instantaneous hyperemic diastolic flow velocity-pressure relation was assessed in 52 arteries with < 30% diameter stenosis. Sensitivity and specificity of the IHDVPS for the assessment of a flow-limiting stenosis was established by comparing the measurements of IHDVPS in the control group with the measurements obtained in 24 arteries with ≥30% diameter stenosis. The possibility to estimate the pressure at zero flow ($P_{f=0}$) from the extrapolation of the instantaneous diastolic velocity pressure relation was tested in 9 cardiac transplant recipients after inducing a controlled prolonged diastolic cardiac arrest.

METHODS

Patient population

Group I (normal arteries or arteries with < 30% diameter stenosis; n = 52): This group included patients undergoing coronary angiography because of suspected coronary artery disease (n = 12), percutaneous coronary interventions in an artery different from the vessel studied (n = 31) and asymptomatic cardiac transplant

recipients undergoing control follow-up coronary angiography 1-5 years after transplant (n = 9). Age, sex, clinical characteristics and type of artery studied for the patients undergoing a successful assessment are indicated in Table 1. The studied arteries were examined by two experienced angiographers and classified as normal (n = 23) or with minimal lumen irregularities (n = 29). The absence of ≥30% diameter stenosis was confirmed, when necessary, using a subsequently described quantitative angiographic technique. In no cases angiographically visible collaterals originated from the artery studied. None of the cardiac transplant recipients had angiographically visible signs of small coronary vessel disease. In all cases left ventriculography showed a normal left ventricular function in the territory of distribution of the artery studied. Twenty-nine patients (56%) of this group were under antianginal and/or antihypertensive treatment at the time of the study.

Group II (arteries with ≥ 30% diameter stenosis; n = 24): this group included 21 patients with ≥50% diameter stenosis studied before a coronary intervention and 3 patients with ≥30% but < 50% diameter stenosis undergoing a diagnostic coronary angiogram. Patients with acute myocardial infarction, arterial occlusion/subocclusion {Thrombolysis in Myocardial Infarction (TIMI) flow class 0-1} or presence of an open aorto-coronary bypass graft on the vessel studied were not included in the study. Clinical characteristics and type of vessel studied in the group undergoing a successful assessment are reported in Table 2. All patients of this group were under antianginal treatment at the time of the study.

Catheterization procedure

After intravenous administration of 10,000 I.U. of heparin and 250 mg of acetylsalicylic acid, a 7-8 Fr guiding catheter was advanced up to the ostium of the artery studied. The Doppler guidewire was introduced into the proximal or mid-segment of the vessel to be studied (Group I) or distal to the stenosis (Group II). After optimization of the Doppler signal and 3-5 min after intracoronary injection of a bolus of 2-3 mg of isosorbide-dinitrate, baseline flow velocity and proximal coronary pressure were recorded and a cineangiogram was performed in order to measure the cross-sectional area at the site of the Doppler sample volume and the geometric characteristics of the stenosis (when present). The flow velocity measurement was then repeated at the peak effect of an intracoronary bolus injection of papaverine (8 mg: right coronary; 12.5 mg: left coronary and saphenous vein bypass graft) [30]. Care was taken to avoid impairment of flow during maximal hyperemia due to the presence of the guiding catheter in the coronary ostium. If damping occurred, the guiding catheter was withdrawn from the coronary ostium immediately after the injection of papaverine. In 6 cardiac transplant recipients, left ventricular and aortic pressure were measured simultaneously using a double sensor high-fidelity pig-tail catheter (Sentron, Roden, the Netherlands). In these cases a previously described automated analysis system [31] was used to measure peak positive and negative first derivative of the left ventricular pressure (+dP/dt and −dP/dt), the maximal velocity of left ventricular isovolumic contraction (V_{max}) and the constant of isovolumic relaxation (τ_1). In all the 9 cardiac transplant recipients, during the phase of maximal

Table 1. Clinical and hemodynamic characteristics of the patients studied with a simultaneous recording of transstenotic pressure gradient and flow velocity.

Pts	Age	Sex	Hypert	Vessel	CSA_2 (mm^2)	Aortic pressure range (mmHg)		Flow velocity range (cm/s)		CFR	IHDVPS	IHDVPS variab.	$P_{f=0}$	$P_{f=0}$ variab.	r^2
						max	min	max	min		cm/s/mmHg	%	mmHg	%	
921137	67	M	y	LAD	4.07	96	71	83	39	2.4	1.2	5	32	12	0.85
921335	53	M	n	LCX	9.07	102	85	135	82	2.8	2.5	15	44	16	0.82
921343	67	M	n	RCA	9.38	96	54	63	28	2.5	0.8	13	14	53	0.94
921248	43	M	n	RCA	4.71	108	81	124	65	2.9	1.3	15	22	33	0.81
921238	55	M	n	LCX	4.10	121	91	132	54	2.6	2.4	16	66	13	0.91
920859	45	M	n	LCX	5.85	112	85	176	99	3.0	2.6	9	43	15	0.94
920931	70	M	n	LAD	3.34	100	70	45	14	2.0	0.9	12	52	8	0.90
921117	59	F	n	LAD	5.11	100	69	116	67	2.5	1.6	25	22	41	0.86
921146	45	M	n	LAD	3.43	108	84	119	63	2.7	2.1	10	51	7	0.95
921613	58	M	n	RCA	7.05	88	72	87	60	2.5	1.7	7	34	6	0.84
920613	66	M	n	LCX	5.78	127	97	97	53	3.7	1.4	6	53	8	0.86
921603	42	M	n	LCX	9.49	92	75	107	59	3.1	2.6	6	53	3	0.95
921671	59	M	y	LCX	4.12	139	112	106	76	3.0	1	12	29	35	0.85
921878	45	M	n	LCX	8.59	107	86	131	88	3.0	1.9	8	38	11	0.88
921787	64	F	y	LCX	7.31	111	84	84	59	2.8	1	10	19	36	0.90
921453	71	M	y	RCA	6.27	120	73	67	29	2.2	0.6	19	17	40	0.72
921953	65	F	y	LCX	6.30	80	58	36	24	1.3	0.5	4	5	39	0.91
921645	52	M	y	LCX	1.69	80	63	82	61	1.7	1.1	11	8	55	0.79
921581	53	F	n	LAD	3.88	116	85	64	36	2.1	0.8	7	44	11	0.91

Pts	Age	Sex	Hypert	Vessel	CSA (mm^2)	Aortic pressure range (mmHg)		Flow velocity range (cm/s)		CFR	IHDVPS	IHDVPS variab.	$P_{f=0}$	$P_{f=0}$ variab.	r^2
920813	51	M	n	LCX	3.34	75	63	73	60	2.6	3.2	15	55	3	0.85
920705	45	F	y	LAD	14.1	103	87	89	56	4.5	1.6	13	47	8	0.89
922007	58	M	y	RCA		108	88	54	29	3.5	1.5	14	66	7	0.79
922038	56	M	n	LCX		103	84	103	68	3.2	1.5	20	34	33	0.60
921757	42	M	n	LAD	8.82	71	66	78	59	4.5	2.8	33	43	25	0.77
921475	61	M	n	LAD	9.01	102	76	116	58	3.5	2.3	6	48	3	0.93
921097	51	M	y	LAD	10.82	71	58	55	41	2.0	1.1	16	28	26	0.69
921384	50	M	y	RCA	-	75	61	71	40	3.3	2.1	39	31	36	0.75
920966	54	M	y	RCA	-	82	71	82	62	3.5	1.7	16	33	22	0.85
921134	50	M	y	LAD	6.12	105	93	143	99	2.3	3.1	15	59	27	0.78
921922	55	M	y	RCA	-	66	54	51	33	3.0	1.2	21	23	28	0.88
920896	31	F	y	LCX	6.07	94	74	97	50	3.8	1.7	13	36	17	0.81
921961	57	M	y	LCX	7.55	108	79	100	70	3.3	0.9	14	10	49	0.82
920952	67	M	n	SVBG	8.66	121	100	54	25	2.2	1.1	4	73	4	0.72
922002	67	M	n	SVBG	-	86	71	101	53	2.6	2.6	7	44	7	0.78
921548	66	M	y	LAD	17.5	90	73	73	43	1.6	1.6	8	44	6	0.87
930194	53	M	n	LCX	9.69	106	91	37	24	2.0	0.9	11	62	6	0.89
921983	48	M	n	LAD	9.56	90	77	94	71	4.9	1.7	13	34	16	0.92
930053	46	M	n	LAD	3.83	98	83	127	85	2.8	2.8	25	55	13	0.87
930242	68	M	y	LAD	3.84	119	87	85	48	2.7	1.0	7	31	17	0.79
930264	68	M	n	RCA	7.02	98	81	89	52	1.7	2.2	11	56	6	0.85
930131	73	F	n	LCX	7.11	99	77	87	54	3.6	1.4	11	34	17	0.84
930399	47	F	n	LAD	-	118	91	133	80	2.2	1.9	18	44	19	0.84
930090	58	M	y	RCA	5.35	110	79	53	27	2.4	0.8	15	38	36	0.88
921884	57	M	n	LAD	7.26	83	73	98	59	3.8	1.8	16	36	8	0.7
MEAN ± SD	55 ±8					99 ±18	77 ±14	93 ±32	56 ±21	2.9 ±0.7	1.7 ±0.7	14 ±8	37 ±16	22 ±15	0.85 ±0.07

CSA = cross/sectional area; CFR = coronary flow reserve; IHDVPS = instantaneous hyperemic velocity pressure slope; $P_{f=0}$ = (X-axis intercept); r^2 = squared correlation coefficient.

Table 2. Clinical and hemodynamic characteristics of the patients with > 30% diameter stenosis.

Pts	Age yrs	Sex	MI	Hyp	Vessel	DS %	MLCSA	CSA Doppler site	Aortic pressure range (mmHg)		Flow velocity range (cm/s)		CFR	IHDVPS (cm/s/mmHg)	IHDVPS variab.	$P_{f=0}$ mmHg	$P_{f=0}$ var.	r^2
							mm^2	mm^2	max	min	max	min			%		%	
921880	37	F	y	n	LAD	35	1.82	3.30	81	69	32	22	2.4	0.7	10	38.6	17	0.83
921858	52	M	y	n	LCX	67	1.1	10.2	96	81	20	15	2	0.2	13	7.6	27	0.95
921792	56	M	y	n	LAD	56	1.83	8.76	95	73	47	29	1.8	0.6	7	14.3	24	0.85
920707	73	M	n	n	RCA	78	0.5	9.5	84	58	50	32	1.5	0.6	19	0	52	0.76
920922	59	M	n	n	RCA	76	1.27	4.64	93	67	41	18	1.8	1	14	45	5	0.82
920908	63	F	n	n	RCA	55	1.17	8.70	101	78	33	20	1.5	0.5	24	34	42	0.86
921238	55	M	n	n	LAD	68	0.87	2.49	89	70	21	12	1.1	0.3	32	26	50	0.70
920945	69	M	y	y	LAD	55	2.18	4.22	88	75	31	21	1.7	0.6	8	28.7	12	0.72
921504	50	M	n	y	LAD	45	1.46	6.2	96	77	57	30	1.9	0.7	29	28.9	19	0.60
921834	49	F	y	n	RCA	69	0.59	6.5	125	75	50	18	1.3	0.5	12	26.6	22	0.92
921118	48	M	y	y	LAD	56	1.06	5.47	95	80	66	52	1.4	0.7	12	2	70	0.72
921774	66	M	n	n	LAD	60	1.02	6.38	67	54	38	21	1.7	0.8	10	27.9	9	0.68
930228	60	F	y	n	LAD	54	2.49	5.55	112	70	202	94	3.3	2.3	11	20	27	0.93
930201	51	M	y	n	LAD	52	2.07	7.99	111	75	61	37	2.1	0.6	5	9	48	0.94
922038	56	M	y	n	RCA	66	0.79	6.21	62	49	57	37	1.9	1.5	13	24.7	17	0.92
MEAN ± SD	58 ±10					60 ±12	1.2 ±0.5	6.20 ±2.39	90 ±16	70 ±10	42 ±14	25 ±11	1.7 ±0.3	0.7 ±0.3	16 ±8	23.4 ±14	28 ±19	0.79 ±0.1

MI = myocardial infarction; % DS = percent diameter stenosis; MLCSA = minimal luminal cross-sectional area;
CSA = cross-sectional area; IHDVPS = instantaneous hyperemic diastolic velocity pressure slope; CFR = coronary flow reserve.

hyperemia after papaverine injection, an intracoronary bolus of 3 mg of adenosine was used to induce a prolonged diastolic cardiac arrest. Ventricular pacing was used, when necessary, to restore cardiac contraction.

Quantitative angiographic measurements

The guiding catheter, filmed devoid of contrast medium, was used as a scaling device. A previously validated [32] on-line analysis system operating on digital images (ACA-DCI, Philips Medical Systems, Best, The Netherlands) was used during the catheterization procedure. In this system, after automatic detection of the vessel centerline, a weighted first and second derivative function with predetermined continuity constraints is applied to the brightness profile on each scan line perpendicular to the vessel centerline. In all patients a user-defined diameter was measured at the site of the Doppler sample volume and the corresponding cross-sectional area was calculated assuming a circular cross-section. In Group II, minimal luminal diameter (MLD) was measured and percent luminal diameter stenosis was calculated using an automatic interpolated technique to measure the reference diameter.

Doppler guidewire and flow velocity measurements

The Doppler angioplasty guidewire is a 0.018" (diameter 0.45 mm, cross-sectional area 0.17 mm^2) 175 cm long flexible and steerable guidewire with a very flexible shapable distal end mounting a 12 MHz piezoelectric transducer at the tip (Cardiometrics Inc., Mountain View, CA) [28]. The sample volume is positioned at a distance of 5.2 mm from the transducer and has an approximate width of 2.25 mm due to the divergent ultrasound beam so that a large part of the flow velocity profile is included in the sample volume also in case of eccentric positions of the Doppler guidewire. After real-time processing of the quadrature audio signal a fast-Fourier transform algorithm is used to increase the reliability of the analysis [33], the Doppler system calculates and displays on-line several spectral variables including the instantaneous peak velocity and the time-averaged (mean of 2 beats) peak velocity (Figure 1A). The flow velocity measurements obtained with this system have been validated in vitro and in an animal model using simultaneous electromagnetic flow measurements for comparison [28]. Mean flow velocity was calculated as time-averaged peak velocity/2, assuming a fully developed parabolic flow velocity profile [29]. Coronary flow reserve was defined as the ratio between maximal flow velocity at the peak effect of the papaverine injection and in baseline conditions.

Instantaneous assessment of the flow velocity-pressure relation

A continuous acquisition of the instantaneous peak Doppler flow velocity, of the pressure measured through the guiding catheter and of the electrocardiogram was performed with a 12 bits analog-to-digital converter (DataQ Instr., Akron, OH) connected to a PC. Electrocardiogram, proximal coronary pressure and instantaneous

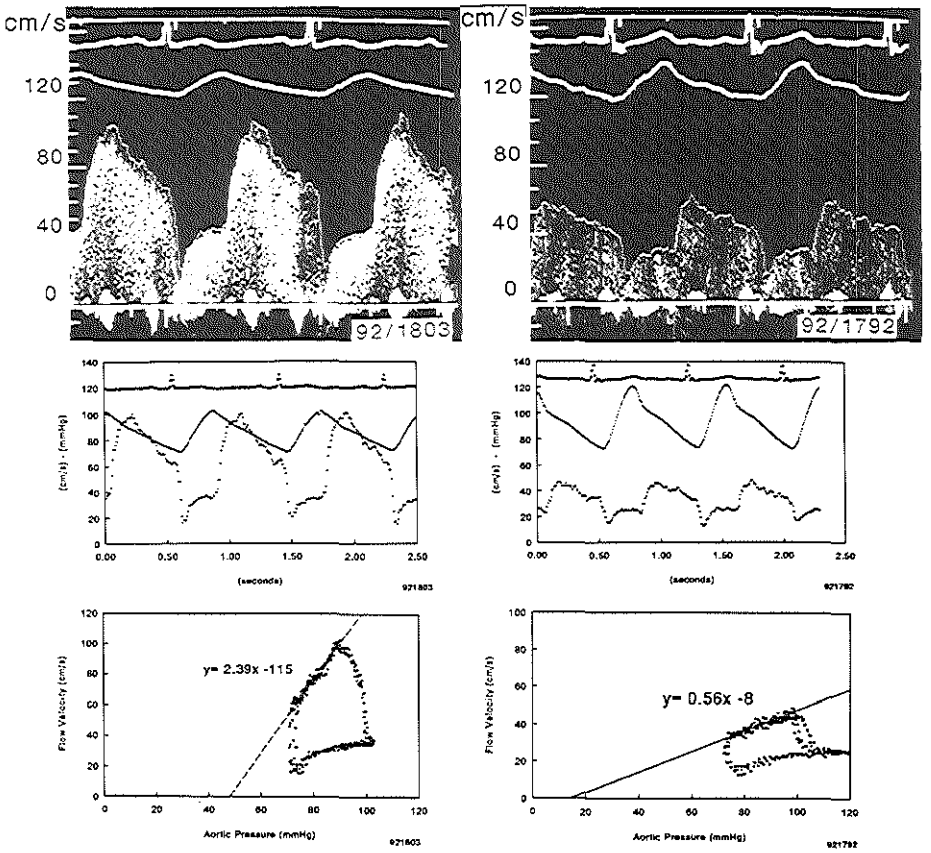

Fig. 1. Top panel) Flow velocity measurements during maximal hyperemia in a left circumflex artery with minimal wall irregularities (left side) and in a left anterior descending coronary artery distal to a significant stenosis (56% diameter stenosis, right side). Mid-panel) From top to bottom electrocardiogram, aortic pressure and peak velocity of the same beats acquired in a digital format (125 Hz). The maximal velocity and the rapid decrease in velocity due to the beginning of myocardial contraction are used as the start and end point for the analysis of the diastolic hyperemic pressure velocity relation. Bottom panel) Pressure flow velocity loop of the same beats. The regression line was calculated from the datapoints of the mid-diastolic interval indicated above. Note the steeper slope of the pressure velocity relation in the normal artery.

peak coronary blood flow velocity were sampled at 125 Hz per channel and stored for off-line analysis (Figure 1B). Using dedicated software (ACodas, DataQ, Akron, Ohio), the acquired signals were displayed in an X-Y scatterplot, so that the progressive variations of the instantaneous peak flow velocity-pressure loop from baseline to hyperemia could be monitored and 4 consecutive cardiac cycles without recording artifacts could be selected at peak hyperemia. The diastolic interval to be analyzed was selected using as start point the maximal diastolic velocity and as end-point the beginning of the phase of rapid decrease of flow velocity induced by the ventricular contraction (Figure 1C). After identification of the interval of analysis for

each cycle, linear regression was used to calculate the individual IHDVPS in order to study the variability among different cardiac cycles. Afterwards, the data of the 4 selected diastolic intervals were pooled and the mean IHDVPS was calculated. The reproducibility of the measurements was tested in 10 randomly chosen cases of Group I in which the same 4 cardiac cycles were independently assessed by a second observer. In the 6 patients in whom a left ventricular high-fidelity pressure was available during the measurements, the slope of the hyperemic diastolic flow velocity-pressure relation was assessed in the same beats using the start- and end-points proposed by Mancini et al. (20 ms after peak left ventricular $-dP/dt$ and upstroke of $+dP/dt$) [24].

Velocity-pressure relation during controlled diastolic cardiac arrest

In 9 cardiac transplant recipients a second injection of papaverine intracoronary was performed, followed after 30-45 s by an intracoronary bolus of adenosine 3 mg (Figure 2). Using a previously introduced right ventricular pacing catheter, pacing was performed when necessary (4 cases) to restore a normal cardiac contraction. Flushing was reported by 4/9 patients. None of the patients complained of chest discomfort.

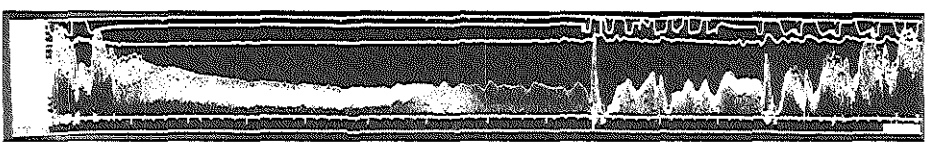

Fig. 2. Prolonged diastolic pause induced by the intracoronary injection of 3 mg of adenosine during maximal hyperemia induced by papaverine. A progressive decrease of flow velocity and aortic pressure is observed during the 6 seconds of cardiac arrest. In the first beats induced by ventricular pacing, note the presence of a large systolic flow component, indicating refilling of the capacitance of the epicardial coronary artery. The dotted tracing at the top of the Doppler envelope indicates the instantaneous peak velocity (automatically detected on-line and used for the analysis of the pressure-velocity relation).

Statistical analysis

The results were expressed as mean ± standard deviation (SD). The beat-to-beat variability of the IHDVPS was calculated as the ratio between the standard deviation and the mean of the slopes measured over 4 consecutive cardiac cycles. The mean ± SD of the signed differences of corresponding measurements was used to test the interobserver variability and the variability of the measurements obtained defining the diastolic interval of analysis from the flow velocity signal or from the left ventricular pressure. Covariance analysis was used in Group I to estimate the independency of the IHDVPS from heart rate, mean diastolic aortic pressure, cross-sectional area at the site of the velocity measurements and left ventricular $+dP/dt$ and $-dP/dt$, Vmax and τ_1. A two-tailed Student's t-test for unpaired data was performed

to compare the measurements of IHDVPS in patients with and without > 30% diameter stenosis.

To test the linearity of the individual velocity-pressure relations during long diastolic pauses, the data were fit with a linear and a second order polynomial function. A relation was considered non linear when the coefficient of the second order term of the polynomial fit was significant at $p < 0.01$ and when the F-statistic for the polynomial fit was statistically better at $p < 0.01$ than the linear fit [34].

RESULTS

Feasibility, reproducibility, beat-to-beat variability and dependence on hemodynamic variables of the measurement of IHDVPS

Feasibility: A reliable, automatic detection during maximal hyperemia of the progressive decrease in flow velocity of peak velocity in mid-late diastole was obtained in 44/52 patients of Group I (85%) and in 15/24 patients of Group II (62%). A poor quality of the Doppler signal or the presence of multiple artifacts impairing the accuracy of the automatic analysis was the reason for exclusion in all the 8 failed measurements in Group I and in 4 failed measurements in Group II. In the remaining 5 patients excluded in Group II the reason of failure was the presence of a flat diastolic flow velocity curve, without a clear proto-mid diastolic peak usable as start-point for analysis. In all the patients with this pattern a severe coronary obstruction (> 75% diameter stenosis) was observed.

Variability: The mean difference between measurements of IHDVPS performed independently by two observers (n = 10) was 0.004 ± 0.0001 $cm \cdot s^{-1} \cdot mmHg^{-1}$ (observer 1 minus observer 2), equal to $2 \pm 1\%$ of the mean of the two measurements. A beat-to-beat variability of $13 \pm 7\%$ was observed in Group I (individual measurements in Table I) and of $15 \pm 8\%$ in Group II (Table II). The IHDVPS calculated using start- and end-points for the definition of the diastolic interval derived from the flow velocity tracing or from the left ventricular pressure tracing (n = 6) showed a mean difference of 0.009 ± 0.005 $cm \cdot s^{-1} \cdot mmHg^{-1}$ (measurement with interval selected on the velocity pattern minus measurement with interval selected from the left ventricular tracing, $3 \pm 2\%$).

Dependence on hemodynamic variables: In Group I IHDVPS showed no significant correlation with heart rate, mean aortic diastolic pressure, type of vessel studied and luminal cross-sectional area at the site of the Doppler sample volume. In 6 patients of the same group in whom a high-fidelity left ventricular pressure was recorded, no correlation between IHDVPS and +dP/dt, −dP/dt, V_{max} and τ_I was observed.

IHDVPS in patients with and without coronary stenoses

The patients with and without > 30% diameter stenosis in the artery studied showed no significant differences in heart rate (69 ± 12 versus 63 ± 7 beats/min, NS), mean diastolic aortic pressure (88 ± 13 vs 82 ± 7 mmHg, NS) and cross-sectional area at

the site of the Doppler measurement (6.9 ± 3.1 vs 6.3 ± 2.2 mm^2, NS). Maximal diastolic velocity was significantly higher in Group I than in Group II (91 ± 31 vs 54 ± 43 cm/s, $p < 0.005$). Coronary flow reserve was also significantly higher in Group I than in Group II (2.9 ± 0.7 vs 1.7 ± 0.3, $p < 0.00005$). The IHDVPS was significantly higher in the normal or near-normal arteries of Group I than in the arteries with ≥30% diameter stenosis (1.65 ± 0.71 vs 0.77 ± 0.52 $cm \cdot s^{-1} \cdot mmHg^{-1}$, $p < 0.0001$), (Figure 3). A significant correlation was observed between IHDVPS and CFR ($r = 0.51$, $p < 0.0005$). In Group II the IHDVPS showed no correlation with the angiographically measured minimal luminal cross-sectional area and with percent diameter stenosis ($r = 0.39$ and 0.01, respectively, both NS).

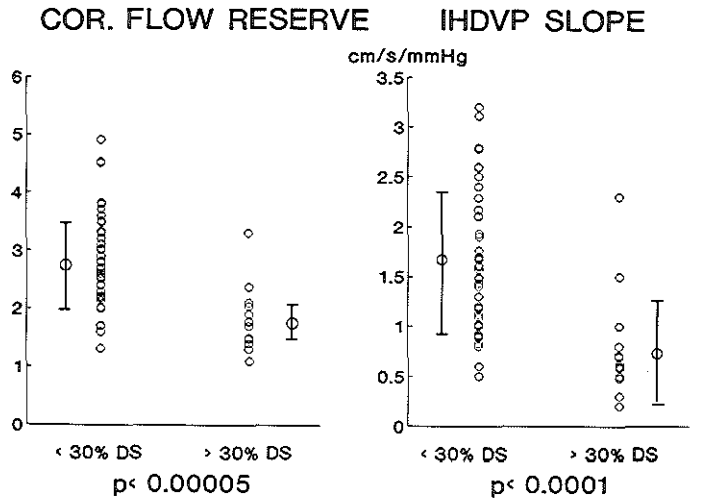

Fig. 3. Individual measurements of coronary flow reserve and IHDVPS in patients with and without > 30% diameter stenosis. Both the indices showed a significant difference in the two groups. The measurements of IHDVPS showed a smaller overlap in the two groups and a slightly higher sensitivity in the detection of the absence of ≥30% diameter stenosis.

IHDVPS during long-diastolic pauses

In 6/9 heart transplant recipients (66%) the injection of 3 mg of adenosine intracoronary was followed by a diastolic pause sufficiently long to induce a reduction of the minimal aortic pressure to ≤45 mmHg. Two of these patients were excluded because of deterioration of the flow velocity signal in the lower pressure range. Sinus node arrest was observed in 3 patients while a 3rd degree atrio-ventricular block was the cause of the arrest of the left ventricular contraction in the remaining 3 patients.

The individual curves of the 4 longest pauses observed in these patients are plotted in Figure 4. The curvilinear relation between velocity and pressure was confirmed by the analysis of the residuals after fitting a linear and a second order polynomial equation (Figure 5) and by the F-test, showing that the polynomial fit was better at

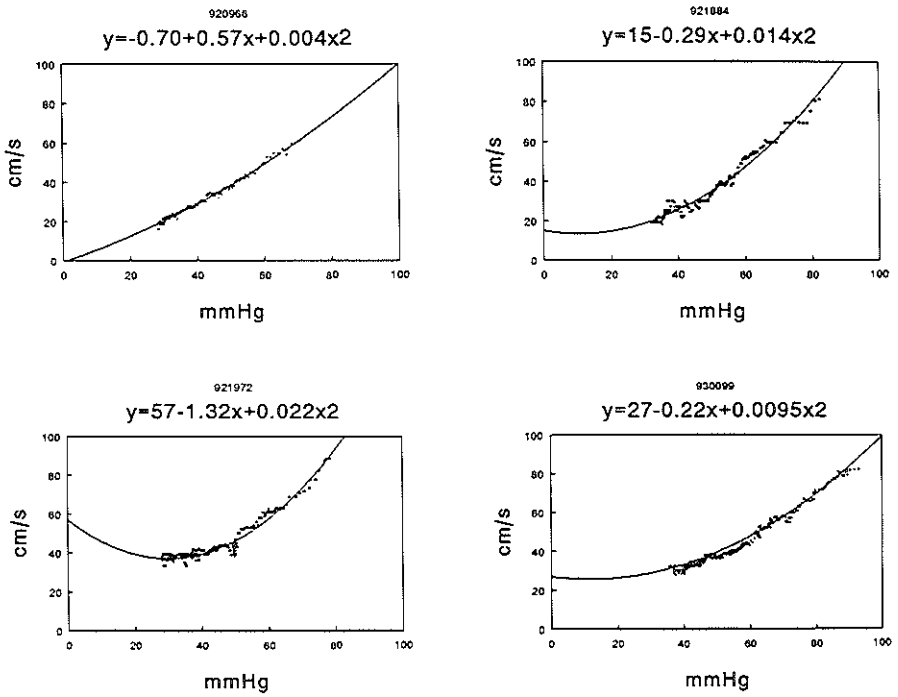

Fig. 4. The instantaneous hyperemic peak velocity from maximal diastolic velocity to the restoration of cardiac contraction is plotted versus aortic pressure during a prolonged cardiac arrest induced by an intracoronary injection of adenosine 3 mg intracoronary. In all the cases a second order polynomial equation is applied for analysis. In the case in the left upper panel, however, the F-test showed no significant difference between a linear and the displayed second order polynomial function. The curvilinearity in all the other cases is evident and was confirmed by the F-test. Note the absence of the intercept on the pressure axis in these last three cases.

$p < 0.01$ in 3/4 cases. In order to ascertain whether the curvilinear relation between velocity and pressure was present over the entire range of measurements, an automated calculation of IHDVPS was performed using linear regression over progressively smaller ranges of measurements, starting from the lowest pressure (Figure 6 A) and progressively increasing the lowest pressure by 1 mmHg up to a final smallest range examined including the measurements obtained in the highest 15 mmHg pressure range (Figure 6 F). This series of slopes was then plotted against the corresponding lowest pressure. The results of this analysis showed that a rather constant IHDVPS was present in a pressure range > 60 mmHg (Figure 6). Similarly, the intercept with the pressure axis showed a progressive increase in the lower pressure range, while stable higher values were observed in the physiologic pressure range.

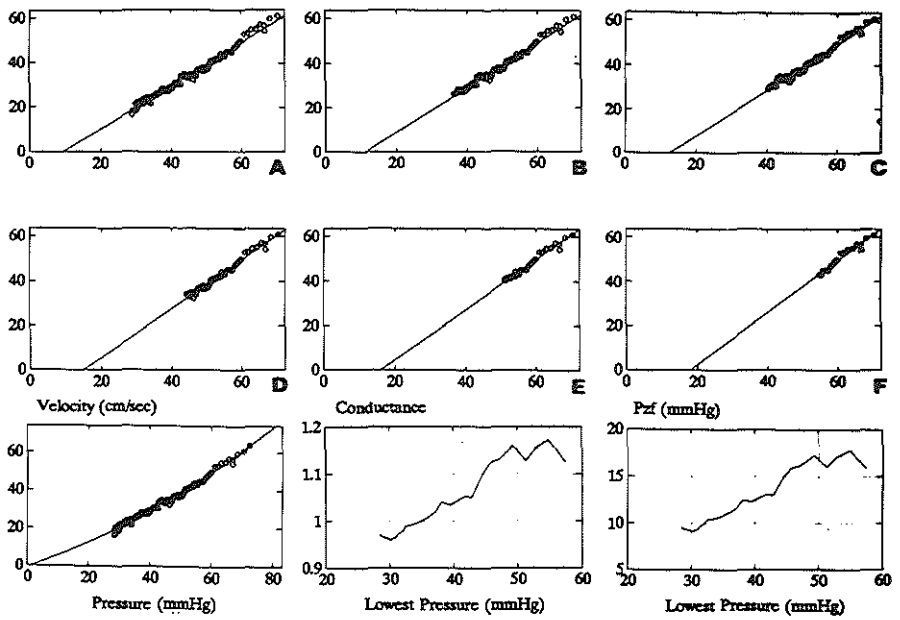

Fig. 5. The IHDVPS (Conductance) and the X-intercept (P_{zf}) are calculated using linear regression analysis over progressively smaller ranges of measurements, starting in the lowest pressure range (A) and progressively increasing the minimal pressure up to the higher 15 mmHg pressure range (F). The calculated IHDVPS (Conductance, lower mid-panel) and $P_{f=0}$ (P_{zf}, lower right panel) are plotted against the lowest pressure of the sample analyzed. Note the progressive increase in the 30-45 mmHg range and the more stable values at higher pressure.

DISCUSSION

The instantaneous velocity-pressure relation for the assessment of stenosis severity

In this first application in humans of the index proposed by Mancini et al. [24-27], special attention was paid to the assessment of the feasibility of the measurement. In the vast majority of the studied arteries the IHDVPS could be assessed. A manual tracing of the peak velocity from the Doppler spectrum could have increased the number of cases with a successful assessment when the presence of artifacts in the automatically detected peak velocity was the reason of failure. This method, however, is cumbersome, requires an-off line analysis so that the results cannot be immediately available at the time of the assessment and is prone to a considerable subjectivity. The presence of a flat diastolic flow velocity curve was the second most important reason of failure in the assessment of the IHDVPS. This pattern was observed only in very severe stenoses for which the assessment of an additional index of functional severity could be considered of limited additional clinical value.

Despite a careful selection of the beats analyzed, a relatively large beat-to-beat variability was observed. Respiratory changes can be advocated as a possible explanation but the effect of respiration should be minimal during maximal hyperemia. A technical limitation is the most likely explanation of this variability. The automatic detection of the peak diastolic velocity and, in particular, of the maximal velocity which was used as the start point for analysis and is an essential determinant of the final outcome of the analysis, is very sensitive to the presence of noise. The original method proposed by Mancini et al. [24] required a high fidelity measurement of the left ventricular pressure in order to detect the diastolic interval of interest for analysis. Measurements obtained in a subset of patients demonstrated that the simplified approach used in this study yields results similar to those obtained selecting the interval for analysis from the left ventricular pressure tracing.

Mancini et al. [24-27] could independently manipulate the hemodynamic parameters in the animal model used to assess the correlation of CFR and flow-pressure slope with each hemodynamic variable. A similar approach could not be used in a clinical study but the lack of correlation in the population studied between IHDVPS and heart rate, aortic pressure and indices of left ventricular contractility and relaxation at the time of the assessment suggests that also in humans this index is independent from these hemodynamic variables. The IHDVPS measured in arteries with ≥ 30% diameter stenosis was less than half the IHDVPS measured in normal or near-normal coronary arteries. Due to the small overlap between the two groups, if an arbitrary cut-off of ≥ 0.8 $cm \cdot s^{-1} \cdot mmHg^{-1}$ was chosen, the sensitivity and specificity of this index in the detection of the absence of a ≥30% diameter stenosis were 95 and 91%, respectively, with a sensitivity only minimally greater than coronary flow reserve and a similar specificity. The assessment of a larger group of patients with flow limiting stenoses is required to establish the potential advantage of IHDVPS over CFR in the assessment of an impairment of coronary conductance. In particular, these studies should address the usefulness of this index for the assessment of the changes of coronary conductance after coronary interventions. In this setting, the IHDVPS has the great potential advantage over CFR to be independent from changes in baseline velocity and from the hemodynamic conditions at the time of the assessment.

A substantial difference between the approach of Mancini and our approach is the use of flow velocity instead of absolute coronary flow normalized for the myocardial mass. The approach used in this study has the advantage of an easier applicability in the clinical setting but has also the potential disadvantage that the velocity-pressure slope can be influenced by the dimension of the artery under assessment so that slopes measured in arteries of different diameter can not be compared. The results of this study in normal or near-normal arteries, however, showed that the IHDVPS is independent from the cross-sectional area at the site of the velocity measurement. In the coronary system, the presence of a progressive, moderate increase in total cross-sectional area from proximal to distal has been suggested in accordance with the principles of limited/adaptive vascular shear stress, minimum vascular volume at bifurcations and minimum viscous energy loss [35]. After three-dimensional reconstruction of the arterial tree from orthogonal cineangiograms in

humans, Seiler et al [35] calculated a ratio between area of the mother vessel and mean of the areas of the daughter vessels of 1.647, similar to the ratio predicted based on the previously mentioned principles (1.588). These considerations explain why only a moderate decrease of mean velocity, inversely proportional to the moderate increase in total cross-sectional area, occurs from proximal to distal in the epicardial coronary arteries. The maintenance of a relatively constant flow velocity despite the changes in cross-sectional area and in perfused myocardial bed partially limits the inaccuracy consequent to the lack of correction for the perfused myocardial mass which can not be easily determined in humans.

The changes of flow velocity can be considered a reliable indicator of the changes in coronary flow only in the presence of a constant cross-sectional area. The minimal reduction in cross-sectional area occurring during the meso-telediastolic phase of the cardiac cycle is likely to induce a negligible reduction in cross-sectional area and, consequently, a negligible underestimation of the true flow-pressure slope estimated from the flow velocity.

The IHDVPS assesses changes in coronary conductance which can be induced both by the presence of a severe epicardial stenosis and by the presence of an impaired vasodilatation of the coronary microvasculature. A different approach can be used to distinguish these two components of coronary resistance, but this approach requires the additional measurement of the post-stenotic pressure. Gould et al. [36] correlated in dogs the severity of experimentally induced coronary stenoses with the changes in the transstenotic pressure gradient-flow velocity relation. Using a high-fidelity pressure transducer mounted on an angioplasty guidewire in combination with a separate Doppler guidewire, this approach has been recently repeated in humans [22,37]. A different analysis of the same recordings can be performed to study the relation between flow velocity and post-stenotic pressure, an indicator of the maximal vasodilatory response of the distal coronary bed. When a high-fidelity pre- and post-stenotic pressure and flow velocity signals are available, two types of relation can be used to separate the functional characteristics of the stenosis and of the distal vascular bed: the instantaneous relation between transstenotic pressure and velocity, assessing the stenosis hemodynamics as in an isolated hydraulic model, independently from the hemodynamic conditions and from the properties of the distal vascular bed, and the relation between flow velocity and post-stenotic pressure, correlated to the conductance of the distal vasculature [22].

The instantaneous velocity-pressure relation for the assessment of the zero-flow pressure

The extrapolation of the pressure-flow relation during a long diastolic pause was used in the original report by Bellamy [38] to assess the pressure at zero flow. His observation that $P_{f=0}$ was higher than the coronary venous pressure has initiated a great deal of experimental work to better define mechanism and physiologic and clinical importance of this phenomenon.

Mechanisms of regulation of the $P_{f=0}$

Bellamy, discussing the importance of a $P_{f=0}$ greater than the coronary venous pressure as a determinant of coronary resistance [39], interpreted this phenomenon as the effect of a vascular waterfall due to active vascular constriction or to the effect of a tissue pressure higher than the intravascular pressure. The lack of a direct demonstration of vascular collapse at the arteriolar level and the persistence of venous outflow after cessation of the arterial flow [40] have suggested alternative mechanisms. The effect of capacitative flow due to the blood stored in the extramural coronary arteries and discharged into the myocardium because of the progressive reduction of epicardial arterial volume at low pressures, suggests that the $P_{f=0}$ at the microvascular level is overestimated by a measurement in a proximal artery. After correction for the capacitative effects, Eng et al. [41] calculated a $P_{f=0}$ similar to the right atrial pressure during maximal hyperemia. Canty et al. [42], however, confirmed the persistance of a $P_{f=0}$ during maximal hyperemia greater than venous pressure using a capacitance free model. The presence of a large intramyocardial compliance with long time-constants for blood discharge has been proposed as a model alternative to the presence of a vascular waterfall to explain the cessation of flow in the epicardial arteries at a pressure higher than the right atrial pressures [43]. Whatever mechanism is involved in the regulation of the $P_{f=0}$, there is a consensus that the presence of an elevated $P_{f=0}$ (up to 50 mmHg) occurs only in conditions of coronary autoregulation and that much lower pressures are present at the cessation of the arterial flow when the coronary vasculature is maximally vasodilated [44].

Morphology of the diastolic pressure-flow relation

The diastolic flow-pressure relation during maximal hyperemia was found to be concave upwards towards the flow axis in many experimental reports [41,42,45]. This curvilinearity may be explained by a discharge of blood from the upstream epicardial vessels and by a progressive increase in vascular resistance due to the pressure-dependent decrease of arterial diameter [45]. If this curvilinearity is ignored or if the pressure-flow relation is not explored in the low pressure range, falsely elevated measurements of $P_{f=0}$ are obtained. In this study the measurements were obtained during a long diastolic pause, with pressures at the end of the period of cardiac arrest < 45 mmHg. However, the use of flow velocity instead of flow introduced an additional bias in the estimation of the pressure-flow relation. If the arterial cross-section at the site of the velocity measurement is reduced simultaneously to the reduction in flow velocity, the velocity decrease underestimates the true flow reduction. The phenomenon is relevant for flow velocity measurements obtained in the low pressure range because a curvilinear relation between distending pressure and arterial cross-section is present, with larger changes in cross-section in the low pressure range [46]. Therefore, the marked curvilinearity present in the flow velocity-pressure relation at low pressures, without a positive intercept with the pressure axis, precluded the use of the flow velocity-pressure relation for the assessment of the $P_{f=0}$. The simultaneous use of intracoronary Doppler and two-dimensional ultrasound imaging has the potential to overcome this limitation and allow the estimation of the $P_{f=0}$ in conscious humans in the catheterization laboratory [47]. In the physiologic

range of pressures, however, the relation between flow velocity and pressure remained linear so that linear regression could be used to estimate arterial conductance.

CONCLUSION

The instantaneous velocity-pressure relation during maximal hyperemia can be reliably assessed using intracoronary Doppler in the catheterization laboratory, is highly reproducible, has a moderate beat-to-beat variability and is independent from heart rate, aortic pressure or indexes of left ventricular contractility-relaxation at the time of the assessment. The slope of this relation can distinguish arteries with and without significant coronary stenoses, suggesting that this index is a potential alternative to coronary flow reserve for the assessment of stenosis severity.

The curvilinearity of the velocity-pressure relation during long diastolic pauses precludes the use of the flow velocity-pressure relation for the assessment of the zero-flow pressure.

ACKNOWLEDGMENTS

The contribution to the acquisition of the data by the medical, technical and nursing staff of the Catheterization Laboratory is gratefully acknowledged. Dr. P.D. Verdouw and Dr. C.J. Slager are acknowledged for their contribution and suggestions in the preparation of this manuscript.

REFERENCES

1. Reiber JHC, Serruys PW, Kooijman CJ, Wijns W, Slager CJ, Gerbrands JJ, et al. Assessment of short-, medium-, and long-term variations in arterial dimensions from computer-assisted quantitation of coronary cineangiograms. *Circulation* 1985;71:280-8.
2. Tenaglia AN, Buller CE, Kisslo KB, Stack RS, Davidson CJ. Mechanisms of balloon angioplasty and directional coronary atherectomy as assessed by intravascular ultrasound. *J Am Coll Cardiol 1992*; 20: 685-91.
3. Young DF, Cholvin NR, Roth AC. Pressure drop across artificially induced stenoses in the femoral arteries of dogs. *Circ Res* 1975; 36: 735-43.
4. Lipscomb K, Hooten S. Effect of stenotic dimensions and blood flow on the hemodynamic significance of model coronary arterial stenoses. *Am J Cardiol* 1978; 42: 781-92.
5. Serruys PW, Reiber JHC, Wijns W, van den Brand M, Kooijman CJ, ten Katen HJ, et al. Assessment of percutaneous transluminal coronary angioplasty by quantitative coronary angiography: diameter versus densitometric area measurements. *Am J Cardiol* 1984; 54: 482-8.
6. Araujo LI, Lammertsma AA, Rhodes CG, McFalls EO, Iida H, Rechavia E, et al. Non-invasive quantification of regional myocardial blood flow in coronary artery disease with oxygen-15-labeled carbon dioxide inhalation and positron emission tomography. *Circulation* 1991; 83: 875-85.
7. Krivokapich J, Huang SC, Schelbert HR. Assessment of the effects of dobutamine on myocardial blood flow and oxidative metabolism in normal human subjects using nitrogen-13 ammonia and carbon-11 acetate. *Am J Cardiol* 1993; 71: 1351-6.

8. Gould KL. Identifying and measuring severity of coronary artery stenosis. Quantitative coronary arteriography and positron emission tomography. *Circulation* 1988; 78: 237-45.
9. Gould KL, Lipscomb K, Hamilton GW. Physiologic basis for assessing critical coronary stenosis. Instantaneous flow response and regional distribution during coronary hyperemia as measures of coronary flow reserve. *Am J Cardiol* 1974;33:87-94.
10. Klocke FJ. Measurements of coronary flow reserve: defining pathophysiology versus making decisions about patient care. *Circulation* 1987;76:1183-9.
11. McGinn AL, White CW, Wilson RF. Interstudy variability of coronary flow reserve. Influence of heart rate, arterial pressure and ventricular preload. *Circulation* 1990; 81: 1319-30.
12. Rossen JD, Winniford MD. Effect of increases in heart rate and arterial pressure on coronary flow reserve in humans. *J Am Coll Cardiol* 1993; 21: 343-8.
13. Wilson RF, Marcus ML, White CW. Prediction of the physiologic significance of coronary arterial lesions by quantitative lesion geometry in patients with limited coronary artery disease. *Circulation* 1987;75:723-32.
14. Harrison DG, White CW, Hiratzka LF, Doty DB, Barnes DH, et al. The value of lesion cross-sectional area determined by quantitative coronary angiography in assessing the physiologic significance of proximal left anterior descending coronary artery stenoses. *Circulation* 1984; 69: 1111-9.
15. Zijlstra F, van Ommeren J, Reiber JHC, Serruys PW. Does the quantitative assessment of coronary artery dimensions predict the physiologic significance of a coronary stenosis? Circulation 1987; 75: 1154-61.
16. Laarman GJ, Serruys PW, Suryapranata H, van der Brand M, Jonkers PR, de Feyter PJ, et al. Inability of coronary flow reserve measurements to assess the efficacy of coronary angioplasty in the first 24 hours in unselected patients. *Am Heart J* 1991; 122: 631-9.
17. Wilson RF, Johnson MR, Marcus ML, Aylward PEG, Skorton DJ, Collins S, et al. The effect of coronary angioplasty on coronary flow reserve. *Circulation* 1988; 77: 873-85.
18. Serruys PW, Juilliere Y, Zijlstra F, Beatt KJ, De Feyter PJ, Suryapranata H, et al. Coronary blood flow velocity during percutaneous transluminal coronary angioplasty as a guide for assessment of the functional result. *Am J Cardiol* 1988;61:253-259.
19. Kern MJ, Deligonul U, Vandormael M, Labovitz A, Gudipati CV, Gabliani G, et al. Impaired coronary vasodilator reserve in the immediate postcoronary angioplasty period: analysis of coronary artery flow velocity indexes and regional cardiac venous efflux. *J Am Coll Cardiol* 1989;13:860-72.
20. Segal J, Kern MJ, Scott NA, King SB III, Doucette JW, Heuser RR, Ofili E, et al. Alterations of phasic coronary artery flow velocity in humans during percutaneous coronary angioplasty. *J Am Coll Cardiol* 1992;20:276-86.
21. Ofili EO, Kern MJ, Labovitz AJ, St. Vrain J, Segal J, Aguirre FV, et al. Analysis of coronary blood flow velocity dynamics in angiographically normal and stenosed arteries before and after endolumen enlargement by angioplasty. *J Am Coll Cardiol* 1993; 21: 308-16.
22. Serruys PW, Di Mario C, Meneveau N, de Jaegere P, Strikwerda S, de Feyter PJ, et al. Intracoronary pressure and flow velocity from sensor tip guidewires: a new methodological approach for assessment of coronary hemodynamics before and after coronary interventions. *Am J Cardiol* 1993; 71: 41D-53D.
23. Uren NG, Crake T, Lefroy DC, de Silva R, Davies GJ, Maseri A. Delayed recovery of coronary resistive vessel function after coronary angioplasty. *J Am Coll Cardiol* 1993; 21: 612-21.
24. Mancini GBJ, Mc Gillem MJ, DeBoe SF, Gallagher KP. The diastolic hyperemic flow versus pressure relation: a new index of coronary stenosis severity and flow reserve. *Circulation* 1989; 80: 941-50.
25. Mancini GBJ, Cleary RM, DeBoe SF, Moore NB, Gallagher KP. Instantaneous hyperemic flow-versus-pressure slope index. Microsphere validation of an alternative to measures of coronary reserve. *Circulation* 1991; 84: 862-70.
26. Cleary RM, Aron D, Moore NB, DeBoe SF, Mancini GBJ. Tachycardia, contractility and volume loading alter conventional indexes of coronary flow reserve, but not the instantenous hyperemic flow versus pressure slope index. *J Am Coll Cardiol* 1992; 20: 1261-9.
27. Cleary RM, Moore NB, DeBoe SF, Mancini GBJ. Sensitivity and reproducibility of the

instantaneous hyperemic flow versus pressure slope index compared to coronary flow reserve for the assessment of stenosis severity. *Am Heart J* 1993; 126: 57-65.

28. Doucette JW, Corl PD, Payne HM, Flynn AE, Goto M, Nassi M, et al. Validation of a Doppler guide wire for intravascular measurement of coronary artery flow velocity. *Circulation* 1992;85:1899-911.
29. Serruys PW, Di Mario C, Kern MJ. Intracoronary Doppler. In Topol EJ (ed) Textbook of Interventional Cardiology (2nd ed). Philadelphia, Saunders, 1993, in press.
30. Zijlstra F, Serruys PW, Hugenholtz PG. Papaverine: the ideal coronary vasodilator for investigating coronary flow reserve? A study of timing, magnitude, reproducibility and safety of the coronary hyperemic response after intracoronary papaverine. *Cathet Cardiovasc Diagn* 1986;12:298-303.
31. Serruys PW, Wijns W, van den Brand M, Mey S, Slager C, Schuurbiers JHC, et al. Left ventricular performance, regional blood flow, wall motion, and lactate metabolism during transluminal angioplasty. *Circulation* 1984; 70: 25-36.
32. Haase J, Di Mario C, Slager CJ, van der Giessen WJ, den Boer A, de Feyter PJ, et al. In-vivo validation of on-line and off-line geometric coronary measurements using insertion of stenosis phantoms in porcine coronary arteries. *Cathet Cardiovasc Diagn* 1992;27:16-27.
33. Di Mario C, Roelandt JRTC, de Jaegere P, Linker DT, Oomen J, Serruys PW. Limitations of the zero-crossing detector in the analysis of intracoronary Doppler: a comparison with fast Fourier transform analysis of basal, hyperemic and transstenotic blood flow velocity measurements in patients with coronary artery disease. *Cathet Cardiovasc Diagn* 1992; 28: 56-64.
34. Zar JH. Biostatistical analysis (2nd ed). Englewood Cliffs: Prentice Hall, 1984.
35. Seiler C, Kirkeeide RL, Gould KL. Basic structure-function relations of the epicardial coronary vascular tree. Basis of quantitative coronary angiography for diffuse coronary artery disease. *Circulation* 1992; 85: 1987-2003.
36. Gould KL. Coronary artery stenosis". New York: Elsevier, 1991:41-52.
37. Di Mario C, de Feyter PJ, Slager CJ, de Jaegere P, Roelandt JRTC, Serruys PW. Intracoronary blood flow velocity and transstenotic pressure gradient using sensor-tip pressure and Doppler guidewires: a new technology for the assessment of stenosis severity in the catheterization laboratory. *Cathet Cardiovasc Diagn* 1993; 28: 311-9.
38. Bellamy RF. Diastolic coronary artery pressure-flow relation in the dog. *Circ Res* 1978; 43: 92-101.
39. Bellamy RF. Calculation of coronary vascular resistance. *Cardiovasc Res* 1980; 14: 261-9.
40. Chilian WM, Marcus ML. Coronary venous outflow persists after cessation of coronary arterial inflow. *Am J Physiol* 1984; 247: H984-H990.
41. Eng C, Jentzer JH, Kirk ES. The effects of the coronary capacitance on the interpretation of the diastolic pressure-flow relationships. *Circ Res* 1982; 50: 334-41.
42. Canty JM Jr, Klocke FJ, Mates RE. Characterization of capacitance-free pressure-flow relations during single diastoles in dogs using an RC model with pressure dependent parameters. *Circ Res* 1987; 60:273-82.
43. Spaan JAE. Coronary diastolic pressure-flow relation and zero flow pressure explained on the basis of intramyocardial compliance. *Circ Res* 1985; 56: 293-309.
44. Hoffman JIE, Spaan JAE. Pressure-flow relations in coronary circulation. *Physiol Rev* 1990; 70: 331-390.
45. Klocke FJ, Weinstein IR, Klocke JF, Ellis AK, Kraus DR, Mates RE, et al. Zero-flow pressures and pressure-flow relationships during single long diastoles in the canine coronary bed before and during maximum vasodilatation. Limited influence of capacitative effects. *J Clin Invest* 1981; 68: 970-80.
46. Nichols WW, O'Rourke MF. Properties of the arterial wall. In McDonald's blood flow in arteries: theoretic, experimental and clinical principles. 3rd ed. London: Edwards Arnold, 1990: 77-124.
47. Sudhir K, MacGregor JS, Brzabant SD, Foster E, Fitzgerald PJ, Chatterjee K, et al. Assessment of coronary conductance and resistance vessel reactivity in response to nitroglycerin, ergonovine and adenosine: in vivo studies with simultaneous intravascular two dimensional and Doppler ultrasound. *J Am Coll Cardiol* 1993; 21: 1261-8.

CHAPTER 14

RESPONSE OF CONDUCTANCE AND RESISTANCE CORONARY VESSELS TO SCALAR CONCENTRATIONS OF ACETYLCHOLINE

Assessment with quantitative angiography and intracoronary Doppler in 29 patients with coronary artery disease

Carlo Di Mario, M.D., Sipke Strikwerda, M.D., Ph.D., Robert Gil, M.D., Pim J. de Feyter, M.D., Ph.D., Peter de Jaegere, M.D., Ph.D., Patrick W. Serruys, M.D., Ph.D.

From the Cardiac Catheterization Laboratory, Division of Cardiology, Thoraxcenter, Erasmus University, Rotterdam

Reprint from Serruys PW, Foley DP, de Feyter PJ (eds). QCA in clinical practice. Dordrecht, Kluwer Academic Publishers, 1993.

19. Response of conductance and resistance coronary vessels to scalar concentrations of acetylcholine. Assessment with quantitative angiography and intracoronary doppler in 29 patients with coronary artery disease

CARLO DI MARIO, SIPKE STRIKWERDA, ROBERT GIL, PIM J. DE FEYTER, NICOLAS MENEVEAU and PATRICK W. SERRUYS

The in vitro observations of Furchgott and Zawadzki [1] and the in vitro and in vivo reports from the group of Moncada [2, 3] have shown that an endothelium-derived-relaxing-factor, identified as nitric oxide [2], modulates vascular tone in response to physiologic and pathologic stimuli (increase in wall shear stress, serotonin, bradykinin, histamine, thrombin, sympathetic stimulation, acetylcholine, endotoxins, etc.). Endothelial damage, leading to a decreased formation or release of nitric oxide from its precursor L-arginine, or reduced penetration due to the presence of subendothelial intimal thickening, are possible explanations of the impairment of endothelium-mediated vasodilatation observed in patients with systemic hypertension [4], hypercholesterolemia, diabetes mellitus [5], atherosclerosis [6].

The presence of paradoxical vasoconstriction induced by acetylcholine has been shown in coronary patients at sites of severe stenosis or moderate wall irregularities [7] and in angiographically normal segments [8–10]. Coronary spasm after acetylcholine infusion has also been demonstrated in patients with variant angina, with and without angiographically visible changes [11, 12]. The observed vasoconstriction or vasodilatation after acetylcholine is the net effect of the conflicting action of this substance on the endothelial cells (stimulation to the release of endothelium-derived relaxing factor) and on the smooth muscle cells (vasoconstriction due to the direct effect on the cholinergic receptors). With the use of intracoronary Doppler, an impairment of the endothelial derived vasodilatation was observed also after more physiologic stimuli such as the increase of blood flow [13–15]. The flow dependent vasodilatation is an essential mechanism of adjustment of coronary tone to prevent endothelial damage due to a pathologic increase in wall shear stress [12]. An abnormal vasoconstriction in response to sympathetic stimulation [16] or release of platelet-derived vasoconstrictors [17, 18] was observed if the direct effect of these substances on the muscular media was not antagonized by a preserved endothelium-mediated vasodilatation. Nitric oxide has also a powerful anti-aggregatory activity. Yao et al. [19] showed a protective effect of endogenous nitric oxide in the prevention of cyclic flow variations due to platelet aggregation at the site of endothelial injury. Endothelial

P.W. Serruys, D.P. Foley and P.J. de Feyter (eds.), Quantitative Coronary Angiography in Clinical Practice, 329–353.

dysfunction, therefore, is not only a potential mechanism of aggravation of ischemia in patients with coronary atherosclerosis but it increases the risk of endothelial injury and impairs the antithrombotic reaction, thus facilitating the development of acute coronary syndromes and the release of platelet-derived growth factors which may predispose to progression of atherosclerosis. An impairment of endothelium-mediated vasodilatation has been shown in patients with risk factors for coronary atherosclerosis but without angiographically visible atherosclerotic changes [9, 20]. A possible limitation of these studies is the poor sensitivity of angiography in the detection of early atherosclerotic changes. More recently, the presence of endothelial dysfunction also in patients with structurally normal coronary arteries but with hypertension, hyyperlipidemia, family history of coronary artery disease or smoking has been confirmed using two-dimensional intracoronary ultrasound [21]. A complete loss of endothelium-mediated vasodilatation was present in arteries with angiographically visible atherosclerotic changes. Angiographically normal arteries of patients with hypercholesterolemia showed a normal flow-mediated vasodilatation following papaverine but an abnormal vasoconstriction after acetylcholine [21].

The possible presence of opposite effects of acetylcholine infusion on epicardial and resistance coronary arteries have been reported by Hodgson et al. [22]. The observed increase of coronary flow after acetylcholine was prevented by the pretreatment with methylene blue, an inhibitor of endothelium-derived relaxing factor. Zeiher et al. [23] reported a significantly lower flow increase after acetylcholine in patients with coronary artery disease than in control subjects. These findings confirmed previous experimental results showing that the impairment of endothelial function in atherosclerotic arteries may extend into the coronary microcirculation [24–26]. The presence of an impaired endothelium-dependent vasodilatation of the resistance vessels may induce or facilitate the development of myocardial ischemia in response to neurohumoral stimulation or increased myocardial work [27]. The epicardial arteries and the arterioles have large structural differences and show a different involvement in the atherosclerotic process, mainly confined to the large epicardial coronary arteries. Both types of arteries, however, are likely to show a similar response to pathologic stimuli on the endothelial cells impairing the intracellular production and release of nitric oxide. The presence of an impaired diffusion or of an increased extracellular degradation of nitric oxide in the thickened intima is a phenomenon limited to the epicardial arteries and may explain an earlier and more severe impairment of the endothelium-mediated vasodilatation of these vessels.

Aim of this study is the simultaneous assessment of the endothelium-mediated vasodilatation of conductance and resistance vessels in coronary arteries without significant stenosis (<30% diameter stenosis). During selective infusion of scalar increasing concentrations of acetylcholine the changes of coronary cross-sectional area over a proximal/mid segment and a distal segment of the studied artery were measured with quantitative coronary

angiography and correlated with the changes in coronary flow, derived from the flow velocity measured with a Doppler guidewire and used as an index of vasodilatory response of the resistance vessels.

Methods

Patient population

Twenty-nine patients (age 57 ± 9 years, 24 men and 5 women) undergoing elective percutaneous transluminal angioplasty because of disabling stable angina pectoris were studied. Previous myocardial infarction was present in 8/29 patients (26%), in no cases involving the territory of distribution of the studied artery. Systemic hypertension was defined as a chronically elevated arterial blood pressure (≥150/90 mmHg) and was present in 9/29 patients (31%). Three patients were current smokers (10%). A previous history of smoking was present in 18 patients (62%). No patient had anemia (mean hemoglobin 8.8±0.57 mmol/l) or anamnestic/biohumoral signs of diabetes mellitus or hyperthyroidism. The angiographic selection criteria included absence of >30% diameter stenosis in one of the 3 major coronary arteries without visible collaterals originating from this vessel and with a normal left ventricular contraction of the segments of distribution of the studied artery. Angiographically visible wall irregularities were present in 19/29 patients (66%). The studied artery was the left anterior descending coronary artery in 7 patients (24%), the left circumflex in 13 (45%) and the right coronary artery in 9 (31%). Written informed consent was obtained in all cases. The protocol was approved by the Ethics Committee Erasmus University-Rotterdam Dijkzigt Hospital (protocol #MEC 114.542/1991/61). All vasoactive medication, with the exclusion of short-acting sublingual nitrates, was withheld at least 48 hr before the catheterization. No sublingual, intravenous or intracoronary nitrates were used in the 6 hr before or during the catheterization procedure.

Catheterization procedure

After systemic anticoagulation with 10,000 I.U. of heparin and 250 mg of acetylsalicylic acid intravenously and sedation with 5–10 mg diazepam intravenously, the artery to be studied was instrumented using a 9F giant lumen (inner lumen = 0.084″) Amplatz or Judkins guiding catheter (left coronary artery) or a 7F Judkins diagnostic catheter (right coronary artery). A 0.018″ Doppler angioplasty guidewire was then advanced to a normal or near-normal straight proximal segment of the artery to be studied where a stable flow velocity signal could be obtained. A 3.6 F flexible infusion catheter (Tracker 25, Target Therapeutics, San Jose, CA) was then inserted over the Doppler wire into the proximal segment of the coronary artery in order to

obtain a selective injection into the left anterior descending or left circumflex artery [28]. Care was taken to avoid a too selective cannulation of the large guiding catheter into the left main coronary artery in order to avoid limitation of flow during maximal hyperemia. For the right coronary artery a selectively engaged 7 F diagnostic catheter was used for the infusion. Heart rate and mean aortic pressure were automatically measured using a previously described computer-assisted system [29] by averaging 16 consecutive seconds of recording. After the baseline acquisition of flow velocity, heart rate and blood pressure, the measurements were repeated 30 s after a bolus injection of 7 mg of papaverine diluted in 1.5 ml. After a recovery period of 8 min, new basal measurements were performed followed by a cineangiogram suitable for quantitation. Scalar concentrations of acetylcholine at 37°C (0.036, 0.36, 3.6 μg/ml) were infused at a flow rate of 2 ml/min using a precision pump-injector (Mark V, Medrad, Pittsburgh, PA). With these dilutions and flow rates and assuming a coronary blood flow of 80 ml/min in the studied artery, intracoronary blood concentrations of 10^{-8}, 10^{-7} and 10^{-6} M were estimated. Five min after the beginning of the infusion of each concentration blood flow velocity and hemodynamic measurements were acquired and a new cineangiogram performed. Five min after the end of the series of acetylcholine infusions a new baseline flow velocity was acquired and, 1 min after a bolus injection of 3 mg of isosorbide dinitrate, a new cineangiogram was performed.

Doppler guidewire and flow velocity measurements

The Doppler angioplasty guidewire is a 0.018″ (diameter = 0.46 mm) 175 cm long flexible and steerable guidewire with a floppy shapable distal end mounting a 12 MHz piezoelectric transducer at the tip (FloWire, Cardiometrics Inc., Mountain View, CA). The sample volume was positioned at a distance of 5.2 mm from the transducer in order to avoid the area of distortion of flow profile due to the presence of the Doppler guidewire. At this distance the sample volume has approximately a diameter of 2.25 mm due to the divergent ultrasound beam so that a large part of the flow velocity profile is included in the sample volume even in case of eccentric position of the Doppler guidewire. In order to increase the reliability of the analysis of the Doppler signal [30] a real-time fast-Fourier transform algorithm was applied to the quadrature audio signal. The Doppler system used (FloMap, Cardiometrics, Mountain View, CA) performs a real-time spectral analysis of the Doppler signal and calculates and displays on-line several spectral variables including the instantaneous peak velocity and the time-averaged (mean of 2 beats) peak velocity (Fig. 1). The flow velocity measurements obtained with this system have been validated in vitro and in an animal model using simultaneous electromagnetic flow measurements for comparison [31]. Coronary flow reserve was defined as the ratio between maximal flow velocity at the peak effect of the papaverine injection and in baseline conditions.

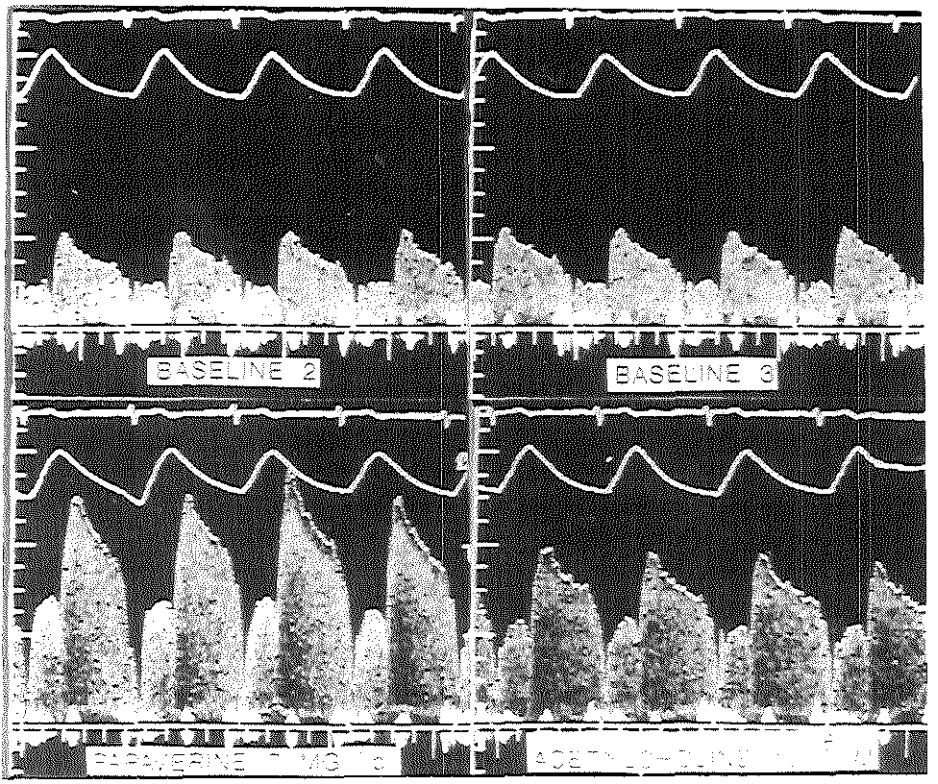

Figure 1. Flow velocity measurement in a proximal left circumflex artery before the injection of increasing concentrations of acetylcholine (Baseline 2), 5 min after the end of the infusion of acetylcholine (Baseline 3) and at the peak effect of papaverine and acetylcholine 10^{-6}M. Note the stable flow velocity in baseline condition, the large velocity increase after papaverine and the moderate increase after the maximal concentration of acetylcholine. APV = time-averaged peak velocity.

Electrocardiogram, coronary pressure and peak coronary blood flow velocity were continuously sampled at 125 kHz per channel using a 12 bits analog-to-digital converter. The ACodas software package (DataQ Instr., Akron, OH) was used for off-line analysis.

Quantitative angiographic measurements

The preformed coronary catheter, filmed not filled with contrast medium, was used as a scaling device [32]. Before the study, when necessary, a previously validated on-line analysis system operating on digital images (ACA-DCI, Philips, Eindhoven, The Netherlands) [33] was used to exclude the presence of > 30% diameter stenosis. Coronary angiography was per-

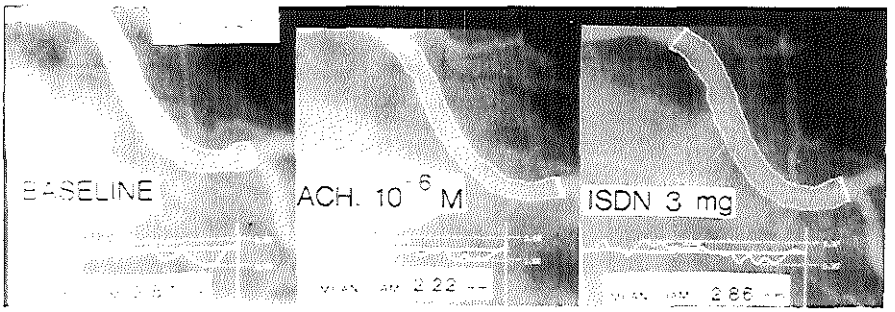

Figure 2. Quantitative angiographic measurements of the mean diameter of a proximal segment of the left circumflex artery. Two side branches are used as landmark to facilitate consistent repeated measurements of the same segment throughout the procedure. Note the severe decrease in mean coronary diameter (−22%) after the maximal concentration of acetylcholine (Ach 10^{-6} M). ISDN = isosorbide dinitrate.

formed with a manual injection of 6–10 ml of iopamidol (Iopamiro 370, Schering, Berlin, Germany). A 5″ or 7″ field-of-view of the image intensifier was used. No changes of the position of the patient or of the X-ray gantry were performed throughout the procedure. The same angiographic view was maintained during the study, avoiding foreshortening or vessel superimposition of the arterial segments of interest. A previously validated [34] cine-film based off-line system (CAAS System, Pie Medical Data, Maastricht, The Netherlands) was used to measure the mean diameter over a 2–3 cm long proximal/mid and distal coronary segment, using easily visible side-branches as anatomical landmarks to allow the analysis of the same segments in the successive cineangiograms (Fig. 2). In 14 cases (48%) a second order arterial branch (diagonal, obtuse marginal, postero-lateral, right ventricular branch) was analyzed as distal segment. In the remaining cases (15, 52%) the distal segment of one of the three major coronary arteries was used. After automatic detection of the vessel centerline, the system applies a weighted first and second derivative function with predetermined continuity constraints to the brightness profile of each scan line perpendicular to the vessel centerline [35]. A user-defined reference diameter was measured at the site of the Doppler sample volume [36]. Cross-sectional area was calculated from the corresponding diameter assuming a circular arterial cross-section. Coronary flow was calculated as:

$$\text{Coronary flow (ml/min)} = \text{CSA}(\text{mm}^2)\,\frac{\text{Time-Averaged Peak Vel (cm/s)}}{2}\,0.6$$

where CSA is the arterial cross-sectional area at the site of the Doppler sample volume. Coronary flow resistance was calculated as:

$$\text{Cor. flow resistance (mmHg·min·ml}^{-1}\text{)} = \frac{\text{Mean aortic pressure (mm Hg)}}{\text{Coronary flow (ml/min)}}$$

Statistical analysis

The significance of the differences between flow velocity and cross-sectional area measurements and derived indexes in baseline conditions and after papaverine, acetylcholine and isosorbide dinitrate was tested using a two-tailed Student's t test for paired data. A two-tailed Student's t test for unpaired data was used to compare the diameter and flow changes observed in patients with different clinical angiographic characteristics. Linear regression analysis was used to correlate the changes observed in cross-sectional area and in coronary flow and in coronary flow resistance. Analysis of variance for repeated measurements was used to test the time-response and the variability of the flow velocity changes after infusion of acetylcholine. Statistical significance was defined as $p < 0.05$. All data were expressed as mean±SD.

Results

The heart rate was stable throughout the study, with a significant increase in heart rate only after the bolus injection of isosorbide-dinitrate (Fig. 3A). In two cases during the maximal infusion of acetylcholine short lasting epysodes of Mobitz I atrio-ventricular block, not requiring ventricular pacing, were observed.

Aortic pressure was stable in baseline conditions and during the infusion of the different concentrations of acetylcholine. A slight but significant decrease was observed at the peak effect of the papaverine and isosorbide-dinitrate infusions (− 7 and − 5%, respectively) (Fig. 3B).

Flow velocity changes

Table 1 reports the individual changes in blood flow velocity in the studied patients.

In Fig. 4 the changes of time-averaged peak blood flow velocity were expressed as a percent of the baseline velocity (baseline 2). A moderate decrease of blood flow velocity was observed between the first baseline measurement (beginning of the study) and the second/third baseline measurement (5 min after papaverine and after the maximal concentration of acetylcholine, respectively, $p < 0.05$). On the contrary, a large increase was observed after papaverine injection, with a peak velocity 2.8±0.83 times higher than in basal conditions (baseline 2). The lowest concentration of

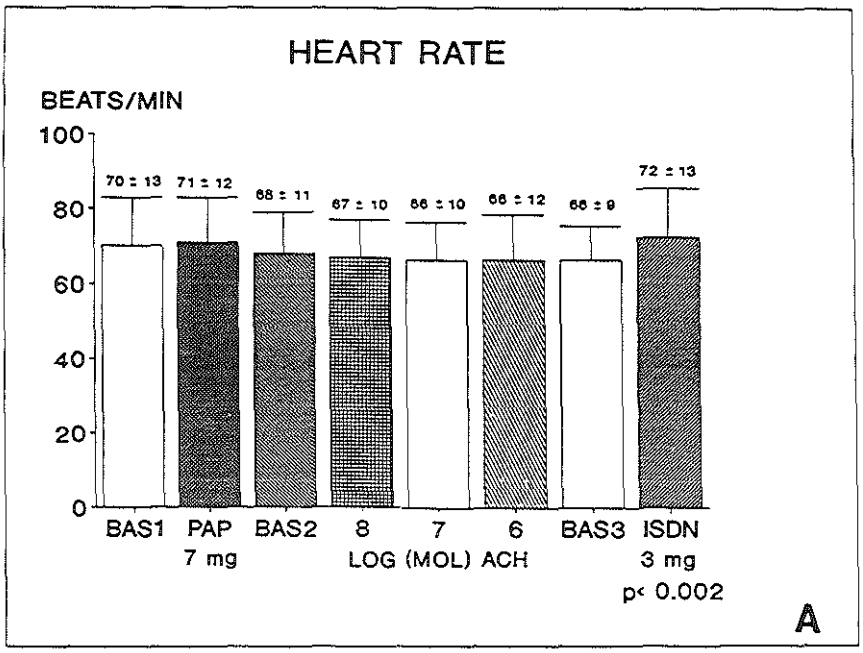

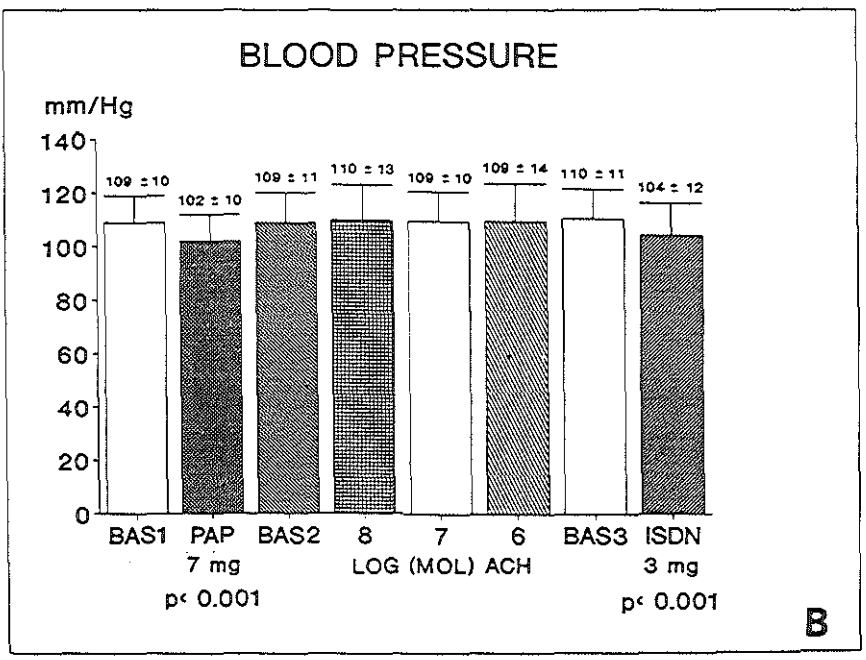

Figure 3. A) Heart rate and B) mean aortic blood pressure during the various phases of the study. ACH: acetylcholine; BAS: baseline; ISDN: isosorbide dinitrate.

Table 1. Clinical characteristics and flow velocity changes after papaverine and acetylcholine.

Patient	Age yrs	Sex	Hypert.	Choles mmol/l	Vessel	Wall irreg.	BAS1 cm/s	PAV cm/s	BAS2 cm/s	Ach 10^{-8} cm/s	Ach 10^{-7} cm/s	Ach 10^{-6} cm/s	BAS3 cm/s	ISDN cm/s
1	70	M	y	5.5	LAD	y	22	44	22	21	18	20	21	30
2	63	M	n	5.7	RCA	y	20	48	19	16	22	33	22	35
3	68	F	y	7.3	RCA	y	19	40	20	20	21	32	24	22
4	58	M	n	4.9	LCX	y	33	60	26	29	24	50	26	24
5	49	M	y	5.8	LCX	y	44	79	26	25	25	23	23	28
6	59	M	n	6.5	LCX	y	32	89	22	29	30	49	25	33
7	50	M	n	6.4	RCA	y	11	41	14	19	19	26	15	24
8	53	M	y	5.6	LCX	y	23	70	21	23	35	53	23	65
9	48	M	y	7.2	LAD	y	17	39	17	22	41	66	20	32
10	53	M	n	5.5	LAD	n	38	56	32	29	30	32	26	42
11	66	F	y	7.7	LCX	y	27	65	20	19	20	37	16	26
12	52	F	n	7.4	LCX	y	25	80	19	19	35	44	17	25
13	59	M	n	6.6	LCX	y	22	52	24	26	28	46	24	38
14	42	M	n	5.2	LCX	n	33	53	24	24	23	24	22	36
15	54	F	n	5.9	LCX	y	28	71	28	28	27	43	28	43
16	45	M	n	7.1	LCX	y	42	120	39	39	41	65	39	66
17	45	M	y	6.1	LAD	n	27	77	25	25	32	48	26	29
18	44	M	n	7.7	RCA	y	32	68	23	21	22	67	23	43
19	67	M	n	5.8	LAD	n	27	70	17	19	25	31	19	22
20	67	M	n	6.9	RCA	y	25	66	27	27	36	72	30	39
21	71	M	n	4.7	RCA	n	25	57	21	19	34	69	23	23
22	45	F	n	7.0	LAD	n	36	90	55	40	35	120	n.r.	n.r.
23	46	M	y	6.8	LAD	n	23	44	21	16	24	17	17	18
24	58	M	n	5.4	RCA	n	26	66	24	20	20	18	21	30
25	66	M	n	4.9	LCX	y	15	52	11	14	42	89	17	26
26	69	M	n	5.4	RCA	y	28	65	28	28	27	29	25	40
27	65	M	n	5.9	LCX	n	21	34	15	15	22	39	21	24
28	54	M	y	5.3	RCA	n	12	43	9	19	9	15	9	21
29	56	M	n	7.1	LCX	y	32	65	23	17	19	18	23	19
Mean	57			6.2			26	62**	23‡	23	27*	44**	22‡‡	32**
±SD	9			0.9			8	18	8	7	8	24	5	12

‡: $p < 0.02$ vs BAS1; ‡‡: $p < 0.005$ vs BAS1; *: $p < 0.05$ vs BAS2; **: $p < 0.002$ vs BAS2. Ach = acetylcholine; BAS = baseline; Choles = cholesterol; ISDN = isosorbide dinitrate; n.r. = not recorded; PAV = papaverine; yrs = years.

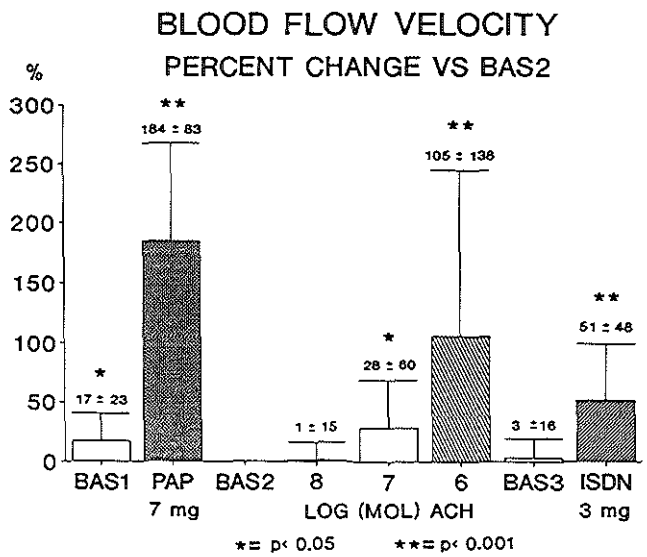

Figure 4. Flow velocity changes expressed as a percent of the baseline flow velocity. Legends as in Fig. 3.

acetylcholine did not induce significant changes in blood flow velocity. A 28±60% increase was observed after 5 min of infusion of acetylcholine 10^{-7} M ($p < 0.05$). At the end of the highest acetylcholine concentration (10^{-6} M) a more than twofold increase in flow velocity was observed (+ 105±138%, $p < 0.001$).

Time-response of the flow velocity change and flow velocity variability during acetylcholine infusion

In Fig. 5 the time-response of the flow velocity changes during the infusion of the maximal concentration of acetylcholine is reported for the entire group (Fig. 5–A) and for all the individual cases. A significant increase of flow velocity was observed within 30" from the beginning of the infusion. Afterwards, during the remaining infusion period, no significant flow velocity changes were observed in the overall study population. However, if the individual response is considered, only in 10 patients (Fig. 5–B) a relatively stable flow velocity was observed during infusion. In the remaining patients, despite the constant rate of infusion and the stable hemodynamic conditions, a large variability was observed, with cases showing a progressive increase or decrease during the final phase of infusion (Fig. 5–C and D, respectively) or a bell-shaped or biphasic response (Fig. 5–E and F, respectively; example in Fig. 6). The variability was more evident in the patients with a large velocity increase after acetylcholine.

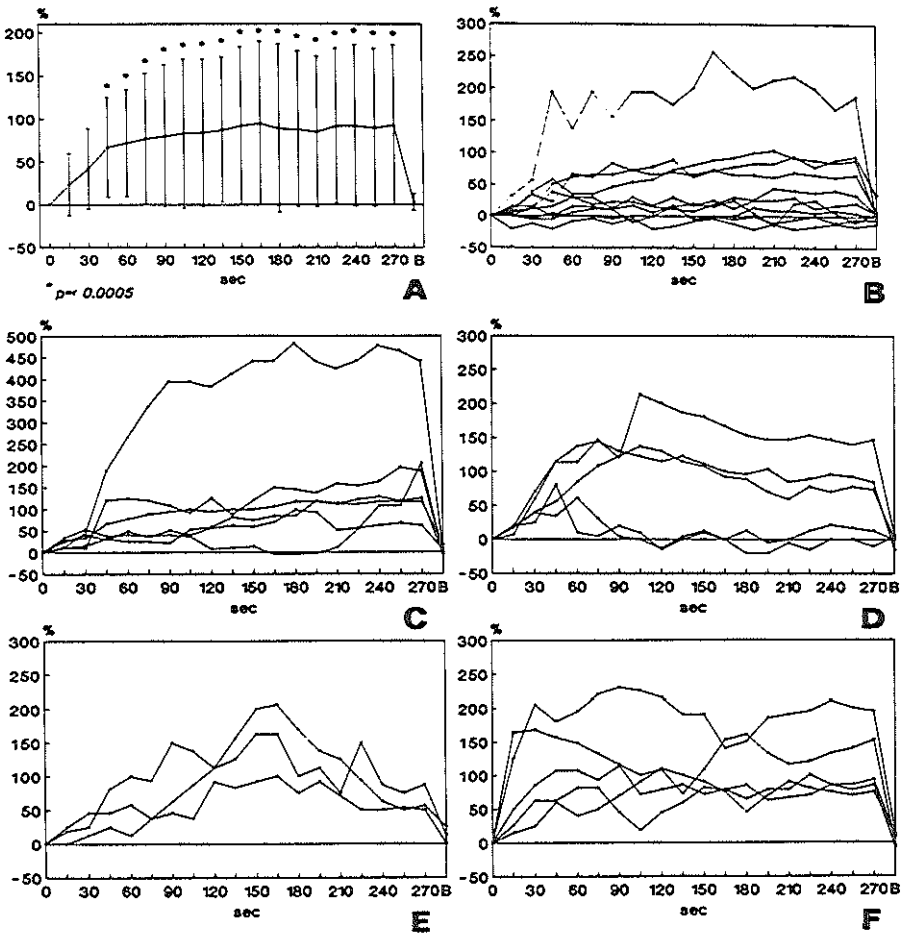

Figure 5. Temporal changes in flow velocity during infusion of the highest concentration of acetylcholine expressed as a percent of the value before infusion (time 0). A: mean±standard deviation; B: 10 individual curves showing a relatively stable flow velocity; C and D: 6 and 5 patients showing, respectively, a progressive increase and a progressive decrease from the beginning to the end of the infusion; E-F: 3 and 5 cases with a bell-shaped or a biphasic response during infusion. B: baseline 3 (5 min after the end of the acetylcholine infusion).

Coronary artery cross-sectional area

Table 2 indicates the individual measurements of the mean cross-sectional area of the proximal and distal coronary segments. In Fig. 7 the changes in cross-sectional area after the three increasing concentrations of acetylcholine and the bolus of isosorbide dinitrate are expressed as a percent of the basal cross-sectional area. The injection of the two lowest concentrations of

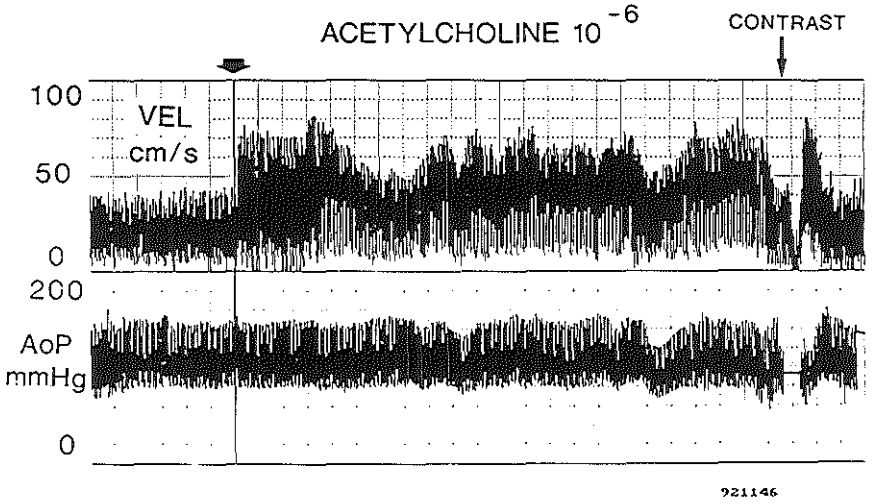

Figure 6. Continuous flow velocity (upper panel, VEL) and aortic pressure (lower panel, AoP) recorded continuously during the infusion of acetylcholine (10^{-6} M). Note the rapid increase in flow velocity after the beginning of inflation (arrow), followed by a moderate decrease in spite of a stable aortic pressure. Flow velocity variations are present also in the following minutes of infusion, before contrast injection (5 min).

acetylcholine induced a moderate but significant reduction of the mean cross-sectional area both in the proximal segment and in the distal segment. A larger decrease was observed after the highest concentration of acetylcholine ($-24 \pm 20\%$ and $-22 \pm 20\%$ of the mean cross-sectional area of the proximal and distal coronary segments, respectively, $p < 0.00001$). At this concentration almost all the studied arteries showed a variable degree of vasoconstriction (26/29 arteries, 90%), (Fig. 8-A). In no cases a $> 75\%$ mean cross-sectional area reduction was observed. At the end of the infusion of the highest concentration of acetylcholine, focal vasoconstriction of the more distal branches of the studied artery was observed in 8 patients. In these cases also quantitative angiography showed a more severe vasoconstriction ($-32 \pm 25\%$ vs $-18 \pm 22\%$ cross-sectional area reduction of the analyzed segments with and without focal arterial spasm, respectively, NS).

The presence of a preserved vasodilatory capacity of the studied artery was confirmed by the diffuse cross-sectional area increase after bolus injection of a direct smooth muscle vasodilator such as isosorbide dinitrate ($+16 \pm 26\%$ and $+18 \pm 26\%$ cross-sectional area increase vs baseline for the proximal and distal coronary segments, respectively, $p < 0.002$).

Coronary flow changes

A significant increase of coronary flow was observed only after the maximal concentration of acetylcholine ($+43 \pm 83\%$, $p < 0.001$). The large variability

Table 2. Quantitative angiographic changes after acetylcholine infusion.

Patient	Mean diameter proximal segment (mm)					Mean diameter distal segment (mm)				
	BAS	Ach 10^{-8}	Ach 10^{-7}	Ach 10^{-6}	ISDN	BAS	Ach 10^{-8}	Ach 10^{-7}	Ach 10^{-6}	ISDN
1	1.89	1.74	1.65	1.58	1.84	1.24	1.30	1.20	1.14	1.46
2	2.82	2.82	2.50	2.36	2.87	2.87	2.40	2.59	2.21	2.69
3	2.36	2.33	2.67	2.35	3.05	2.74	2.71	2.57	2.35	3.02
4	2.41	2.39	2.49	2.30	2.79	1.78	1.82	1.69	1.60	1.94
5	2.48	2.09	2.15	1.99	2.60	1.74	1.50	1.34	1.36	1.8
6	2.87	2.19	2.12	2.22	2.86	2.27	1.86	1.66	1.83	2.42
7	4.00	4.08	4.13	4.28	4.21	2.23	1.95	1.89	1.92	2.06
8	2.75	2.57	2.73	2.60	3.16	1.58	1.55	1.40	1.57	1.95
9	1.48	1.28	1.41	1.15	1.54	1.17	0.97	1.12	1.10	1.44
10	1.67	1.42	1.52	1.52	1.92	1.32	1.30	1.37	1.26	1.67
11	3.00	2.98	2.85	2.62	3.06	1.40	1.42	1.39	1.21	1.47
12	1.66	1.62	1.62	1.59	1.82	1.48	1.39	1.33	1.31	1.43
13	2.30	n.a.	1.97	1.38	2.02	2.15	n.a.	1.66	1.05	1.8
14	2.91	2.90	3.00	2.85	2.90	1.66	1.66	1.82	1.77	1.67
15	3.20	3.18	3.15	2.96	3.12	1.50	1.37	1.28	0.98	1.36
16	3.11	2.77	2.59	2.43	3.41	1.42	1.21	1.29	1.32	1.71
17	2.17	1.91	1.90	1.74	1.94	1.99	1.78	1.82	n.a.	1.77
18	2.69	2.51	2.54	2.41	2.96	1.33	1.21	1.26	1.40	1.52
19	2.59	2.28	2.23	2.07	2.62	1.60	1.32	1.31	1.30	1.76
20	3.13	2.52	2.72	2.42	3.16	1.78	1.57	1.67	1.69	1.83
21	2.96	3.27	3.14	3.15	3.57	1.71	1.73	1.54	1.60	2.08
22	1.52	1.43	1.62	1.49	2.21	1.36	1.46	1.42	1.09	1.99
23	2.22	2.24	2.06	2.12	2.26	1.76	1.76	1.74	1.88	2.12
24	3.03	2.70	2.91	2.41	3.23	2.35	2.23	2.35	2.31	2.62
25	2.28	1.90	1.77	1.39	2.37	1.66	1.55	1.48	1.18	1.94
26	2.72	2.72	2.71	2.41	3.20	1.74	1.74	1.67	1.42	2.11
27	2.47	2.40	1.96	1.91	2.63	1.11	1.17	0.95	1.09	1.23
28	3.16	3.22	3.28	3.28	3.09	1.90	1.77	1.73	1.67	1.75
29	2.47	2.26	2.18	1.81	2.68	1.46	1.31	1.29	1.29	1.56
Mean	2.56	2.42*	2.39*	2.23***	2.73**	1.73	1.61*	1.58**	1.50***	1.85*
±SD	0.56	0.62	0.62	0.66	0.60	0.43	0.38	0.39	0.38	0.42

*: $p < 0.002$ vs baseline; **: $p < 0.0005$ vs baseline; ***: $p < 0.00001$ vs baseline; Ach = acetylcholine; BAS = baseline; ISDN = isosorbide dinitrate.

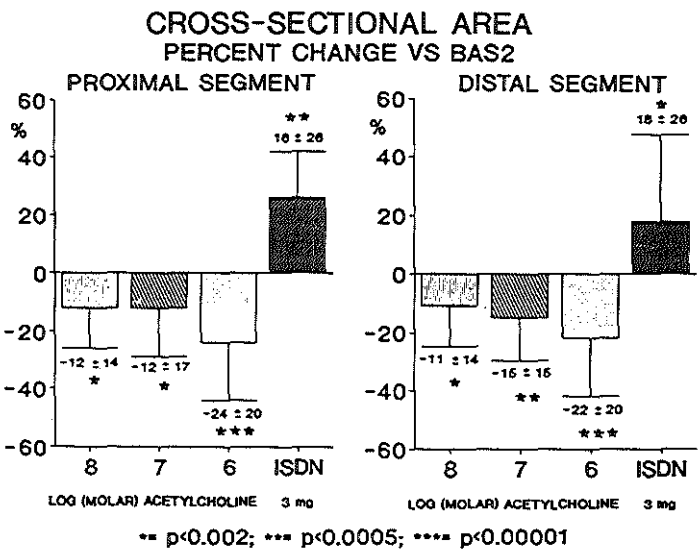

Figure 7. Mean cross-sectional area changes in the proximal and distal segment expressed as a percent of the baseline cross-sectional area. Legends as in Fig. 3.

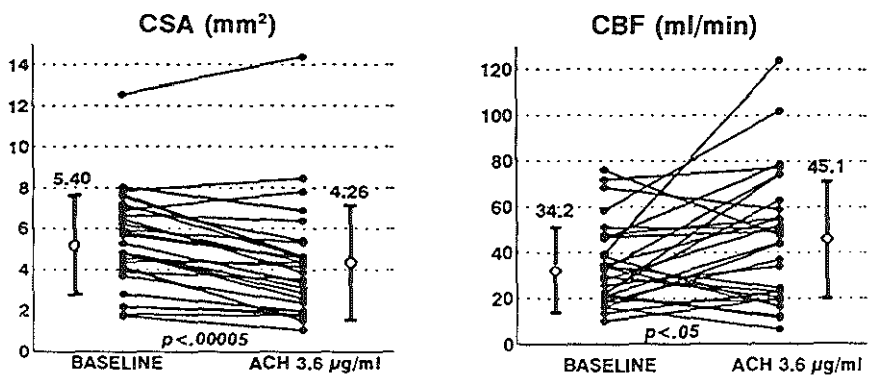

Figure 8. Cross sectional area (CSA) and coronary blood flow (CBF) in baseline conditions (baseline 2) and after infusion of the maximal concentration of acetylcholine (Ach 10^{-6} M). Note the almost uniform decrease in cross-sectional area and the large variability of the individual flow change.

of the individual measurements for the highest concentrations of acetylcholine is shown in Fig. 8-B. Note that at the peak concentration of acetylcholine 10 patients showed a decrease of absolute flow and increase in coronary resistance.

Correlation of the observed results with the clinical-angiographic characteristics

The flow velocity, cross-sectional area and flow changes after acetylcholine showed no correlation with age, sex, presence of systemic hypertension, total cholesterol, HDL cholesterol, HDL cholesterol/total cholesterol ratio, plasma triglycerides, type of studied artery and basal coronary luminal diameter.

The presence of wall irregularities was associated with a larger decrease in luminal cross-sectional area ($-27 \pm 20\%$ change vs baseline in the 19 arteries with angiographically visible wall irregularities and $-16 \pm 20\%$ in the angiographically normal arteries). The difference, however, was not statistically significant. The arteries with wall irregularities showed also a smaller flow increase after the last concentration of acetylcholine ($+47 \pm 30\%$ vs $+68 \pm 56\%$ in the group with smooth arterial contours, NS).

A poor correlation was observed between flow velocity changes after acetylcholine and papaverine ($r^2 = 0.18$ for the maximal concentration of acetylcholine). Similarly, the percent increase of lumen diameter after isosorbide dinitrate was not correlated with the changes observed after acetylcholine infusion.

The flow changes and flow resistance changes after the maximal dose of acetylcholine infusion showed a poor correlation with the cross-sectional area changes observed in the proximal/distal coronary segments. Figure 9 shows the linear regression analysis performed using the cross-sectional area changes of the proximal segments. Also in the distal coronary segment analyzed a very poor correlation was observed, with a squared correlation coefficient of 0.01 and 0.05 for coronary flow and flow resistance.

Discussion

Acetylcholine is the prototype and the most frequently used pharmacological stimulus with a primary endothelium-independent contractile action on the vascular smooth muscle cells and an opposite endothelium-mediated vasodilatory activity which is predominant in normal conditions and at physiologic concentrations [37, 38]. Acetylcholine was used in the in vitro experiments in which the role of intact endothelium in the regulation of vascular tone was established (1) and in the first in vivo study showing that acetylcholine induces severe vasospasm in human coronary arteries with significant stenoses [6]. The induction of an endothelium-dependent vasodilatation in canine femoral [39] and coronary [40] arteries after the application of acetylcholine on the arterial adventitia suggests a role of acetylcholine, the mediator of the parasympathetic stimulation, in the modulation of vascular tone. The circadian rhythm of the parasympathetic activity has been advocated to explain the higher incidence of acute coronary syndromes such as vasospastic

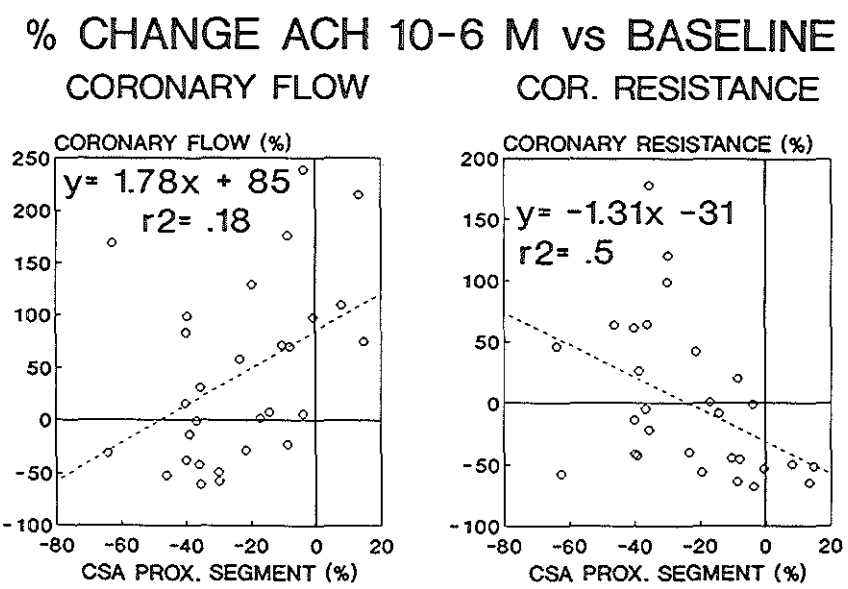

Figure 9. Linear regression analysis of the percent changes in mean cross-sectional area (CSA) of the proximal segment studied and of the percent changes of coronary flow and resistance. Note the poor correlation over the entire range of measurements.

angina and myocardial infarction in the early morning. Selective intracoronary infusion of acetylcholine elicited vascular responses comparable to those observed after serotonin [41], a substance that is released after platelet activation and may contribute to the development of myocardial ischemia in acute coronary syndromes [17, 42, 43].

In this study, concentrations and flow rate of acetylcholine were the same used in recent reports [14, 20, 23] in order to facilitate the comparison of the results. Papaverine and isosorbide dinitrate were infused selectively in doses sufficient to induce a maximal vasodilatation of the resistance and conductance coronary arteries with a limited systemic effect [44]. With these drugs, the presence of an aspecific impairment of vascular relaxation due to structural changes of the epicardial and resistance coronary vessels could be excluded.

Cross-sectional area changes

The arteries studied included both angiographically normal and minimally diseased arteries. In this latter group the severity of coronary vasoconstriction was similar to that reported in two comparable series of patients by the group of Freiburg (−27% decrease in the present study vs −29% and −34% cross-sectional area decrease from baseline at the same concentration of

acetylcholine) [16, 23]. The angiographically normal arteries showed a 16% decrease in cross-sectional area from baseline, similar to the 23% decrease reported by Vrints et al. [12] for normal segments of the left anterior descending coronary artery at this concentration. In the present study the arteries without angiographically visible lesions showed a less pronounced vasoconstriction after the maximal concentration of acetylcholine. No significant differences were present, however, between arteries with and without angiographically visible wall irregularities. A possible explanation is that the atherogenic factors that have already induced a severe symptomatic coronary stenosis in our study population can be sufficient to induce the development of a diffuse endothelial damage also in the absence of large atherosclerotic changes. An alternative explanation is that angiography is not sufficiently sensitive to detect initial atherosclerotic changes. Epicardial and intracoronary ultrasound imaging have shown that diffuse atherosclerotic changes are present in patients with coronary artery disease also in segments which have an angiographically normal lumen and smooth vascular contours [45–47]. Pathological reports have explained this phenomenon with the presence of an overall vascular enlargement able to preserve a normal vascular lumen despite large areas of wall encroachment [48]. In this study no patient showed a severe focal or diffuse spasm inducing a critical flow reduction and the development of symptoms and signs of myocardial ischemia. The characteristics of the studied population, including only patients with stable angina and, for the vast majority, single vessel coronary disease, may explain the different results observed in previous studies [7, 11, 22]. The absence of >75% cross-sectional area reduction from the basal measurement suggests that the impairment of flow after acetylcholine is not due to a critical vasoconstriction of the epicardial arteries. A flow limitation due to focal or diffuse vasoconstriction of small distal branches, not analyzable with quantitative angiography but visually detectable in 8 cases, is more difficult to be ruled out. In these patients, however, the flow changes after the maximal concentration of acetylcholine were similar to those observed in the remaining cases.

A diffuse vasoconstriction was present after the maximal concentration of acetylcholine in 90% of the patients studied (26/29). A progressive dose-response was observed with increasing concentrations of acetylcholine. The proximal and distal segments showed a similar decrease of lumen dimension. A moderate difference between proximal and distal segments was observed only after the intermediate concentration of acetylcholine (cross-sectional area decrease from baseline $-12\pm17\%$ in the proximal segment and $-15\pm15\%$ in the distal segment, $p < 0.05$). At the peak concentration of acetylcholine, however, no differences were observed between proximal and distal arterial segments. Vrints et al. [12] have confirmed the presence of similar changes of proximal and distal segments of the left anterior descending coronary artery. A more significant vasoconstriction after acetylcholine of the distal coronary segments was reported by Rande' et al. [49] in a very limited patient population (5 cases). The variability of the response to

acetylcholine of the proximal and distal segments observed in individual patients can explain this difference and probably reflects a different severity of atherosclerotic involvement of the two segments.

Coronary flow and flow velocity changes

Intracoronary Doppler was used to assess coronary flow velocity in this study. Technical improvements have recently increased the reliability of this technique for the assessment of coronary flow velocity. In particular the large Doppler sample volume and the use of peak blood flow velocity, allowed by the spectral analysis of the signal, avoid changes of the measured velocity in response to minor variations of the position of the Doppler probe inside the artery. It was so possible to minimize manipulation and repositioning of the Doppler probe and to avoid to exclude patients because of poor quality of the Doppler recordings. The accuracy in the calculation of absolute coronary flow from the corresponding mean flow velocity and cross-sectional area, however, is still limited by the difficulty of an exact measurement of the mean velocity and by the impossibility to acquire simultaneously the two measurements. In the presence of rapid changes of flow and cross-sectional area such as after the injection of a bolus of nitrates, papaverine or adenosine, the delay between flow velocity measurement and cineangiogram may result in a significant inaccuracy of the flow measurements. In this study no cineangiograms were performed at the maximal effect of the injection of papaverine. For this reason, absolute coronary flow after papaverine could not be calculated. The presence of a larger cross-sectional area at the peak effect of papaverine than in baseline conditions may explain the relatively low coronary flow reserve (2.8 ± 0.8) observed in this study. Based on previously reported angiographic measurements after papaverine, a 15–20% underestimation of the true flow reserve is expected [50, 51]. In this study, however, papaverine was used only to confirm a normal response of the coronary resistance vessels to a direct smooth muscle vasodilator to exclude structural alterations of the microvasculature as the factor limiting the flow increase.

The lack of simultaneous flow velocity/cross-sectional area measurements is a serious limitation also to explain the changes observed during infusion of acetylcholine. Variations of flow velocity during infusion of acetylcholine have not been previously reported. With the previous generation of Doppler probes the Doppler signal was highly dependent from minor changes in the position of the the Doppler sample volume [52]. These changes, therefore, could have been misinterpreted as artifacts due to an unstable position of the catheter in the artery. The previously described characteristics of the Doppler guidewire and the modalities of signal analysis (fast Fourier transform, continuous automatic measurement of peak flow velocity) are ideal conditions for the assessment of these moderate flow velocity variations. Two causes can be suggested for these flow velocity variations: a true change in flow as the result of a variable vasodilatation of the resistance vessels over

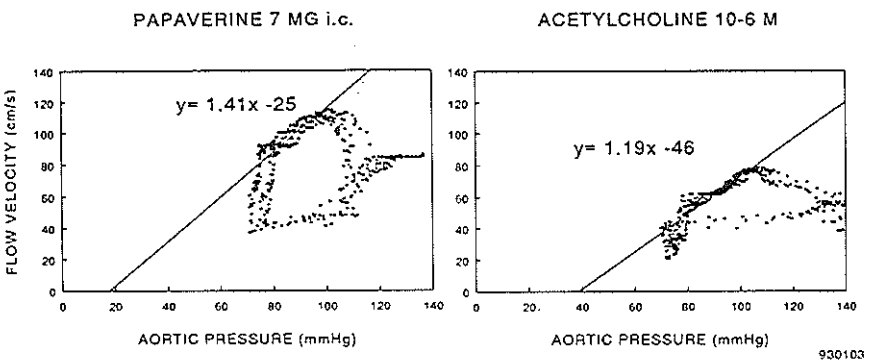

Figure 10. Pressure-flow velocity loop of 4 consecutive beats at the peak effect of the injection of papaverine and after 5 min of infusion of the highest concentration of acetylcholine. The regression line has been calculated from the mid-diastolic data-points. Note the steeper slope of the pressure-velocity relation after papaverine and the lower pressure-intercept.

time, or a change of the cross-sectional area at the site of the Doppler sample volume (flow velocity changes but coronary flow remains the same). In the absence of a simultaneous continuous assessment of lumen cross-sectional area the mechanism of these flow velocity changes remains speculative. In the near future the combination of intravascular ultrasound imaging and Doppler may allow a continuous assessment of coronary cross-sectional area and flow velocity and facilitate the assessment of the dynamics of the flow/area changes after acute pharmacological interventions [53].

In this study the flow velocity changes after acetylcholine have been expressed as a percent change from baseline and not as a percent of the maximal flow increase (after papaverine) because a moderate (−7%) but significant aortic pressure reduction was observed at the peak effect of papaverine. A constant pressure is a prerequisite for a reliable comparison of a flow measured in autoregulatory conditions and during maximal vasodilatation [54]. Recently, the slope of the instantaneous hyperemic diastolic pressure-flow relation has been used in animal experiments as an index of coronary conductance and has been shown to be independent from changes in aortic pressure, heart rate and cardiac contractility [55, 56]. The instantaneous hyperemic diastolic pressure-flow velocity relation can be reproducibly assessed also in humans [57, 58]. The possibility to measure an index of coronary conductance independent from the hemodynamic conditions at the time of assessment during different pharmacologic interventions and during maximal vasodilatation is a of great potential interest (Fig. 10). This approach, however, still requires a more extensive clinical validation.

Experimental data have demonstrated that atherosclerotic animals show an abnormal endothelium-dependent vasodilatation of the coronary resistance arteries, despite the absence of structural atherosclerotic lesions [24].

The comparison of the flow response to acetylcholine in patients with coronary artery disease and in control subjects has confirmed an impaired flow increase in the coronary patients, despite the absence of significant lesions of the epicardial coronary arteries [23]. In this study a large variability of the flow changes was observed after the highest doses of acetylcholine. A dose dependent vasodilatation after acetylcholine was present in most cases, with flow increase up to 3 times the baseline flow. In 10 patients, however, a flow decrease was observed after the maximal concentration of acetylcholine. The mean flow increase from baseline was $+44 \pm 24\%$ at the maximal concentration of acetylcholine, an increase much lower than the flow increase observed in normal controls at the same acetylcholine concentration [23, 59]. No clinical or angiographic predictors of these large individual differences could be observed.

A reduction of the endothelium-dependent relaxation is present in animals chronically maintained at an atherogenic diet with an high content of cholesterol [60, 61]. In hypercholesterolemic patients without angiographic evidence of coronary artery disease, an impaired endothelium-mediated vasodilatation of the epicardial coronary arteries and of the resistance coronary vessels have been demonstrated [16]. Thirteen of the study patients had a total cholesterol level ≥ 6.4 mmol/l (250 mg/dl). This group, however, showed no significant differences in terms of flow increase and vascular diameter changes after acetylcholine. The importance of the relative amount of HDL and LDL cholesterol has recently been reported to correlate more closely than total cholesterol with the degree of impairment of the endothelium-mediated vasodilatation [62]. In the studied group, however, also the use of the HDL/total cholesterol ratio did not identify a subset of patients with a different response to acetylcholine.

Correlation of coronary area/flow changes after acetylcholine

In this study mean arterial cross-sectional area of the epicardial arteries and coronary flow have been considered as independent indices of response of conductance and resistance coronary vessels. This assumption has three potential limitations: the possibility that a flow-limiting vasoconstriction occurs in an epicardial artery; the development of a vasodilatation of the epicardial arteries secondary to the increase of flow; the use of a cross-sectional area measured along the analyzed segment to calculate coronary flow. In spite of all these potential reasons for interdependance, the flow or flow resistance changes after the maximal concentration of acetylcholine showed only a poor correlation with the corresponding cross-sectional area changes. The discrepancy between flow and cross-sectional area reflects a different response of the conductance and resistance arteries to acetylcholine. The large arteries are the preferential target of the atherosclerotic process. At this level the presence of intimal thickening may constitute a barrier to the diffusion of nitric oxide from the endothelial cells to the muscular media

[63]. A macrophagic infiltration or the presence of a lipidic component of the intimal plaque may also accelerate the degradation of nitric oxide and prevent its action on the underlying muscular layer [37]. The importance of these mechanisms in atherosclerotic human arteries is indirectly confirmed by the frequent development of focal vasoconstriction after acetylcholine. Myocardial perfusion is regulated predominantly by resistance arteries < 200 micron [64]. These arteries do not show signs of atherosclerotic involvement at histology, suggesting that biochemical or ultrastructural changes are the most likely mechanisms underlying the abnormal endothelium-dependent relaxation.

These observations have potential clinical implications. A prolonged treatment aimed at the regression of the atherosclerotic intimal changes may be required to restore an impaired endothelium-mediated response when the presence of an intimal barrier is the main operative mechanism [65]. On the contrary, acute pharmacologic interventions or a short lasting treatment may be sufficient to normalize the endothelial function when metabolic abnormalities are involved. The possibility to normalize the endothelial response in hypercholesterolemia with a short-term infusion of L-arginine has been shown in animal experiments [66] as well as in human coronary arteries [49, 67]. Similarly, different classes of drugs have shown the ability to restore a normal endothelium-mediated vascular reactivity in experimental animals [68–70].

Conclusions

In angiographically normal or minimally diseased arteries of symptomatic patients with coronary artery disease, also very low doses of acetylcholine induced a significant coronary vasoconstriction of the epicardial coronary arteries. The resistance vessels showed a variable response, with a trend towards a moderate vasodilatation (flow increase in 2/3 of the patients after the highest concentration of acetylcholine). The presence of hypercholesterolemia or wall irregularities was not correlated with the diameter/flow changes after acetylcholine. The poor correlation observed between cross-sectional area and flow changes after acetylcholine suggests that different mechanisms induce impairment of endothelium-mediated vasodilatation in conductance and resistance coronary vessels.

Acknowledgements

We gratefully acknowledge the support given by Hoffmann-La Roche Research Laboratories to this study. The contribution to the acquisition of the data of the medical, technical and nursing staff of the Cath Lab is gratefully acknowledged. Mrs. Jolanda van Wijk, Research Assistant, Dept. Clinical

Epidemiology, Thoraxcenter, is gratefully acknowledged for her essential contribution to the acquisition and analysis of data.

References

1. Furchgott RF, Zawadzki JV. The obligatory role of endothelial cells in the relaxation of smooth muscle by acetylcholine. Nature 1980; 288: 373–6.
2. Palmer RM, Ashton DS, Moncada S. Vascular endothelial cells synthetize nitric oxide from L-arginine. Nature 1988; 333: 664–6.
3. Vallance P, Collier J, Moncada S. Effects of endothelium-derived nitric oxide on peripheral arteriolar tone in man. Lancet 1989; 2: 997–1000.
4. Panza JA, Quyyumi AA, Brush JEJR, et al. Abnormal endothelium-dependent vascular relaxation in patients with essential hypertension. N Engl J Med 1990; 323: 22–7.
5. Johnstone MT, Gallagher SJ, Scales KM, Cusco JA, Lee B, Creager MA. Endothelium-dependent vasodilatation is impaired in patients with insulin-dependent diabetes mellitus (abstr). Circulation 1992; 68: I-618.
6. Fostermann U, Mugge A, Alheid U, et al. Selective attenuation of endothelium-mediated vasodilatation in atherosclerotic human coronary arteries. Circ Res 1988; 62: 185–90.
7. Ludmer PL, Selwyn AP, Shook TL, et al. Paradoxical vasoconstriction induced by acetylcholine in atherosclerotic coronary arteries. N Engl J Med 1986; 315: 1046–51.
8. Werns SD, Walton JA, Hsia HH. et al. Evidence of endothelial dysfunction in angiographically normal coronary arteries of patients with coronary artery disease. Circulation 1989; 79: 287–91.
9. Vita JA, Treasure CB, Nabel EG, et al. Coronary vasomotor response to acetylcholine relates to risk factors in coronary artery disease. Circulation 1990; 81: 491–7.
10. Yasue H, Matsuyama K, Okumura K, et al. Responses of angiographically normal human coronary arteries to intracoronary injection of acetylcholine by age and segment. Circulation 1990; 81: 482–90.
11. Okumara K, Yasue H, Matsuyama T, et al. A study of coronary hemodynamics during acetylcholine induced coronary spasm in patients with variant angina: endothelium-dependent dilatation in the resistence vessels. J Am Coll Cardiol 1992; 19: 1426–34.
12. Vrints CJM, Bult H, Hitter E, Herman AG, Snoeck JP. Impaired endothelium-cholinergic coronary vasodilatation in patients with angina and normal coronary arteriograms. J Am Coll Cardiol 1992; 19: 21–31.
13. Cox DA, Vita JA, Treasure CB, et al. Atherosclerosis impairs flow-mediated dilation of coronary arteries in humans. Circulation 1989; 80: 458–65.
14. Nabel EG, Selwyn AP, Ganz P. Large arteries in humans are responsive to changing blood flow: an endothelium-dependent mechanism that fails in patients with atherosclerosis. J Am Coll Cardiol 1990; 16: 349–56.
15. Drexler H, Zeiher AM, Wollschlager H, Meinertz T, Just H, Bonzel T. Flow-dependent coronary artery dilatation in humans. Circulation 1989; 80: 466–74.
16. Zeiher AM, Drexler H, Wollschlager H, et al. Coronary vasomotion in response to sympathetic stimulation in humans: importance of the functional integrity of the endothelium. J Am Coll Cardiol 1989; 14: 1181–90.
17. McFadden EP, Clarke JG, Davies GJ, et al. Effect of intracoronary serotonin on coronary vessels in patients with stable angina and in patients with variant angina. N Engl J Med 1991; 342: 648–54.
18. Zeiher AM, Schachinger V, Weitzel SH, et al. Intracoronary thrombus formation causes focal vasoconstriction of epicardial arteries in patients with coronary artery disease. Circulation 1991; 83: 1519–25.
19. Yao SK, Ober JC, Willerson JT, et al. Endogenous nitric oxide protects against platelet

aggregation and cyclic flow variations in stenosed and endothelium injured arteries. Circulation 1992; 86: 1302–9.
20. Zeiher AM, Drexler H, Wollschlager H, Just H. Modulation of coronary vasomotor tone in humans. Progressive endothelial dysfunction with different early stages of coronary atherosclerosis. Circulation 1991; 83: 391–401.
21. Hodgson J, Nair R, Sheehan HM, Reddy KG. Endothelial dysfunction in coronary arteries precedes ultrasonic evidence of atherosclerosis in patients with risk factors (abstr). J Am Coll Cardiol 1992; 19: 323A.
22. Hodgson JB, Marshall JJ. Direct vasoconstriction and endothelium dependent vasodilation. Circulation 1989; 79: 1043–51.
23. Zeiher AM, Drexler H, Wollschläger H, Just H. Endothelial dysfunction of the coronary microvasculature is associated with impaired coronary blood flow regulation in patients with early atherosclerosis. Circulation 1991; 84: 1984–92.
24. Selke FW, Armstrong ML, Harrison DG. Endothelium-dependent vascular relaxation is abnormal in the coronary microcirculation of atherosclerotic primates. Circulation 1990; 81: 1586–93.
25. Chillian WM, Dellsperger KC, Layne SM, et al. Effects of atherosclerosis on the coronary microcirculation. Am J Physiol 1990; 258: H-529–H-39.
26. Yamamoto H, Bossalier C, Cartwright J, Henry PD. Videomicroscopic demonstration of defective cholinergic arteriolar vasodilatation in atherosclerotic rabbit. J Clin Invest 1988; 81: 1752–8.
27. Chesebro JH, Fuster V, Webster MWI. Endothelial injury and coronary vasomotion. J Am Coll Cardiol 1989; 14: 1191–2.
28. Hibbard MD, Holmes DR. The Tracker catheter: a new vascular access system. Cathet Cardiovasc Diag 1992; 27: 309–16.
29. Meester Gt, Bernard N, Zeelenberg C, et al. A computer-system for real-time analysis of cardiac catheterization data. Cathet Cardiovasc Diag 1975; 1: 113–32.
30. Di Mario C, Roelandt JRTC, de Jaegere P, Linker DT, Oomen J, Serruys PW. Limitations of the zero-crossing detector in the analysis of intracoronary Doppler. A comparison with fast Fourier transform of basal, hyperemic and transstenotic blood flow velocity measurements in patients with coronary artery disease. Cathet Cardiovasc Diag 1993; 28: 56–64.
31. Doucette JW, Douglas Corl P, Payne HP, et al. Validation of a Doppler guide wire for intravascular measurement of coronary artery flow velocity. Circulation 1992; 85: 1899–911.
32. Di Mario C, Hermans WRM, Rensing BJ, Serruys PW. Calibration using angiographic catheters as scaling devices. Importance of filming the catheters not filled with contrast medium (letter). Am J Cardiol 1992; 69: 1377–8.
33. Haase J, Di Mario C, Slager CJ, et al. In vivo validation of on-line and off-line geometric coronary measurements using insertion of stenosis phantoms in porcine coronary arteries. Cathet Cardiovasc Diagn 1992; 27: 16–27.
34. Di Mario C, Haase J, den Boer A, Reiber JHC, Serruys PW. Videodensitometry versus edge detection for the assessment of in vivo intracoronary phantoms. Am Heart J 1992; 124: 1181–9.
35. Reiber JHC, Serruys PW, Koojman CJ, et al. Assessment of short-, medium-, and long-term variations in arterial dimensions from computer-assisted quantitation of coronary cineangiograms. Circulation 1985; 71: 280–8.
36. Di Mario C, de Feyter PJ, Slager CJ, de Jaegere P, Roelandt JRTC, Serruys PW. Intracoronary blood flow velocity and transstenotic pressure gradient using sensor-tip pressure and Doppler guidewires. Cathet Cardiovasc Diag 1993; 28: 311–19.
37. Bassenge E, Busse R. Endothelial modulation of coronary tone. Progr Cardiovasc Dis 1988; 30: 349–80.
38. Newman CM, Maseri A, Hackett DR, et al. Response of angiographically normal and atherosclerotic left anterior descending coronary artery to acetylcholine. Am J Cardiol 1990; 66: 1070–6.

39. Busse R, Trogisch G, Bassenge E. The role of endothelium in the control of vascular tone. Basic Res Cardiol 1985; 80: 475–90.
40. Angus JA, Campbell GR, Cocks TM, et al. Vasodilatation by acetylcholine is endothelium-dependent. A study by sonomicrometry in canine femoral artery in vivo. J Physiol 1983; 344: 209–44.
41. Vrints C, Bosmans J, Bult H, Herman A, Snoeck J. Close parallelism between the coronary vasomotor responses to acetylcholine and to serotonin (abstr). J Am Coll Cardiol 1992; 19: 323A.
42. Golino P, Piscione F, Willerson JT, et al. Divergent effects of serotonin on coronary artery dimensions and blood flow in patients with coronary atherosclerosis and coronary patients. N Engl J Med 1991; 324: 641–8.
43. Hillis DL, Lange RA. Serotonin and acute ischemic heart disease. N Engl J Med 1991; 342: 688–9.
44. Zijlstra F, Serruys PW, Hugenholtz PG. Papaverine: the ideal coronary vasodilator for investigating coronary flow reserve? A study of timing, magnitude, reproducibility and safety of the coronary hyperemic response after intracoronary papaverine. Cathet Cardiovasc Diag 1989; 12: 298–303.
45. McPherson DD, Johnson MR, Alvarez NM, et al. Variable morphology of coronary atherosclerosis: characterization of atherosclerotic plaque and residual arterial lumen size and shape by epicardial echocardiography. J Am Coll Cardiol 1992; 19: 593–9.
46. Nissen SE, Gurley JC, Grines CL, et al. Intravascular ultrasound assessment of lumen size and wall morphology in normal subjects and patients with coronary artery disease. Circulation 1991; 84: 1087–99.
47. StGoar FG, Pinto F, Alderman EL, Fitzgerald PJ, Stinson EB, Popp RL. Detection of coronary atherosclerosis in young adult hearts using intravascular ultrasound. Circulation 1992; 86: 756–763.
48. Glagov S, Weisenberg E, Zarins CK, et al. Compensatory enlargement of human atherosclerotic coronary arteries. N Engl J Med 1986; 316: 1371–5.
49. Dubois-Rande' JL, Zelinsky R, Roudot F, et al. Effects of infusion of L-arginine into the left anterior descending coronary artery on acetylcholine-induced vasoconstriction of human atheromatous coronary arteries. Am J Cardiol 1992; 70: 1269–75.
50. Zijlstra F, Reiber JHC, Serruys PW. Does intracoronary papaverine dilate epicardial coronary arteries? Implications for the assessment of coronary flow reserve. Cathet Cardiovasc Diag 1988; 14: 1–6.
51. Mügge A, Heublein B, Kuhn M, Nolte C, Lichtlen PR. Impaired coronary dilator response to substance P and impaired flow-dependent dilator response in heart transplant patients with graft vasculopathy. J Am Coll Cardiol 1993; 21: 163–175.
52. Serruys PW, Di Mario C, Kern M. Intracoronary Doppler. In: Topol E. editor. Textbook of Interventional Cardiology, 2nd Ed. Philadelphia, Saunders, 1993, in press.
53. Sudhir K, MacGregor JS, Barbant S, Gupta M, Yock PG, Chatterjee K. In vivo demonstration of role for nitric oxide in the regulation of coronary vascular tone by simultaneous intravascular two-dimensional and Doppler ultrasound. J Am Coll Cardiol 1993; 21: 1261–68.
54. Klocke FJ. Measurements of coronary flow reserve: defining pathophysiology versus making decisions about patient care. Circulation 1987; 76: 245–253.
55. Mancini GBJ, Cleary RM, DeBoe SF, et al. Instantaneous hyperemic flow-vs-pressure slope index. Microsphere validation of an alternative to masures of coronary flow reserve. Circulation 1991; 84: 862–71.
56. Cleary RM, Aron D, Moore NB, DeBoe SF, Mancini GBJ. Tachycardia, contractility and volume loading alter conventional indexes of coronary flow reserve, but not the instantenous hyperemic flow versus pressure slope index. J Am Coll Cardiol 1992; 20: 1261–8.
57. Serruys PW, Di Mario C, Meneveau N et al. Intracoronary pressure and flow velocity from sensor-tip guidewires. A new methodological comprehensive approach for the assessment

of coronary hemodynamics before and after coronary interventions. Am J Cardiol 1993; 71: 41D–53D.
58. Di Mario C, Meneveau N, De Feyter P, Gil R, Serruys PW. Assessment of the pressure-flow velocity relation using an intracoronary Doppler guidewire (abstr). J Am Coll Cardiol 1993; 21: 348A.
59. Treasure CB, Klein L, Vita JA, Selwyn AP, Ganz P, Alexander RW. Hypertension and left ventricular hypertrophy are associated with impaired endothelium-mediated relaxation in human coronary resistance vessels. Circulation 1993; 87: 86–93.
60. Verbeuren TJ, Jordaens FH, Zonnekeyn LL, Hove CE, Coene MC, Herman AG. Effect of hypercholesterolemia on vascular reactivity in the rabbit. Circ Res 1986; 58: 552–64.
61. Takahishi M, Yui Y, Yasumoto H, Aoyama T, Morishita H, Hattori R, Kawai C. Lipoproteins are inhibitors of endothelium-dependent relaxation of rabbit aorta. Am J Physiol 1990; 258: H1–H8.
62. Drexler H, Zeiher AM, Doster W, Zeh W, Wieland H. Endothelial dysfunction in the coronary circulation in hypercholesterolemia: protective effect of high HDL cholesterol (abstr). Circulation 1992; 86: I–117.
63. Lerman A, Burnett JC. Intact and altered endothelium in regulation of vasomotion. Circulation 1992; 86: III-12–III-9.
64. Chillian WM, Easthman CL, Marcus ML. Microvascular distribution of coronary vascular resistance in beating left ventricle. Am J Physiol 1986; 20: H779–H88.
65. Harrison DG, Armstrong ML, Freiman PC, Heistad DD. Restoration of endothelium-dependent relaxation by dietary treatment of atherosclerosis. J Clin Invest 1987; 80: 1808–11.
66. Cooke JP, Andon NA, Girerd XJ, Hirsch AT, Creager MA. Arginine restores cholinergic relaxation of hypercholesterolemic rabbit thoracic aorta. Circulation 1991; 83: 1057–62.
67. Drexler H, Zeiher AM, Meinzer K, Just H. Correction of endothelial dysfunction in coronary microcirculation of hypercholesterolemic patients by L arginine. Lancet 1991; 338: 1546–51.
68. Auch-Swelk W, Bossaler C, Claus M, Graf K, Schuler S, Fleck E. ACE-inhibitors potentiate endothelium-dependent relaxation to threshold concentrations of bradykinin in coronary arteries (abstr). J Am Coll Cardiol 1992; 19: 190A.
69. Dohi Y, Criscione L, Pfeiffer K, Luscher TF. Normalization of endothelial dysfunction of hypertensive mesenteric resistance arteries by chronic therapy with benazepril or nifedipine (abstr). J Am Coll Cardiol 1992; 19: 226A.
70. Williams JK, Adams MR, Herrington DM, Clarkson TB. Short-term administration of estrogen and vascular responses of atherosclerotic coronary arteries. J Am Coll Cardiol 1992; 20: 452–7.

CONCLUSIONS

Coronary angiography provides a rapid overview and effective road-map during diagnostic or interventional procedures, has low cost and enjoys widespread availability. These advantages, coupled with the continuous improvement in image quality and possibility of on-line quantitative analysis, suggest that angiography will continue to be the principal imaging technique for coronary interventional procedures.

However, the importance of knowing the morphological composition and functional significance of coronary stenoses is increasingly being recognized. The two intracoronary ultrasound techniques described in this thesis provide a unique insight into the nature of a coronary lesion. Recent investigations with intracoronary ultrasound imaging and Doppler have contributed significantly to our knowledge of coronary artery disease and to our understanding of the response to therapeutic procedures.

Whether these two techniques will prove to be cost-effective and find their own niche in clinical practice or whether they will be limited to academic research remains to be determined. As a logical continuation of the work reported in this thesis, our group has promoted or is participating in on-going multicenter studies addressing this question (GUIDE II and PICTURE for ultrasound imaging, DEBATE for intracoronary Doppler).

SAMENVATTING

Het hemodynamisch belang van een vernauwing kan beter worden vastgesteld, indien we geïnformeerd zijn over de morphologische kenmerken van de atherosclerotische lesie (bv excentriciteit, samenstelling van de lesie) en indien we de verandering van de bloedstroom ten gevolge van de vernauwing nauwkeurig hebben vastgesteld.

De toepassing van ultrageluid en Doppler gedurende diagnostische onderzoekingen en therapeutische procedures in het catheterisatie laboratorium is mogelijk geworden, doordat de ultra geluids catheters uiterst klein zijn gemaakt en door de recente ontwikkeling van een Doppler-piezo-elektrisch kristal die gemonteerd is op een voerdraad.

Het hoofdthema van dit proefschrift is het onderzoek naar de morphologische en functionele karakteristieken van vernauwingen in het coronair systeem met intracoronair ultrageluid.

In hoofdstuk 1 wordt een algemene inleiding gegeven betreffende 2-dimensioneel intracoronair ultrageluid. In hoofdstuk 2 worden de voor- en nadelen van intracoronair ultrageluid en kwantitatieve angiografie om vasculaire afmetingen vast te stellen beschreven. In hoofdstuk 3 worden de problemen van de 3-dimensionele reconstructie op basis van opeenvolgende intracoronaire ultrageluidsbeelden belicht. In de hoofdstukken 4 en 5 worden de resultaten van twee studies beschreven die de nauwkeurigheid van intravasculair ultrageluid bestuderen om structuur en samenstelling van de normale en zieke kransvatwand en de veranderingen van de vaat elasticiteit bij pharmacologische interventies vast te stellen. In hoofdstuk 6 wordt het effect van de variaties van de invalshoek van de geluidsbundel op de intensiteit van reflectie van de geluidsbundel door de wand van de kransslagaderen beschreven.

Hoofdstuk 7 geeft een algemene inleiding van het tweede gedeelte van het proefschrift. Hierin worden de nieuwe mogelijkheden beschreven welke intracoronaire Doppler biedt om het belang van coronaire stenosen vast te stellen.

In hoofdstuk 8 worden de voordelen van spectrale analyse boven de zero-crossing techniek beschreven. In hoofdstuk 9 wordt de ernst van een kransslagader vernauwing bepaald met behulp van de maximale bloedstroomsnelheid ter plaatse van de vernauwing, gebruikmakend van de continuïteitsvergelijking. In hoofdstuk 10 worden de beperkingen beschreven van het bepalen van de "coronary flow reserve" om de resultaten van ballon angioplastiek vast te stellen. In hetzelfde hoofdstuk en de hoofdstukken 11, 12 en 13 worden andere mogelijkheden voorgesteld om de ernst van coronaire stenoses vast te stellen gebaseerd op de relatie tussen gelijktijdig geregistreerde transstenotische druk gradient en bloedstroom snelheid tijdens de hartcyclus.

In het laaste hoofdstuk wordt een studie beschreven die werd uitgevoerd bij 29 patiënten om het effect van selectieve infusie van de endothelium afhankelijke vaatverwijder acetylcholine op de afmetingen van de epicardiale kransslagaderen en de bloedstroom snelheid vast te stellen. Door middel van deze methode werd de relatie tussen endothelium afhankelijke veranderingen van de epicardiale en de weerstands kransvaten onderzocht.

ACKNOWLEDGEMENTS

When, after the attendance of the 1989 Congress of Echocardiography in Rotterdam, I expressed for the first time my interest to be involved in a research project in the field of intravascular ultrasound at the Thoraxcenter, I did not realize that two short telephone conversations with Prof. Roelandt and Prof. Serruys would have changed my work and life so completely for the following three years and possibly for many years in the future. This change would have not been possible without the availability of a Research Fellowship of the European Society of Cardiology and I am grateful for this opportunity to start to work in this exciting field of research.

The confidence and full support of Prof. Serruys were essential to successfully complete the research projects reported in this thesis. I hope that in this thesis some characteristics of his scientific approach to research are apparent: originality of study design, meticulous acquisition of the data and complete and rigorous analysis of the results.

Prof. J.R.T.C. Roelandt taught me that the quality of a good scientific paper is the identification of an essential message, conveyed to the reader using a well-documented but simple and straighforward presentation. I was deeply impressed by his ability to clarify this message in his original and thorough review of many of the manuscripts of this thesis. His comments have certainly contributed to improve the baroque style of the initial version of these manuscripts although the length of the last chapter shows that there is still some more work to do.

My co-promotor Dr. P.J. de Feyter and my "paranimf" Dr. P. de Jaegere have introduced me to the practice of interventional cardiology at the Thoraxcenter. I have learnt from them that a meticulous preparation, planning and follow-up of the intervention are the key of a successful procedure and an essential prerequisite to combine advanced research and good patient care. I am also indebted for many insightful comments in the preparation of these manuscripts. The experience and suggestions of Dr. M. van den Brand were of great support in many procedures. I am grateful to Dr. S. Strikwerda for the pleasant collaboration in the study reported in Chapter 14.

An invaluable help to overcome the obvious problems related to a new research and work experience in a foreign country was given by the nursing, technical and administrative staff of the Catheterization Laboratory of the Thoraxcenter. Only a deep personal motivation for research oriented academic activity and the idea (which I fully share) that intravascular ultrasound will improve patient care in the future, may explain how they accepted to work during long interventional procedures surrounded by many trolleys carrying echomachines, control units of angioscopes or pressure guidewire systems connected by a network of cables to computers, angiographic screens and video-mixers, taking care of the preparation and careful handling of these multiple devices on the Catheterization table and of the optimization of the recording. I would also like to thank them for their friendly and patient attitude, shared by all my colleagues and by the nursing staff of the Departments of Cardiology (CCU, dag-behandeling, MCU and 3-Zuid) towards my still pitiful attempts to communicate in Dutch with them and the patients.

I believe that much of the secret of the continuous success of the Thoraxcenter 25 years after its foundation is the collaboration in the same Institute of Departments of Clinical Cardiology and Biomedical Technology and of an Experimental Animal Laboratory. Prof. N. Bom gave me the first opportunity to participate in a research program in intravascular ultrasound, in collaboration with the active group of Dr. E.J. Gussenhoven, Dr. S. The and Ir. L. Wenguang, and continuous advice and encouragment for the clinical studies carried out in the Catheterization Laboratory. Dr. C.J. Slager, Dr. H. Schuurbiers and Dr. J. Ommen have contributed to the analysis of the results of many Chapters in this thesis. I would also like to express my gratitude to my "paranimf" Dr. R. Krams for his constructive criticism and his tolerance for the simplifications required to try to apply in clinical practice physiologic concepts adapted from complex animal models. The proposers of these models, and in particular Dr. L. Gould and R.L. Kirkeede, Houston, Texas, and Dr. J. Mancini, Vancouver, Canada, must be acknowledged as a source of the concepts applied in humans using the new guidewire technology. Prof. P.D. Verdouw, Dr. W. van den Giessen, Dr. L. Soei and Mr. R. van Bremen are also acknowledged for their support in the experimental part of this thesis.

Another of the secrets of the success of the Thoraxcenter is its great capability to rapidly integrate in its research programs doctors coming from many countries and with different levels of research experience behind them. A short list of these "United Nations of the Thoraxcenter" who have directly or indirectly contributed to the work presented in this thesis include Dr. K.J. Beatt, London, U.K.; Dr. P. Widimsky, Prague, Czech Republic; Dr. T. Forster, Szeged, Hungary; Dr. M.S. El-Said, Cairo, Egypt; Dr. A. Violaris, London, U.K.; Dr. E. Murphy, Portland, Oregon, who had started the clinical application of a spectral analyzer during Doppler studies at the Thoraxcenter; Dr. R. Wilson, Associate Professor of Cardiology in Portland, Oregon, who had coordinated the study presented in Chapter V; Dr. B. H. Strauss, Toronto, Canada; Dr. Jürgen Haase, Frankfurt, Germany; Dr. N. Meneveau, Besancon, France and Dr. R. Gil, Szczecin, Poland, who have worked with me for many months late at night to complete the analysis of the Doppler tracings; Dr. J. Escaned, La Coruna, Spain, with whom I am endebted for many stimulating discussions; Dr. Hakan Emanuelsson, Professor of Cardiology in Göteborg, Sweden, who gave a great impulse to the application of high-fidelity pressure transducers at the Thoraxcenter; Dr. D. Foley and Dr. D. Keane, Dublin, Ireland; Dr. J. Baptista, Lisbon, Portugal, and Dr. Y. Ozaki, Nagoya, Japan.

I have been fortunate to work together with a great expert in intracoronary Doppler ultrasound such as Dr. M.J.Kern for one of the book chapters of this thesis. I am also thankful for the superb technical support obtained from the manufacturers of the Doppler and the ultrasound imaging systems used for most of these studies (Cardiometrics, CA and Cvis, CA) and from the distributor of these systems in Holland (TDM BV, The Netherlands).

Many others working at the Thoraxcenter who have provided help and support deserve acknowledgment: E.J. Montauban van Swijndregt, Marie-Angel Morel, H. Luijten, M. Eichkoltz, M. Bokslag, V. Umans, N. van den Putten, N. Bruining, E. Boersma, Anja van Huuksloot, Paolo Fioretti, Stanley Madrestma, Arno Breeman,

M. van den Linden, W. Hermans, B. Rensing, J.P. Herrman, Aggie Balk, Robert J. van Suylen, Machteld de Kroon, Harm ten Hoff, Nico de Jong, Jaap Pameyer, Jollanda van Wijk.

Almost all the photographic material presented in this thesis is the result of the high professional skills and tireless work of Mr. J. Tuin.

During my training at the University of Padua, Prof. S. Dalla Volta transmitted to me his love for Cardiology and his passion for research. Prof. M. Vincenzi and my Colleagues of the Division of Cardiology as well as the Hospital Administration of Vicenza have kindly allowed me a two years' temporary leave during which most of this thesis was completed. I hope that they will understand reading this thesis the scientific motivation for continuing my professional carreer at the Thoraxcenter.

This thesis would have not been possible without the continuous support and encouragement of my family and my wife's parents.

I am also endebted to the many persons who have helped my wife and me to settle in this country and in particular to Mrs. D. Serruys, Mrs. M. Roelandt, Dr. A. Balk, Mrs. M. Fioretti, Dr. Conny Tirtaman, Dr. F. and M.G. Verheijen and Mrs. S. de Jaegere.

CURRICULUM VITAE

Carlo Di Mario
Born in Modena, Italy, on May 11, 1955
Married, two sons.

School education

1974	Grammar High School at the "Liceo Classico R. Franchetti", Venezia-Mestre, with final marks of 60/60.
1980	Graduated in Medicine at the University of Padua with the maximum score of 110/110 cum laude. Score average of the exams: 30/30.
1980	Passed the Italian Medical licensure examination.
1984	Specialization in Cardiology at the University of Padua (Director Prof. S. Dalla Volta) with the maximal score of 70/70 cum laude.
1987	Specialization in Sports Medicine (Director Prof. C. Brandi) at the University of Padua.
1993	Certification as Cardiologist in the Netherlands

Prizes and Associations

1982	Passed the E.C.F.M.G. examination.
1983	Member of the Italian Society of Cardiology (S.I.C.).
1983	Research Award from the University of Padua
1984	Member of the National Association of the Hospital Cardiologists (A.N.M.C.O.).
1987	Member of the Working Group on Coronary Circulation of the European Society of Cardiology.
1991	Fellow of the European Society of Cardiology.

Post-university education and research activity

1986	Research and clinical training (1 month) at the Cardiac Catheterization Laboratory of the University of Pavia (Prof. G. Specchia).
1987	Research training (4 months) at the Cardiac Catheterization Laboratory, Thoraxcenter, Erasmus University, Rotterdam (Prof. P.W. Serruys).
1991	Research Fellowship of the European Society of Cardiology with a project on intravascular ultrasound; Project Supervisors: Prof. P.W. Serruys, Prof. J.R.T.C. Roelandt; Institute: Thoraxcenter, Rotterdam; duration: 1 year.
1980-93	15 abstracts presented as first Author in ESC/AHA/ACC Congresses; 9 lectures as Invited Speaker in International Congresses. 95 publications.
1993	Director Intracoronary Imaging Laboratory, Thoraxcenter, Rotterdam.

Hospital and University Appointments

80-84	Residency at the Department of Cardiology, Padua University Hospital (Director Prof. S. Dalla Volta).
84-87	Junior Registrar ("Assistente") of the Division of Cardiology of Cittadella General Hospital.
87-88	Senior Registrar ("Aiuto") of the Division of Cardiology, Bassano General Hospital.
88-91	Senior Registrar ("Aiuto") of the Division of Cardiology, "S.Bortolo" Regional Hospital, Vicenza (Institute Affiliated to the University of Verona).
1991	Research Fellow, Experimental Laboratory and Cardiac Catheterization Laboratory, Thoraxcenter, Erasmus University, Rotterdam.
1992	University Lecturer, Department of Cardiology, Thoraxcenter, Erasmus University, Rotterdam.
1993	Senior Staff Member, Cardiac Catheterization Laboratory, Department of Cardiology, Thoraxcenter, Erasmus University, Rotterdam.

ORIGINAL MANUSCRIPTS

(International journals/English text)

1. Di Mario C, Beatt KJ, de Feyter PJ, et al. Percutaneous aortic balloon valvuloplasty for calcific aortic stenosis in elderly patients: immediate hemodynamic results and short-term follow-up. Br Heart J 1987; 58: 644-52.
2. Di Mario C, Veen van LCP, Serruys PW, et al. Computed tomography during experimental balloon dilatation for calcific aortic stenosis. A look into the mechanism of valvuloplasty. J Intervent Cardiol 1988; 1: 95-107.
3. Serruys PW, Di Mario C, Essed CE. Restenosis three months after successful percutaneous aortic valvuloplasty. A clinico-pathological report. Internat J Cardiol 1987; 17: 210-14.
4. Di Mario C, Zanchetta M, Maiolino P. Coronary aneurysms in a case of Ehlers-Danlos syndrome. Japan Heart J 1988; 29: 491-94.
5. Serruys PW, Luijten HE, Di Mario C, et al. Percutaneous balloon valvuloplasty for calcific aortic stenosis. A treatment "sine cure"? Eur Heart J 1988; 9: 782-94.
6. Serruys PW, Di Mario C, Koning R, et al. The "long-sheath" technique in percutaneous aortic balloon valvuloplasty. J Intervent Cardiol 1988; 1: 85-93.
7. Hartog H, Di Mario C, van den Brand M, et al. Closure of an acquired coronary fistula in a heart transplant recipient. Cathet Cardiovasc Diagn 1993; in press.
8. Plante S, Veen van LCP, Di Mario C, et al. Aortic valvuloplasty of calcific aortic stenosis with monofoil and trefoil balloon catheters: practical considerations. Internat J Cardiac Imaging 1990; 5: 249-60.
9. Serruys PW, Di Mario C, KJ Beatt KJ, et al. Valvuloplasty for calcific aortic stenosis. Cardiac Imaging Video J 1989; 2: n.4.
10. Plante S, Beatt KJ, Di Mario C, et al. Assessment of the long sheath technique for percutaneous aortic balloon valvuloplasty. Cathet Cardiovasc Diag 1989; 19: 301-310.
11. Di Mario C, Compostella L, Cucchini F, et al. Onset of cardiovascular action after oral ibopamine. Early hemodynamic effects of single and repeated doses in patients with idiopathic dilated cardiomyopathy. Arzneim Forsch/Drug Res 1990; 5: 65-77.
12. Di Mario C, Iavernaro A, Cucchini F. Acute hemodynamic effect of gallopamil in patients with coronary artery disease. Eur Heart J 1991; 12: 1006-11.
13. Cucchini F, Di Mario C, Bolognesi R, et al. Peak aortic blood acceleration: a possible indicator of initial left ventricular impairment in patients with coronary artery disease. Eur Heart J 1991; 12: 860-68.
14. Di Mario C, Serruys PW, Roelandt JRTC, et al. Detection and characterization of vascular lesions by intravascular ultrasound. An in vitro qualitative and quantitative correlation with histology. J Am Soc Echocardiogr 1992; 5: 135-46.
15. Wenguang L, Gussenhoven WJ, Di Mario C, et al. Validation of quantitative analysis of intravascular ultrasound. Internat J Cardiac Imag 1991; 6: 247-53.
16. Escaned J, Foley P, Di Mario C, et al. Quantitative angiography during coronary angioplasty using a single angiographic view. A comparison of automated edge detection and videodensitometric techniques. Am Heart J 1993, in press.
17. van den Brand M, Essed CE, Di Mario C, et al. Histologic changes in the aortic valve after balloon aortic valvuloplasty: evidence for a delayed healing process. Br Heart J 1992; 67: 445-49.
18. Di Mario C, Linker D, Serruys PW, et al. The angle of incidence of the ultrasound beam: a critical factor for the image quality in intravascular ultrasound. Am Heart J 1993; 125: 442-48.
19. Haase J, Di Mario C, Serruys PW. Validation and comparison of on-line and off-line quantitative coronary analysis systems using an in-vivo intracoronary insertion of stenosis phantoms. Cathet Cardiovasc Diag 1992; 22: 16-27.
20. Di Mario C, Roelandt JRTC, Serruys PW. Limitations of the zero-crossing detector for the analysis of intracoronary Doppler. A comparison with fast Fourier transform analysis of basal, hyperemic and transtenotic blood flow velocity in patients with coronary artery disease. Cathet Cardiovasc Diag 1993; 28: 56-64.
21. Di Mario C, Reiber JH, Serruys PW, et al. Edge detection vs densitometry in the quantitative

assessment of stenosis phantoms: an in vivo comparison in porcine coronary arteries. Am Heart J 1992; 124: 1181-89.
22. Di Mario C, Strikwerda S, Serruys PW, et al. Response of conductance and resistance coronary vessels to scalar concentrations of acetylcholine. Assessment with quantitative angiography and intracoronary Doppler in 29 patients with coronary artery disease. Am Heart J 1994; in press.
23. Di Mario C, de Feyter PJ, Serruys PW, et al. Intracoronary blood flow velocity and transstenotic pressure gradient using sensor tip pressure and Doppler guidewires. Cathet Cardiovasc Diagn 1993; 28: 311-19.
24. Haase J, Di Mario C, Serruys PW, et al. Digital geometric measurements in comparison to cinefilm analysis of coronary artery dimensions. Cathet Cardiovasc Diag 1992; 27: 16-27.
25. Serruys PW, Di Mario C, Meneaveau N, et al. Intracoronary pressure and flow velocity from sensor-tip guidewires. A new methodological approach for the assessment of coronary hemodynamics before and after coronary interventions. Am J Cardiol 1993; 17: 41D-53D.
26. Di Mario C, Meneveau N, Gil R, et al. Maximal blood flow velocity in severe coronary stenoses measured with a Doppler guidewire. Am J Cardiol 1993; 17: 54D-61D.
27. Di Mario C, Krams R, Serruys PW, et al. Intracoronary Doppler flow velocity indices for the assessment of coronary interventions. Eur Heart J; 1993, in press.

BOOK CHAPTERS/REVIEWS

English text

1. Roelandt JRTC, Di Mario C, de Feyter PJ, et al. Intravascular Ultrasound: instrumentation, image interpretation, promises and pitfalls. In Hanrath P, Uebis R, Krebs W (eds):"Cardiovascular Imaging by Ultrasound", Kluwer Academic Publishers, Dordrecht-Boston-London, 1992, pp. 325-341.
2. Serruys PW, Di Mario C, Roelandt JRTC, et al. Intravascular (coronary) Doppler catheter assessment.In Roelandt JRTC, Sutherland GR, Iliceto S, Linker DT (eds): "Cardiac Ultrasound", Churchill-Livingstone, London, 1993, pp. 1011-28.
3. Di Mario C, Serruys PW, Roelandt JRTC. Clinical applications of intravascular ultrasound. In Roelandt JRTC, Sutherland GR, Iliceto S, Linker DT (eds): "Cardiac Ultrasound", Churchill-Livingstone, London, 1993, pp. 938-49.
4. Razzolini R, Chioin R, Di Mario C, et al. Medium-term assessment of isosorbide-5-mononitrate in effort angina. Dependancy of efficacy on basic hemodynamic conditions. In Julian DG, Rittinghausen R, Uterbacher HJ (eds): "Mononitrate II", 1987, Springer-Verlag, Berlin , 1982.
5. Haase J, Di Mario C, Serruys PW, et al. How reliable are geometric coronary measurements? Validation and comparison of digital and cinefilm analysis systems. In Serruys PW, Foley DP, de Feyter PJ (eds): "Quantitative coronary angiography in clinical practice", Kluwer Academic Publishers, Dordrecht/London/New York, pp. 42-50.
6. Haase J, Di Mario C, Serruys PW, et al. Accuracy and relevance of angiocardiographic coronary measurements. In Onnasch D, Simon R (eds): Quality assurance in digital angiocardiography. Commett, p. 20-23, Kiel 1992.
7. Hermans W, Di Mario C, Serruys PW, et al. Immediate and late assessment of the results of coronary interventions. In Faxon D (ed): "Practical Angioplasty", Raven Press, 1993: 153-172.
8. Di Mario C, Serruys PW, Roelandt JRTC. Intravascular ultrasound. Cardioscopies 1992; 5: 130-136.
9. Di Mario C, Li W, Roelandt JRTC, et al. Three dimensional reconstruction in intravascular ultrasound. In: Marzilli M, Klugmann S (eds): "Invasive Cardiology 1992", in press.
10. Di Mario C, Haase J, Serruys PW. In vivo and in vitro, off-line and on-line validation of quantitative coronary angiography. Chapter III: Validation of videodensitometry in the assessment of stenosis phantoms. An in vitro and in vivo study. In Serruys PW, Foley DP, de Feyter PJ (eds): "Quantitative coronary angiography in clinical practice", Kluwer Academic Publishers, Dordrecht/London/New York, 1993, pp. 51-68.
11. Di Mario C, Slager C, Serruys PW. Assessment of coronary stenosis severity from simultaneous measurement of transstenotic pressure gradient and flow. A comparison with quantitative

angiography. In Serruys PW, Foley DP, de Feyter PJ (eds): "Quantitative coronary angiography in clinical practice", Kluwer Academic Publishers, Dordrecht/London/New York, 1993, pp. 283-306.
12. Di Mario C, Roelandt JRTC, Serruys PW, et al. Intravascular ultrasound: an evolving rival for quantitative coronary angiography. In Serruys PW, Foley DP, de Feyter PJ (eds): "Quantitative coronary angiography in clinical practice", Kluwer Academic Publishers, Dordrecht/London/New York, 1993, pp. 695-715.
13. Di Mario C, Roelandt JRTC. Intravascular ultrasound imaging with mechanical probes. In: Marzilli M, Klugmann S (eds): "Invasive Cardiology 1992", in press.
14. Roelandt J, Di Mario C, Linker DT, et al. Intracoronary ultrasound: state of the art. In: Chierchia S, Grossi A: "Cardiology Today and Tomorrow", Centro Scientifico Editore, 1992: 37-41.
15. Roelandt J, Di Mario C, Linker DT, et al. Intravascular ultrasound: rationale, image interpretations and overview of applications. In Taylor DJE, Vannan MA, Pandian NG (eds): "Echocardiography. State of the art", Pergamon Press, 1992: 1-5.
16. Emanuelsson H, Dohnal M, Lamm C, Di Mario C, et al. Measurement of coronary artery pressure and stenosis gradients. Clinical applications. In Serruys PW, Foley DP, de Feyter PJ (eds): "Quantitative coronary angiography in clinical practice", Kluwer Academic Publishers, Dordrecht/London/New York, 1993, pp. 167-179.
17. The SHK, Di Mario C, Gussenhoven EJ, et al. Normal and atherosclerotic arterial wall examined with intravascular ultrasound. Borgatti A (ed) :"Follow-up and prevention of the atherosclerotic plaque", Centro Scientifico Editore, 1992, Torino, 89-102.
18. de Feyter PJ, Vos J, Di Mario C, et al. Progression or regression of atherosclerosis. Asssessment with quantitative coronary angiography. In Serruys PW, Foley DP, de Feyter PJ (eds): "Quantitative coronary angiography in clinical practice", Kluwer Academic Publishers, Dordrecht/London/New York, 1993, pp. 635-49.
19. Serruys PW, Di Mario C, Kern M. Intracoronary Doppler. In Topol EJ (ed): "Interventional Cardiology. 2nd Edition", Saunders WB, 1993, Philadelphia (in press).
20. Wenguang L, Gussenhoven WJ, Zhong Y, The SHK, Di Mario C, et al. Validation of quantitative analysis of intravascular ultrasound images. In: S. Iliceto, P. Rizzon, JRTC Roelandt (eds) Ultrasound in coronary artery disease, Kluwer Academic Publishers 1991; 6: 247-53.
21. Di Mario C, Wenguang L, Roelandt J, et al. Three-dimensional intracoronary ultrasound. Goals and practical problems. Int J Cardiac Imaging 1993; 63-77.
22. Strauss BH, Escaned J, Foley DP, Di Mario C, et al. Technological considerations and practical limitations in the use of quantitative angiography during percutaneous coronary recanalization. Progr Cardiovasc Dis, in press.
23. Foley DP, Escaned J, Strauss BH, Di Mario C, et al. Quantitative coronary angiography in interventional cardiology. Application to scientific research and clinical practice. Progr Cardiovasc Dis, in press.
24 Escaned J, Doriot P, Di Mario C, et al. Does coronary lumen morphology influence vessel cross-sectional area estimation? An in-vitro comparison of intravascular ultrasound and quantitative coronary angiography. In Serruys PW, Foley DP, de Feyter PJ (eds): "Quantitative coronary angiography in clinical practice", Kluwer Academic Publishers, Dordrecht/London/New York, 1993, pp. 681-693.
25. Escaned J, Haase J, Foley DP, Di Mario C, et al. Videodensitometry in percutaneous coronary interventions: a critical appraisal of its contribution and limitations. In Serruys PW, Foley DP, de Feyter PJ (eds): "Quantitative coronary angiography in clinical practice", Kluwer Academic Publishers, Dordrecht/London/New York, 1993, pp. 69-87.
26. Herrman JPR, Keane D, di Mario C, Serruys PW. Advances in pharmacological treatment in the prevention of restenosis. In Maresta A, Invernizzi E (eds): Advances in Interventional Cardiology and Cardiac Surgery, 1993, in press.
27. Di Mario C, Baptista J, Keane D, Umans V, Herrman JPR, Ozaki Y, de Jaegere P, de Feyter PJ, Roelandt JRTC, Serruys PW. Intracoronary imaging and non-imaging techniques for guidance of coronary interventions. In Maresta A, Invernizzi E (eds): Advances in Interventional cardiology and Cardiac Surgery, 1993, in press.
28. Haase J, Keane D, Di Mario C, et al. Percutaneous implantation of coronary stenosis phantoms in

an anesthetized swine model to validate current quantitative angiography analysis systems. In Reiber JHC, Serruys PW (eds): Quantitative coronary arteriography 1993, Kluwer Academic Publishers, Dordrecht, 1994, in press.
29. Di Mario C, Krams R, Serruys PW. The instantaneous hyperemic coronary pressure-flow velocity relationship in conscious humans. In Reiber JHC, Serruys PW (eds): Quantitative coronary arteriography 1993, Kluwer Academic Publishers, Dordrecht, 1994, in press
30. Di Mario C, Strkwerda, Serruys PW, et al. Response of conductance and resistance coronary vessels to scalar concentrations of acetylcholine. In Serruys PW, Foley DP, de Feyter PJ (eds): "Quantitative coronary angiography in clinical practice", Kluwer Academic Publishers, Dordrecht/London/New York, pp. 230-53.
31. de Feyter PJ, Di Mario C, Serruys PW, Roelandt JRTC. How to assess regression of the atherosclerotic plaque. Biochem Soc Trans 1993; 21: 642-47.

LETTERS

1. Di Mario C, Hermans W, Serruys PW, et al. Calibration using the catheter as a scaling device. Importance to film the catheter not filled with contrast media. Am J Cardiol 1992; 69: 1377-78.
2. Di Mario C, Slager CJ, Serruys PW et al. Quantitative assessment of coronary artery stenosis by intravascular Doppler catheter technique. Circulation 1992; 88: 2016.

ORIGINAL ARTICLES
(non-English text/English abstract)

1. Di Mario C, Al Bunni M, Maiolino P, et al. Inferior myocardial infarction. Coronaro-ventriculographic correlations in 80 patients. Rev Lat Cardiol 1988; 6: 376.
2. Di Mario C. Zanchetta M, Carlon R, et al. Myocardial infarction below age 45: clinical usefulness of coronary arteriography in asymptomatic patients. G Ital Cardiol 1986; 16: 76.
3. Permutti B, Maddalena F, Di Mario C, et al. Preoperative clinical and angiographic profiles of the candidates to aorto-coronary bypass surgery. Differences dependent on patient gender. Boll Soc Ital Cardiol 1981; 26: 51.
4. Permutti B, Di Mario C, Dei Tos GA, et al. Factors predicting recurrence of angina in patients undergoing coronary bypass surgery. A 4-7 years follow-up study. Cardiologia 1982; 27: 237.
5. Permutti B, Dei Tos G, Di Mario C, et al. Return to work in patients undergoing aorto-coronary bypass surgery. Cardiologia 1983; 28: 93.
6. Permutti B, Dei Tos GA, Di Mario C, et al. Pre- and post-operative findings predicting long-term mortality after aortocoronary bypass surgery. G Ital Fisiopat Clin Cardiovasc 1983; 1: 239.
7. Permutti B, Di Mario C, Dei Tos GA, et al. Aorto-coronary bypass in the elderly. Min Med 1983; 74: 1301.
8. Di Mario C, Permutti B, Corbara F, et al. Functional improvement in patients undergoing aorto-coronary bypass surgery. G Ital Fisiopat Clin Cardiovasc 1983; 2: 269.
9. Di Mario C, Permutti B, Stritoni P, et al. Regional left ventricular wall motion in patients with coronary artery disease. Angiographic findings in 244 patients. G Ital Fisiopat Clin Cardiovasc 1983; 2: 275.
10. Dalla Volta S, Corbara F, Di Mario C, et al. Long-term results after aorto-coronary bypass implantation in a multicentric Italian Registry. G Ital Cardiol 1982; 12: 214.
11. Carlon R, Zanchetta M, Di Mario C, et al. Correlations among clinical, ergometric and angiographic findings 1-6 months after aorto-coronary bypass surgery. Il Cuore 1987; 4: 509.
12. Compostella L, Bellotto F, Chioin R, Roncon L, Carlon R, Di Mario C, et al. Serum enzymes behaviour after acute myocardial infarction. Effects of early thrombolytic therapy. Cardiologia 1983; 28: 31.
13. Razzolini R, Chioin R, Corbara F, Calvanese A, Miraglia G, Egloff C, Maiolino P, Di Mario C,

et al. Clinical results of isosorbide-5-mononitrate in chronic effort angina. Basi Raz Ter 1986; 16: 73.
14. Permutti B, Miraglia G, Maddalena F, Di Mario C, et al. Correlations between clinical and hemodynamic findings in 244 coronary patients. Cardiologia 1982; 27: 553.
15. Zanchetta M, De Lio U, Di Mario C, et al. Influence of the implantation of internal mammary arteries on the native coronary vessels. Short- and medium-term angiographic results. G Ital Cardiol 1988; 18: 10.
16. Scognamiglio R, Fasoli G, Di Mario C, et al. Chronic mitral insufficiency: preoperative left ventricular function and post-operative low cardiac output syndrome. G Emodinam 1984; 4: 129.
17. Carlon R, Zanchetta M, Di Mario C, et al. Percutaneous transluminal coronary angioplasty: long-term results. Riv Cardiol Prev Riabil 1986; 4: 99.
18. Al Bunni M, Franceschetto L, Carrozza A, Zanchetta M, Di Mario C, Maiolino P. Initial experience with a new VDD pacing system. Cardiostimolazione 1987; 5: 183.
19. Di Mario C, Zanchetta M, De Lio U, Maiolino P. Coronary anomalies and myocardial infarction. Report of 2 cases. G Emodinam 1985; 5: 119.
20. Allegri P, Di Mario C, Maiolino P. Anomalous origin of the left circumflex artery from the pulmonary trunk. G Emodinam 1987; 6: 167.
21. Serruys PW, Luijten HE, Essed CE, Di Mario C, de Feyter PJ, van den Brand M. Percutane transluminale ballonvalvuplastiek bij oudere patienten met een verworen aortaklepstenose. Nederlands Tijdschr Geneeskunde 1987; 131: 1269.
22. Di Mario C, Pedon L, Zanchetta M, et al. Effects on left ventricular function and effort myocardial ischemia of the aortic implantation of the anomalous left coronary artery in an adult case of Bland-White-Garland syndrome. Il Cuore 1988; 5: 381.
23. Zanchetta M, Dalle Mule J, Di Mario C, et al. Evaluation of post-operative flow reserve in internal mammary artery coronary grafting. G Ital Cardiol 1988; 19: 234.
24. Meneveau N, Di Mario C, de Jaegere P, de Feyter PJ, Serruys PW. La relation instantanee pression-velocité du flux coronaire, alternative a la mesure de la reserve coronaire: etude de faisabilité et reproductibilité de la methode. Arch Mal Coeur 1993; 86: 975-85.
25 Gil R, Di Mario C, P.W. Serruys, et al. Intravascular ultrasound: a substitute for angiography? Kardiologia Polska (Polish Heart Journal) 1982; 38: 327.

REVIEWS/BOOK CHAPTERS

(non-English text)

1. Di Mario C, Luijten HE, Serruys PW. Primary success and restenosis after percutaneous transluminal coronary angioplasty. Are common definitions possible today? G Ital Cardiol 1987; 17: 360.
2. Di Mario C, Beatt KJ, Verdouw PD, Serruys PW. Synchronized diastolic coronary sinus retroperfusion. Technique, physiologic and experimental grounds, clinical experiences and future perspectives. Cardiologia 1988; 33: 1017.
3. Permutti B, Dei Tos GA, Di Mario C, et al. Medical treatment after aorto-coronary bypass surgery. A review. Basi Raz Ter 1983; 13: 297.
4. Permutti B, Compostella L, Bellotto F, Bressan M, Di Mario C, et al. Ischemic heart disease in the elderly. Acta Geront 1983; 37: 231.
5. Bellotto F, Cirillo M, Compostella L, Carlon R, Bruni A, Di Mario C, et al. Dissociation between electric and mechanical activity in acute myocardial infarction. Proceedings of the XXXV National Congress of the Italian Society of Anesthesia, Analgesia and Intensive Care, 1983; 2: 299.
6. Di Mario C, Beatt KJ, Serruys PW. Synchronized diastolic coronary sinus retroperfusion during percutaneous coronary angioplasty. In Stritoni P, Violini R (eds): "Hemodynamics 1987", p. 281, Scoop srl, 1988, Naples.
7. Cucchini F, Di Mario C, Iavernaro A. Immediate effects of an intravenous bolus of gallopamil on cardiac hemodynamics. In Caturelli G (Ed): "Cardiological Intensive Care '89", p.65, Canal Press, 1989, Venice.

8. Vincenzi M, Arfiero S, Di Mario C, Mosele GM. Preventing sudden death: light and shadows. G Ital Cardiol 1991; 21: 203.
9. Arfiero S, Di Mario C, La Vecchia L, et al. Pharmacologic prevention of cardiac sudden death. Basi Raz Ter 1991; 21: 211-21.
10. Di Mario C, Arfiero S, Bedogni F, et al. Prevention and treatment of cardiac sudden death. A review of the available non-pharmacologic tools. Basi Raz Ter 1991; 21: 275-85.

Met dank aan:

Hoffmann La Roche, Nederland B.V., Schneider, Radi Medical Systems, Cardiometrics, Cvis, Baxter Laboratories, Cordis, Cadsand, Medicor, Spectranetics, TD Medical